Evolution of Neotropical biodiversity : phylogeny, ecology, and biogeography of Mesoeucrocodylia (Vertebrata Crocodyliformes) from the Miocene of Peruvian Amazonia

Rodolfo Salas-Gismondi

UNIVERSITÉ DE MONTPELLIER

THÈSE

Pour obtenir le grade de

DOCTEUR DE L'UNIVERSITÉ DE MONTPELLIER

Préparée au sein de l'école doctorale : Systèmes Intégrés en Biologie, Agronomie, Géosciences, Hydrosciences, Environnement (SIBAGHE)

Spécialité : Paléontologie

Présentée par RODOLFO SALAS-GISMONDI

EVOLUTION OF NEOTROPICAL BIODIVERSITY:
PHYLOGENY, ECOLOGY, AND BIOGEOGRAPHY OF THE MESOEUCROCODYLIA
(VERTEBRATA: CROCODYLIFORMES)
FROM THE MIOCENE OF PERUVIAN AMAZONIA

Soutenue le 14 décembre 2015 devant le jury composé de

M. Emmanuel Douzery, Professeur, Université de Montpellier	Président
M. Torsten Scheyer, Chercheur, Université de Zurich	Rapporteur
M. Diego Pol, Directeur de Recherches, Trelew	Rapporteur
M. Christian de Muizon, Directeur de Recherches, MNHN, Paris	Examinateur
M. Pierre-Olivier Antoine, Professor, Université de Montpellier	Directeur de thèse
M. Armando Valdés Velásquez, Professeur, Université Cayetano Heredia	Co-directeur de thèse
M. John J. Flynn, Professeur, Conservateur, AMNH New York	Invité
M. Stéphane Jouve, Conservateur-adjoint, Muséum de Marseille	Invité

ACKNOWLEDGMENTS

First of all, I have to say that this work did not start with the Ph.D. program itself, this work started many years ago with the help of many people of different countries that, in one way or another, supported my dream of becoming a paleontologist. In this section I will express my gratitude in the language I can better explain my deep recognition to all of them.

Dicho esto, quiero empezar agradeciendo a mis dos asesores, Pierre-Olivier Antoine y Armando Valdés Velásquez, por haber confiado en mi para realizar esta investigación. Yo les agradezco profundamente por su paciencia y apoyo durante estos tres años, por haberme motivado y conducido para dar este importante paso profesional en mi vida.

Por consiguiente, agradezco profundamente a Pierre-Olivier Antoine, mi guía y aliado, el maestro y amigo que no vaciló nunca en hacer un esfuerzo adicional para que este proyecto se concrete. Gracias por todo el tiempo invertido, lo aprecio y respeto. Cada uno de sus consejos y enseñanzas durante estos tres años, y desde que nos conocimos, tanto haciendo trabajo de campo en la Amazonía de Iquitos como en el laboratorio, traslucieron su calidad humana y científica. He aprendido mucho sobre paleontología en todas nuestras conversaciones, por las cuales le estaré siempre agradecido. Además, estoy muy agradecido por el tiempo que pasé en Montpellier, por haberme hecho sentir como en casa, por proveerme de las mejores condiciones de trabajo y oportunidades para que esta investigación sea mejor cada día. Muchas gracias a Pierre-Olivier porque él y su familia –Maëva y Aloys –, fueron la mía en Montpellier.

Yo le agradezco sinceramente a Armando Valdés Velásquez quien ha co-dirigido esta investigación desde Lima, Perú. A pesar de recién haberme conocido, Armando aceptó sin vacilar ser mi co-director. Le agradezco por las enseñanzas en cada conversación que tuvimos y la confianza que depositaste en mi, mostrando un compromiso desinteresado por llevar este proyecto adelante.

Quiero agradecer a los revisores de la tesis, Torsten Scheyer y Diego Pol, por mostrar gran interés por mi trabajo y por haber aceptado evaluar esta investigación. Sus importantes carreras y obras científicas siempre me fueron inspiradoras. Asimismo, quiero expresar mi agradecimiento a los miembros del jurado, Emmanuel Douzery, Christian De Muizon, John Flynn y Stéphane Jouve. Agradezco a Stéphane por compartir sus conocimientos e ideas sobre cocodrilos fósiles conmigo en muchas conversaciones y misivas.

Quiero hacer un reconocimiento especial a Christian de Muizon y a John Flynn. Desde que conocí a Christian hace muchos años en Lima cuando era director del Instituto Francés de Estudios Andinos (IFEA), nos apoyó a Mario Urbina y a mi, para desarrollar la paleontología de vertebrados en el Perú. De allí en adelante siempre fue incondicional y su ayuda se hizo sentir en momentos decisivos de mi carrera. Junto a Jean Vacher y Niels Valencia, Christian me incentivó para que estudiara ciencias biológicas con ayuda de una beca del IFEA otorgada durante la gestión de Jean Vacher, a quien agradezco y aprecio. Asimismo, las oportunidades

que Christian me dio para trabajar por algunos meses en el Museum national d'Histoire naturelle (MNHN) sirvieron para que yo revisara y estudiara las vastas colecciones de cocodrilos y así, empezara la revisión de los caracteres de los cocodrilos fósiles y actuales registrados en la matriz filogenética que en esta tesis incluyo. Christian me enseñó las bases de la ciencia llamada paleontología, por lo que lo considero mi mentor. A John Flynn lo conocí en el 2004 durante la primera expedición en la que yo participé a los yacimientos paleontológicos de la zona de Iquitos. Desde ese año, en cada campaña a Iquitos, cada descubrimiento lo hemos vivido y trabajado juntos, palmo a palmo, y lo hemos celebrado juntos con Siete Raíces Sour. A John le agradezco por haberme apoyado en la decisión incluir los cocodrilos de Iquitos como parte importante de mi doctorado. Además le tengo que agradecer por haberme facilitado estadías y becas para trabajar en la colección de cocodrilos del American Museum of Natural History (AMNH). Incluso me brindó un espacio en el AMNH para enclaustrarme el último mes antes de entregar el manuscrito de mi tesis y poder terminarla a tiempo. También le agradezco por todos los intercambios epistolares en los que discutimos aspectos científicos de los artículos conformantes de esta tesis. Del AMNH, quiero agradecer a Ana Balcárcel por su extraordinario trabajo en el campo y en la preparación de fósiles en el laboratorio y a Carl Mehling por brindarme acceso a las colecciones de reptiles fósiles.

Asimismo, expreso mi agradecimiento a Bruce MacFadden por haberme permitido ocupar por cuatro meses la Biblioteca Simpson del University of Florida Natural History Museum para escribir el segundo artículo de la tesis. Aprecio y agradezco mucho a Valerie DeLeon por haberme aceptado como alumno libre en la clase de morfometría geométrica en la University of Florida (UF); a Christopher Brochu, Paula Bona, Torsten Scheyer, Jorge Moreno-Bernal, Orángel Aguilera y Stéphane Jouve por facilitarme imágenes de cocodrilos fósiles; a Salvador Bailón del MNHN, Richard Hulbert y Kenneth Krysko de la UF, a Eberhard "Dino" Frey del Staatliches Museum für Naturkunde Karlsruhe, Karlsrhue, Germany (SMNK), y a R. Schoch del Staatliches Museum für Naturkunde Stuttgart, Stuttgart (SMNS) por amablemente brindarme acceso a las colecciones de cocodrilos fósiles y actuales a su cargo.

Quisiera expresar mi agradecimiento y respeto a todos y cada uno de los miembros del Institute des Sciences de l'Evolution (ISEM). En el ISEM hice muchos y grandes amigos, entre ellos mi compañero de oficina Abdou Mahboubi y el "big chief" Laurent Marivaux. Agradezco a Maëva Orliac por su constante ayuda en análisis de filogenia, conversaciones sobre arte científico y por acogerme en su oficina los meses antes de la sustentación. Agradezco a Julien Claude y Renaud Lebrun por sus valiosas enseñanzas sobre morfometría geométrica. Aprecio mucho la ayuda que me brindó Anusha Ramdarshan para evaluar el mircrodesgaste en dientes de caimanes "moledores".

Agradezco profundamente a la Escuela Doctoral Franco-Peruana de Ciencias de la Vida (EDFPCV) por otorgarme una beca por tres años, sin la cual no habría sido posible hacer esta investigación; a José Espinoza, director de la EDFPCV y a Rebeca Caldas de contabilidad por su constante preocupación y ayuda. Asimismo, a las personas e instituciones, peruanas y francesas que conforman la EDFPCV y que siempre estuvieron dispuestas a resolver cualquier situación adversa durante estos tres años: a Fabiola León-Velarde, rectora de la Universidad Peruana Cayetano Heredia; a Gisella Orjeda, presidenta del

Concejo Nacional de Ciencia, Tecnología e Innovación Tecnológica; a Philippe Benassi agregado de Cooperación Universitaria de la Embajada de Francia en Lima y a su asistente Eliana Noriega; y particularmente a Jean-Loup Guyot, director en Lima del Institut de recherche pour le developpement (IRD), quien me ha brindado su consejo y amistad en todo momento requerido.

Tengo que ofrecer un profundo agradecimiento a todos los que participaron en las expediciones a Iquitos y Fitzcarrald y que hicieron posible que los magníficos fósiles de cocodrilos tema de esta tesis fueran descubiertos, como son John Flynn, Pierre-Olivier Antoine, Patrice Baby, Nicolas Espurt, Ana Balcarcel, Julia Tejada, Dario De Franceschi, Ysabel Calderón, Stéphane Brusset, François Pujos, Mouloud Benammi, Anjali Goswami, Bruce Shockey, Andy Wyss, Martin Roddaz, Denis Uyhen, Badis Kouidrat y Rolando Bolaños. Uno de los gestores de la epopeya Amazónica, junto a Pierre-Olivier Antoine y John Flynn, es mi gran amigo Patrice Baby. Le quiero manifestar mi admiración por haberme demostrado su gran talento para buscar sitios fosilíferos en la Amazonía. Le agradezco por habernos conducido hasta los lugares más alejados de los ríos Mapuya, Inuya, Sepa y Urubamba para encontrar nuevos yacimientos. Le agradezco también por todo su apoyo y las oportunidades que me ha brindado constantemente para participar en nuevos proyectos que siempre culminan con descubrimientos paleontológicos únicos y espectaculares. Sobre todo le quiero agradecer y expresarle todo mi aprecio por su incondicional amistad. Gracias a Patrice por haber convencido a Badis Kouidrat (de Lacoste) frente a un *cassoulet* de financiar (y participar de) la expedición y exhibición Fitzcarrald 2005. Gracias a Badis por confiar en el éxito de este proyecto que significó el descubrimiento de una fauna de mamíferos y cocodrilos de Fitzcarrald, estos últimos estudiados en esta tesis; a Rafael Barbarán y Jorge Arrunategui por haber cuidado de nosotros con "valentía" durante toda la expedición; a nuestros guías Billy Evans, Paco Sanz y un agradecimiento especial al gran conocedor de la selva Victor Tante Marsano, que nos dejó prematuramente, no sin antes convertirse en el mejor anfitrión y amigo de Atalaya. Agradezco también a nuestro guía y motorista Michel en Iquitos.

Ahora toca agradecer a todos y cada uno de los miembros del Departamento de Paleontología de Vertebrados del Museo de Historia Natural de la Universidad Nacional Mayor de San Marcos, Lima, Perú (DPV). En primer lugar a Mario Urbina por haber sido el compañero de esta larga y dura travesía paleontológica, sin quien podría no haber siquiera empezado; a Niels Valencia por su constante apoyo y consejo incondicional como director del Museo de Historia Natural, como amigo y como miembro honorario del DPV; a Walter Aguirre y Eusebio Díaz, técnicos del DPV, por su excelente trabajo de preparación de fósiles en condiciones muy adversas; a Rafael Varas por haber conducido impecablemente el DPV en mi ausencia durante el doctorado; a los jóvenes estudiantes Aldo Benites y Manuel Burga por su ayuda haciendo fotografías de cocodrilos en Lima y tomar datos para mi que luego fueron fundamentales en los resultados de mi tesis; a Joan Chauca por conseguirme la mejor versión de photoshop que podía haber en el mercado. Un cálido agradecimiento a Kevin Montalván Rivera por su excelente trabajo de reconstrucción de la apariencia externa del *Gnatusuchus pebasensis* y a Javier "Canelita" Herbozo por su magnífica recreación pictórica de los caimanes y el ambiente Pebas.

Tengo que agradecer a mi más cercana familia: a mi mamá, Mafalda Gismondi; a mi hermana, Mafalda Tay Gismondi, a mi papá, Rudy Salas; y a Fico, Federico Tay, por haberme apoyado en mi cuestionable decisión de dedicarme a la paleontología en el Perú. Gracias a ellos por todo su amor. Les agradezco por la educación que me dieron en la casa y el constante apoyo económico que me permitió estudiar el colegio, idiomas carreras universitarias, etc. Sin esta ayuda hubiera sido muy difícil alcanzar la meta anhelada. Nunca olvidaría a mi abuelita Julia, quien fue la más maravillosa abuelita del mundo y que desde donde se encuentre seguro sigue cuidándome, como cuando era un niño.

Finalmente, quiero agradecer a Julia Tejada, la mujer de mi vida, la compañera inspiradora, la persona que con su amor me ha ayudado a ser y querer ser cada día una mejor persona. Tengo que agradecerle haberme repetido incansablemente que debería postular para hacer un doctorado, que me haya prácticamente empujado a hacer cada trámite, cada carta. Le agradezco por todas las profundas y acaloradas conversaciones sobre ciencia, sobre nuestro país, la nostalgia que nos ocasiona estar lejos de él y cuanto lo amamos. A Julia le dedico esta tesis.

CONTENTS

CHAPTER I – INTRODUCTION

CHAPTER I – INTRODUCTION

Amazonia is one of the most species-rich biomes on earth. With almost 7 million km^2 and including territories of nine countries in South America, this tropical basin is the largest of the world. As such, it encompasses heterogeneous habitats, landscapes, and biotic communities (Rylands et al., 2002; Hoorn et al., 2010a, b). The origin of this complex mosaic of extreme biodiversity is the result of an evolutionary history closely linked to the Andean uplift and the ecological control of these rapid-growing mountains over the foreland proto-Amazonian basin during Cenozoic and, more particularly, Miocene times (Mora et al., 2010). Indeed, before the establishment of the Amazonian River System, a distinct aquatic ecosystem –known as the Pebas Mega-Wetland System– florished in western proto-Amazonia for more than ten million years, between around 23 and 11 million years ago (Wesselingh & Salo, 2006; Figueiredo et al., 2010; Hoorn et al., 2010a, 2010b). The role of this stage in the development of extant Amazonian biota has been emphasized recently in several scientific contributions (Wesselingh et al., 2002, Wesselingh & Salo, 2006; Hoorn et al., 2010a; Salas-Gismondi et al., 2015a). Independent phylogenetic analyses based on either paleontological or molecular data reveal that origin and diversification of several Amazonian clades of animals and plants occurred during the Miocene epoch (Albert et al., 2006; Hoorn et al., 2010b; Roncal et al., 2015).

Finding fossil evidence in forested tropical areas is a real challenge, though. Fossiliferous localities are usually small spots, confined to river or creek banks, and located in remote, inaccessible territories. However, despite the lack of extensive outcrops and favorable conditions to look for fossils in the Amazonian basin, pioneer scientists and explorers made remarkable paleontological discoveries during the late nineteenth and early twentieth century, some of them inspiring deeply our own search (Fig. I.1; Gervais, 1876; Barbosa-Rodrigues,

1892; Mook, 1921a, 1941; Spillmann, 1949; Matthiessen, 1961; Price, 1964; Langston, 1965; Willard, 1966).

Figure I.1. Pioneer explorers and scientists. (*a*) Paul Gervais (1816-1879); (*b*) Joao Barbosa Rodrigues (1842-1909); (*c*) Charles C. Mook (1887-1966); (*d*) Llewellyn I. Price (1905-1980); (*e*) Franz Spillmann (1901-1988); (*f*) Wann Langston Jr. (1921-2013); (*g*) Peter Matthiessen (1927-2014); (*h*) Harvey Bassler (1882-1950). (*c*) is from the Vertebrate Paleontology Archives, Division of Paleontology, AMNH. (*f*) is from The University of Texas at Austin. (*g*) Photograph by Jill Krementz. (*h*) is from Lehigh University Archives.

Nevertheless, these first approaches denoted other potential limitations of paleontological evidence in tropical areas, mainly related to surface collection on riverbanks, and leading to poor stratigraphic control. In the last three decades, several international teams overcame most barriers limiting our understanding of Amazonian history by performing

constant fieldwork and compiling with extreme rigor abundant geological, biological, climatic, and paleontological data (e.g., Hoorn 1993; Monsch, 1998; Nuttall, 1999; Wesselingh et al., 2002; Muñoz-Torres et al., 2006; Wesselingh & Salo, 2006; Wesselingh et al., 2006a; Figueiredo et al., 2010; Hoorn, et al., 2010a, b; Mora et al., 2010; Antoine et al., submitted). The results obtained by these indefatigable workers now constitute the fundamental framework to which any new research on the Neotropical evolution unarguably will be assembled.

In 2004, following the steps of those early explorers, for the first time our team was able to carry out investigative expeditions to lowland Peruvian Amazonia in search of new geological and paleontological data. The scope of our international team has been focused on the evolution of the proto-Amazonian biota during the Cenozoic. These collaborative projects were lead by French, North American, and Peruvian scientific institutions, including the Université de Toulouse (France), Université de Montpellier (France), Institut de Recherche pour le Développement (France), Muséum national d'Histoire naturelle (France); American Museum of Natural History (USA), PeruPetro (Peru), and Museo de Historia Natural-UNMSM (Peru). For about ten years now, we have explored different sedimentary rocks outcropping within Amazonian riverbanks, notably in Loreto (Iquitos and Contamana areas), Ucayali (Fitzcarrald Arch), and Cusco Departments (Upper Madre de Dios Basin). These areas soon revealed the existence of well-preserved paleontological resources documenting the Eocene and Miocene epochs, such as invertebrate and vertebrate remains and, in some cases, they provided exceptional fossilization of soft-bodied organs and fragile organisms, like leaves and minute arthropods included in amber (Salas-Gismondi et al., 2006, 2007, 2011; Antoine et al., 2007; Pons & De Franceschi, 2007; Goillot et al., 2011; Petrulevičius et al., 2011; Tejada et al., 2011). Among vertebrates, fossil mammals were particularly relevant since they added new clues on the early evolution and diversification of rodents and primates

in South America (Antoine et al., 2011, 2013; Marivaux et al., 2012). Considering the still brief record of paleontological data in tropical South America, these discoveries represent invaluable evidence on the ancient biotic events underlying modern Amazonian diversity.

From the initial findings to our own discoveries, the abundance of Miocene fossil remains belonging to mesoeucrocodylians (sensu Sereno et al., 2001) depicted that these archosaur sauropsids were conspicuous components of South American communities during most of the Cenozoic (Fig. I.2; Bravard, 1858; Gervais, 1876; Burmeister, 1883; Scalabrini, 1887; Rovereto, 1912; Mook, 1921a; Rusconi, 1933; Price, 1964; Langston, 1965, 2008; Sill, 1970; Buffetaut & Hoffstetter, 1977; Buffetaut, 1982; Busbey, 1986; Bocquentin-Villanueva et al., 1989; Bocquentin-Villanueva & Souza Fhilo, 1990; Langston & Gasparini, 1997; Kraus, 1998; Brochu & Rincón, 2004; Aguilera et al., 2006; Sánchez-Villagra & Aguilera, 2006; Paolillo & Linares, 2007; Salas-Gismondi et al., 2007, 2015a; Riff & Aguilera, 2008; Riff et al., 2010; Scheyer & Moreno-Bernal, 2010; Bona et al., 2013; Hastings et al., 2013; Scheyer et al, 2013; Fortier et al., 2014; Aureliano et al., 2015). In South America, mesoeucrocodylians comprises "true" crocodylians (crown-grouped Crocodylia sensu Brochu et al., 2009) and two non-crocodylian clades: the "terrestrial" sebecids (Notosuchia, Sebecosuchia; see Pol & Powel, 2011), and the long- and short-snouted dyrosaurids (Mesoeucrocodylia, ?Neosuchia; see Hastings et al., 2014). The "true" crocodylian clade was largely represented by gavialoids and caimanines, as well as by the enigmatic putative crocodyloid *Charactosuchus* (see Brochu, 1999, 2004; Langston, 1965). Besides dyrosaurids that apparently did not surpass the Paleocene-Eocene boundary in South America (Hastings et al, 2014), the other Cenozoic mesoeucrocodylian clades were either originated within the Americas during the Mesozoic times (i.e., caimanines: Brochu, 1999; sebecids: Pol & Powell, 2011) or incorporated to the South American and Caribbean faunas later by some kind of dispersal during Paleogene times (i.e., gavialoids: Vélez-Juarbe et al., 2007).

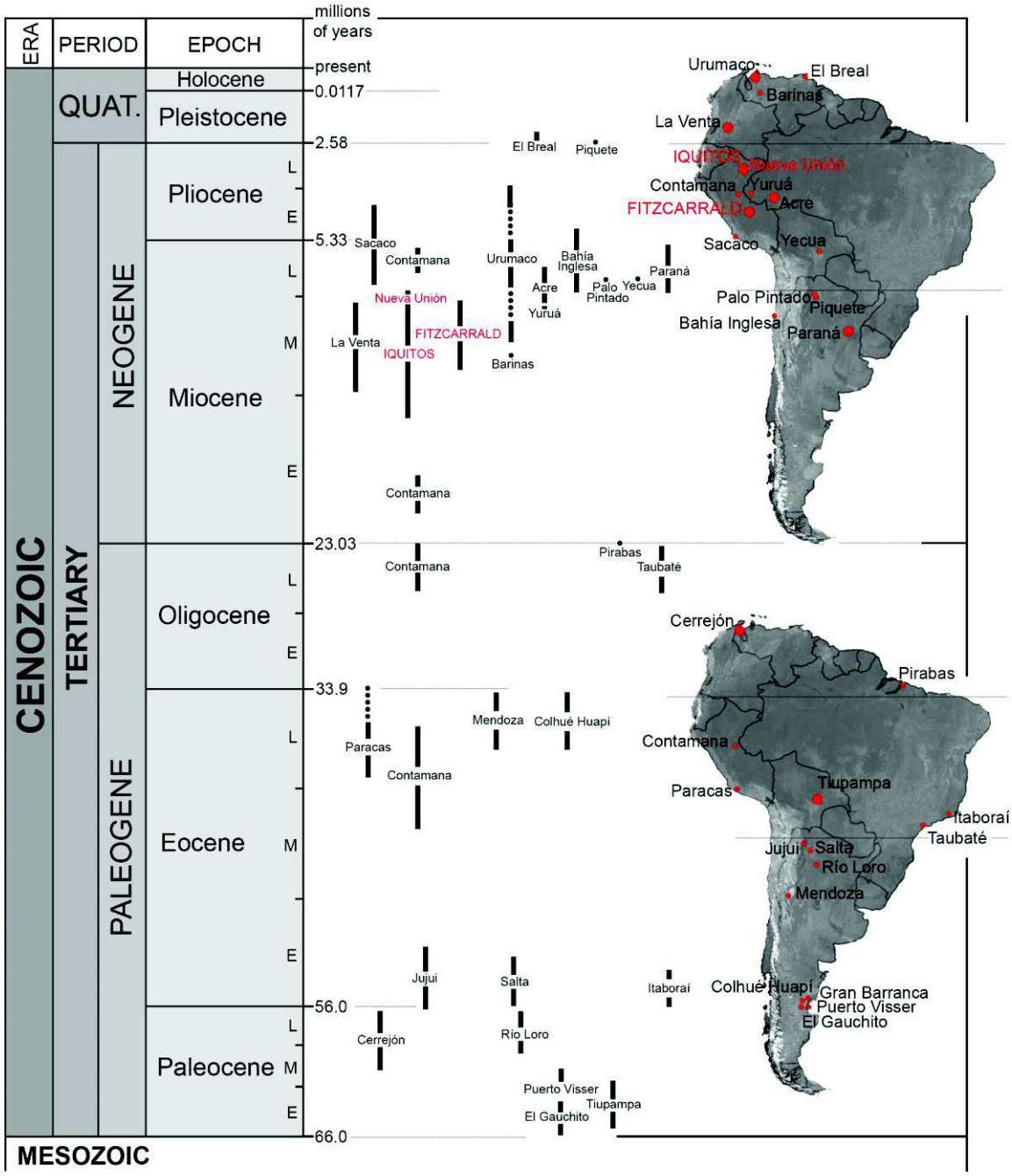

Figure I.2. Cenozoic time scale and South American mesoeucrocodylian localities in the Paleogene and Neogene. Paleogene: Cerrejón (Hastings et al., 2010); El Gauchito (Bona, 2007); Itaboraí (Pinheiro, 2012); Jujui (Gasparini, 1984); Tiupampa (Buffetaut, 1991); Salta (Gasparini, 1986); Contamana (Salas-Gismondi et al., 2013; Antoine et al., submitted); Paracas (Salas-Gismondi et al., 2013); Mendoza (Rusconi, 1946); Río Loro (Pol & Powel, 2011); Puerto Visser (Rusconi, 1937); Colhué Huapí (Simpson, 1933); Taubaté (Chiappe, 1988); Neogene: Contamana (Antoine et al., submitted); La Venta (Langston, 1965); Iquitos (Salas-Gismondi et al., 2015a); Nueva Unión (Salas-Gismondi et al., 2015); Fitzcarrald (Salas-Gismondi et al., 2006); Yuruá, (Price, 1964); Acre (Cozzuol, 2006); Urumaco (Sánchez-Villagra & Aguilera, 2006); Palo Pintado (Bona et al., 2014); Yecua (Tineo et al., 2014); Bahía Inglesa (Walsh & Suárez, 2005); Sacaco (Kraus, 1997); El Breal (Fortier & Rincón, 2013). Bigger dots represent the record of mesoeucrocodylian assemblages within those localities.

In summary, sebecids, gavialoids, and caimanines (eventually *Charactosuchus* too) became the typical mesoeucrocodylian assemblage of inland Neotropical environments during the Middle Miocene, as documented in La Venta (Colombia; e.g., Langston, 1965) and Fitzcarrald faunas (Peru; Salas-Gismondi et al., 2007; this work). "Terrestrial" sebecids probably have gone extinct sometime after the Middle Miocene, since they are absent from the large crocodylian sampling recovered in the Late Miocene localities of Acre (Brazil; Cozzuol, 2006) and Urumaco (Venezuela; Sánchez-Villagra & Aguilera, 2006). These localities provided the highest taxonomic and morphological diversity of crocodylians from all times (Hoorn et al., 2010b; Scheyer et al., 2013; Salas-Gismondi et al., 2015a), thus raising questions about the niche structure and trophic dynamics of Miocene aquatic ecosystems. For example, several coeval species with long and slender rostra among gavialoids and *Charactosuchus* occupied relatively close areas within aquatic environments of northernmost South America (Sánchez-Villagra & Aguilera, 2006). On the other hand, the extreme diversification of caimanines into distinct snout morphotypes resulted in the evolution of macro- and micro-predators, such as the giant *Purussaurus* (Aureliano et al., 2015) and the duck-faced caiman *Mourasuchus* (Langston, 1965), respectively. Little is known about the crocodylian faunas through the Pliocene epoch, but apparently the diversity of snout morphotypes and ecologies reached by Miocene crocodylians was dramatically affected during this time interval (Scheyer et al., 2013). Rocks from the early Pliocene barely document the latest South American gavialoids (Sill, 1970; Kraus, 1998) and the arrival of crocodylines (*Crocodylus* and allies) to the Neotropics (Scheyer et al., 2013). Modern day crocodylian faunas are restricted to six caimanines (*Caiman crocodilus*, *C. yacare*, *C. latirostris*, *Melanosuchus niger*, *Paleosuchus trigonatus*, and *P. palpebrosus*) and two crocodylines (*Cr. acutus* and *Cr. intermedius*), with no species bearing dramatic disparate proportions in snout morphotypes and feeding ecology (see Blanco et al., 2014).

This short recapitulation of the main facts regarding the mesoeucrocodylian history in tropical South America set out several scientific issues related with our knowledge of the Cenozoic evolution of this particular clade.

First, the fossil record in tropical South America gives virtually no clues about the origin and diversification of crocodylians prevailing in the landmass during the Miocene. Besides the early Paleogene caimanine remains unearthed in the southern cone of the continent (Simpson, 1933; Buffetaut & Marshall, 1991; Gasparini et al., 1993; Bona, 2007), the two rich Neotropical Paleogene localities known so far (Fig., I.2; Cerrejón coal mine and Tiupampa: Paleocene of Colombia and Bolivia, respectively) yielded exclusively dyrosaurids and sebecids (Buffetaut & Marshall, 1991; Hastings et al, 2010, 2011, 2014). However, fragmentary remains of Paleogene crocodylians suggest that caimanines and putative gavialoids have roamed proto-Amazonia at least since Eocene times (Salas-Gismondi et al., 2013; Antoine et al., submitted). The high global temperatures of the Paleogene interval favored the evolution of the first Neotropical rainforest in northern South America and a peak of plant diversity during the Middle Eocene Climate Optimum (Jaramillo et al., 2006; Wing et al., 2009). Main topographic reliefs were dominated by the Guyana and Brazilian Cratons, as well as by the growing Andean mountains. Between these elevated areas, the proto-Amazonian basin was connected with the Caribbean by a northern flow drainage. Marine incursions and fluvial environmental conditions were relatively common during this time interval (Hoorn et al., 2010a).

Second, the available evidence of the Miocene mesoeucrocodylians is remarkable and abundant, but still inadequate to reveal major aspects of their phylogenetic relationships, biogeography, and ecology. In this case, our knowledge regards mainly on three rich localities: one Middle Miocene in age (Fig. I.2; La Venta, Colombia: Langston, 1965; Langston & Gasparini, 1997) and two from the Late Miocene (Acre, Brazil: Cozzuol, 2006;

Urumaco, Venezuela: Sánchez-Villagra & Aguilera, 2006; Scheyer et al., 2013). An additional remarkable vertebrate fossiliferous site from the Middle Miocene is also known, but until now it has been only briefly reported for its mesoeucrocodylian fauna (Fitzcarrald, Peru; Salas-Gismondi et al., 2007; Tejada-Lara et al., 2015a). Numerous studies have provided phylogenetic and biogeographic contexts for some of these taxa and suggested that they inhabited highly productive, aquatic environments connecting different regions of tropical South America (e.g., Aguilera et al., 2006; Salas-Gismondi et al., 2007; Riff & Aguilera, 2008; Hoorn et al., 2010b; Scheyer et al., 2013). However, only few attempts provided an integrative phylogenetic vision on the evolution of the crocodylian communities in association with major changes of environmental conditions during the early Neogene (Scheyer et al., 2013). Thus, in this matter crucial questions remain to be addressed. For example, can proto-Amazonian mesoeucrocodylian snout morphotypes provide information about characteristics of habitat preferences and environmental conditions? Or inversely, which features of terrestrial and aquatic ecosystems might have fostered the diversification of a specific snout morphotype through time? Can phylogenetic diversity at each time interval in Amazonia provide clues about trends in landscape evolution? Regarding morphotypes of mesoeucrocodylians absent in recent Amazonian ecosystems, is it possible to infer their general ecology? Is that possible to infer hypothetical ancestral snout-morphotype and ecology underlying the extreme diversification of Miocene caimanines? Why did extant caimans survived while other crocodylians had become extinct in Amazonia? Are there some clues in cranial morphology to discrimate ecology within long-snouted crocodylians? Can we use crocodylians as a proxy to constrain the establishment of modern aquatic ecosystems in Amazonia?

Last but not least, to deal with all these unknown significant pieces of the mesoeucrocodylian evolution in the Neotropics, it is necessary to comprehensively evaluate

the dominant biotic feature existing throughout the Miocene: The Pebas Mega-Wetland System (Fig. I.3). Major data about this long-lasting paleoenvironment has been gathered from a bunch of boreholes and outcrops belonging to the Pebas/Solimões Formation within the territories around the junction of Colombia, Brazil, and Peru (Wesselingh et al., 2002, 2006a). Around 23 million years ago, a peak of Andean mountain building seems to control the origin of this distinctive Miocene mega-wetland by generating subsidence in the foreland basin (Roddaz et al., 2005, 2010; Hoorn et al., 2010a). Initially, the Pebas System encompassed mainly riverine environments, but a transition to lacustrine-dominated conditions is evidenced in Middle Miocene deposits (Hoorn et al., 2010a). Then, main areas of this depositional system were located in present-day western Amazonia, between the Andean mountains and the ancient cratonic reliefs (Wesselingh & Salo, 2006). As a prominent feature, aquatic environments were connected to the Caribbean Sea through a drainage of northern flow. A marine connection with the Pacific Ocean across the Cuenca Basin (Ecuador) has been proposed as well (Hoorn, 1995; Vonhof et al., 1998). Multiple aquatic environments dominated the region and fragmented forested, land areas. Events of marine incursions produced marginal marine conditions during several intervals througthout the Miocene (Gingras et al., 2002; Hovikoski et al., 2007; Boonstra et al., 2015). The distinctive Pebasian sedimentary deposits indicate that dysoxic muddy bottoms within shallow lakes and swamps were prevalent (Wesselingh et al., 2002; 2006a). Most levels document mollusks, pollen, and ostracods, providing a relatively precise biostratigraphic framework for the Pebas Formation (Hoorn, 1993; Muñoz-Torres et al., 2006; Wesselingh & Salo, 2006). Around 13 million years ago, the Pebas Mega-Wetland System reached more than one million km^2 and attained extreme plant and animal diversity (Wesselingh et al, 2006a). This particular stage is finely documented in rocks of the Pebas Formation outcropping along the riverbanks of the Iquitos area (Wesselingh et al., 2002; Wesselingh

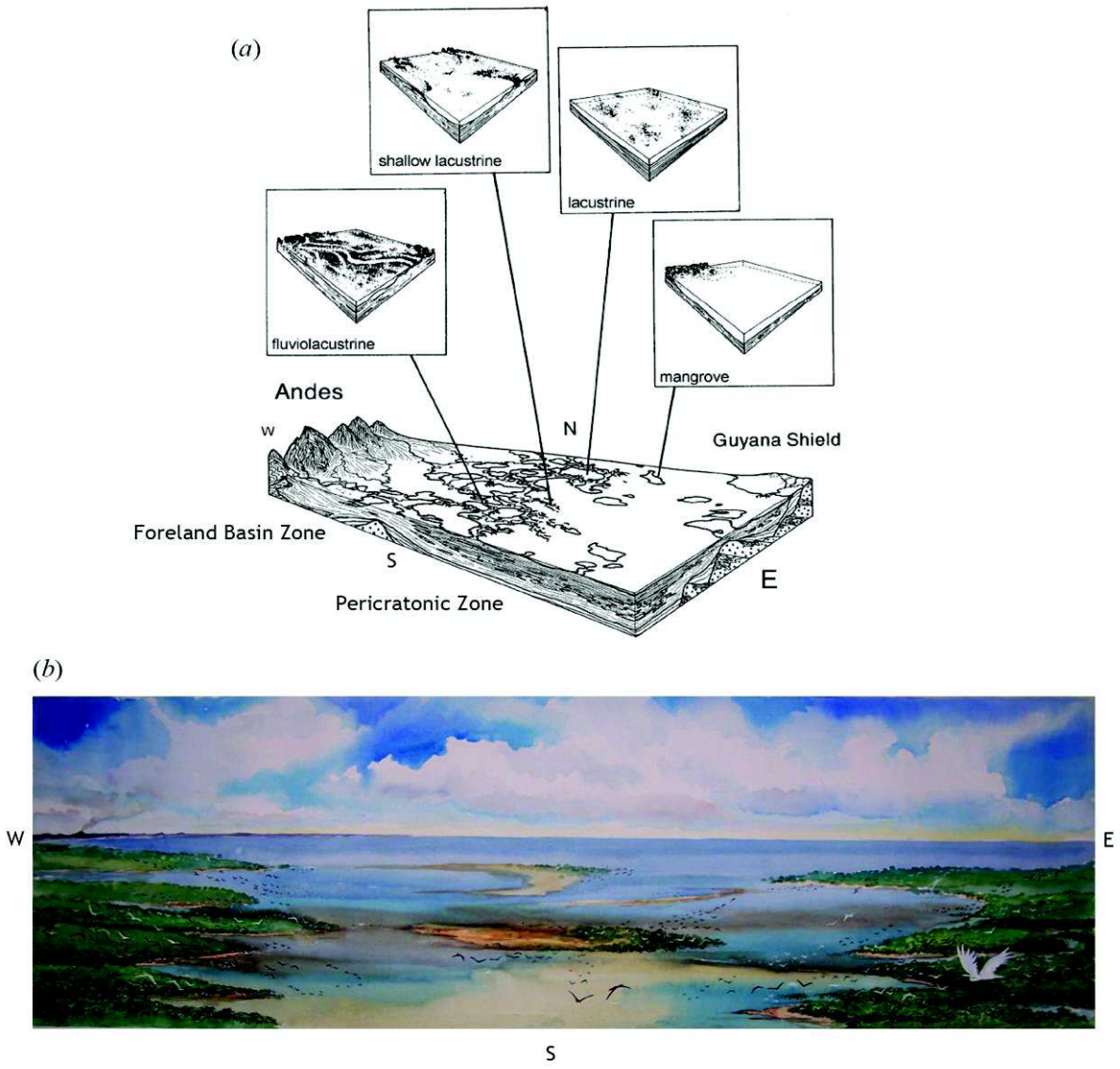

Figure I..3. Paleoenvironmental reconstructions of the Pebas Mega-Wetland System. (*a*) Environmental model from Wesselingh et al. (2002). (*b*) Hypothetical iew of the Pebas System from the Fitzcarrald Arch towards the north, with the growing Andean mountains the west and the wetland to the northeast. Watercolor painting by Daniel Peña.

& Salo, 2006; Antoine et al., 2006). Fossil plants from these levels (i.e., leaves, fruits, and logs) depict less rainfall seasonality than in modern Amazonia (Pons & De Franceschi, 2007). Including bivalves and gastropods, more than 85 co-occurring mollusc species, mostly endemic, inhabited the corresponding aquatic environments (Wesselingh & Salo, 2006; Wesselingh et al., 2006a). Although large vertebrate remains have been recognized in these deposits (Hoorn, 1994), they were only briefly reported (Monsch, 1998; Pujos et al., 2009). At this time, the Pebas Mega-Wetland embraced a complex collage of rivers flowing from the

Andean and cratonic mountains to the shallow lakes, swamps, embayments, and fluvio-tidal environments located in the basin lowlands (Fig. I.3; Wesselingh et al., 2006a; Hoorn et al., 2010a). La Venta (Colombia) and Fitzcarrald (Peru) strata are coeval with those of the Pebas formation in the Iquitos area, and represent fluvial and fluvio-tidal-dominated settings within the Pebas System as well, but closer to the Andean influence (Kay & Madden, 1997; Lundberg et al., 1998; Salas-Gismondi et al., 2007; Hoorn et al., 2010a; Tejada-Lara et al., 2015a).

The end of the distinctive conditions of the Pebas System occurred about 10.5 million years ago with a new peak in the Andean uplift and the subsequent onset of the transcontinental flow of the Amazon River System (Lundberg et al., 1998; Figuereido et al., 2010; Hoorn et al., 2010a, 2010b; Roddaz et al., 2010; Shephard et al., 2010). This Late Miocene stage in the evolution of the Neotropics in known as the Acre Phase and is characterized by the recess of the dysoxic lacustrine environments and the establishment of fluvio-tidal-dominated conditions (Hoorn et al., 2010a). The growing northern Andean mountains dissected proto-Amazonia into the Amazonian, Orinoco, and Magdalena basins (Hoorn et al., 2010a). The Acre Phase of the Amazonian basin is well represented in rocks of the Madre de Dios and Marañon basins (Peru), and particularly in the Acre region, eastern Brazil (Hoorn et al., 2010a). Late Miocene deposits in this latter area document abundant continental vertebrates, including a diversified fauna of mammals, turtles, and crocodylians (Cozzuol, 2006; Negri et al., 2010; Riff et al., 2010). In contrast, molluscan faunas are relatively poor in diversity and resemble present-day fluvial Amazonian faunas (Wesselingh et al., 2006b). Located in northernmost South America, Urumaco is another emblematic Late Miocene fossil-yielding Formation of the Neotropics (Sánchez-Villagra & Aguilera, 2006). The corresponding local fauna records abundant vertebrates living within the paleo-Orinoco basin, in close proximity to the Caribbean Sea. Giant crocodylians, such as *Purussaurus* and

Mourasuchus, are representative of this Late Miocene stage (Bocquentin-Villanueva et al., 1989; Aguilera et al., 2006; Aureliano et al., 2015). Southeastern to Iquitos (Peru), outcrops of the "uppermost Pebas Formation" in the Nauta area correspond to Late Miocene tidally-influenced deposits (Rebata et al., 2006).

Chapters of this thesis are devoted to describe the anatomy, phylogenetic relationships, and ecology of the mesoeucrocodylian fauna recovered from several new outstanding Middle and Late Miocene bonebeds in Peruvian Amazonia. As each new fauna represents different ecological or time assemblages, they may be crucial pieces for reconstructing regional environmental conditions during the peak and initial demise of the Pebas Mega-Wetland System. Particularly enlightening evidence comes from the Middle Miocene Iquitos bonebed assemblage, since it documents the hyperdiverse crocodylian community that evolved within dysoxic lacustrine environments (Chapter IV). With up to five new taxa, this highly endemic assemblage greatly expands our understanding on the phylogenetic and morphological diversity reached by caimanines and gavialoids in South America. However, probably the most substantial contribution of these new faunas is the possibility to explore the ecology, habitat, and feeding strategies in fossil crocodylians using distinct rostral and snout morphologies as proxies. In this matter, besides the known role of temperature and climate in the distribution of crocodyliforms (e.g., Carvalho et al., 2010; Martin et al., 2014), the correspondence between habitat and snout morphotypes has been only superficially studied despite the manifest adaptive value of the crocodylian rostral shapes (Brochu, 2001). Why rostral features deserve particular attention? It is well documented that, compared with the conservative post-cranial features, rostral shapes of crocodyliforms are highly plastic (e.g., Langston, 1976). Therefore, based on this simple statement, most characteristics that evolved in response to peculiar environmental conditions and feeding preferences might be concentrated in the rostrum (Chapter V). The crocodyliform history also

reveals that, underlying this morphological plasticity, only a limited number of rostral solutions exist for a given ecological problem (Brochu, 2001), emphasizing the putative match between rostral patterns, habitat preferences, and/or feeding strategy. I used phylogenetic relationships of crocodylians as a backbone for analyzing adaptive radiation, trends of the evolutionary ecology, and cases of parallel evolution in the rostral patterns within caimanines and gavialoids.

In the context of the Miocene Neotropical ecosystems, this study provides novel insights on the history of the Pebas Mega-Wetland System, the dominant biome occurring before the establishment of the transcontinental Amazonian drainage. This proto-Amazonian biome included a complex and dynamic mosaic of terrestrial and aquatic environments plethoric of mesoeucrodylians (Hoorn et al., 2010a). As at least members of the crocodylian clade are ectothermic and aquatic (Brochu, 2001; Hillenius & Ruben, 2004), they are responsive to climate changes and their distribution depends on the existence of aquatic pathways. Thus, here they are considered prime data to explore historical biogeography, paleogeography, and environmental changes in aquatic environments. Based on an integrative approach of current paleoenvironmental knowledge of the Miocene Pebas ecosystems and the ecological value of mesoeucrocodylian assemblages, I propose hypotheses on the diversification, community structure, prevalence, and extinction of certain clades (Chapter VI). My ultimate goal is to provide further evidence for recognizing key ecological stages and events in the evolution of the Amazonian biome.

CHAPTER II – MATERIAL

CHAPTER II – MATERIAL

A. Geological context

A.1 Pebas and "uppermost Pebas" Formations, Iquitos and Nueva Unión areas

In the Iquitos area, the Pebas Formation is comprised of transgressive and regressive bay-margin deposits. Parasequences are formed by fossiliferous blue to gray clays interbedded with unconsolidated sands, which are typically capped by lignite layers and mollusc shell beds (Hovikoski, 2001; Gingras et al., 2002; Roddaz et al., 2005). Lacustrine brackish-water, sometimes tidally influenced, megawet-land deposits are indicated by most of the studies in the lower and middle parts of the Pebas Formation. The time span of the Pebas Formation ranges approximately from the early Miocene (ca. 23 Ma) to the early Late Miocene (ca. 10.5 Ma; Hoorn et al., 2010a). The biostratigraphic framework of the Pebas Formation is based on pollen, ostracod, and particularly on the abundant and diverse molluscan faunas preserved throughout the unit (Hoorn, 1993; Muñoz-Torres et al., 2006; Wesselingh et al., 2006a). Fossiliferous deposits are located along the Amazon River banks and tributaries of the so-called Iquitos Arch, which correspond to the modern forebulge of the northwestern Amazonia foreland basin (Fig. II.1; Roddaz et al., 2005). Thirty-three localities yield vertebrate remains in the Iquitos area. Fossil vertebrates are found mainly in lignitic bonebeds (Salas-Gismondi et al., 2015a). These localities (IQ) are mapped within the Molluscan Zones (MZ) proposed by Wesselingh et al., (2006a) for the study area (Fig. II.1). These localities documented the highest diversity within a crocodylian community, including the shoveling mollusk-crushing caiman *Gnatusuchus pebasensis*, as well as *Kuttanacaiman iquitosensis*, *Caiman wannlangstoni*, *Purussaurus neivensis*, *Mourasuchus atopus*, *Paleosuchus* sp., and a new gavialoid taxon (Salas-Gismondi et al., 2015a; see Chapters IV & V). Other fossil vertebrate remains, such as fishes, aquatic turtles, and mammals, also are abundant.

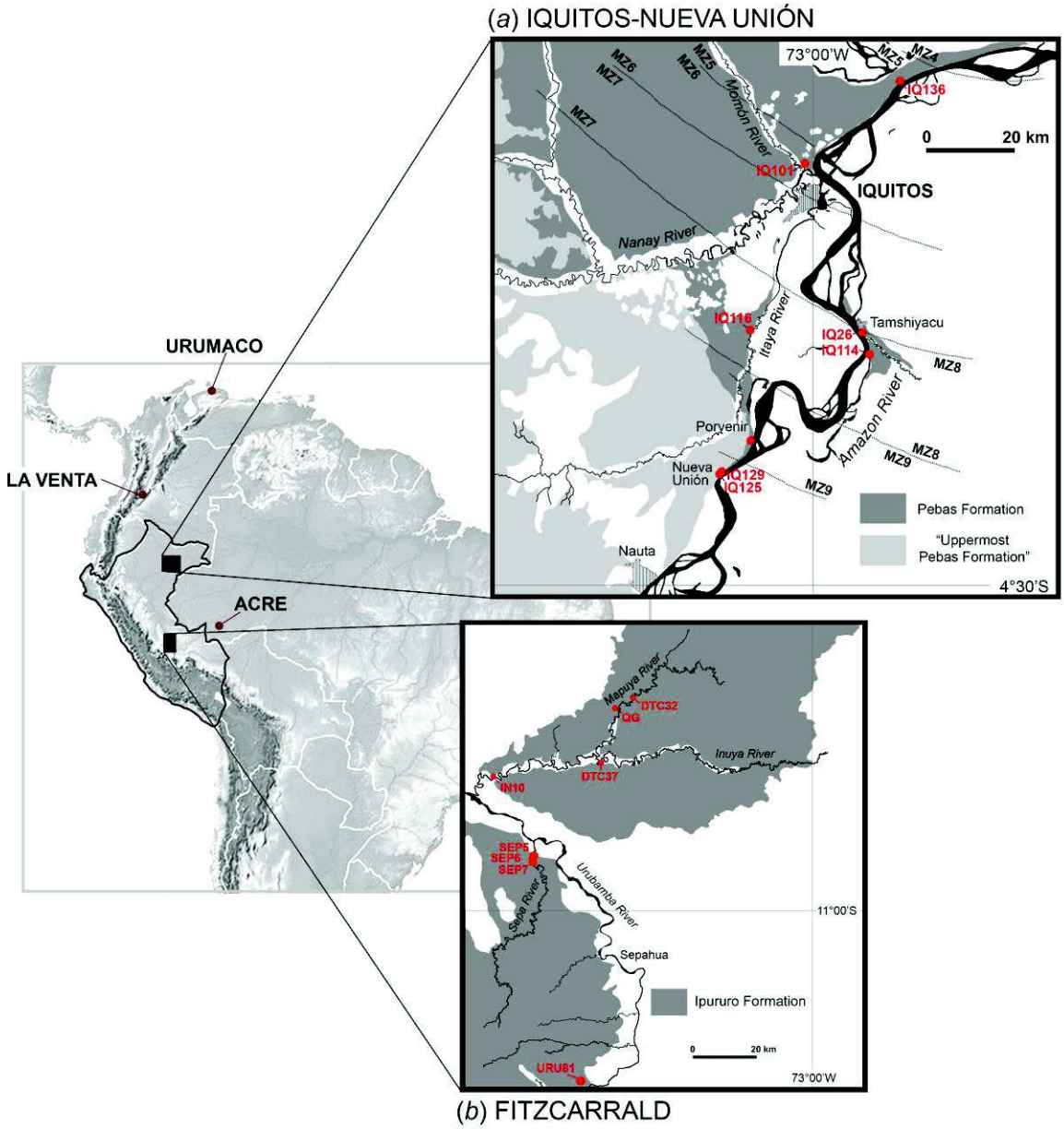

Figure II.1. Maps of the Iquitos-Nueva Unión and Fitzcarrald fossiliferous localities. (*a*) The Iquitos-Nueva Unión map shows the spatial distribution of the Mollucan Zones (MZ; after Wesselingh et al., 2006a) in the Pebas and "uppermost" Pebas Formations. Geological data after Rebata et al. (2006). (*b*) The Fitzcarrald map showing localities along the Mapuya, Inuya, Sepa, and Urubamba Rivers is after Tejada-Lara et al. (2015a). QG is Quebrada Grasa Locality.

Fossiliferous lignite layers are common in the Pebas Formation (Fig. II.2*b*, *c*). For several outcrops (Räsänen et al., 1998; Wesselingh et al., 2006a) the genesis of such layers is linked to lowstand/early transgression in recurring depositional sequences in the megalake system (Hoorn et al., 2010a). The duration of each such sequence was probably within an

orbital cycle scale (Wesselingh et al., 2006c), and no indication of massive reworking and time averaging has ever been found (extensive wear and ecological incompatible taxa – either vertebrates and invertebrates – are notably lacking in the lignites). Furthermore, the vertebrate fossils are often extremely well preserved and complete, and occasionally include various associated elements of the same individual, indicating lack of transport and in-situ deposition within the concerned bonebeds. We therefore consider the studied fossil assemblages from lignite beds IQ26, IQ114, and IQ116 to be autochthonous.

The rich late Middle Miocene Iquitos lignitic bonebed localities that correspond to MZ8 (Wesselingh et al., 2006a) are located in the Fernando Lores District (IQ26 and IQ114) and along the Itaya River (IQ116; Fig. II.1). These three bonebeds each have yielded remains of the new short-snouted, crushing-dentition caimanine crocodylian *Gnatusuchus pebasensis* (Fig. II.2*d*; Salas-Gismondi et al., 2015a). *Gnatusuchus* remains in IQ26 were found in the "upper lignite", laterally equivalent to the lignitic deposits of IQ114 a few kilometers farther south (MZ8). IQ26 and IQ114 share the same seven crocodylian taxa, although fossil evidence of a putative eighth taxon is recovered from the former locality (see crocodylian material by field locality in Chapter II.C1).

IQ26 provides a thick section (~10 m) of MZ7-MZ8 within the Pebas Formation. This sedimentary succession consists of coarsening-upwards parasequences capped by lignites. The bonebed corresponds to the last capping regressive lignite and ~20 m^2 was exposed in the outcrop. This makes this new lignite slightly younger than lignite from which amber faunas were reported. The upper lignite bonebed is referred to the MZ8, contrary to the amber-yielding "lower lignite," referred to MZ7 (Antoine et al., 2007). Underlying mud beds include ichnofossils and mollusc shells (Gingras et al., 2002). The IQ114 lignite bonebed is laterally equivalent to the IQ26 upper parasequence and is located in the same capping regressive lignite (Fig. II.2*e*). This lignitic bonebed covers a surface of ~200 m^2 at IQ114.

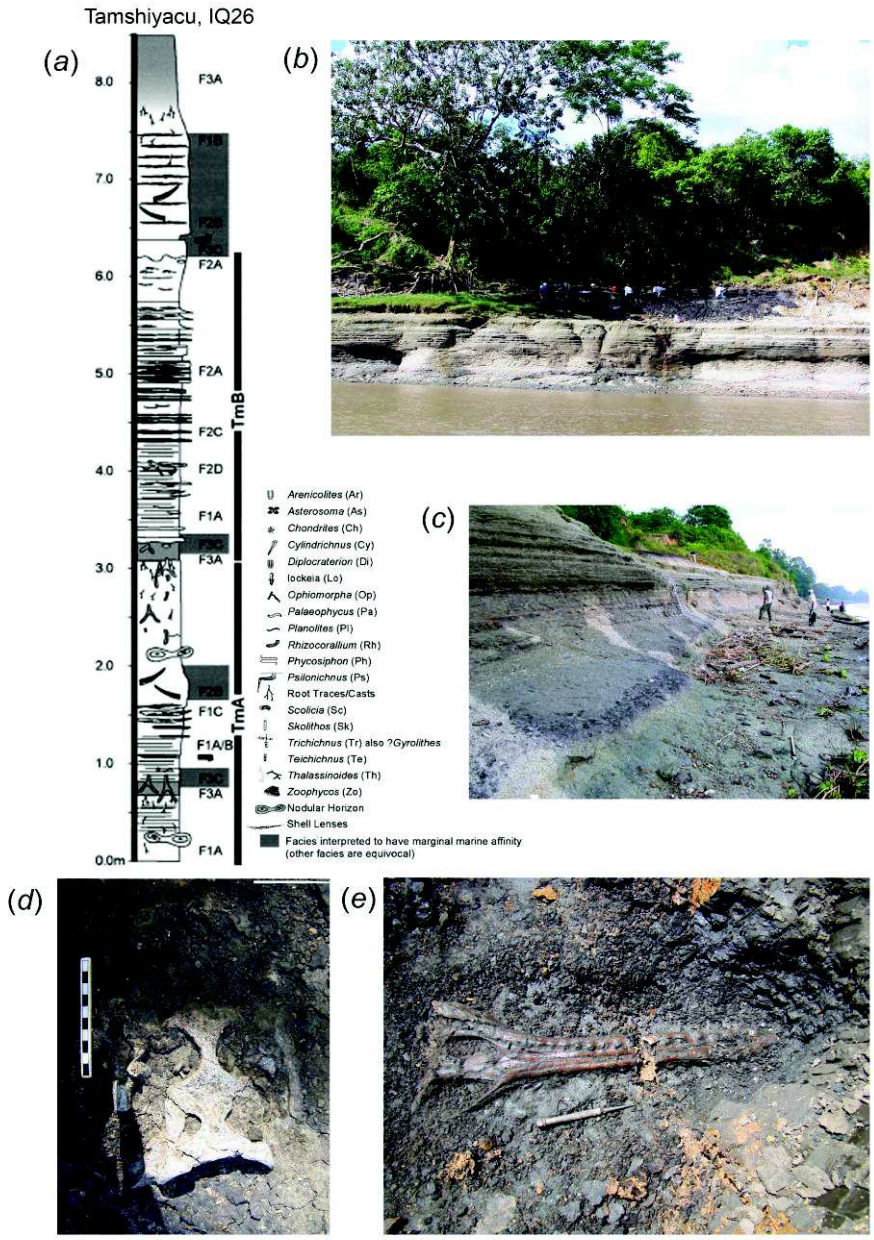

Figure II.2. The lignitic bonebed localities of the Pebas Formation at Iquitos area. (*a*) Stratigraphic section of IQ26 showing the coarsening-upwards successions, Parasequences A (TMA) and B (TMB). Ichnological evidence and stratigraphic section from Gingras et al. (2002). (*b*) General view of IQ26 locality with the paleontological team working at the MZ9 lignite bonebed level. Photograph by Pierre-Olivier Antoine. (*c*) Lower MZ8 levels in IQ26 with molluscs and amber. Photograph by Dario De Franceschi. (*d*) Skull of holotype of *Gnatusuchus pebasensis* at IQ114. (*e*) Skull of *Gryposuchus* nov. sp. at IQ114.

Outcrops at the Itaya River (IQ116) are restricted to a 1-2 meter thick capping lignite level overlying a gray mud with shell beds. They are possibly lateral equivalents of IQ26 and IQ114 sequences.

Southern to the Iquitos area, early Late Miocene localities at Nueva Union (IQ125 and IQ129) belong to MZ9 or even younger intervals (Figs. II.1 and II.3*a*; Rebata et al., 2006; Wesselingh et al., 2006a). They are referred here to the "Uppermost Pebas" Formation following Rebata et al. (2006). Outcrops consist of fine-grained fluvial sandstones, floodplain clays and silts, and paleosols (Fig. II.3*b*). These levels are lignite poor and they lack mollusc remains (Rebata et al., 2006).

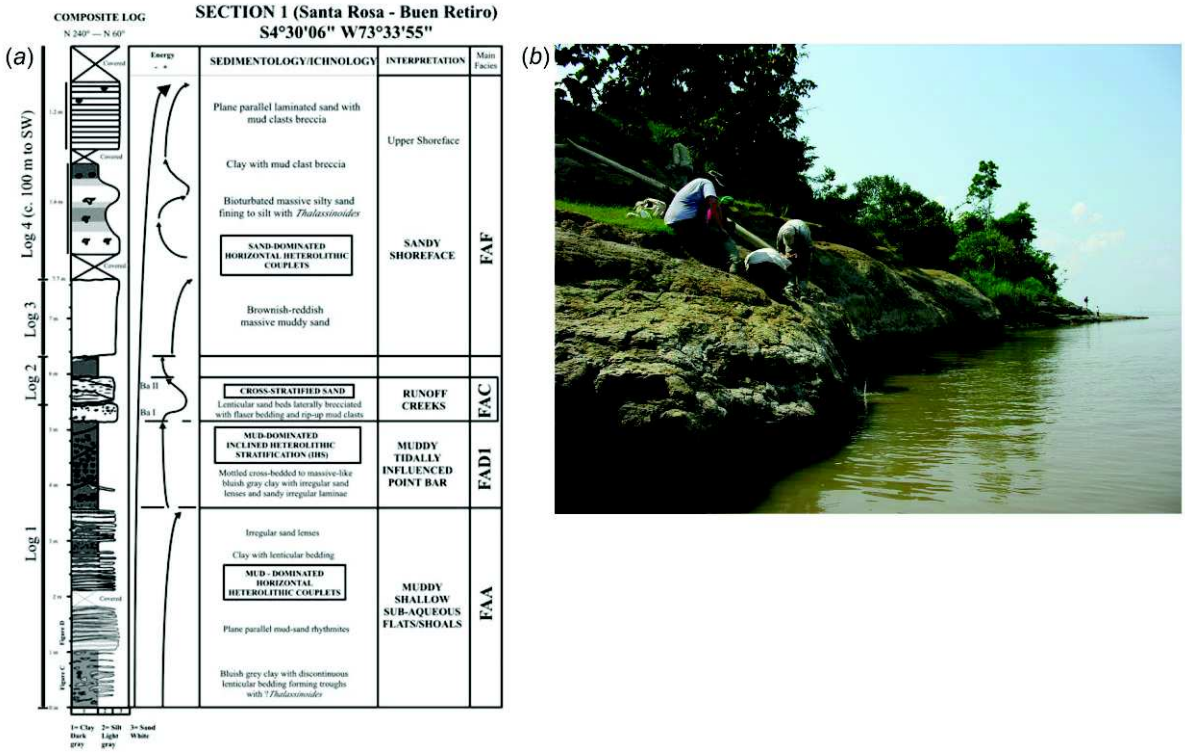

Figure II.3. Nueva Unión localities of the "uppermost Pebas" Formation. (*a*) Composite section at Santa Rosa-Boca Retiro (Nueva Unión) from Rebata et al. (2006). (*b*) Fossiliferous locality IQ125 at Nueva Unión. Photograph by Anjali Goswami.

Approximately 50 vertebrate taxa were recovered in-situ during our surveys of the Pebas and "uppermost Pebas" Formations, between 2002 and 2013. The faunal assemblages, ranging from one up to 30 vertebrate taxa at each locality, are widely dominated by chelonians and crocodyliforms, which are found in virtually every outcrop. Fishes (actinopterygians and chondrichthyans) also are common. On the other hand, mammalian remains are scarce, found in only 18 localities. Ophidians (snakes and lizards) occur in six localities, and birds (aquatic pelecaniform and gruiform) in two. Among chelonians,

pelomedusid (*Podocnemis* and *Stupendemys*) and chelid (aff. *Chelus*) pleurodirans are recorded, as well as testudinid cryptodiran (*Geochelone*).

Crocodyliforms at Iquitos are both extraordinarily diverse and remarkably complete and well-preserved, with the highest single locality crocodylian species diversity ever recorded in a fossil or living assemblage, and four of the seven taxa being represented by almost entire articulated skulls. The crocodyliform fauna is restricted to the crown-clade Crocodylia: no sebecosuchian was identified, in contrast to the taxa recovered in the coeval Fitzcarrald Local Fauna of southeastern Peru (Salas-Gismondi et al., 2007). Within this hyperdiverse crocodylian assemblage, a new gavialoid (Fig. II.2*e*) is the only longirostrine crocodylian recognized in the Iquitos area (four localities), whereas caimanines are represented by six taxa, such as the very large-bodied taxa *Purussaurus neivensis* (ten localities) and *Mourasuchus atopus* (three localities), as well as *Paleosuchus* sp. (two localities). These occurrences coincide with the first unambiguous fossil record of the latter genus, previously known only from extant forms (see also Chapter VI). The three new "crusher" caimans (with crushing-dentition, interpreted as durophagous), namely *Gnatusuchus pebasensis* (recovered from five localities), *Kuttanacaiman iquitosensis* (recovered from three localities), and *Caiman wannlangstoni* (recovered from two localities), were formally named in a recent work (Salas-Gismondi et al., 2015a) and further described in the present work (see main text).

A.2 Ipururo Formation, Fitzcarrald Arch

The Fitzcarrald Arch is a major geomorphic feature of the western Amazonian basin (Baby et al., 2005; Espurt et al., 2006). It is located in the eastern flank of the Peruvian Central Andes and projects into western Brazil, generating a radial drainage that separates northern and southern foreland basins (Espurt et al., 2007). Neogene outcrops depicting tidally-influenced marine environments like those of the Pebas Mega-Wetland System were

initially identified in the southern area of the Arch (Hovikoski et al., 2005, 2010). Our studies were focused in the northwestern region of the Fitzcarrald Arch, where brave explorers discovered amazing remains of fossil vertebrates in the mid twentieth century (Spillmann, 1949; Matthiessen, 1961; Willard, 1966). We identified fourteen Late Middle Miocene bonebed localities in the Inuya, Mapuya, Urubamba, and Sepa Rivers (Fig. II.4; Salas-Gismondi et al., 2006, 2007; Antoine et al., 2007; Tejada-Lara et al. 2015a). Fossiliferous strata are bonebeds assigned to the Ipururo Formation (Espurt et al., 2006; Tejada-Lara et al., 2015a) and interpreted as storm deposits in a fluvially influenced nearshore marine environment (Baby et al., 2005; Espurt et al., 2006, 2010). The fossil vertebrates were accumulated mainly in conglomerates of sand and mud with the bones incorporated in a sandy or muddy matrix (Espurt et al., 2006; Tejada-Lara et al., 2015a). Geomorphological, sedimentological, and paleontological data indicate that the fossiliferous deposits of the Ipururo Formation in this region are coeval with those of the Pebas Formation in the Iquitos area (MZ8 and MZ9 of Wesselingh et al., 2006c; Espurt et al., 2006, 2007; Tejada-Lara et al., 2015a). The Fitzcarrald fauna includes fishes, turtles, mesoeucrocodylians, and a diversified assemblage of mammals, including xenarthrans, litopterns, rodents, notoungulates, astrapotheres, and a putative carnivorous marsupial (Antoine et al., 2007; Pujos et al., 2013; Tejada-Lara et al., 2015a). The mammalian fauna has been assigned to the late Midde Miocene Laventan Age, based on the presence of mammals belonging to the '*Miocochiliu s* Assemblage' defined in La Venta, Colombia (Madden et al., 1997). The crocodyliform community from Fitzcarrald is consistent with these interpretations (Salas-Gismondi et al., 2007). In the section measured at Locality DTC32, paleomagnetic polarity results provide a potential numerical age around 13.20, 12.83 or 12.58 Ma, owing to Laventan biochronology (Madden et al., 1997) and Global Magnetic Polarity Time Scale (GMPTS). Pliocene

conglomerates and Pleistocene terraces unconformably overlay the rocks of the Miocene Ipururo Formation (Regard et al., 2009).

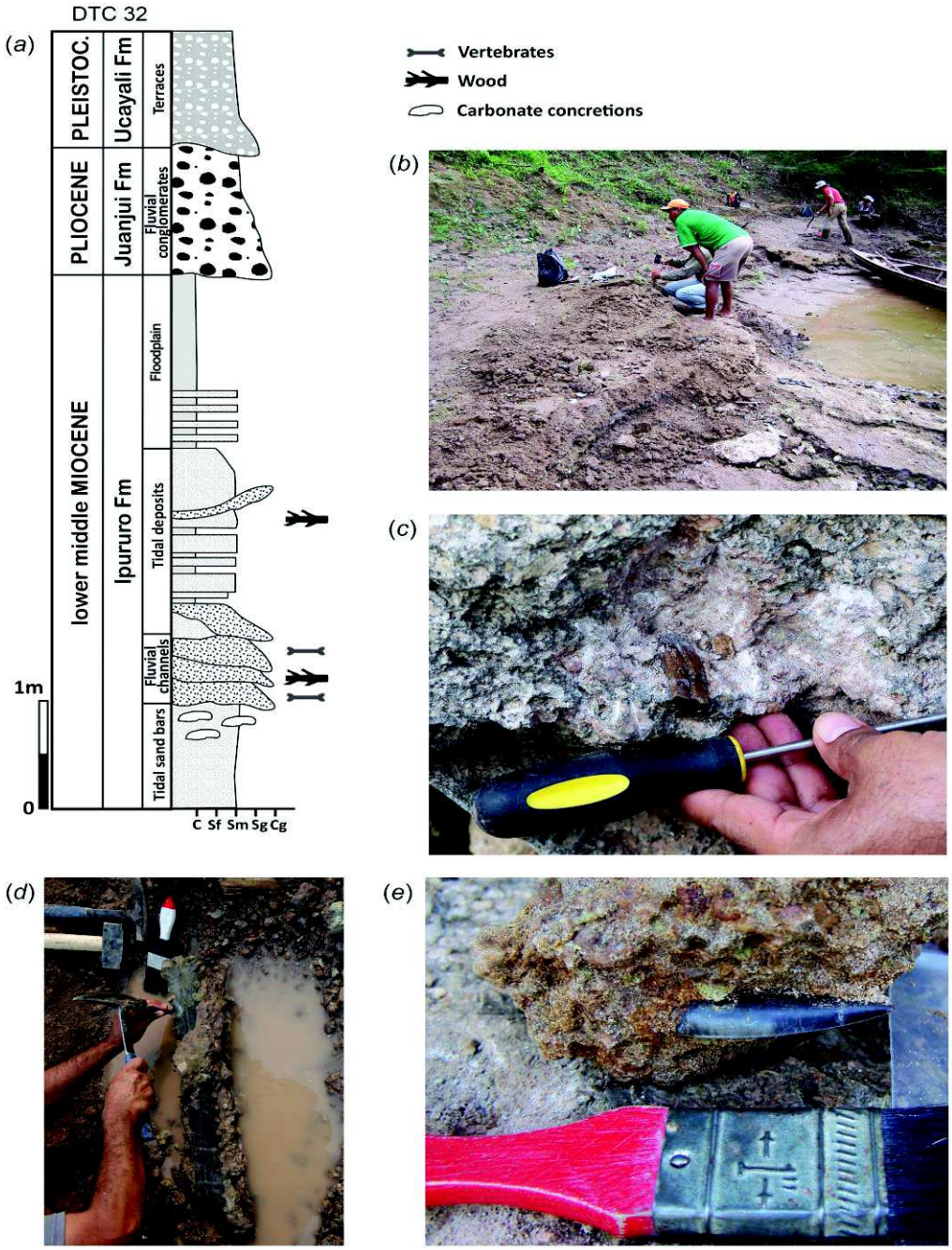

Figure II.4. Fitzcarrald localities of the Ipururo Formation. (*a*) Synthetic stratigraphic section for the Fitzcarrald Arch area from Tejada-Lara et al., 2015. (*b*) Bonebed locality DTC32 at the Mapuya River Photograph by Pierre-Olivier Antoine. (*c*) Notoungulate tooth at the conglomeratic levels of locality DTC20. Photograph by Pierre-Olivier Antoine. (*d*) *Gryposuchus colombianus* mandible at locality DTC20. Photograph by Patrice Baby. (*e*) Tooth of *Sebecus* at locality IN008. Photograph by RS-G.

B. Iquitos, Nueva Unión, and Fitzcarrald fossil material

Peruvian Institutional Abbreviations. MUSM, Vertebrate Paleontology Collection of the Natural History Museum of San Marcos University, Lima, Peru. MRU: Museo Regional de Ucayali, Pucallpa, Perú.

B.1 Mesoeucrocodylian material by field locality, Iquitos and Nueva Unión areas

Field Locality IQ136 (MZ5; Indiana, Iquitos area)

- *Gryposuchus* nov. sp: MUSM 1681, partial skull; MUSM 1682, juvenile partial mandible.

Field Locality IQ101 (MZ6; Momón River, Iquitos area)

- *Gryposuchus* nov. sp.: MUSM 987, right mandible.

Field Locality IQ26 (MZ8; Fernando Lores District, Iquitos area)

- *Gnatusuchus pebasensis*: MUSM 1722, right mandible lacking the retroarticular process; MUSM 1730, left mandible.

- *Kuttanacaiman iquitosensis*: MUSM 1490, skull and jaws (**holotype**); MUSM 1736, left mandible without splenial; MUSM 1937, portion of left dentary.

- *Caiman wannlangstoni*: MUSM 2377, partial skull (**holotype**); MUSM 926, partial left dentary and splenial; MUSM 1495, partial right dentary and splenial; MUSM 1906, left mandible; MUSM 1935, anterior portion of right dentary; MUSM 2381, juvenile maxilla.

- *Paleosuchus* sp.: MUSM 1724, right maxilla; MUSM 1985, right maxilla; MUSM 1934, partial left premaxilla; MUSM 2380, partial right premaxilla.

- *Mourasuchus atopus*: MUSM 1726, partial left maxilla; MUSM 1734, partial left maxilla; MUSM 1735, left jugal; MUSM 1762, partial left maxilla; MUSM 1933, left premaxilla; MUSM 2077, posterior left maxilla; MUSM 2378, skull table; MUSM 2379, jaw elements, humerus, cervical vertebra, scapula.

- *Purussaurus neivensis*: MUSM 1731, left premaxilla; MUSM 1733, skull table; MUSM 1392, right dentary; MUSM 2413, skull table.

- Caimaninae indet: MUSM 1728, skull table and articular region.

- *Gryposuchus* nov. sp.: MUSM 1428, right mandible; MUSM 1439, juvenile mandibular symphysis; MUSM 1440, posterior portion of right mandible; MUSM 1727, partial rostrum.

Field Locality IQ114 (MZ8; Fernando Lores District, Iquitos area)

- *Gnatusuchus pebasensis*: MUSM 990, skull (**holotype**); MUSM 925, anterior portion of right dentary with 1-5 alveoli; MUSM 1437, edentulous right premaxilla; MUSM 1465, edentulous premaxillae; MUSM 1737, left mandible; MUSM 1739, left splenial; MUSM 1761, anterior portion of right dentary with 1-6 alveoli; MUSM 1979, right mandible; MUSM 2040, left dentary and splenial with one globular tooth; MUSM 2051, right squamosal, exoccipital, and quadrate.

- *Kuttanacaiman iquitosensis*: MUSM 1942, associated left mandible, left maxilla, and skull table; MUSM 1928, juvenile partial skull table; MUSM 2394, juvenile partial skull table, MUSM 2078, partial left dentary.

- *Caiman wannlangstoni*: MUSM 928, right maxilla; MUSM 1983, associated maxilla, mandible with teeth, and partial skull table.

- *Paleosuchus* sp.: MUSM 1740, portion of right dentary; MUSM 1927, posterior portion of left maxilla; MUSM 1939, portion of left dentary; MUSM 1945, posterior portion of maxilla; MUSM 1989, partial right maxilla, jugal, and ectopterygoid.

- *Mourasuchus atopus*: MUSM 1966, right quadrate; MUSM 2074, right jugal.

- *Purussaurus neivensis*: MUSM 2075, tooth; MUSM 2076, tooth, MUSM 3189, tooth.

- *Gryposuchus* nov. sp.: MUSM 1981, skull without occipital and pterygoid region (**holotype**); MUSM 1428, right mandible; MUSM 1988, juvenile skull table; MUSM 2407, mandibular symphysis.

Field Locality IQ116 (MZ8; Itaya River, Iquitos area)

- *Gnatusuchus pebasensis*: MUSM 662, left jaw preserved from the anterior tip of the dentary to the posterior process of the angular.

- cf. *Kuttanacaiman iquitosensis*: MUSM 2080, frontal.

- *Purussaurus* sp: MUSM 916, tooth.

- *Gryposuchus* nov. sp.: MUSM 900, skull without snout; MUSM 2032, skull table and portion of the snout.

Field Locality IQ124 (MZ9; Porvenir, Iquitos area)

- *Gryposuchus* nov. sp.: MUSM 2471, portion of posterior right maxilla.

Field Locality IQ125 and IQ129 (MZ9 or younger intervals; Nueva Unión area)

- *Gnatusuchus pebasensis*: MUSM 2393, posterior portion of right mandible.

- *Purussaurus* sp.: MUSM 2426, ten associated teeth; MUSM 2262, giant tooth.

- *Mourasuchus* sp.: MUSM 2427, left jugal; MUSM 2428, osteoderm; MUSM 2429, distal femur.

- *Gryposuchus* cf. *colombianus*: MUSM 2430, left postorbital.

B.2 Mesoeucrocodylian material by field locality, Fitzcarrald Arch area

Field Locality IN008 (Inuya River, Fitzcarrald Arch, Ucayali Department)

- *Sebecus* cf. *huilensis*: MUSM 912, tooth; MUSM 2422, tooth.

Field Locality DTC20 (Mapuya River, Fitzcarrald Arch, Ucayali Department)

- *Purussaurus* sp.: MUSM1261, tooth (formerly referred to *Balanerodus logimus* by Salas-Gismondi et al., 2007)

- *Gryposuchus colombianus*: MUSM 650, symphyseal region of a mandible.

- *Paleosuchus* sp. MUSM 929, portion of right dentary.

Field Locality DTC32 (Mapuya River, Fitzcarrald Arch, Ucayali Department)

- *Sebecus* cf. *huilensis*: MUSM 2421, tooth.

- *Gryposuchus colombianus*: MUSM 906, juvenile partial symphysis.

- *Mourasuchus* sp.: MUSM 930, portion of right dentary including third and fourth alveoli; MUSM 931, partial left premaxilla

-*Paleosuchus* sp. MUSM 1673, portion of right dentary.

Field Locality DTC34 (Mapuya River, Fitzcarrald Arch, Ucayali Department)

- *Purussaurus* sp.: MUSM 1262, tooth (formerly referred to *Balanerodus logimus* by Salas-Gismondi et al., 2007)

Field Locality Quebrada Grasa (Mapuya River, Fitzcarrald Arch, Ucayali Department)

- *Sebecus* cf. *huilensis*: MUSM 1266, tooth.

- *Purussaurus* new species: MRU 17, virtually complete rostrum (MUSM 1982, cast)

- cf. *Eocaiman* sp.: MUSM 2082, anterior portion of right dentary.

- *Barinasuchus arveloi*: partial snout, specimen currently lost.

Field Locality SEP002 (Sepa River, Fitzcarrald Arch, Ucayali Department)

- *Purussaurus* sp.: MUSM 2631, tooth.

Field Locality SEP006 (Mapuya River, Fitzcarrald Arch, Ucayali Department)

- *Mourasuchus* sp.: MUSM 1672, associated postcranial elements, including vertebrae, ribs, ilium, and multiple osteoderms.

CHAPTER III – METHODS

CHAPTER III – METHODS

A. Phylogenetic Analyses

A.1 Phylogenetic background

In this study, I follow definitions established by Sereno et al. (2001), Brochu (2003) and Brochu et al. (2009) for Mesoeucrocodylia and Crocodylia clades (Fig. III.1). Therefore, Mesoeucrocodylia (*sensu* Sereno et al., 2001) includes Crocodylia and the paraphyletic mesosuchians and is defined as "the most inclusive clade containing *Crocodylus niloticus* (Laurenti, 1768) but not *Protosuchus richardsoni* (Brown, 1933)". Crocodylia is restricted to the crown group and is defined as "the last common ancestor of *Gavialis gangeticus*, *Alligator mississippiensis*, and *Crocodylus niloticus* and all its descendants" (Clark, 1986; Brochu, 2003). Other ingroup definitions can be found in Brochu (2003).

Several authors have attempted phylogenetic relationships of the non-eusuchian Mesouecrocodylian clades, with special emphasis on the Thalattosuchia (e.g., Clark, 1994; Jouve, 2009; Pol & Gasparini, 2009; Young et al., 2010; Wilberg, 2015), dyrosaurids (e.g., Jouve et al., 2008; Hastings et al., 2010, 2011, 2014), advanced notosuchians (e.g., Pol et al., 2014), and Sebecidae (Pol & Powell, 2011; Pol et al., 2012). Among them, exclusively the sebecids survived until the Neogene. Late Middle Miocene representatives of this clade are *Barinasuchus* (Peru and Venezuela; Buffetaut & Hoffstetter, 1977; Paolillo & Linares, 2007) and *Sebecus huilensis* (Colombia and probably Peru; Langston, 1965; Salas-Gismondi et al., 2007). As no living crocodylian, these animals are representatives of the oreinirostral morphotype of Busbey (1995), characterized by a deep, laterally compressed rostrum (Fig. III.2*c*). Similar cranial trophic structures in sebecids and large theropod dinosaurs agree with hypotheses that sebecids were fully land-dwelling predators (Molnar, 2012).

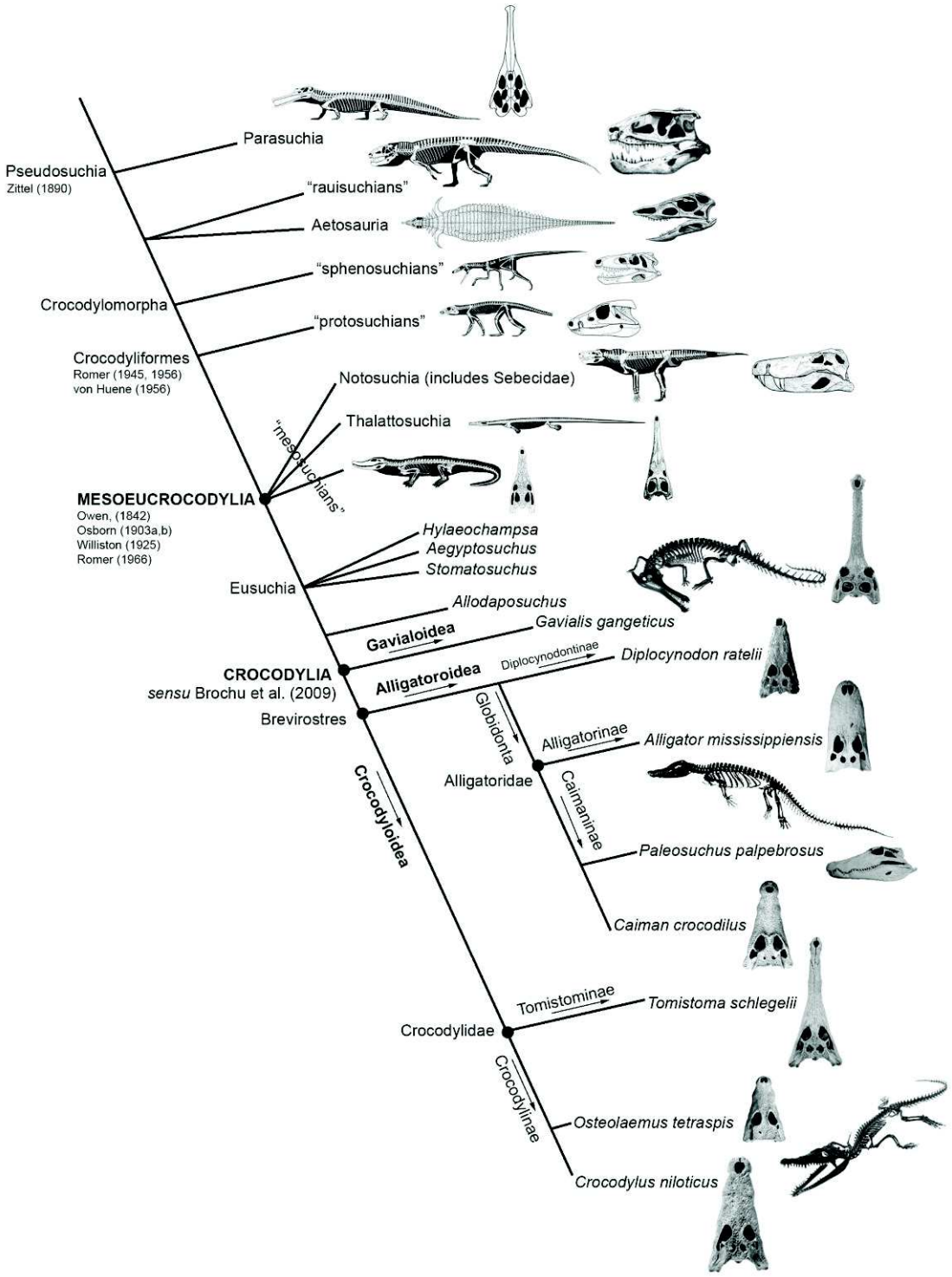

Figure III.1. Synthetic phylogenetic relationships and nomenclature of the Mesoeucrocodylia clade and their relatives within the pseudosuchians. Skulls in lateral and dorsal views denote the oreinirostral or platyrostral clade/taxa morphotype, respectively (*sensu* Busbey, 1995). Modified from Brochu (2001) and Brochu et al. (2009).

Following Pol & Powell (2011), *Sebecus huilensis* is an advanced sebecid lying in a polytomy with *S. icaeorhinus*, *S. querejazus*, and the Lumbrera form, supporting the allocation of the Colombian species from La Venta to the long-range genus *Sebecus* (Fig. III.3). On the other hand, *Lorosuchus*, from the Paleocene of Argentina, and *Barinasuchus* are regarded as the most basal and second most basal sebecids, respectively (Pol & Powell, 2011). Here we use this phylogenetic hypothesis. The phylogenetic position of the Sebecidae within mesoeucrocodylians is not clear due to the lack of comprehensive anatomical descriptions on them, and on Cretaceous peirosaurids and baurusuchids (Pol & Powell, 2011).

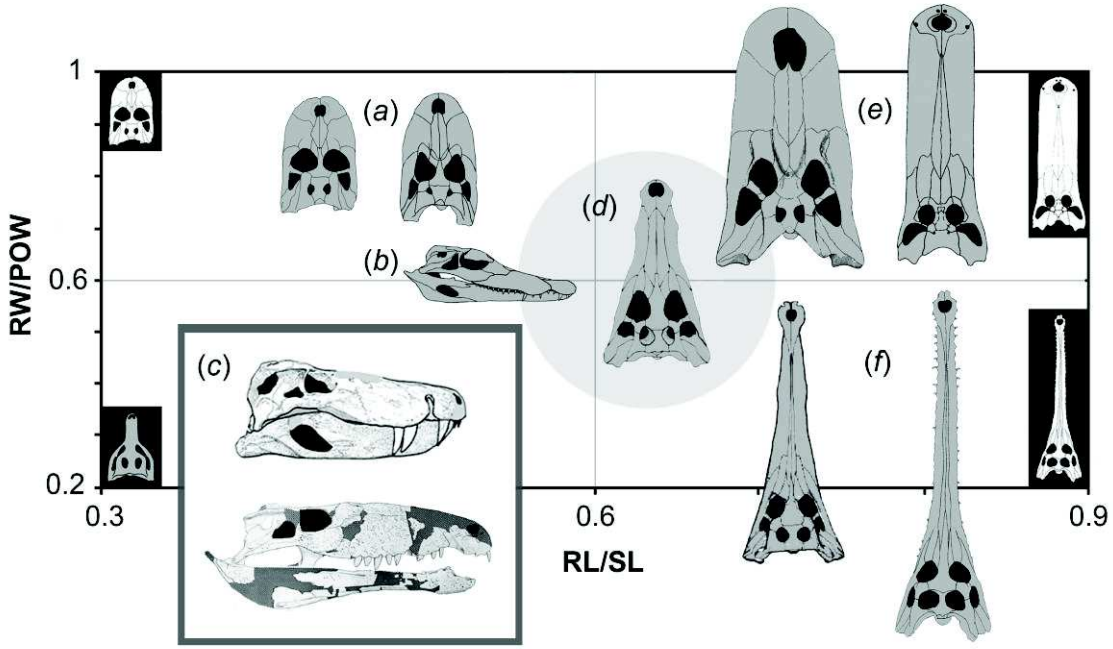

Figure III.2. Snout morphotypes. Main snout morphotypes are indicated in a bivariate plot of relative snout width and length modified from Busbey (1995) and Salas-Gismondi et al. (2015a). Quadrants correspond to the four potential combinations of the bidimensional snout-shaped morphotypes. Within this plot, no crocodylian occupies the lower left quadrant that represents the short and narrow snout-shaped morphotype. This last morphology is closer to that observed in protosuchians and some notosuchians having deep snouts and putative terrestrial habitus. (*a*) blunt-snouted morphotype, e.g. *Gnatusuchus*, *Kuttanacaiman*; (*b*) Generalized, moderately short and deep, e.g. *Paleosuchus*; (*c*) oreinirostral morphotype, e.g. *Baurusuchus*, *Sebecus*; (*d*) generalized morphotype, indicated by the position of the gray circle, e.g. *Borealosuchus*; (*e*) duck-faced morphotype, e.g. *Mourasuchus*, *Purussaurus*; (*f*) longirostrine morphotype, e.g. *Piscogavialis, Mecistops*. Abbreviations: RW/POW, rostral width – postorbital width index; RL/SL, rostral length – skull length index.

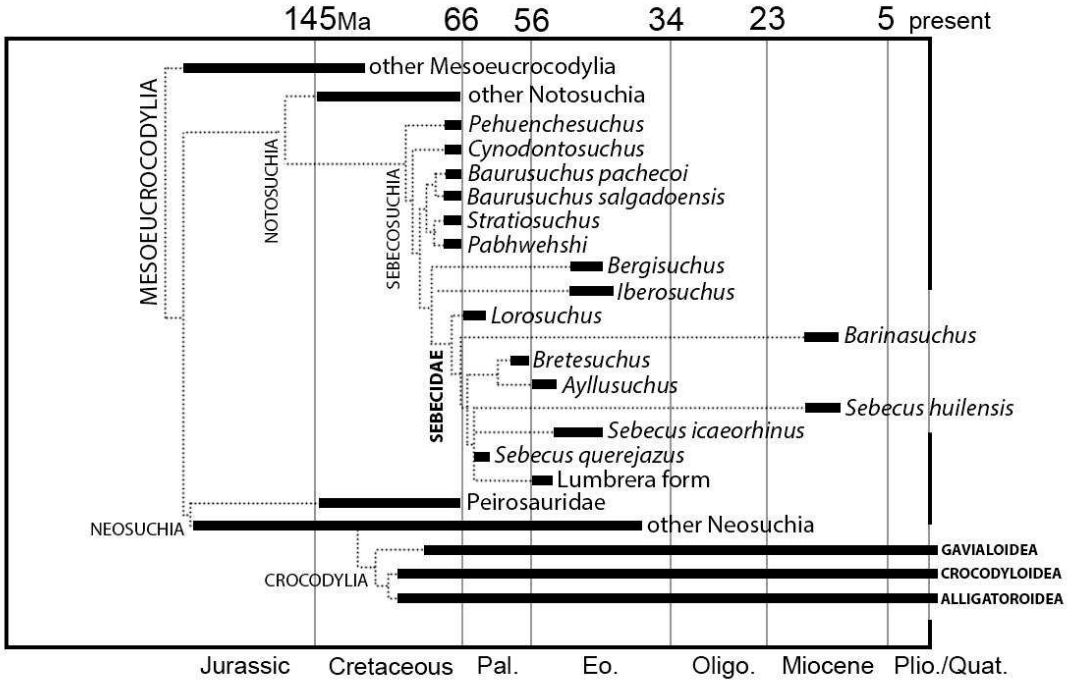

Figure III.3. Time-calibrated phylogenetic relationships of the sebecosuchian mesoeucrocodylians. Based on Pol & Powell, 2011.

The crown group Crocodylia includes Gavialoidea, *Borealosuchus*, planocranids, and Brevirostres, the later clade encompassing Crocodyloidea and Alligatoroidea (Fig. III.4; Brochu, 2003, 2013). These groups were already differentiated before the end of the Mesozoic Era. Earliest gavialoids and alligatoroids are recorded from the early Late Cretaceous of North America and Europe (Campanian), whereas crocodyloids occurred no before the latest Cretaceous (Maastrichtian; see Brochu, 2003). All gavialoids —from Cretaceous "thoracosaurs" to the sole extant species *Gavialis gangeticus* (the Indian gharial)— present specialized long, tubular, and slender snout, namely the longirostrine morphotype (Fig. III.2*f*; see Brochu, 2004a, Jouve et al., 2008). This morphotype has been developed independently in gavialoids, tomistomines, thalattosuchians, dyrosaurids, and pholidosaurids (e.g., Clark, 1994; Jouve et al., 2006; Hastings et a., 2014), obscuring their phylogenetic affinities (see below). Gavialoids experimented a large adaptive radiation in

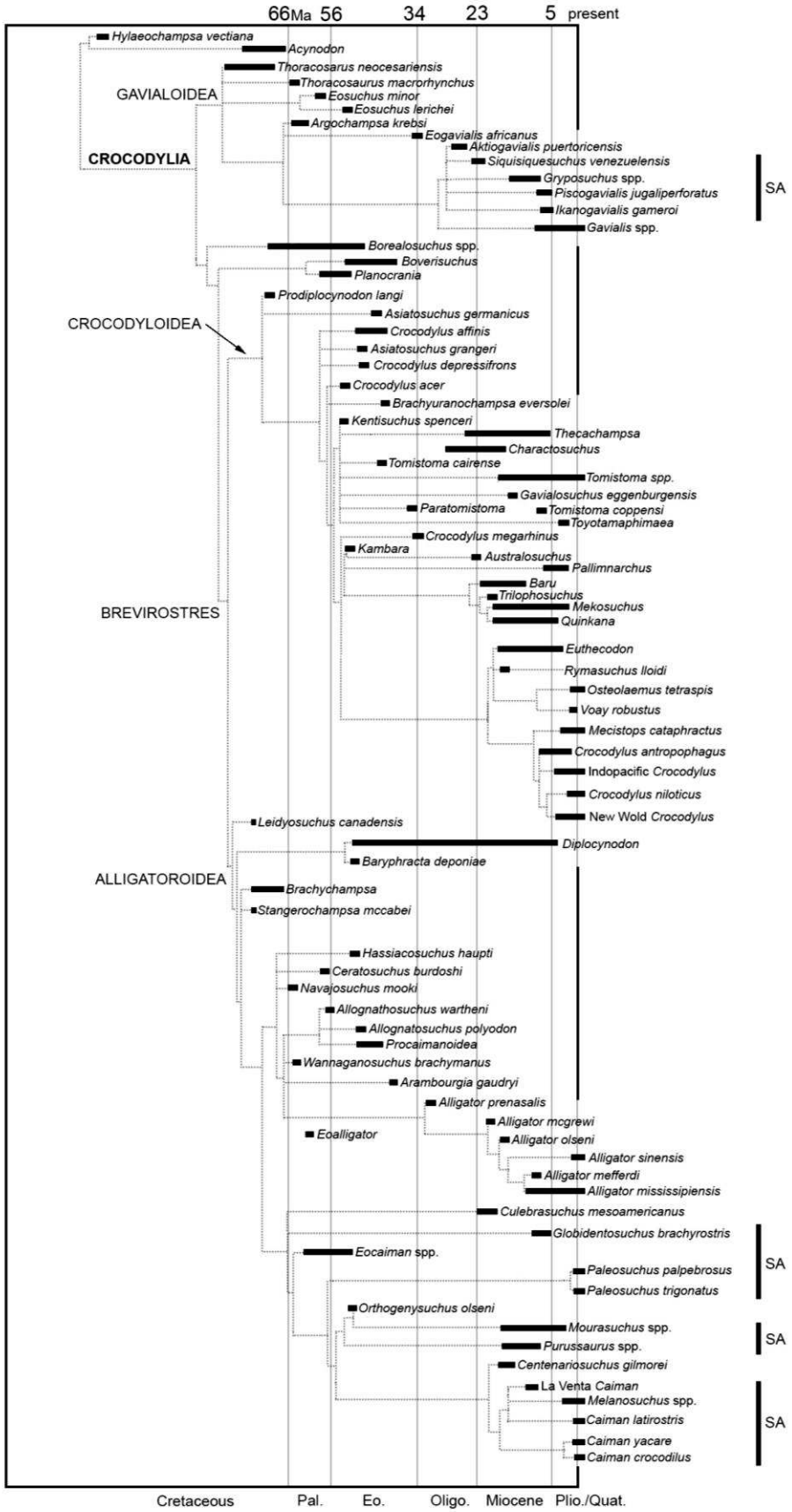

Figure III.4. Time-calibrated phylogenetic relationships of the Crocodylia. Based on Brochu (2003) and updated with recent crocodylian phylogenetic researches using morphological data. SA indicates crocodylian species with record in South America.

coastal marine Tethyan environments and particularly during the early Neogene of South America (e.g., Buffetaut, 1982; Brochu & Rincón, 2004; Jouve et al., 2008). Within the same long-snouted morphotype, South American gavialoids bear distinctive rostral and orbital patterns (Sill, 1970; Buffetaut, 1982; Kraus, 1998), including some advanced species probably related to the Indian gharial *Gavialis* (Langston, 1965; Langston & Gasparini, 1997; Jouve et al., 2008; Riff & Aguilera, 2008). Although ancestral rostral shape of gavialoids remains unknow, we can speculate that it might resemble the generalized snout morphotype of *Borealosuchus*, the most basal non-gavialoid crocodylian (Fig. III.4). The generalized snout morphotype, as that of *Borealosuchus*, is dorsoventrally compressed, medium in length, and tapering gradually toward the naris (Fig. III.2*d*; Busbey, 1995; Brochu, 2001). This snout morphotype is also observed at the base of the Alligatoroidea and the Crocodyloidea, in the taxa *Leidyosuchus* and *Diplocynodon*, respectively (Fig. III.4). Thus, the generalized morphotype might represent the ancestral condition for Brevirostres as well (Brochu, 2003). The clade Globidonta evolved in the early Late Cretaceous of North America, immediately after the appearance of the basalmost alligatoroids. This group includes extant alligatorines and caimanines, and ancestrally they possessed a relatively short and broad snout, typically representing the blunt-snouted morphotype (Figs. III.2*a* and III.4; Brochu, 2004b). This morphotype is usually associated with having globular dentition and a durophagous diet (Abel, 1928; Carpenter & Lindsey, 1980). Although Globidonta has robust character support (Brochu, 1999), ingroup relationships (i.e., between caimanines, alligatorines and Cretaceous globidontans) are not fully resolved, in part by the poor fossil evidence of Paleogene caimans (Simpson, 1933; Rusconi, 1937; Bona, 2007; Brochu, 2010; 2011; Pinheiro et al., 2013). No alligatorine has been identified in South America even though species with caimanine-like morphology existed in the Eocene of North America (Westgate, 1989; Brochu, 1999, 2010) and the early Miocene of Panama (Hastings et al., 2013). The crown group caimanine

includes the jacareans (*Centenariosuchus* + *Caiman* + *Melanosuchus*), *Paleosuchus*, *Purussaurus*, and *Mourasuchus* (Fig. III.4; Brochu, 1999; Aguilera et al., 2006; Hastings et al., 2013). Phylogenetic analyses indicate that *Purussaurus* and *Mourasuchus* are sister groups, both characterized by their parallel-sided rostrums and wide and long snout, namely duck-faced morphotype (Brochu, 2001; Fig. III.2*e*). The peculiar morphotype of these caimanines emerged in South American fossil record during the Middle Miocene and disappeared by the end of the same epoch (Price, 1964; Langston, 1965; Bocquentin-Villanueva et al., 1989). Most extant caimans have generalized rostrums and few retain blunt snouts (e.g., *Caiman latirostris*). The smooth-fronted caiman *Paleosuchus* has been considered as blunt-snouted but its snout morphology is relatively longer and higher, thus displaying features of generalized and the oreinirostral morphotypes, respectively (Fig. III.2*b*; Busbey, 1995; Brochu, 2001). Extant crocodylian species with a generalized morphotype are generalist carnivorous animals in terms of diet.

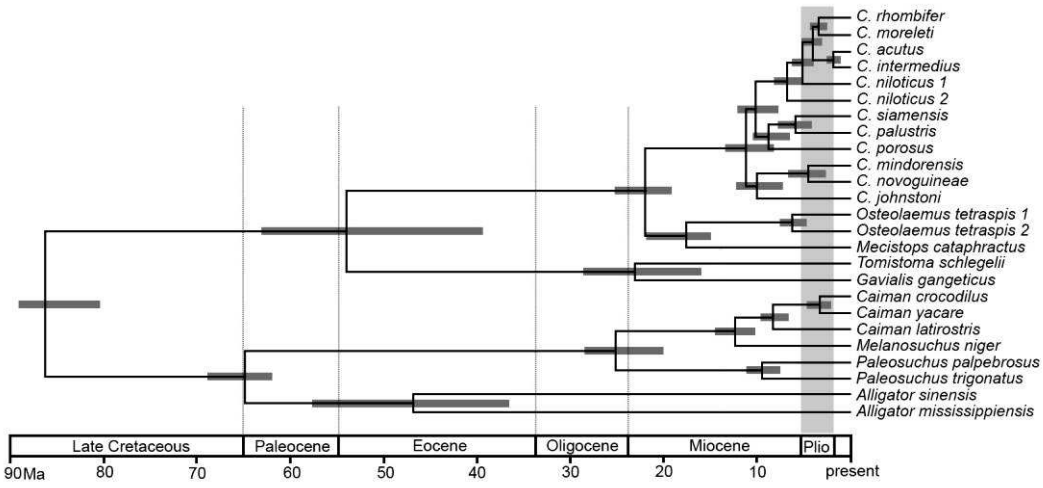

Figure III.5. Phylogenetic relationships of extant crocodylians based on molecular data. Mean node ages of divergence are indicated with gray horizontal bars. Vertical bar (light gray) marks the Pliocene interval, when major diversification of New World *Crocodylus* occurred. From Oaks, 2011.

In the past four decades, molecular data has provided remarkable discoveries regarding phylogenetic relationships and divergence time of crocodylians (Fig. III.5; Densmore, 1983; Gatesy & Amato, 1992; Dessauer et al., 2002; Gatesy et al., 2004; Oaks,

2011; Meredith et al., 2011). In general, these attempts confirmed analyses based on morphological datasets from fossil and modern species, such as the closer affinities between *Caiman-Paleosuchus* and *Alligator* than these species with *Crocodylus* (Leclercq et al., 1981; Perutz et al., 1981) and the divergence *Crocodylus-Alligator* time dating back to the Cretaceous (Fig. III.5; Hass et al., 1992; Roos et al., 2007). Comprehensive molecular analyses have elucidated long-lasting unresolved issues on the evolutionary radiation of *Crocodylus* and *Osteolaemus*, providing evidence on the more recent diversification and higher taxonomic diversity than that established based on morphology (Fig. III.5; McAliley et al., 2006; Eaton et al., 2009; Oaks, 2011). In absolute congruence with paleontological evidence, a mitochondrial DNA-based research indicates that the New World *Crocodylus* might have migrated from Africa during the Pliocene (Meredith et al., 2011).

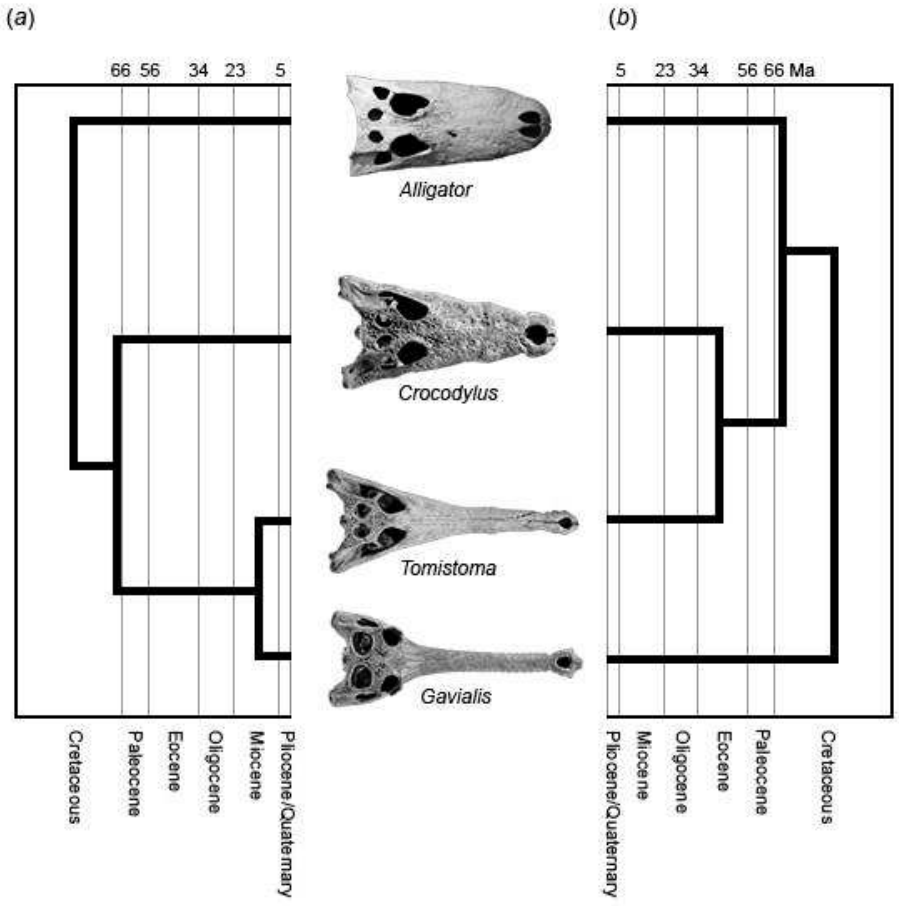

Figure III.6. Molecules vs. Morphology. Relationships and divergence timing of crocodylians based on molecules (*a*) and morphology (*b*). From Brochu, 2003.

However, an important controversy between molecular and morphological datasets has captured the attention of most systematic studies: whereas morphology traditionally placed *Gavialis* outside the remaining living crocodylians (Fig. III.6*a*; Kälin, 1931, 1955; Tarsitano et al., 1989; Norell, 1989; Brochu, 1997; 2003, 2004; Hua & Jouve, 2004; Jouve et al, 2008), molecules consistently support sister-taxon affinities between *Gavialis* and the Indonesian false gharial *Tomistoma* (Fig. III.6*b*; Densmore, 1983; Densmore & Dessauer, 1984; Densmore & Owen, 1989; Densmore & White, 1991; Hass et al., 1992; Aggarwal et al., 1994; Poe, 1996; Gatesy et al., 2003; Dessauer et al., 2002; Harshman et al., 2003; MacAliley et al., 2006; Willis, 2007; Gatesy & Amato, 2008; Oaks, 2011). Although fossil gavialoids are known from Cretaceous rocks of North America, Europe, and Africa (Brochu, 2004a; Jouve et al., 2008), these analyses usually proposed an Eocene or even Miocene divergence time between the Indian and Indonesian species (Densmore & Dessauer, 1984; Hass et al., 1992; Gatesy et al., 2003, Oaks, 2011). Combined analyses of both molecular and morphological-paleontological data support molecular hypotheses (Poe, 1996). However, when excluding fossils from the combined datasets, morphological hypothesis is favored (Brochu, 1997). To date, there is no consensus in this matter, but "new fossils await discovery, and new genes await sequencing" (Brochu, 2003).

A.2 Phylogentic analyses in this study

To determine the phylogenetic relationships of the fossil crocodylian material described here we included them in a data matrix of morphological characters mostly based on C. A. Brochu's and S. Jouve's publications on Alligatoroidea (Brochu, 1999, 2011) and Gavialoidea (Jouve et al., 2008) systematics, respectively. A small number of characters are derived from other analyses (Benton & Clark, 1988; Norell, 1988, 1989; Norell & Clark, 1990; Buscalioni et al., 1992, 2001; Willis, 1993; Clark, 1994; Wu et al., 2001; Brochu, 2004a; Hua & Jouve, 2004; Jouve, 2004; Salisbury et al., 2006; Ösi et al., 2007). For each

analysis, the corresponding data matrix was evaluated with a maximum parsimony analysis using TNT 1.1 (Goloboff et al., 2008). All characters were unordered, non-additive, and had equal weight. To assess nodal support, branches with a minimum length of 0 were collapsed and Bremer support values (decay indices) were calculated and shown on the strict consensus phylogeny. After revising character formulation of Salas-Gismondi et al. (2015a), some character states (i.e., 49, 137, 185, 198, 201, 206) have been modified following Brazeau (2011).

Although most previous publications consistently show a close relationship between *Mourasuchus* species and *Orthogenysuchus olseni* (Brochu, 1999, 2011; Scheyer et al., 2013), the latter taxon was omitted in the current analysis because ongoing detailed preparation and study of the type specimen revealed different scores for key features than in previous analyses. In this study, specimen UCMP 39978 from the late Middle Miocene of La Venta, Colombia, originally identified as *Caiman* cf. *lutescens* (Langston, 1965), is referred to as "La Venta *Caiman*".

Although Brochu (2011) stated that in *Necrosuchus ionensis* the ventral process of the exoccipital was long and slender, this bone barely exceeds the ventral level of the occipital condyle and does not reach the tubera. Conservatively, we thus coded it as unknown for this taxon in present analyses. The angular-surangular suture passing along the ventral margin of the mandibular fenestra is present in *Gnatusuchus* but the suture reaches the fenestra higher, close to the posterior angle, in *Globidentosuchus* and *Kuttanacaiman*. The latter condition also pertains to *Eocaiman cavernensis* and scoring of this taxon (based on the holotype) was changed to fit this new interpretation.

Character 51 of our study differs from that of Brochu (2004b) by the omission of state 1 (i.e., largest dentary alveolus immediately caudal to four is 13 or 14 and the series behind it) in the former. This state regards those taxa among blunt-snouted globidontans with enlarged

rear alveoli linked by the presence of globular dentition, such as *Brachychampsa* and *Allognathosuchus*. The concept of this state has been incorporated into character 198, a new character concerning the mandibular dental morphology posterior to the twelfth or thirteenth alveoli. In "generalized" and long-snouted crocodylians, teeth in these positions are pointed, slightly blunt, or blunt. This is also true for most caimans including *Melanosuchus*, which presents blunt posterior teeth.

However, new discoveries show that some basal caimanines developed posterior globular dentitions as well. Thus, here we discriminate globular from blunt teeth. Globular teeth bear bulbous or globular crowns, with the crown wider than the root. Generally, these teeth are flattened and closely packed to form a crushing unit. In caimanines with globular teeth, the crushing tooth unit within the dentary is composed of at least four posterior subequal sized teeth, whereas other globidontans have globular teeth notably different in sizes within the crushing unit. Some stem eusuchians bear posterior multicusped teeth. Although *Gnatusuchus* bears globular teeth, loci posterior to fourteenth are lost.

In earlier analyses the relative length of the anterior process of the frontal and the contact/separation of the prefrontals were treated as different characters (Brochu, 1999; Jouve et al., 2008). Considering that the morphology of the former determines the condition of the latter, or vice versa, here they are regarded as components of character 129, a combination of character 175 of Jouve et al. (2008) and character 100 of Brochu (1999). Characters 200 and 206 are proposed to record features present in selected advanced gavialoids. These characters deal with variation of circumorbital proportions and shape, temporal fenestrae, and premaxilla.

Character 199 of Jouve et al. (2008) expresses the variation in the shape of the supratemporal fenestrae. Additionally to its shape, I observed that the thickness of its posterior bar varies among gavialoids taxa with wide supratemporal fenestrae. For example,

in *Eothoracosaurus mississippiensis* and *Eogavialis africanum* this bar is thick, whereas in South American gavialoids and *Gavialis gangeticus* the bar is thin. To recognize this latter distinct feature, in these analyses character 191 is based on character 199 of Jouve et al. (2008).

Finally, I propose a new character (character 199) to document the relative size between anterior and posterior dentary alveoli. In most crocodylians, the first and fourth dentary alveoli are larger than the second and the third ones, and neither of them is ever the largest when compared to other mandibular teeth. However, in *Purussaurus* and *Mourasuchus* species, the anterior mandibular dentition has enlarged to a point that the four anterior-most dentary alveoli are larger than any other of the series.

B. Body length assessment

Length estimates are based on (a) Sereno et al. (2001) and Hurlburt et al. (2003). For (a): *Crocodylus moreletii* formula: TL=(10.48)(SL)-6.20. For (b) *Alligator mississippiensis* formula: Log TL=(LogSL)(0.970)+0.954. Results are shown in Table IV.1.

C. Morphometric analysis and phylogenetic mapping

Landmark-based geometric morphometrics is a powerful tool to quantifying shape variation in biological entities (Webster & Sheets, 2010; Polly et al., 2013). Recently, researchers have applied this approach to analyze patterns of skull shape in crocodylians (Pierce et al, 2008, 2009; Pearcy & Wijtten, 2011; Weaver, 2012; Wilberg, 2012; Watanabe & Slice, 2014). Considering that crocodylians have a relatively flat skull construction, these are suitable biological material for studying their dorsal surface morphology with two-dimensional (2D) landmark-based analyses (Watanabe, 2014). Additionally, crocodylians present complex cranial bone sutures visible thoughout their ontogeny. Cranial bone

configuration and sutures are a major topic when studying crocodylian phylogenetic relationships (see Brochu, 1999). On the other hand, evolutionary ecology of crocodylian clades is usually associated with rostral bone rearrangement and snout morphotypes (2001), both features particularly appropriate to be investigated with a phylogeny mapped into morphospaces. By mapping cladograms into morphospaces, evolutionary morphologists can visualize phenetic similarities associated with ecology, reconstruct ancestral morphologies, and test historical transformation hypotheses (Stone, 2003; Friedman, 2011). In Chapter V, we performed a 2D landmark-based geometric morphometric analysis and mapped our phylogenetic hypothesis into this morphospace, in order to the analyze shape variation of a distinct, specific region within crocodylian skull. Detailed procedures of this analysis are described in Chapter V.B.2.

CHAPTER IV – CROCODYLIAN COMMUNITY FROM THE LAKES AND SWAMPS OF THE PEBAS SYSTEM, IQUITOS AREA (CAIMANINAE)

CHAPTER IV – CROCODYLIAN COMMUNITY FROM THE LAKES AND SWAMPS OF THE PEBAS SYSTEM, IQUITOS AREA (CAIMANINAE)

A MIOCENE HYPERDIVERSE CROCODYLIAN COMMUNITY REVEALS PECULIAR TROPHIC DYNAMICS IN PROTO-AMAZONIAN MEGA-WETLANDS

This section corresponds to the extended version of the following article:

Salas-Gismondi, R., Flynn, J., Baby. P., Tejada-Lara J. V., Wesselingh, F., Antoine P-O. 2015 A Miocene hyperdiverse crocodylian community reveals peculiar trophic dynamics in proto-Amazonian mega-wetlands. Proc. R. Soc. B 282: 20142490.

DOI: 10.1098/rspb.2014.2490

Abstract

Amazonia contains one of the world's richest biotas, but origins of this diversity remain obscure. Onset of the Amazon River drainage at approximately 10.5 Ma represented a major shift in Neotropical ecosystems, and proto-Amazonian biotas just prior to this pivotal episode are integral to understanding origins of Amazonian biodiversity, yet vertebrate fossil evidence is extraordinarily rare. Two new species-rich bonebeds from late Middle Miocene proto-Amazonian deposits of northeastern Peru document the same hyperdiverse assemblage of seven co-occurring crocodylian species. Besides the large-bodied *Purussaurus* and *Mourasuchus*, all other crocodylians are new taxa, including a stem caiman—*Gnatusuchus pebasensis*—bearing a massive shovel-shaped mandible, procumbent anterior and globular

posterior teeth, and a mammal-like diastema. This unusual species is an extreme exemplar of a radiation of small caimans with crushing dentitions recording peculiar feeding strategies correlated with a peak in proto-Amazonian molluscan diversity and abundance. These faunas evolved within dysoxic marshes and swamps of the long-lived Pebas Mega-Wetland System and declined with inception of the transcontinental Amazon drainage, favouring diversification of longirostrine crocodylians and more modern generalist-feeding caimans. The rise and demise of distinctive, highly productive aquatic ecosystems substantially influenced evolution of Amazonian biodiversity hotspots of crocodylians and other organisms throughout the Neogene.

Keywords: Miocene, caimanine crocodylians, proto-Amazonia, Pebas System, molluscs, durophagy

A. Introduction

In Western Amazonia, the beginning of the Neogene (at approx. 23 Ma) was marked by a peak in Andean uplift that favored onset and development of the Pebas Mega-Wetland System (Hoorn et al., 2010b). Ten million years later, just prior to establishment of the transcontinental Amazon River drainage, this inland ecosystem attained huge size (more than 1 million km2) and extreme complexity with multiple environments, such as lakes, embayments, swamps and rivers that drained towards the Caribbean (Wesselingh et al., 2002; Hoorn et al., 2010a). The exceptional depositional and fossil record of the Pebas/Solimoes Formations around the Peruvian–Colombian–Brazilian junction permits detailed reconstructions of these Miocene paleoenvironments and their distinctive biotas (Hoorn, 1993; Wesselingh et al., 2002; Antoine et al., 2006; Muñoz-Torres et al., 2006; Wesselingh, 2006; Wesselingh et al., 2006a; Pons & De Franceschi, 2007). Aquatic invertebrates

(ostracods and molluscs) are extremely abundant and diverse within those deposits (Nuttall, 1999; Wesselingh et al., 2002, 2006a; Wesselingh & Salo, 2006), denoting an extensive radiation of endemic lacustrine taxa by about 13 Ma (Wesselingh et al., 2002). The biostratigraphic framework for the Pebas/Solimoes Formation is based on molluscs and pollen (Hoorn, 1993; Wesselingh et al., 2006a). Although fishes (Monsch, 1998) had been reported prior to our exploration of this region, other fossil vertebrates were unknown other than a teid lizard later discovered (Pujos et al., 2009). Since 2002, systematic survey of Peruvian localities of the Iquitos area in northwestern Amazonia has yielded well preserved remains of mammals, turtles, fishes and crocodylians, the latter in great abundance. Two nearby, correlative and contemporaneous lignitic bonebeds in outcrops of approximately 20 and approximately 200 m^2 each document at least seven co-occurring crocodylian species, contrasting with the three species that rarely occur sympatrically within the Amazon biodiversity hotspot today. Here, we report discovery of this new highly diverse and endemic crocodylian community, dominated by small blunt-snouted taxa with crushing dentitions that inhabited the Pebas Mega-Wetland System at its climax, just after the Middle Miocene Climate Optimum (MMCO). We describe three new, sympatric, blunt-snouted caimans to assess distinctive trophic dynamics of proto- Amazonian wetlands and identify a key interval of ecological turnover at the dawn of the Amazon River drainage.

B. Material and methods

B.1 Phylogenetic analysis

The list of characters includes only osteological characters from the skull and jaws (see Appendices), thus postcranial (i.e., 1-46) and soft tissue characters (i.e., 75-78) of Brochu (2011) are omitted in the list. Modifications in selected characters (i.e., 47, 51, 71, 80, 128, 129, 131, 138, 157, 190, 191, 196), due to revised character definitions, enhanced precision or

alternative codings, are indicated in bold font (Salas-Gismondi et al., 2015a, electronic supplementary material). Characters 198 to 201 are new. The last two characters of this study (i.e., characters 200 and 201) are proposed to record features present in selected advanced gavialoids, including Pebasian gavialoid.

Character 138 describes the presence of a topological discontinuity in the ventral orbital margin relative to the presence or absence of an upturned anterolateral orbital rim. Originally, two clear morphologies were proposed regarding this region, to discriminate the condition seen in most crocodylians from that of advanced gavialoids. In crocodylids and most alligatoroids – exclusive of *Mourasuchus* – the orbit is gently circular, with neither an upturned anterior orbital rim nor a ventral notch. In contrast, in advanced gavialoids such as *Gavialis gangeticus* and *Gryposuchus*, the anterior rim is upturned and terminates abruptly in the anteroventral border of the orbit; thus in lateral view a deep notch is seen immediately anterior to the postorbital pillar (Brochu, 1999). However, a variation of this morphology is observed in some South American gavialoids and *Eogavialis africanum*. In these taxa, the anterior orbital rim is clearly upturned, but instead of bearing a ventral orbital notch, the rim progressively descends lateral to the postorbital pillar. Character 138 in this analysis is based on character 139 of Brochu (1999).

The squamosal topology on skull table is treated in character 157 of Brochu (2011). Present research added one state to this character regarding the prominent squamosal eminences observed in some *Mourasuchus* species (Bona et al., 2013).

B.2 Relative snout width and length assessment

The disparity of rostral shapes of the Pebas crocodylians and 69 other eusuchians were included in a bivariate plot to illustrate relative snout length and width based on size-standardizing cranial indices (Appendices). This bivariate plot was modified from Busbey

(1995). Standard measurements and indices are shown in Appendices. Quadrants in figure IV.21 correspond to the four potential combinations of the bi-dimensional snout-shaped morphospace.

Snout length is expressed by the *rostral length-skull length index* (RL/SL). *Rostral length* is measured from the tip of the snout to the anterior end of the orbits in the mid-sagittal plane. *Skull length* is measured from the tip of the snout to the posterior end of the skull table in the mid-sagittal plane. For this index, we chose to use skull length instead of basal skull length of Busbey (1995) because the former measurement is easier to make consistently, and is less affected by distortion, in fossil crocodyliforms.

Snout width is described by the *rostral width-postorbital width index* (RW/POW). *Rostral width* is the transverse diameter of the snout at the level of the fourth maxillary alveoli. Postorbital width is the transverse diameter of the skull at the level of the postorbital bar. For this index, Busbey (1995) measured rostral width at the level of the external nares. The external nares in crocodylians are located just behind the tip of the snout, thus at this position the snout did not attain its average width, particularly in taxa with rostrums tapering anteriorly. Generally, in crocodylians the rostrum width is well developed at the level of the fourth maxillary alveoli. *Postorbital width* is measured at the level of the base of the postorbital pillar.

C. Systematic Paleontology

C.1 Iquitos caimanines

Crocodyliformes Hay, 1930

Alligatoroidea Gray, 1844

Globidonta Brochu, 1999

Caimaninae Brochu, 1999

Gnatusuchus Salas-Gismondi et al., 2015a

Gnatusuchus pebasensis Salas-Gismondi et al., 2015a

Etymology. *Gnatusuchus* from Quechua "Ñatu" for small nose, and Greek "Souchos", crocodile; *pebasensis* from Pebas, after the old Amazonian village of Pebas, Peru for which the source geological formation was named.

Holotype. MUSM 990, nearly complete skull (Figs, IV.1*a-c*, IV.2*d-f*, and IV.21*a*; Table IV.2).

Locality and Horizon. Locality IQ114 (Chapter II.A; Fig. II.1), Iquitos area, Peru; Pebas Formation, late Middle Miocene, ca. 13 Ma; Mollusc Zone 8 (MZ8; Wesselingh et al., 2006*a*).

Referred specimens. MUSM 1465, edentulous premaxilla (Fig. IV.2*a-c*), Locality IQ114; MUSM 1979, right mandible (Figs. IV.3; Table IV.3), Locality IQ114; MUSM 1739, left splenial (Fig. IV.4*a*), IQ114; MUSM 1737; left mandible (Fig. IV.4*b*), Locality IQ114; MUSM 2040, partial left mandible with one posterior tooth (Figs. IV.4*e*, *f* and IV.23*d*), Locality IQ114; MUSM 662, partial left mandible (Figs. IV.1*d* and IV.23*a-c*), Locality IQ116 (Table IV.3); MUSM 1440, MUSM 1730, left mandible with anterior tooth (Fig. IV.4*c*, *d*), IQ26; MUSM 1722, right mandible (Fig. IV.4*g*, *h*), Locality IQ26.

Diagnosis. *Gnatusuchus* is a blunt-snouted caimanine alligatoroid diagnosed by the following combination of characters (autopomorphies within Crocodyliformes are demarcated with an asterisk): skull short and broad, parallel-sided with a reduced rostrum and a wide rounded snout; upturned orbital rims absent; rostral canthi or "spectacle" absent; thick laterosphenoid; attachment scars on ventral surface of quadrate forming a prominent knob; anterior teeth peg-shaped with blunt crowns and posterior teeth globular, both with no

carinae*; dentary with an extensive diastema that separates seven anterior alveoli from four close-packed posterior "cheek teeth" alveoli*; anterior dentary teeth strongly procumbent*; posterior mandibular teeth completely surrounded by the dentary; shovel-like mandible with a long symphysis reaching the level of the eleventh dentary tooth alveolus (of related taxa); large participation of splenial in symphysis; posterior half of the mandibular ramus tilted lateroventrally*.

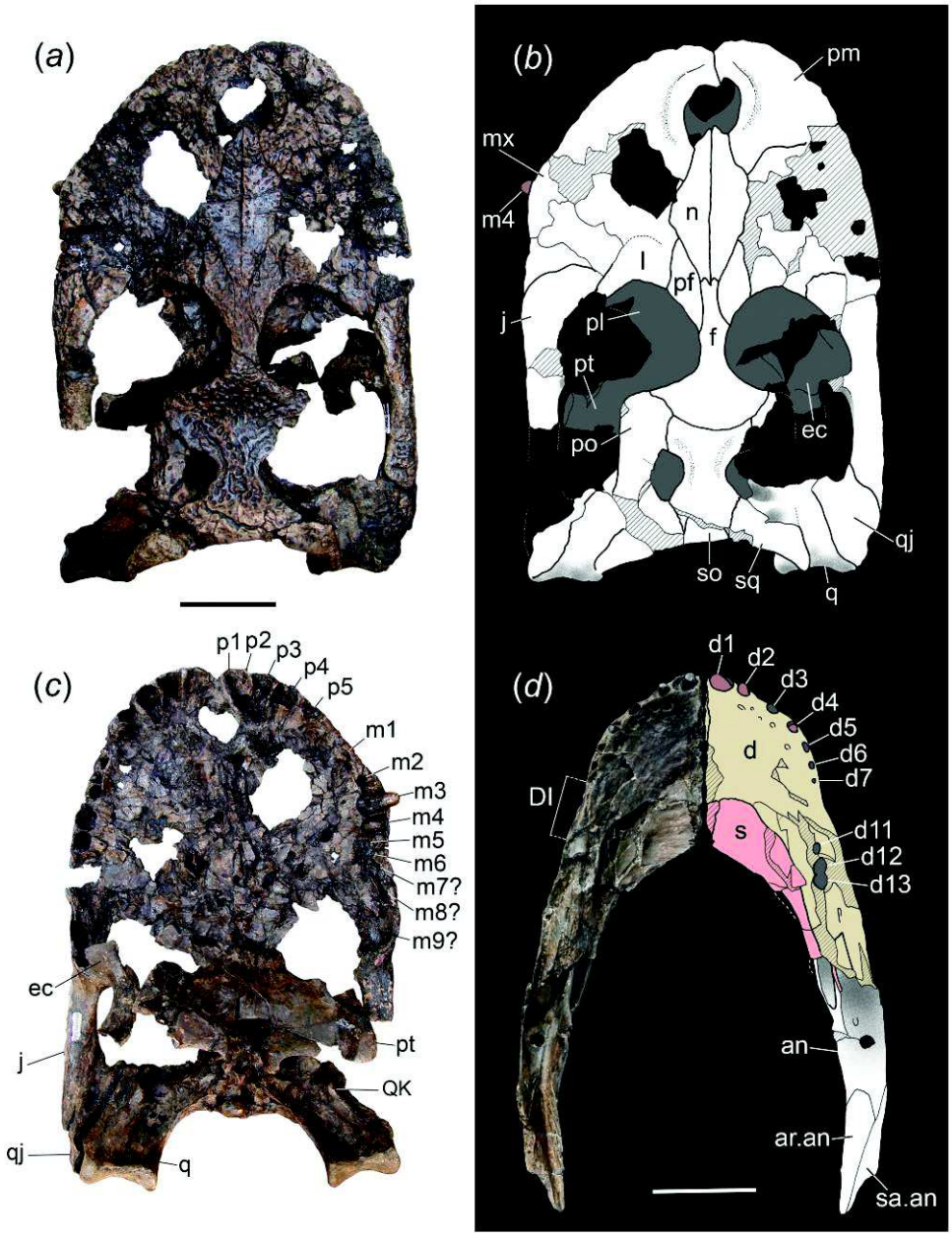

Figure IV.1. ***Gnatusuchus pebasensis.*** Skull (holotype, MUSM 990) in dorsal (*a* and *b*) and ventral (*c*) view. (*d*) Left mandible (MUSM 662) in dorsal view. For anatomical abbreviations see Appendices. Scale bars, 5 cm.

General description. The holotype of *Gnatusuchus pebasensis* (MUSM 990; Figs. IV.21*a*, IV.1*a-c*, and IV.2*d-f*) is a nearly complete skull that is partially flattened in the rostrum region. Palatine bones and maxilla are crushed; tooth alveoli are distorted but not badly damaged. Third and fourth maxillary teeth are preserved in their alveoli (Fig. IV.2*d*). The skull lacks the postorbital bars, left quadratojugal, and portions of bones associated with the infratemporal fenestrae. The skull measures 220 mm in basal length. It might represent the fully adult morphology and size, considering that it bears prominent crests A, B, and D on the anteroventral surface of the quadrate, because among Crocodylia these crests are well developed in old individuals and almost absent in immature specimens (Iordansky, 1976; Wu et al., 2001). Additional material assigned to this taxon comprises cranial fragments and several well-preserved jaws belonging to individuals of equivalent size. Additional material assigned to this taxon comprises cranial fragments and well preserved jaws belonging to individuals of equivalent size. MUSM 662, a left jaw, has a preserved length of 263 mm from the anterior tip of the dentary to the posterior process of the angular. From IQ 26, MUSM 1730 (left mandible) and MUSM 1922 (right mandible without retroarticular process; Fig. IV.4*g*, *h*), measure 275 mm and 234 mm, respectively. From IQ 114, two additional mandibles (MUSM 1737: left mandible; MUSM 1979: right mandible) have a total length of about 308.0 mm and 325 mm. These last specimens are particularly robust and are about 20% larger than previously mentioned ones.

The snout of *Gnatusuchus pebasensis* is substantially wider than long, with a length-breadth index (*sensu* Langston, 1965) of 1.55 – a slightly higher value than the 1.45 index of the bizarre pug-nosed Malagasy Cretaceous crocodyliform *Simosuchus clarki* (Buckley et al., 2000). As in *Acynodon iberoccitanus* (Martin, 2007), the skull is so short that the orbits are situated midway between the anterior tip and posterior margin of the skull. The index of rostral-skull length is 0.49. Skull bone sculpturing is generally moderate, but a little stronger

in the jugal bones and skull table. The external naris is apple-shaped. Orbits are large and nearly circular, but with long axis oriented mediolaterally. The suborbital fenestrae are short, lacking a posterior notch, and appearing to be widely separate from each other. The anterior and lateral rims of the choana lie flush with the surrounding pterygoid bones; the posterior rim is deeply incised. Mandibular articulation of the quadrates is proportionally larger than usually observed in caimans. Tooth loci count probably consisted of a total of five and nine in each premaxilla and maxilla, respectively. *Gnatusuchus* shares with other caimanines small supratemporal fenestrae with overhanging rims (character 152-1), trapezoid supraoccipital on skull table (character 160-4), and slender process of exoccipital ventrally to basioccipital tubera (character 176-2). Total body length estimate is 148.9-167.7 cm (see Table IV.1).

Table IV.1. Length estimates for *Gnatusuchus pebasensis*, *Kuttanacaiman iquitosensis*, and *Caiman wannlangstoni*. For (a): *Crocodylus moreletii* formula: TL=(10.48)(SL)-6.20. For (b) *Alligator mississippiensis* formula: Log TL=(LogSL)(0.970)+0.954. For (b) skull length in mm. SL, skull length; TL, estimated total length in cm. Based on Sereno et al. (2001) and Hurlburt et al. (2003).

Gnatusuchus pebasensis	cm
Length of skull, posterior edge of skull table to tip of snout (SL)	21.92
(a) TL	148.9
(b) TL	167.7
Kuttanacaiman iquitosensis	
Length of skull, posterior edge of skull table to tip of snout (SL)	24.8
(a) TL	171.2
(b) TL	189.1
Caiman wannlangstoni	
Length of skull, posterior edge of skull table to tip of snout (SL)	29.9
(a) TL	210.5
(b) TL	226.7

Skull. The premaxillae and maxillae are collapsed in MUSM 990, thus the real volume of the rostrum is hard to estimate. However, evidence from a specimen comprising both premaxillae suggests that the rostrum was relatively deep, with the snout particularly elevated around the external naris (Fig. IV.2*c*). In this region, each premaxilla bears a crescent-shaped bulge and notch that borders laterally the external naris. A notch of this kind is present in *Alligator* species, *Procaimanoidea utahensis*, and *Arambourgia gaudryi* (see Brochu, 2004b). The posterior process of the premaxillae is short and wide; it reaches the level of the third

maxillary alveolus. The incisive foramen is completely encircled by the premaxillae. This foramen is roughly oval in shape and smaller than the external naris. The suture of the premaxilla with the maxilla seems to be mainly transversal. No occlusion pits are discernable.

As preserved, the dorsal surface of the maxillae appears relatively smooth, with no trace of rostral canthi. No festooning is discernable. Posterior to the level of the fourth maxillary alveolus, the lateral margins of the maxillae are parallel to the longitudinal axis. Ventrally, the maxilla is perforated by tiny "nutritious" foramina lingually to the alveoli. Bigger foramina pierce the left maxilla palatal plate at the level of the fifth alveolus. The palatines are completely distorted and their boundaries with the maxillae cannot be established. However, bone remains in this region depict that the palatines were broad between the suborbital fenestrae.

Table IV.2 – Measurements (mm) of holotype of *Gnatusuchus pebasensis*. MUSM 990, skull. Measurements after Langston (1965). Measurements with missing data are omitted. Abbreviations: e, estimate.

	MUSM 990
Transverse diameter of skull, level of jaw articulation	155.9
Basal length of the skull	220.1
Transverse diameter of skull, level of anterior ends of orbits	163.1
Length of the snout, anterior end of the orbits to tip of the snout	105.1
Length of skull, posterior edge of skull table to tip of snout	219.2
Least transverse diameter, interorbital space	12.0
Length of orbits	49.5
Length of skull table	64.6
Transverse diameter of skull table, posteriorly	95.5
Transverse diameter of skull table, anteriorly	68.1
Transverse diameter of skull, level of postorbital bar	159.7
Width of orbits	50.9
Transverse diameter of nares	24.4
Length of nares, exclusive of narial spine	23.5
Length of the choana	11.4
Transverse diameter of the choana	17.9
Length of suborbital fenestra	49.9e
Length of incisive foramen	18.9
Greatest transverse diameter of incisive foramen	20.3
Height of occipital condyle	10.2
Transverse diameter of occipital condyle	13.8

The nasals make up the posterior margin of the external naris. The anterior process of the nasals (i.e., internarial process) wedged from behind into the external nares. The outline of these paired bones roughly draws an elongated hexagon with diagonal contacts, with the

premaxillae anteriorly and the prefrontals posteriorly. Additionally, the nasals reach the anterior process of the frontal bone behind and contact laterally with the maxillae.

The anterior process of the jugals that overlaps the maxilla is short and vaulted. It does not extend anteriorly beyond the orbit; instead, the anterior process of the jugals is blunt and occupies most of the anterolateral orbital rim. The contact of the jugal with the lacrimal is significantly reduced. The maxillo-jugal suture is smooth and evenly curved. The posterior process of the jugal is stout and constitutes most of the lower bar of the infratemporal fenestra, but fails to reach its posterior angle. The root of the ascending process of the jugal is not deeply inset relative to the horizontal branch as usual in caimanines. One big foramen is located behind the base of the jugal ascending process.

Like the jugal, the lacrimal and prefrontal are relatively short, albeit their relation with the maxilla is not recognizable due to cracking. For example, it is not clear if the maxilla contacts the prefrontal or if the lacrimal interposes between these bones. Thus, it is not conclusive if the anterior limit of the lacrimal equals that of the prefrontal or if it reaches further anteriorly. The lacrimal is broad and concave at the orbital margin. The prefrontal is rhomboid-shaped in dorsal view. The lacrimals, prefrontals, and the frontal bone constitute an even dorsal, slightly convex surface, with no upturned orbital rims, “spectacle” or other cranial adornment. The contact between the prefrontal-frontal inner orbital walls with the dorsal plate of the interorbital bridge is at right angle. The frontal at the interorbital bridge is extremely narrow whereas posteriorly this bone is widely expanded to occupy most of the anterior margin of the skull table. The skull table is a roughly flat surface. As preserved, the left postorbital dorsal plate is thick, robust, and makes up the anterolateral rim of the supratemporal fenestra. Weathering obscures the posterior contact of the postorbital with the squamosal on the lateral side and dorsal surface of the skull table. The otic recess is shallow compared with other alligatoroids, in which the postorbital-squamosal suture is extensively

developed medially ventral to the skull table (i.e., character 146 of Brochu, 2011). At the base of the descending process, facing laterally, there is a single big foramen. The postorbital descending process is not preserved.

The parietal bears a flat, large, and strongly sculptured surface. The frontoparietal suture is concavoconvex and lies entirely on skull table. Surrounding the anteromedial margin of the supratemporal fenestrae, there is a pair of bowed wrinkles that roughly marks the parietal portion that overhangs the fenestrae. Posteriorly, the parietal contacts the trapezoid supraoccipital bone on the skull table. The parietal borders laterally the supraoccipital, but fails to reach the posterior margin of the skull table. On the occipital surface, the supraoccipital bears a U-shaped ventral suture. Details of the postoccipital processes and postemporal fenestrae are not discernable. The sagittal ridge and the parasagittal excavations are well developed.

The squamosals bear a large posterolateral process. This process defines the concave posterior margin of the skull table. The squamosal overhangs the supratemporal fenestra as well as the occipital plate. The left squamosal shows that its lateral margin is thick, but features of the longitudinal groove on the lateral side of the skull table are not preserved.

The paraoccipital process of the exoccipitals is high and projects posterolaterally. The ventral margin of the paraoccipital process is smooth medial to the posterior opening of the cranioquadrate passage. Lateral to the occipital condyle, within a wide and deeply concave surface, the exoccipitals are pierced by a big vagus opening and a smaller foramen for nerve XII. The descending process of the exoccipitals is long and relatively stout compared with that of other caimanines, in which this process is very slender (see Brochu, 1999). The lateral carotid foramen lies on the ventral process of the exoccipital and faces posteriorly (Fig. IV.2*e*).

The basioccipital is bordered laterally by the exoccipitals. Assembled, these bones form a wide, triangular bassioccipital plate. The basioccipital tubera has a prominent bulge-like sagittal process, just behind the medial opening for the eustachian foramen. In front of this foramen, the basisphenoid is broadly exposed as a concave and vertical wall that leans against the posterior margin of the pterygoids.

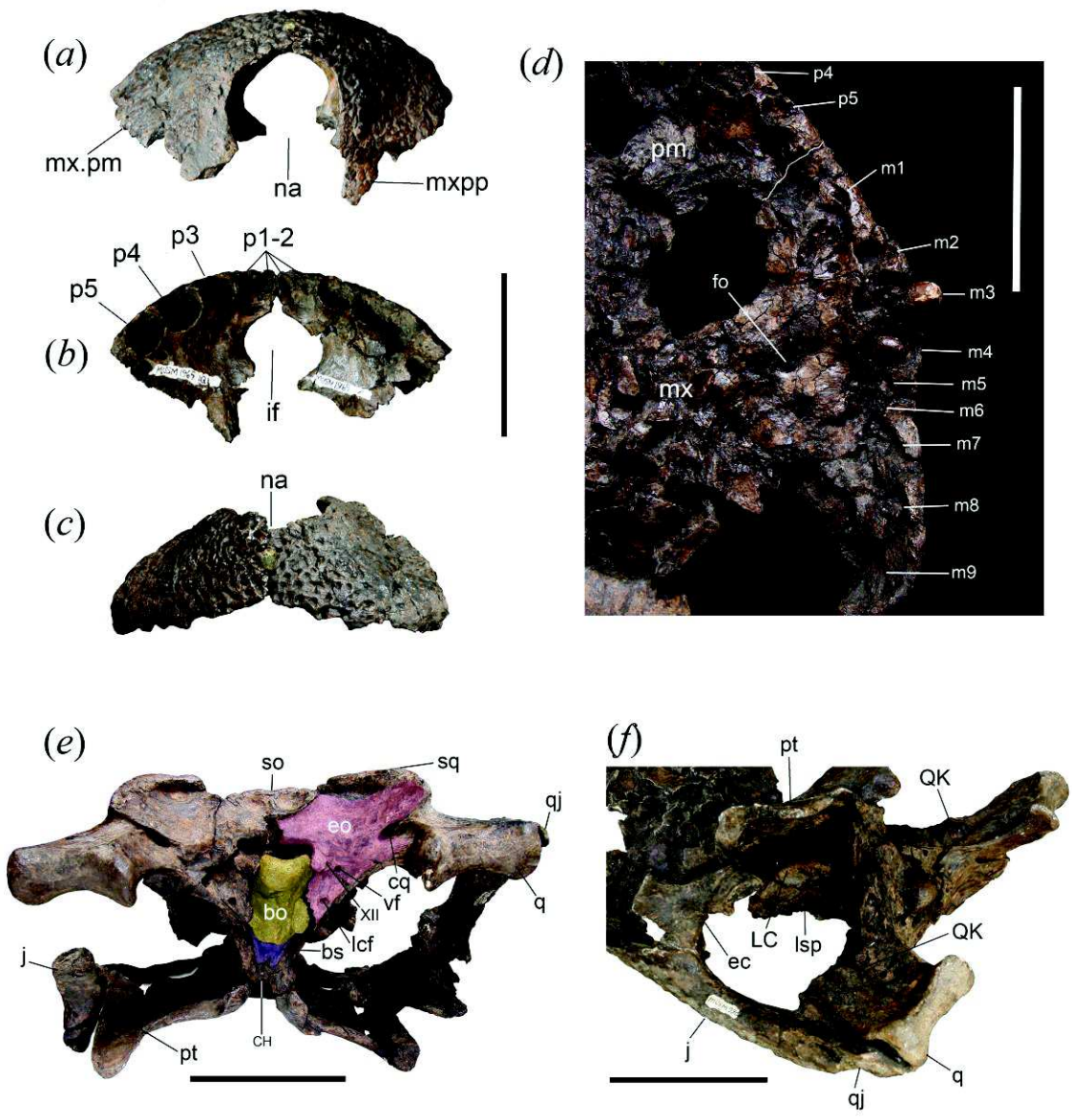

Figure IV.2. ***Gnatusuchus pebasensis*.** Premaxillae (MUSM 1965) in dorsal (*a*), ventral (*b*), anterior (*c*) view. (*d-f*) Skull (holotype, MUSM 990). (*d*) Details of the maxillary dentition in ventral view. (*e*) Occipital and quadrate region in posteroventral view. (*f*) Temporal region in ventrolateral view. Abbreviations: bs, basisphenoid (purple); bo, basioocipital (yellow); eo, exoccipital (red). For other anatomical abbreviations see Appendices. Scale bars, 5 cm.

Contrary to the thin-walled, shell-like constitution of the laterosphenoid bone of most crocodylians, in *Gnatusuchus* this bone is stout, massive, and bears a prominent, thick crest that runs anterolateraly towards the capitate process (Fig. IV.2*f*). The prootics are badly damaged.

The quadrate and quadratojugal together constitute a wide and robust body (Fig. IV.2*e*, *f*). The dorsal surface of the quadratojugal is heavily sculptured and approaches the squamosal medially. The quadratojugal takes part of the posterior corner and margin of the infratemporal fenestra, although the precise extension of its ascending process is unknown. The mandibular condyles of the quadrates are proportionally bigger and more robust than is usually observed in other crocodylians. Whereas the general conficguration of the medial and lateral hemicondyles is similar to other caimanines, the dorsal surface of the quadrate is more convex and bears a sharp longitudinal ridge that separates its medial and lateral portions. The foramen aerum lies on dorsal surface of the quadrate, lateral to this ridge. Anteroventrally, the quadrate is scored by strong crests A, B, and possibly D (*sensu* Iordansky, 1976: Fig. 10). The crest A bears a prominent knob (QK; Fig. IV.2*f*), resembling the condition of *Iharkutosuchus makadii* (see Osi & Weishampel, 2009). The general crest pattern, particularly that of crests A and B, is similar to that observed in *Alligator mississippiensis*.

The pterygoids completely encircle the choana in close proximity to their posteroventral limit. The pterygoid wings are comparatively thick. They are projected posteroventrally as usual in crocodylians. The posterior margin of each wing is concave. The pterygoid torus transiliens is long, parallel-sided, and narrow as in *Alligator mississippiensis*. Sutures between the pterygoids and palatines are not visible.

The anterior process of the ectopterygoid is extremely short and truncated instead of tapering anteriorly as usual in crocodylians. It seems to be that the lateral border of the ectopterygoid is separated from the maxillary tooth row. The medial margin of the

ectopterygoid anterior process bears a deep embayment, thus the suborbital fenestra is bowed and concave medially. The descending process of the ectopterygoid is long, straight, and slender. Its base is thicker and more rounded in section than the flattened condition observed in alligatoroids. The ascending process is damaged.

Mandible. The mandible (Figs. IV.1*d*, IV.3, and IV.4) is short, wide, and massive. The symphyseal region is extremely shallow, broad, and flat, as in early alligatoroids and caimanines, such as *Globidentosuchus brachyrostris* (Scheyer et al., 2013) and *Eocaiman cavernensis* (Simpson, 1933). The symphysis is very long, being about a third of the total length of the mandible, and reaching posteriorly to the level of the eleventh dentary tooth alveolus locus of related taxa.

The dentary bone surrounds all of the mandibular dentition (Fig. IV.4*b*). The splenial participates extensively in the symphysis. The ratio of the splenial length in the symphysis to the total length of the symphysis is 0.30, thus representing almost a third of its total length. In this region, the dentary and the splenial are dorsoventrally compressed and both make up a continuous concave dorsal surface, with the splenial bearing a posterior sharp edge. The splenial constitutes a huge flange medial to the level of posterior alveoli, as in basal Globidonta taxa, such as *Brachychampsa*, *Stangerochampsa*, *Allognathosuchus*, and among caimanines, in *Globidentosuchus brachyrostris* (Fig. IV.4*a*; Carpenter & Lindsey, 1980; Brochu, 2004b; Scheyer et al., 2013). No perforation for the mandibular cranial nerve V is seen on the medial wall of the splenial in MUSM 662, but two foramina are detected in this region in MUSM 1979 and MUSM 1739 (Fig. IV.4*a*). Behind the tooth series, the rami increase in height and, unlike crocodylians, the whole bone structure in this position is tilted lateroventrally. Posteriorly, the articular bone, and therefore the mandibular joint, is displaced medially from the longitudinal axis of the rami. The external mandibular fenestra is proportionally larger and more triangular in profile than usually observed in caimans, due to

the presence of a posterioventral angle and straighter margins (Fig. IV.3*d*). The surangular bridge above the fenestra is quite robust and flattened transversally, as in longirostrine crocodylians (Iordansky, 1976). The surangular-angular suture contacts the external mandibular fenestra at the posterior rim, above the posteroventral angle. The posterior extension of the angular reaches the tip of the retroarticular process, as in extant caimans.

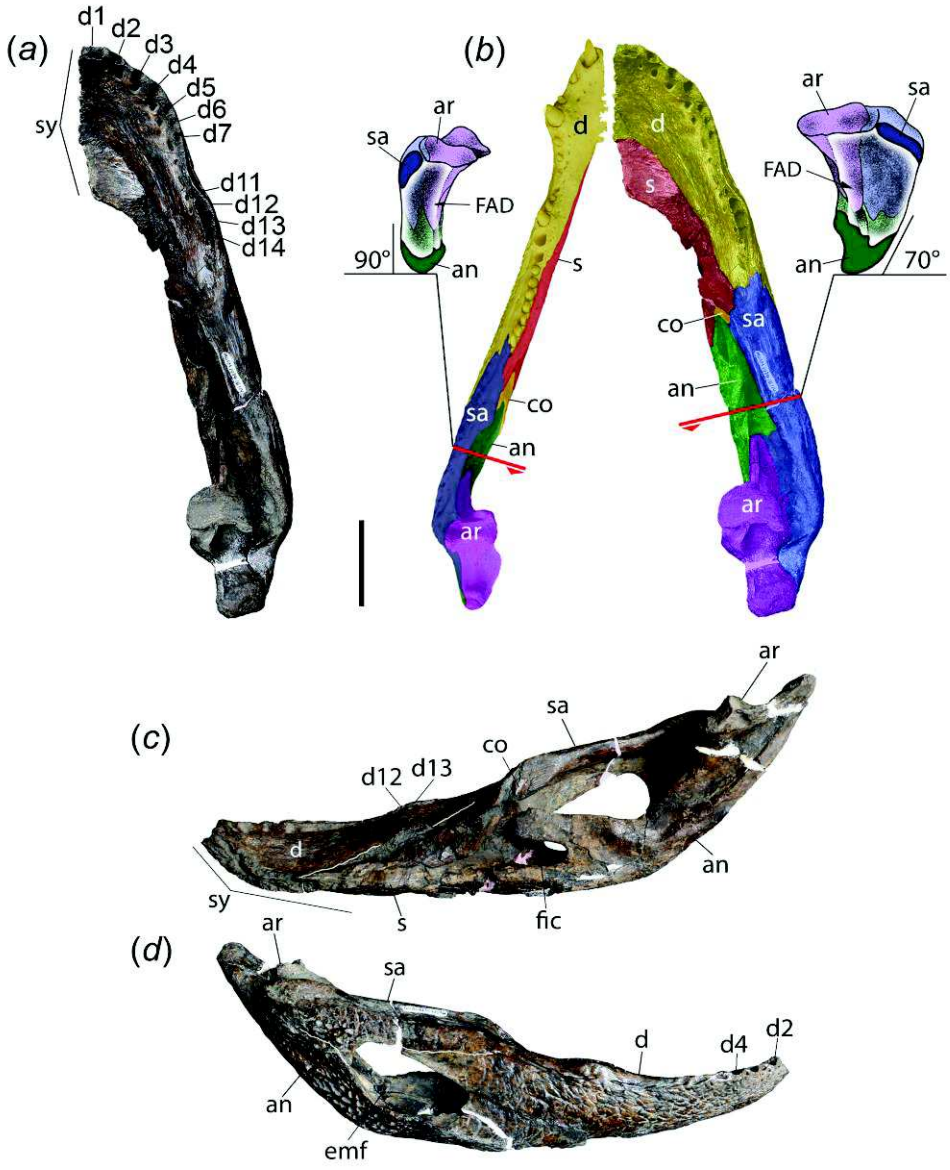

Figure IV.3. *Gnatusuchus pebasensis*. Right mandible (MUSM 1979) in dorsal (*a*), medial (*c*), and lateral (*d*) view. (*b*) Comparison among colored bone photographs of mandible of *Gnatusuchus pebasensis* (right) and *Caiman crocodilus* (left) in in dorsal views and cross sections at the level of the adductor fossa. Values of 70º and 90º indicate the corresponding lateral vertical angle of the mandibular ramus with the horizontal plane. For other anatomical abbreviations see Appendices. Scale bar, 5 cm.

On the medial side, the foramen intermandibularis caudalis (fic) is relatively long. Ventral to this foramen, the posterior process of the splenial meets the angular in an interlocking, trident-like suture. Whereas the angular bounds the fic ventrally, the splenial runs posteriorly along the ventral margin of the mandible until the rear limit of the foramen.

Table IV.3 – Measurements (mm) of mandibles of *Gnatusuchus pebasensis*. MUSM 662, left mandible without articulars. MUSM 1979, complete right mandible. Mandible width at the end of the symphysis was estimated by duplicating the minimum width measurement of the preserved mandibular ramus. Measurements modified from Langston & Gasparini (1997). Abbreviations: e, estimate.

	MUSM 662	MUSM 1979
Mandible length (as preserved)	263	308.0
Symphysis length	83.3	86.3e
Splenial length in symphysis	24.7	25.7
External fenestra length	--	71.0
External fenestra height	--	35.3
Mandible width at end of symphysis	58.3 x 2 = 116.6	61.0 x 2 = 122.0
Mandible height at d4	18.6	--
Greatest mandible height	--	80.0

Feeding musculature inferred from the cranial and mandibular anatomy. The mandibular anatomy of *Gnatusuchus* presents the following peculiar features: the ramus is high, robust, tilted lateroventrally posterior to the symphysis, and the dorsal margin of the surangular is transversely expanded, housing a wider and more capacious adductor fossa. Therefore, this fossa encompasses more surface area and volume for stronger adductor tendons and muscles. A transversally expanded surangular bone is present in longirostrine crocodylians (e.g., *Gavialis*, *Tomistoma*; Iordansky, 1976); this bone bears areas for insertion of m. adductor mandibulae externus (pars superficialis and media) (Schumacher, 1976; Busbey, 1989). In the skull of *G. pebasensis*, the temporal region is characterized by a thickened and crested laterosphenoid bone and by the presence of prominent crests A and B (*sensu* Iordansky, 1964) on the anteroventral surface of the quadrate. Such morphology points to the remarkable size of the temporal muscles, such as the m. pseudotemporalis and the m. adductor mandibulae posterior, respectively (Schumacher, 1976). This latter muscle acts as an

adductor but also functions to firmly fix the jaws during mastication, due to its proximity to the jaw joints (Schumacher, 1976; Busbey, 1989). Strong adductors muscles also might facilitate any crocodylian feeding activity involving strong potentially dislocating jaw forces.

Specialized Dentition. Dentition is a conspicuous feature in *Gnatusuchus pebasensis*. It is distinctly modified in shape and number from the generalized crocodilian pattern. Significant evolutionary loss of several alveoli occurred in the maxilla and the dentary. In the maxilla, this loss took place posterior to the ninth tooth loci of related taxa. In the dentary, it occurred between the seventh and the eleventh tooth loci as well as posterior to the thirteeth alveoli of related taxa. Thus, based on the available material the dental formula of *Gnatusuchus* is estimated in 5 + ?9/11.

In MUSM 990, the premaxilla and the maxilla hold five and probably nine tooth positions, respectively; most of them are distorted or incomplete. In the premaxilla, the alveoli are all evenly and closely spaced. The first and second alveoli are extremely reduced and they might not have carried teeth. The third to fifth are subequal, remarkably large, and probably the largest in the mouth. An extensive diastema separates the fifth premaxillary alveolus from the first of the maxilla. As usual in the brevirostres, the maxillary dentition exhibits two waves of size, with the first peak at the third and fourth alveoli, oddly both of almost equal size. The second peak comprises the mostposterior maxillary teeth, probably corresponding to the seventh, ninth, and tenth. They were implanted very close together and at least the ninth and tenth might have shared a large alveolar groove. No posterior maxillary teeth are preserved *in situ*; however, these positions might have housed relatively big crushing teeth (see below). The fifth and sixth alveoli are small.

Compared with other blunt-snouted or “generalized” caimans, which possess around 18-20 tooth alveoli, the mandibular dentition is extremely reduced in number.

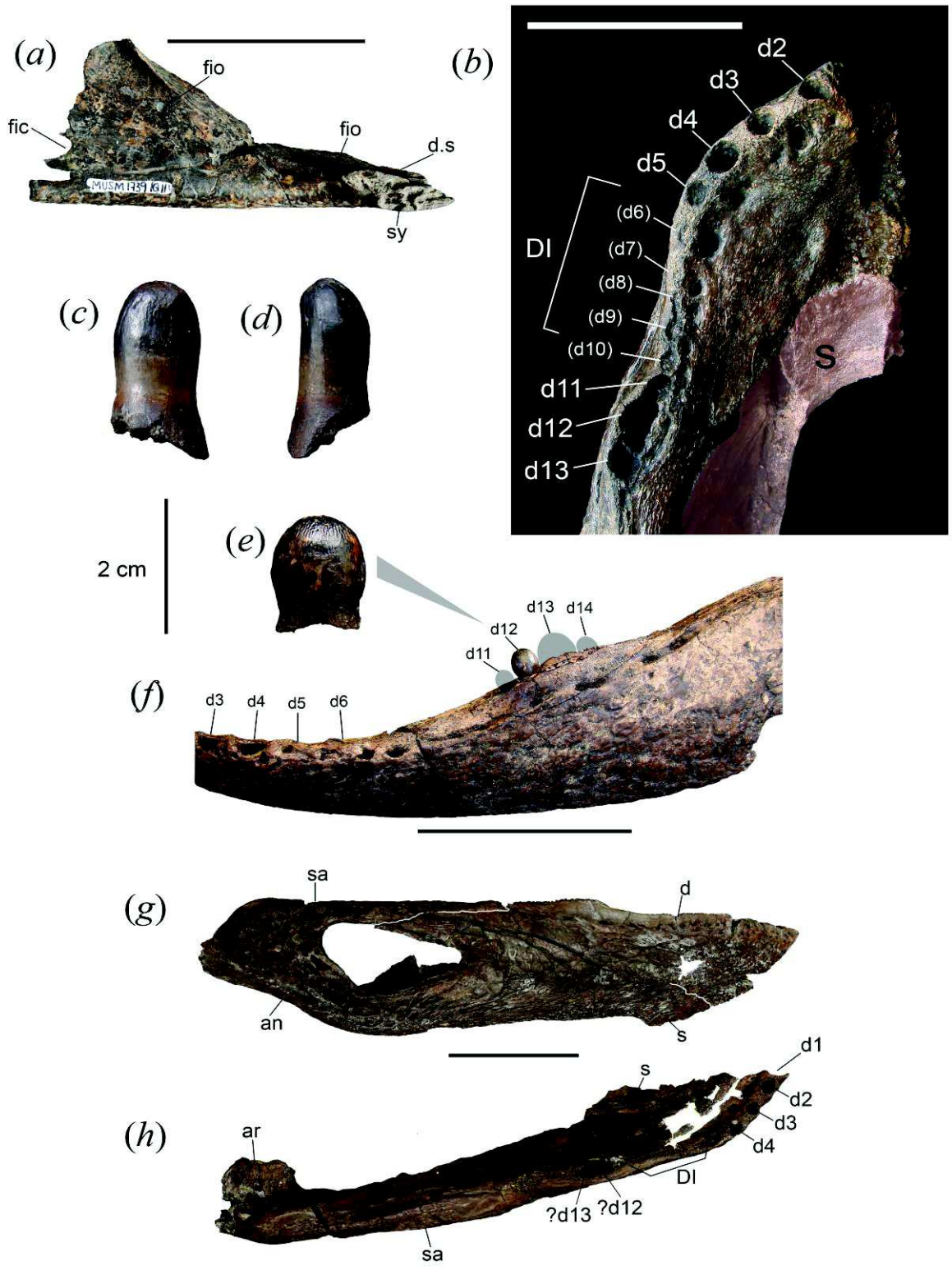

Figure IV.4. ***Gnatusuchus pebasensis*****.** (*a*) Splenial (MUSM 1737) in medial view. (*b*) Left mandible (MUSM 1737) showing symphyseal and alveolar pattern. Anterior tooth (MUSM 1730) in lingual (*c*) and mesial (*d*) view. (*e*, *f*) Left dentary (MUSM 2040) in lateral (*f*) view and close up of posterior tooth (*e*). (*g*, *h*) Right mandible (MUSM 1722) in lateral (*g*) and dorsal (*h*) view. For anatomical abbreviations see Appendices. Otherwise stated, scale bars equal 5 cm.

Mandibular teeth include 11 tooth alveoli grouped into seven anterior teeth and four posterior "cheek" teeth, with these groups separate by a long diastema (Figs. IV.1*d* and IV.4*b*). Tooth positions, dentary shape, and vestigial dental alveoli indicate that the diastema results from the evolutionary loss of at least three tooth alveolus loci (the eighth, ninth, and tenth loci of related taxa). Significant evolutionary loss of several alveoli posterior to the 14th tooth loci also occurred within the rear mandibular dentition, as the ancestral caimanine condition may have included four to six more tooth loci posterior to the 14th locus (Simpson, 1933; Scheyer et al., 2013). Additional alveolar closure within tooth loci posterior to the fourth is observed among most individuals, but it might be a consequence of secondary bone filling (i.e., bone resorption) after tooth loss that probably occurred during *in vivo* feeding activity on hard food (e.g., durophagy).

In MUSM 662, the first, second, and fourth dentary teeth are preserved in their alveoli (Fig. IV.1*d*). Apart from size differences among them, all are equivalent in morphology; likely they represent the morphology of all anterior tooth loci. Anterior alveoli decrease in size posteriorly, with the first alveolus being the largest in the mandible. The third and fourth alveoli are generally subequal in size. The first four alveoli are aligned along the frontal edge with the tips oriented outwards. Fifth, six, and seventh alveoli are reduced in diameter. Large vascular and neural foramina occur distal to the anterior alveoli. Behind the diastema, the four posterior tooth positions most likely represent the eleventh to 14th tooth loci of related taxa. The eleventh and 14th alveoli are small and generally comparable in size and shape to the fifth or sixth. The twelfth and 13th alveoli are large. Posterior teeth are closely spaced (Fig. IV.4*b*).

Teeth are distinctly modified in shape from the generalized crocodylian pattern. Anterior teeth are thin and peg-like in shape, bearing blunt crowns with no carinae ridges or striae. Preserved teeth show apical wear. Anterior teeth are notably procumbent. In MUSM

2040, one posterior tooth is preserved in the twelfth dentary position (Fig. IV.4*e, f*). This tooth is globular in shape with a distinct neck at the base of the crown. Similar morphology is expected for adjoining teeth from edentulous loci.

Dental patterns suggest that specific, distinct roles were performed by the anterior and posterior teeth series. Incisor-like procumbent anterior teeth with apical wear possibly functioned for holding, scooping, or scratching. The posterior dental series bears just four functional globular, molar-like teeth. Although reduced in number relative to other caimanines, they are closely packed and located at the top of the posterior convex arch, in a prominent lateral expansion of the alveolar border (Figs. IV.3 and IV.4). These teeth most likely served for crushing or grinding of hard prey.

Kuttanacaiman Salas-Gismondi et al., 2015a

Kuttanacaiman iquitosensis Salas-Gismondi et al., 2015a

Etymology. *Kuttana* from Quechua for "grinding or crushing machine", and *caiman*, referring to tropical American alligatoroids; *iquitosensis* from the Iquitos native ethnic group inhabiting the Maynas province close to the Peruvian Amazonian city of Iquitos near the specimen locality.

Holotype. MUSM 1490, nearly complete skull and mandibles in anatomical connection (Figs. IV.5 and IV.21*b*; Table IV.4).

Locality and Horizon. Locality IQ26 (Chapter II.A; Fig. II.1), Iquitos area, Peru; Pebas Formation, late Middle Miocene, ca. 13 Ma; Mollusc Zone 8 (MZ8; Wesselingh et al., 2006a).

Referred specimens. MUSM 1942, associated left mandible, maxilla, and skull table (Figs. IV.6*a-d*, IV.7*a, b*, and IV8*b*; Table IV.5), Locality IQ114; MUSM 1736, left mandible

without splenial (Fig. IV.6*e, f*), Locality IQ26; MUSM 2394, juvenile partial skull table (Fig. IV.7*e*), Locality IQ26; MUSM 1928, juvenile partial skull table (Fig. IV.7*f*), Locality IQ26.

Diagnosis. *Kuttanacaiman* is a small caimanine diagnosed by the following combination of characters: robust, blunt, and short snout; interobital bridge flat and slender; posterior maxillary and dentary teeth closely packed, globular, low, and laterally compressed. Symphysis reaching level of the sixth dentary alveolus, splenial excluded from mandibular symphysis, anterior dorsal process of splenials turned medially; abrupt elevation of surangular dorsal margin posterior to dentary series; first and fourth dentary teeth piercing premaxilla; angular-surangular suture contacting external mandibular fenestra at posterior angle; maxillary bearing a broad shelf extending into suborbital fenestra; palatine lateral margins extending into suborbital fenestra anteriorly and posteriorly; parietal excluded from posterior margin of skull table.

General description. The holotype of *Kuttanacaiman iquitosensis* (MUSM 1490, IQ26; Fig. IV.5) is a smashed skull and mandibles in anatomical connection. Although some skull bones are distorted, most limits are discernable. The left jugal, quadrato-jugal, postorbital, and squamosal are lacking. Anatomical connection in the holotype obscures palatal region of the skull and alveolar series of the mandibles. The posterior mandible bones are badly damaged. From the same type locality, MUSM 1736 comprises a left mandible lacking the splenial and the coronoid. From IQ114, MUSM 1942 are cranial and mandibular elements of a slightly bigger individual, including the left maxilla, jugal, and pterygoid; the skull table and quadrates; and the left mandible without the articular.

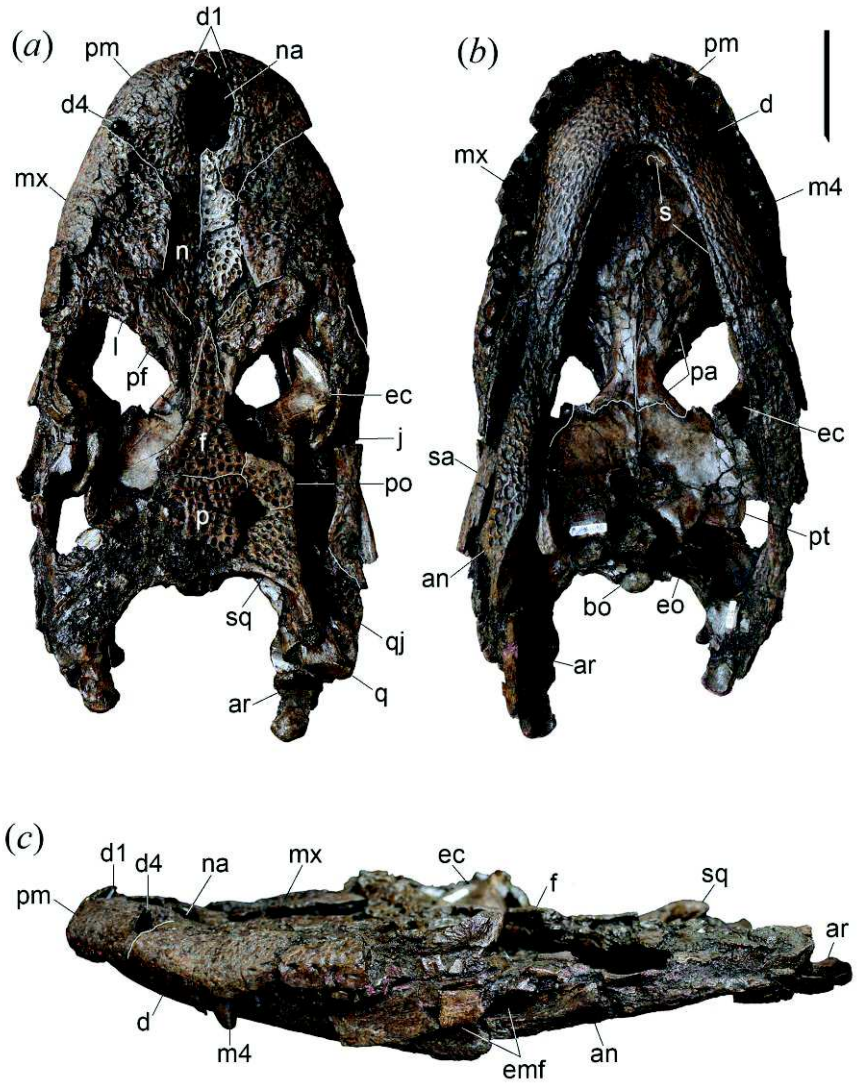

Figure IV.5. *Kuttanacaiman iquitosensis*. Skull and mandibles (holotype, MUSM 1490) in dorsal (*a*), ventral (*b*), and left lateral (*c*) view. For anatomical abbreviations see Appendices. Scale bar, 5 cm.

The skull (holotype) measures 253 mm in basal length. It bears a short and wide rostrum. The snout is blunt and rounded. Lateral rostral margins are slightly convex, without significant transverse expansion posteriorly. The index of rostral-skull length is 0.52 (Fig. IV.21). The narial opening projects dorsally and appear longer than wide. The nasal bones form the posterior rim of narial opening. Nasals and lacrimals are not in contact. The orbits are large, long, and subtriangular in shape, with anterior angle displaced laterally as in *Globidentosuchus brachyrostris* and *Eocaiman cavernensis*.

Table IV.4 – Measurements (mm) of holotype of *Kuttanacaiman iquitosensis*. MUSM 1490, skull. Measurements after Langston (1965). Measurements with missing data are omitted. Abbreviations e, estimate; m4, fourth maxillary alveolus.

	MUSM 1490
Transverse diameter of skull, level of jaw articulation	141.0e
Basal length of the skull	253.0e
Transverse diameter of skull, level of anterior ends of orbits	152.0
Length of the snout, anterior end of the orbits to tip of the snout	125.8
Length of skull, posterior edge of skull table to tip of snout	248.0e
Least transverse diameter, interorbital space	16.1
Length of orbits	67.9
Length of skull table	43.0e
Transverse diameter of skull table, posteriorly	80.0e
Transverse diameter of skull table, anteriorly	78.0e
Transverse diameter of skull, level of postorbital bar	145.0
Width of orbits	54.4e
Transverse diameter of nares	22.4
Length of nares, exclusive of narial spine	32.0
Transverse diameter of choana	28.1
Length of suborbital fenestra	54.0e
Greatest transverse diameter of suborbital fenestra	38.0e
Height of occipital condyle	14.8
Transverse diameter of occipital condyle	18.5
Transverse diameter of snout at m4	133.4
Maxillary teeth series length (13 alveoli)	129.0

Interorbital bridge is very slender and flat. The skull table is parallel-sided, proportionally small, and its surface is virtually even and horizontal. The supratemporal fenestrae are circular and small due to overlap of squamosal, parietal, and postorbital bones. The incisive foramen is teardrop-shaped. Suborbital fenestrae are relatively small and roughly triangular. Participation of the pterygoids in the suborbital margin is limited to the posterior angle. The choana is transversally wide and located close to the posterior margin of the pterygoids. The anterior margin of the choana bears everted margins. Posteriorly, the choana is not deeply notched. Skull bones are heavily sculpted with subcircular pits, particularly on rostrum and skull table. It bears five and thirteen alveoli in premaxilla and maxilla, respectively, and 18 alveoli in dentary. *Kuttanacaiman* differs from *E. cavernensis* in having palatine processes projecting anteriorly into suborbital fenestrae (character 119-1), ectopterygoid-pterygoid flexure present throughout ontogeny (character 126-1), enlarged

twelfth dentary alveolus (character 51-1), and posterior teeth laterally compressed (character 79-1) and globular (character 198-2). It differs from *Gnatusuchus pebasensis* and *Globidentosuchus brachyrostris* in lacking splenial symphysis (character 54-2). Total body length estimate is 171.2-189.1 cm (see Table IV.1).

Skull. The premaxillae are wide, relatively low, and smooth around the narial opening. In lateral view, festooning of the premaxillary and maxillary ventral border is moderate. The posterior process of the premaxillae is short and stout. It reaches the level of the third maxillary alveolus. The left first and fourth mandibular teeth pierced the premaxillae whereas in the right side only the first mandibular tooth pierces the corresponding premaxilla. The lateral walls of premaxillary-maxillary contact seem to remain throughtout the ontogeny. The perforation of the first mandibular tooth is located close to the anterior margin of the narial opening. Each premaxilla bears five alveoli. The first alveolus is not preserved. The third premaxillary alveolus is slightly bigger than the fifth, but both sensibly smaller than the fourth. The second alveolus and probably the first one were the smallest in the series. In the holotype, other details of the palatal plate of the premaxillae are covered by the mandibular symphysis.

The maxillae are relatively low and bear no rostral ridges (i.e., canthi rostralii). The contact between the maxilla and the nasal is bowed laterally. Posteriorly, the maxilla sutural contacts with the prefrontal and the lacrimal are not well preserved in any specimen. In this region, the maxillae probably met only the anterolateral corner of the prefrontal, thus this condition might differ to that of *Caiman* and *Melanosuchus* species in which the maxillae are in large contact with the prefrontals. Ventrally, the palatal surface of the maxillae is wide and relatively short. The premaxillary-maxillary suture is virtually transversal. The maxilla bears thirteen alveoli. Anterior region of maximum alveolar diameter is projected ventrally and includes the first to sixth alveoli, all of them circular in section. In MUSM 1942, the sixth

alveolus is closed, probably as a consequence of secondary bone resoption. The posterior alveoli (i.e., the seventh to 13th) are close together and laterally compressed. The biggest alveolus in the maxilla is the fourth. In the holotype, the palatal surface is plentiful of cracks, thus maxillary-palatine sutural pattern is not discernable. MUSM 1942 presents three deep occlusion cavities medially to the eighth, ninth, and tenth alveoli. These cavities might be for the reception of the twelfth, thirteenth, and fourteenth dentary teeth. Posteriorly, the maxilla bears a broad shelf extending into the suborbital fenestra. The vomer is not exposed in the palatal plate. The anterior limit of the palatine bones reaches approximately the level of the sixth maxillary alveolus.

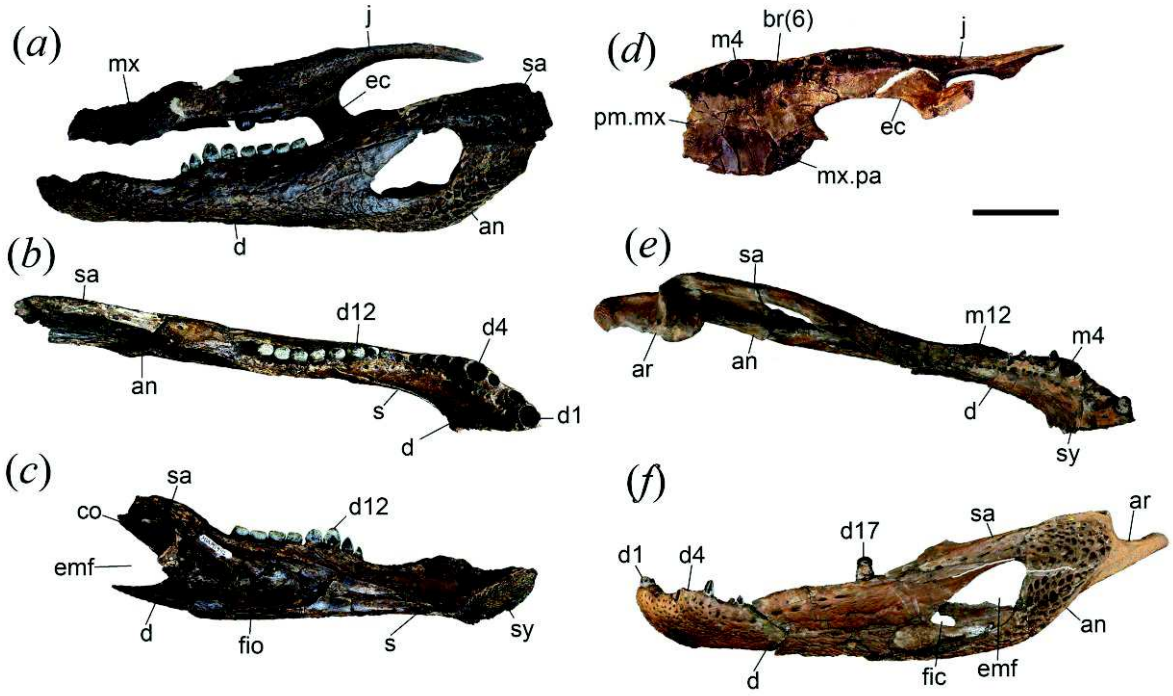

Figure IV.6. ***Kuttanacaiman iquitosensis.*** (*a*-*d*) Incomplete skull and mandibles (MUSM 1942). Left maxilla-ectopterygoid-jugal and partial jaw in lateral view (*a*). Left mandible in dorsal (*b*) and medial (*c*) view. Left maxilla-ectopterygoid-jugal in ventral view. (*e*, *f*) Left mandible (MUSM 1736) in dorsal (*e*) and lateral (*f*) view. br(6) indicates bone resorption in alveolar position 6. For anatomical abbreviations see Appendices. Scale bar, 5 cm.

The nasals are flat and relatively wide. The posterior margin of the nasals surpasses the anterior limit of the orbits. The nasals reach and take part of the posterior margin of the narial opening. The narial opening projects dorsally as in all caimanines, exclusive of *Caiman*

wannlangstoni (Salas-Gismondi et al., 2015a). In this last taxon, the narial opening is anterodorsally oriented.

In the rostrum, the lacrimals and prefrontals seem to reach nearly the same length. The anterior process of frontal is short and fails to reach the level of the anterior margin of the orbits. The prefrontals probably meet medially as in *Caiman yacare* (see Brochu, 1999), and together they make up a discrete arcuate "spectacle". Close to the orbital margin, the prefrontals bear a distint depression that might corresponde to an articular surface for palpebral ossifications.

Table IV.5 – Measurements (mm) of skull and mandible elements of *Kuttanacaiman iquitosensis*. MUSM 1942, associated left mandible, maxilla, and skull table. Maxilla and mandible width at the level of the fourth maxillary (m4) and dentary (d4) alveolus, respectively, was estimated by duplicating the minimum width measured on the preserved side. Measurements modified from Langston (1965) and Langston & Gasparini (1997). Measurements with missing data are omitted. Abbreviation: e, estimate.

	MUSM 1942
Transverse diameter of skull, level of jaw articulation	182.0e
Transverse diameter of skull table, posteriorly	111.0
Transverse diameter of skull table, anteriorly	89.1
Length of skull table	52.4
Height of occipital condyle	15.8
Transverse diameter of occipital condyle	24.6
Transverse diameter of snout at m4	71.4 x 2 = 142.8
Maxillary teeth series length (13 alveoli)	138.8
Mandible length (until half-length of external mandibular fenestra)	226.0
Symphysis length	54.5.
External fenestra length	58.9
External fenestra height	31.6
Mandible width at d4	38.5 x 2 = 116.6
Mandible height at d4	27.9
Greatest mandible height	71.6

The morphology of the jugal is preserved in MUSM1942. This bone is relatively flat and slender. It entirely forms the ventral margin of the orbit and infratemporal fenestra. The anterior process of the jugal is short and evenly rounded, as in *Gnatusuchus pebasensis*. As other caimanines, the root of the postorbital bar is not deeply inset.

The dorsal surface of the frontal presents a slight convexity anteroposteriorly. The fronto-parietal suture lies on the skull table and is concavo-convex in all ontogenetic stages (Figs. IV.5*a* and IV.7*e*, *f*). The postorbitals are restricted to the anterolateral portions of the skull table. Dorsal to the postorbital pillar, they bear two small foramina. The postorbital pillar itself is not preserved. The postorbitals and squamosals limit the supratemporal fenestrae laterally. The parietal takes part of the medial margins of the supratemporal fenestra. Posteriorly, the parietal embraces a triangular-shaped supraoccipital. In MUSM 1942, it approaches the posterior margin of the skull table but fails to reach it.

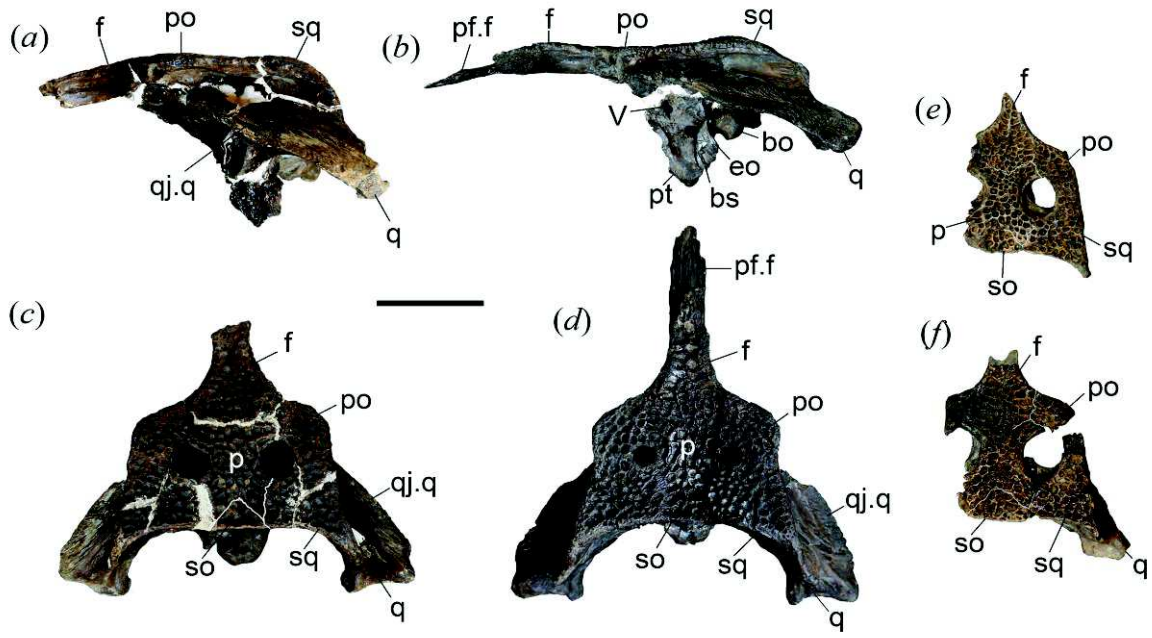

Figure IV.7. Skull tables of *Kuttanacaiman iquitosensis.* MUSM 1942 in left lateral (*a*) and dorsal (*c*) view. MUSM 1728 in left lateral (*b*) and dorsal (*d*) view. (*e*, *f*) Juvenile specimens. MUSM 2394 (*e*) and MUSM1928 (*f*) in dorsal view. For anatomical abbreviations see Appendices. Scale bar, 5 cm.

The squamosals are roughly triangular. The lateral margin of the squamosals is thin and bears a longitudinal groove. The posterior process of the squamosals extends the surface of the skull table behind the medial transversal margin. Between both processes, the posterior border of the skull table is a straight line that largely overlaps the occipital plate.

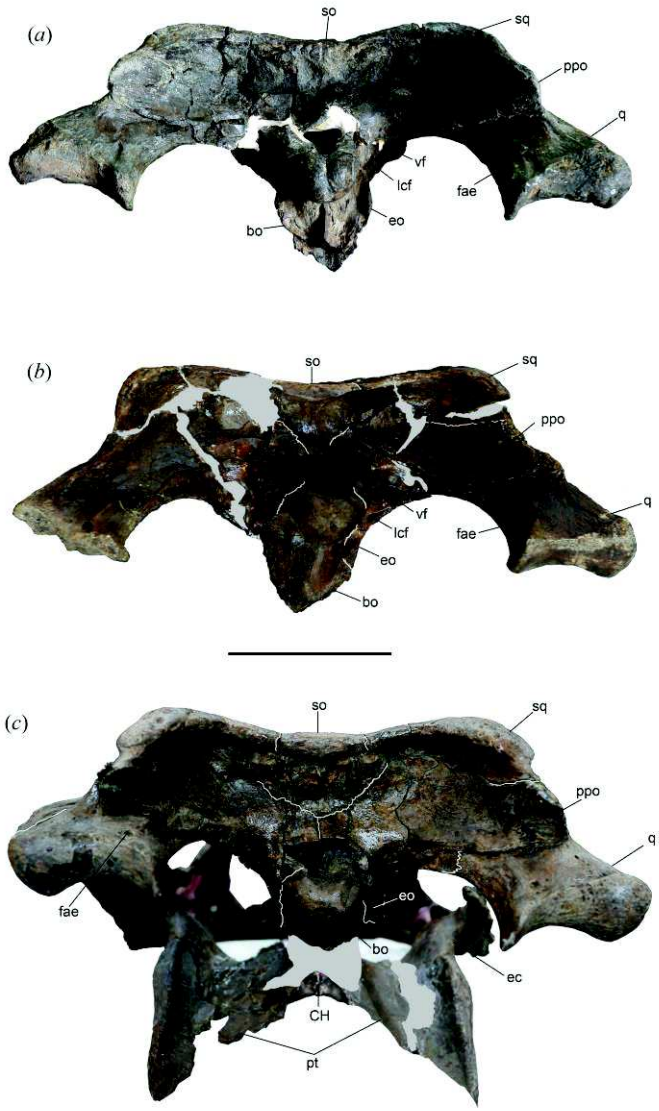

Figure IV.8. Occipital region. (*a*) *Kuttanacaiman iquitosensis*. MUSM 1942. (*b*) cf. *Kuttanacaiman iquitosensis* (MUSM 1728). (*c*) *Caiman wannlangstoni*, MUSM 2377 (holotype). For anatomical abbreviations see Appendices. Scale bar, 5 cm.

In the occipital plate, the squamosals and exoccipitals form concave depressions at each side of the supraoccipital bone. The postoccipital processes are only partially preserved at the medial boundary of these depressions. The ventral margin of the paraccipital processes lies directly on the medial projection of the quadrate, and is not separated from it as in *Caiman* and *Melanosuchus*. Thus, the cranioquadrate foramen in *Kuttanacaiman iquitosensis* is buttonhole-shaped. In MUSM 1942, the big vagi opening perforate the exoccipital at the level

of the foramen magnum. Below this opening, the smaller foramen for cranial nerve XII pierces the same bone lateral to the occipital condyle. In lateral view, the occipital condyle forms an acute angle with the basioccipital plate. The exoccipital ventral processes are long and slender. The medial crest of the basioccipital plate is thin and restricted to the ventral area of the plate.

The quadrates are similar to those of other caiman species, exclusive of *Gnatusuchus pebasensis*. In MUSM 1942, the foramen aerum is located on the dorsal surface of the quadrate. Ventrally, a distinct quadrate crest B is scored laterodorsally to the pterygoids. The quadrate crest A is smaller but particularly noticeable posterior to the infratemporal fenestrae. Although the proportions of the condyles are comparable with those of *Caiman* and *Melanosuchus*, the medial hemicondyle of *Kuttanacaiman* is medially displaced, thus the whole articular condyle has a relatively larger transversal diameter. In *Caiman*, *Melanosuchus*, and most caimanines, the medial condyle is ventrally deflected.

In the holotype, the palatine bones are damaged by minute cracks. These cracks affect mainly to the anterior processes, thus shape pattern and limits with the maxillae are not recognizable. In MUSM 1942, the left maxilla preserves the sutural contact for the palatine bone, indicating that the anterior processes of the palatines were rounded. Between the suborbital fenestrae, the bridge is constricted at the midway. Anterior and posterior to this constriction, the palatine bones flare into the suborbital fenestrae.

The pterygoids are well preserved in the holotype. They project anteriorly beyond the posterior level of the suborbital fenestra due to a sigmoid contact with the palatines, resembling the condition of *Melanosuchus* and *Eocaiman* (Simpson, 1933). The posterior pterygoid wings are tall. The relations between pterygoids and basisphenoids are not preserved.

Mandible. The mandible is wide at the symphysis region (Fig. IV.6). The dorsal profile of the dentary is gently curved. In MUSM 1736 and MUSM 1942, the dentary bears fifteen alveoli. The first and fourth alveoli are similar in size and the biggest in the series. Behind the fourth alveolus, the biggest one is the twelfth. From twelfth to 18th, the alveoli are laterally compressed, close together, and positioned within a straight, horizontal dorsal section of the ramus. The mandibular symphysis is relatively flat as in *Globidentosuchus brachyrostris*, but in lesser degree than in *Eocaiman cavernensis*. Similar to this latter taxon, the dentary symphysis reaches the level of the sixth alveolus and the splenial is excluded from the symphysis.

The splenial covers medially the Meckelian channel. The anterior dorsal process of the splenial is thin and medially deflected. By this process, left and right splenials approach each other at the posterior end of the symphysis but fail to contact. Posteriorly, the splenial gets higher to reach the dental series at the level of the interalveolar space between the 13th and 14th dentary alveoli. Posteriorly to this position, the splenial broadens and forms a relatively wide shelf medial to the alveolar series. In MUSM 1942, the splenial wall bears a single, relatively big opening interpreted here as the posterior aperture of the foramen intermandibularis oralis.

Behind the dental series, at the contact between the dentary and surangular, the dorsal profile of the mandibular ramus composed by the surangular deeply increases its height, differing to the continuous and slightly convex profile seen in *Caiman* and *Melanosuchus* (Fig. IV.6*a, c, f*). The angular-surangular suture contacts the external mandibular fenestra almost at the level of the posterior angle. Both aforementioned features are present in the holotype of *Eocaiman cavernensis* (see Simpson, 1933). The surangular bridge limiting dorsolaterally the adductor fossa is straight, long, and relatively slender. In *Melanosuchus*, this bridge is bowed outward. The adductor fossa is comparatively longer than that of

Paleosuchus and *Caiman* and, in this feature, it is similar to *Melanosuchus*. To the level of the adductor fossa, the posterior process of the dentary forms most of the upper margin of the external mandibular fenestra, thus the surangular is restricted to the posterior angle of the fenestra (MUSM 1736). The retroarticular process is similar to that of *Caiman*, and relatively low compared to that of *Paleosuchus*. The surangular extends to the posterior end of the reatroarticular process.

Dentition. The dental formula is 5 + 13/18. All teeth present a distinct neck at the limit between the crown and the root. In the premaxilla, interalveolar spaces are fairly large, exclusive of the smaller space separating the second and third alveoli. Premaxillary teeth crowns are unknown, but they might have resembled the anterior maxillary teeth preserved in the holotype (i.e., MUSM 1490). The teeth of the anterior region of maximum alveolar diameter in the maxilla, as well as the first eight or nine dentary teeth, are conical in shape, bear sharp carinae, and the crown surface is smooth. Teeth of the posterior region of maximum alveolar diameter are laterally compressed and bear distint minute radial ridges. Among them, from seventh to nineth teeth bear blunt crowns. The last four teeth are globular, flattened, sub-equal in size, and closely packed (Fig. IV.23*e*). The last five dentary teeth show this same morphology. As in living caimans, the largest tooth posterior to the fourth is the twelfth.

Juvenile specimens. MUSM 1928 and MUSM 2394 from IQ114 are skull tables interpreted here as belonging to juvenile ontogenetic stages of *Kuttanacaiman iquitosensis* (Fig. IV.7*e*, *f*). Both specimens differ mainly on their size, representing MUSM 1928 a smaller individual. Like specimens representing adult individuals, MUSM 1928 and MUSM 2394 bear a slender and flat interorbital bridge and a heavily sculpted skull table dorsal surface. Compared to the adult condition observed in MUSM 1942, these specimens bear proportionally longer and larger supratemporal fenestrae with little overhanging rim. The

frontoparietal suture is deeply concave anteriorly. The supraoccipital is comparatively large and roughly trapezoidal whereas this bone in MUSM 1942 is triangular.

Kuttanacaiman Salas-Gismondi et al., 2015a

cf. *Kuttanacaiman iquitosensis* Salas-Gismondi et al., 2015a

Material. MUSM 1728, skull table and articular region (Figs. IV.7*b*, *d* and IV.8*a*)

Locality and horizon. Locality IQ26 (Chapter II.A; Fig. II.1), Iquitos area, Peru; Pebas Formation, late Middle Miocene, ca. 13 Ma; Mollusc Zone 8 (MZ8; Wesselingh et al., 2006a).

Remarks. MUSM 1728 (Figs. IV.7 *b*, *d* and IV.8*a*) represents an individual equivalent in size to MUSM 1942, the latter referred to *Kuttanacaiman iquitosensis*. The general morphology, proportions, and sutural patterns are similar in both specimens, including a slender, short and flat frontal interorbital bridge. Differences between MUSM 1728 and those of *Kuttanacaiman iquitosensis* include a trapezoidal supraoccipital in the skull table (triangular in *K. iquitosensis*), a ventrally deflected quadrate medial hemicondyle (medially deflected in *K. iquitosensis*), and shallow concave deppressions lateral to the supraoccipital bone in the occipital plate (deep concave deppressions in *K. iquitosensis*). Additionally, this specimen bears much smaller supratemporal fenestrae and strong development of the ventral quadrate crests, these highly variable in modern caimans (see Brochu, 1999).

Caiman Spix, 1825

Caiman wannlangstoni Salas-Gismondi et al., 2015a

Etymology. *wannlangstoni* after Wann Langston Jr., for his invaluable contributions to the knowledge of South American fossil crocodylians.

Holotype. MUSM 2377, partial skull (Figs. IV.8*c* and IV9); Table IV.6).

Locality and Horizon. Locality IQ26 (Chapter II.A; Fig. II.1), Iquitos area, Peru; Pebas Formation, late Middle Miocene, ca. 13 Ma; Mollusc Zone 8 (MZ8; Wesselingh et al., 2006a).

Referred specimens. MUSM 1983, associated cranial and mandibular elements (Fig. IV.10*a-e*), Locality IQ114; MUSM 1723, juvenile left dentary (Fig. IV.10*h-j*), Locality IQ26. Also AMU-CURS-49, a right premaxilla and maxilla, from the Urumaco Formation (Sánchez-Villagra & Aguilera, 2006: Fig. 3p, q).

Diagnosis. Small to medium-sized *Caiman* species diagnosed by the following combination of characters: high and blunt snout with lateral margins strongly sinuous and diverging posteriorly; canthi rostralii very prominent; maxilla bearing broad shelf extending into suborbital fenestra, prefrontals contacting medially; edges of orbits upturned; narial opening oriented anterodorsally; crown teeth smooth to ribbed within crown upper half; dentary and maxillary posterior teeth large, globular, tightly-packed, and rounded in section; pterygoid surface pushed inward anterolateral to choana; dentary symphysis extended to level of sixth alveolus.

General description. The holotype of *Caiman wannlangstoni* is a well-preserved partial skull lacking alveolar portions of the right premaxilla, left premaxilla and maxilla, and right jugal and quadratojugal (Fig. IV.9). Some distortion is observed in the left articular region by dorsal compression. In general, alveolar region of the maxillae is badly damaged. Palatines are lacking. MUSM 1983 provides data on the alveolar pattern of the maxillae and the dentaries.

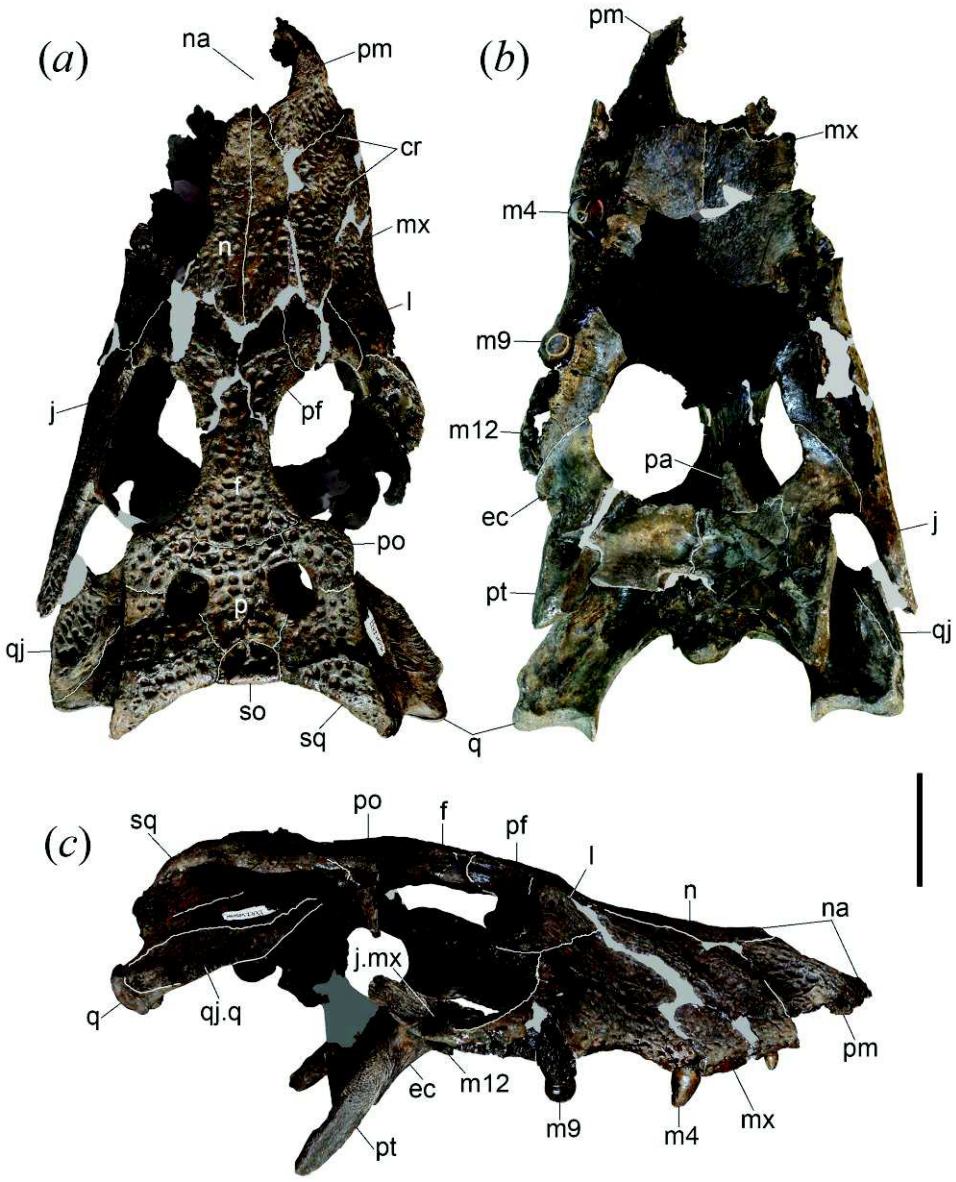

Figure IV.9. ***Caiman wannlangstoni.*** Skull (holotype, MUSM 2377) in dorsal (*a*), ventral (*b*), and right lateral (*c*) view. For anatomical abbreviations see Appendices. Scale bar, 5 cm.

The skull is roughly triangular in dorsal view. It bears a markedly high and robust rostrum. The ornamentation of the dorsal surface of the skull comprises relatively big pits. The nasal bones project into a fairly large narial opening. The orbits are oval and large. The jugal barely reaches the anterior margin of the orbits, thus its medial contact with lacrimal is reduced. The supratemporal fenestrae are constricted, as is typical in caimanines. Posterior margin of skull table is semicircular and overhangs the occipital plate. Configuration of the

skull table bones resembles that of *Caiman latirostris* and *Melanosuchus niger*. *Caiman wannlangstoni* differs from *K. iquitosensis* in having upturned orbital edges (character 137-1), canthi rostralii (character 96-1), alveoli circular in cross section (character 79-0), pterygoid surface lateral and anterior to internal choana pushed inward (character 123-1), and surangular-angular suture intersecting external mandibular fenestra along its ventral margin (character 60-1). Here, we refer AMU-CURS-49, a right premaxilla and maxilla, from the Urumaco Formation (Sánchez-Villagra & Aguilera, 2006) to *C. wannlangstoni* based on the presence of strong sinuous rostral margins and robust globular posterior teeth. UCMP 39978, a partial skull from La Venta (Colombia), was originally referred to *C. lutescens* (Langston, 1965) and more recently to *C. latirostris* (Bona et al., 2013). It shares several features with *C. wannlangstoni* and might belong to this new species as well. However, La Venta *Caiman* lacks the distinctive high rostrum and anterodorsally narial opening observed in *C. wannlangstoni*. Although preserved teeth are blunt, there is no conclusive evidence that La Venta *Caiman* had enlarged and globular posterior teeth.

Table IV.6 – Measurements (mm) of the holotype of *Caiman wannlangstoni*. MUSM 2377, skull. Measurements after Langston (1997). Measurements with missing data are omitted. Abbreviations: e, estimate; m4, fourth maxillary alveolus.

	MUSM 2377
Transverse diameter of skull, level of jaw articulation	182.0
Basal length of the skull	296.0e
Transverse diameter of skull, level of anterior ends of orbits	146.0
Length of the snout, anterior end of the orbits to tip of the snout	163.0e
Length of skull, posterior edge of skull table to tip of snout	299.0e
Least transverse diameter, interorbital space	29.1
Length of orbits	76.6
Length of skull table	68.1
Transverse diameter of skull table, posteriorly	115.0
Transverse diameter of skull table, anteriorly	95.9
Width of orbits	59.4
Transverse diameter of nares	19.4
Transverse diameter of choanae	20.9
Length of suborbital fenestra	55.5
Height of occipital condyle	17.4
Transverse diameter of occipital condyle	24.2
Transverse diameter of snout at m4	119.0e
Maxillary teeth series length (13 alveoli)	155.1

Consequently, we propose to treat it as a distinct entity of uncertain taxonomic affinities until more anatomical data are available. *Caiman brevirostris* from Acre (Brazil) and probably Urumaco (Venezuela) (Fortier et al., 2014) can be distinguished from *C. wannlangstoni* in having a proportionally shorter and parallel-sided rostrum as well as long dorsal premaxillary processes (character 90-1), prefrontals separate by frontal bone (character 129-1), and pterygoid surface lateral and anterior to internal choana flush with choanal margin (character 123-1). Total body length of *C. wannlangstoni* estimate is 210.5-226.7 cm (see Table IV.1).

Skull. The premaxilla is incomplete in the holotype and absent in MUSM 1983. It borders laterally the narial opening (Fig. IV.9). The posterior process of the premaxilla is short. The nasals are massive and widens posteriorly. The canthi rostralii are strong and similar to those of *Melanosuchus*, *Caiman latirostris*, and La Venta *Caiman*. The maxilla of *Caiman wannlangstoni* bears twelve circular alveoli. Festooning of the alveolar edges is particularly pronounced. Anterior region of maximum alveolar diameter is projected laterally and includes the first six or seven alveoli. The level of the eighth maxillary alveolus marks the beginning of the posterior region of maximum alveolar diameter. In this position, the maxilla extends laterally and ventrally. The fouth and ninth maxillary alveoli are the biggest and similar in diameter. The ninth alveolus is around twice the dimeter of the eighth. The twelfth alveolus is around half the diameter of the eleventh. Most alveoli are closed together with the exception of the larger gaps between the sixth and seventh and the seventh and eighth alveoli. Occlusion cavities are present medially sixth, seventh, and eighth maxillary alveoli, but they are shallower than in *K. iquitosensis*. The maxilla bears a broad shelf extending into the suborbital fenestra. The anterior process of the ectopterygoid is short and stout. Posteromedially, the suture of the maxilla with the ectopterygoid bears a flexure as in most advanced caimanines, including *K. iquitosensis*. Palatine-pterygoid suture is located beyond

the posterior margin of the suborbital fenestrae. The posterior process of the pterygoid is prominent and posterolaterally projected.

The lacrimal extends further anteriorly than the prefrontal. The anterior margin of the lacrimal is W-shaped by the presence of a posterior process of the maxilla within the lacrimal (Fig. IV.9). Both prefrontals make up an arcuate "spectacle" as in *Kuttanacaiman iquitosensis*. The postorbital bars are very slender. A small descending process of the postorbital borders posterodorsally the infratemporal fenestra as in other caimanines and *Alligator*. Lateral margin of the skull table is concave (Fig. IV.10*e*). The parietal is exluded from the posterior margin of the skull table. The supraoccipital on the skull table is trapezoidal. The anterior process of the frontal is very short and both prefrontals meet at midline in front of this process. The supratemporal fenestrae are oval in shape. In *Kuttanacaiman iquitosensis* they are comparatively smaller and circular in shape. The lateral quadrate hemicondyle is massive. The medial hemicondyle is ventrally deflected. The posterior margin of the skull table overhangs the occipital plate as in *Kuttanacaiman iquitosensis* (Fig. IV.8). The ventral border of the occipital plate is anteriorly displaced relative to the posterior margin of the skull table as in *Paleosuchus* and other high-rotrum crocodylians.

Mandible. The mandible is more robust and higher at the symphysis than that of *Kuttanacaiman*. The symphysis is composed only by the dentary and reaches posteriorly the level between the fifth and sixth dentary alveolus. Dorsal margin of the dentary is strongly festooned. The mandibles of *C. wannlangstoni* can be distinguished from those of *K. iquitosensis* by having proportionally larger first and fourth dentary alveoli, straighter medial dentary margin, circular posterior teeth and alveoli, concave dorsal margin along the series between the 13th and 18th dentary alveoli, and a surangular-angular suture that contacts the external mandibular fenestra along the ventral margin.

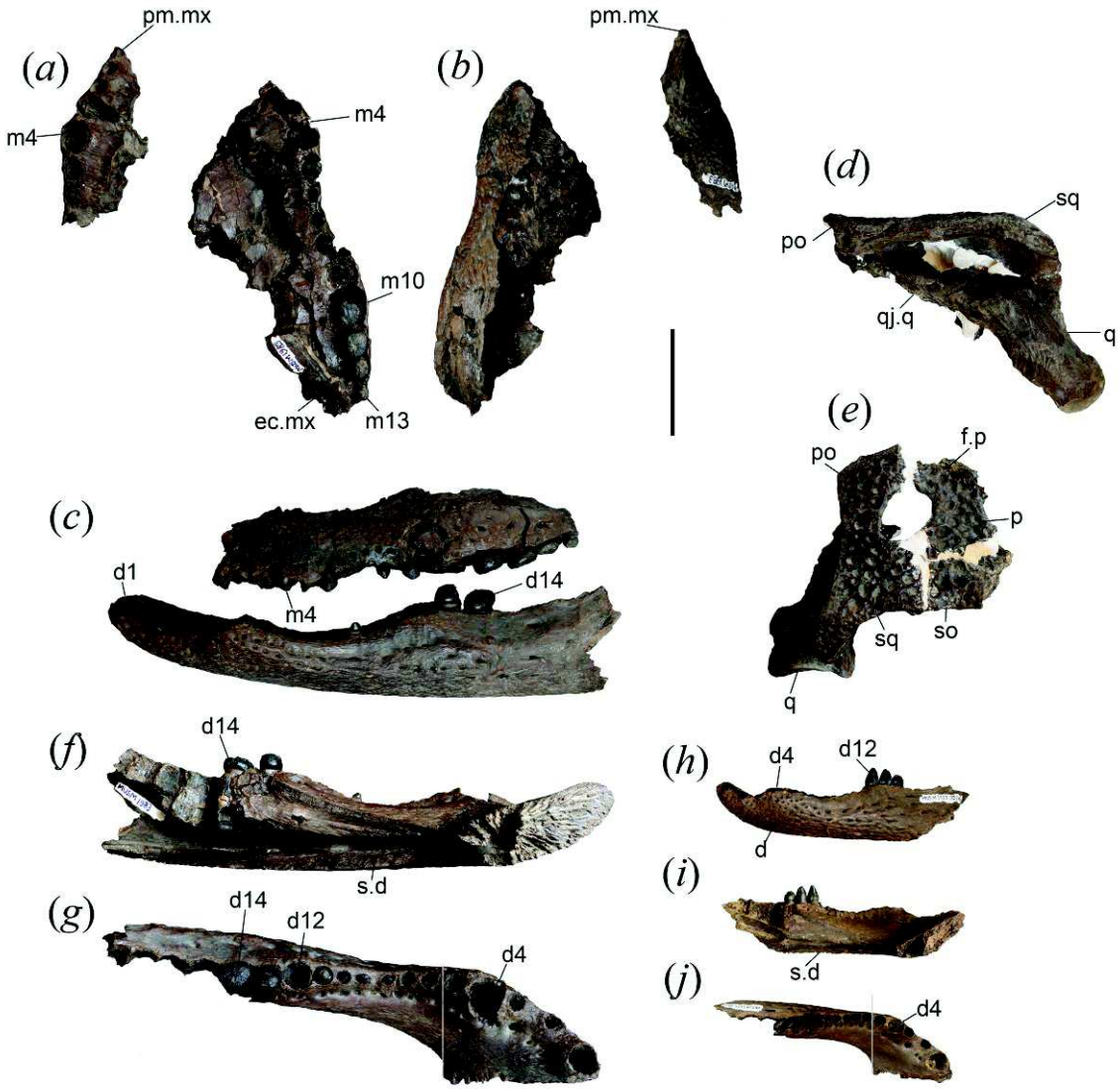

Figure IV.10. ***Caiman wannlangstoni.*** (*a-e*) Partial skull (MUSM 1983). Partial maxilla in ventral (*a*) and dorsal (*b*) view. Left maxilla and dentary in lateral (c) view. Dentary in medial (*f*) and dorsal (*g*) view. Partial skull table and left quadrate in lateral (*d*) and dorsal (*e*) view. (*h-j*) Left juvenile dentary (MUSM 1723) in lateral (*h*), medial (*i*), and dorsal (*j*) view. For anatomical abbreviations see Appendices. Scale bar, 5 cm.

Dentition. The dental formula is ? + 12/18. Dentition is similar to that of *K. iquitosensis*, but differs in having proportionally bigger and stouter globular teeth from the 13th to the 18th alveoli (Fig. IV.23*f*). Most teeth are severely worn.

Juvenile specimen. MUSM 1723 is a left dentary from IQ26 probably belonging to a juvenile of *Caiman wanlangstoni* (Fig. IV.10*h-j*). The splenial is excluded from the symphysis. Twelfth and 13th alveoli are nearly equal in size. Besides the first four alveoli, all

of them are close together. We support our identification of this specimen to *Caiman wannlangstoni* on the similar dorsal alveolar outline and the posterior extension of the symphysis reaching posteriorly the level between the fifth and sixth alveoli. It differs from adult specimens of *C. wannlangstoni* in bearing a broad medial dentary curvature behind the symphysis, similar to that of *Kuttanacaiman*.

Paleosuchus Gray, 1862

Paleosuchus sp.

Locality and Horizon. Locality IQ26 (Chapter II.A; Fig. II.1), Iquitos area, Peru; Pebas Formation, late Middle Miocene, ca. 13 Ma; Mollusc Zone 8 (MZ8; Wesselingh et al., 2006a).

Referred specimens and localities. From Locality IQ26 (MZ8): MUSM 1724, right maxilla (Figs. IV.11*b*, *c*, *e* and IV.13*a*); MUSM 1985, right maxilla (Fig. IV.11*a*, *d*); MUSM 1934, partial left premaxilla (Figs. IV.11*f*, *g* and IV.13*c*); MUSM 2380, partial right premaxilla (Fig. IV.11*h*, *j*). From IQ114 (MZ8): MUSM 1740, portion of right dentary (Fig. IV.12*a*, *c*, *d*). The following material from IQ114 is referred to cf. *Paleosuchus* sp. due to the lack of conclusive evidence on its identity: MUSM 1927, posterior portion of left maxilla; MUSM 1939, portion of left dentary; MUSM 1945, posterior portion of maxilla; MUSM 1989, partial right maxilla, jugal, and ectopterygoid.

Comparative description and remarks. The pebasian *Paleosuchus* species is represented by several rostral elements and one partial dentary of different individuals. All specimens, exclusive of the partial dentary, are similar in size among them and comparatively smaller than homologous elements of a skull of a mature *Paleosuchus trigonatus* available for comparison. This skull (MUSM DPV CR 1) measures 260 mm and belonged to an individual of 176 cm of total body length. The partial dentary (MUSM 1939) is slightly bigger than

MUSM DPV CR1, and therefore probably denoting an animal of larger body length. Total body length of modern species of *Paleosuchus* is normally less than 200 cm (Magnusson, 1992).

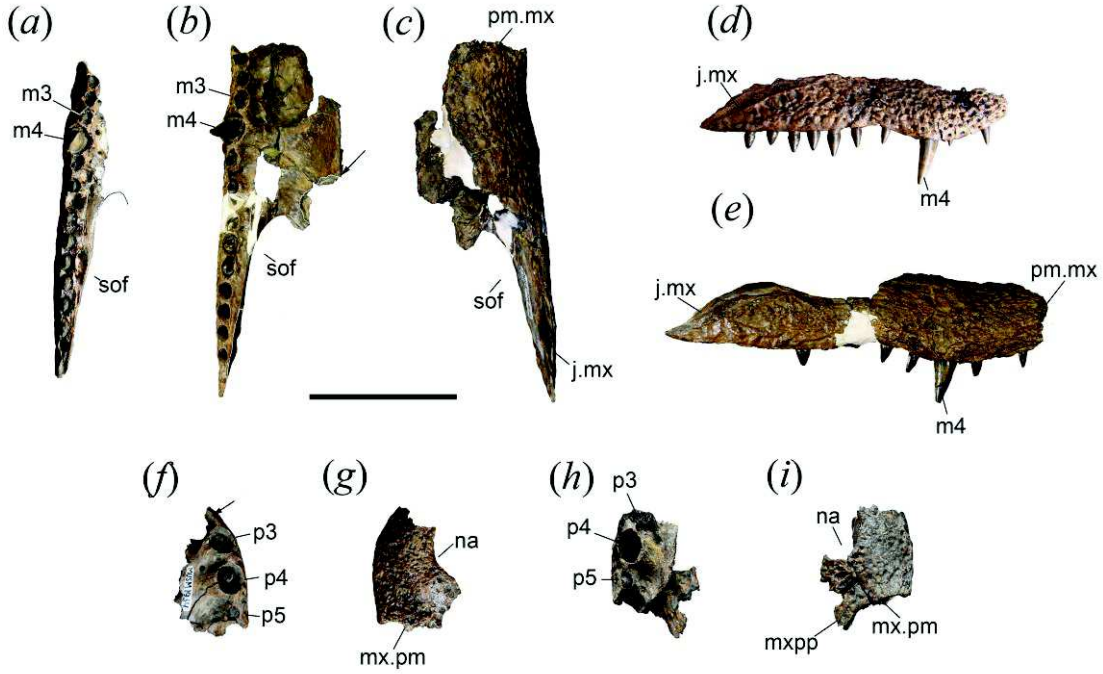

Figure IV.11. *Paleosuchus* sp. (*a*, *d*) Right maxilla (MUSM 1724) in ventral (*a*) and lateral (*d*) view. (*b*, c, *e*) Right maxilla (MUSM 1985) in ventral (*b*), dorsal (*c*), and lateral (*e*) view. (*f*, *g*) Partial left premaxilla (MUSM 1934) in ventral (*f*) and dorsal (*g*) view. (*h*, *i*) Partial left premaxilla (MUSM 2380) in ventral (*h*) and dorsal (*i*) view. For anatomical abbreviations see Appendices. Scale bar, 5 cm.

Rostral evidence depicts a relatively slender and high snout. The premaxilla (i.e., MUSM 1934) lacks of the second minute alveolus present in most crocodylian taxa thus, as the extant *Paleosuchus* species, it might bear four premaxillary alveoli (Fig. IV.13*c*, *d*). The narial opening flushes with the surrounding dorsal surface of the premaxilla. The fourth dentary tooth occludes in a pit within the premaxillary-maxillary contact.

Maxillae are lightly builted with vertically oriented lateral walls. The palatal surface of the maxilla is higher than the alveolar margin as in *Paleosuchus trigonatus*, but not as much as in *Paleosuchus palpebrosus*. The maxilla bears thirteen alveoli whereas extant *Paleosuchus* species have fifteen or sixteen alveoli (Mook, 1921b). The fourth alveolus is the biggest in the

maxilla. All other maxillary alveoli are much smaller and subequal in size, including the third one, which in modern extant *Paleosuchus* species is the second biggest in the maxilla (Mook, 1921b). The anterior margin of the suborbital fenestra reaches the level of the seventh alveolus. The anterior face of the palatine process is notched anteriorly (Fig. IV.13*a*, *b*). This palatine process extends anteriorly until the level of the interalveolar space between the fifth and sixth alveoli (i.e., MUSM 1724). MUSM 1724 and MUSM 1985 are right maxillae preserving total length and measuring 121.6 mm and 108.4 mm, respectively. The right maxilla of MUSM DPV CR 1 measures 145.5 mm.

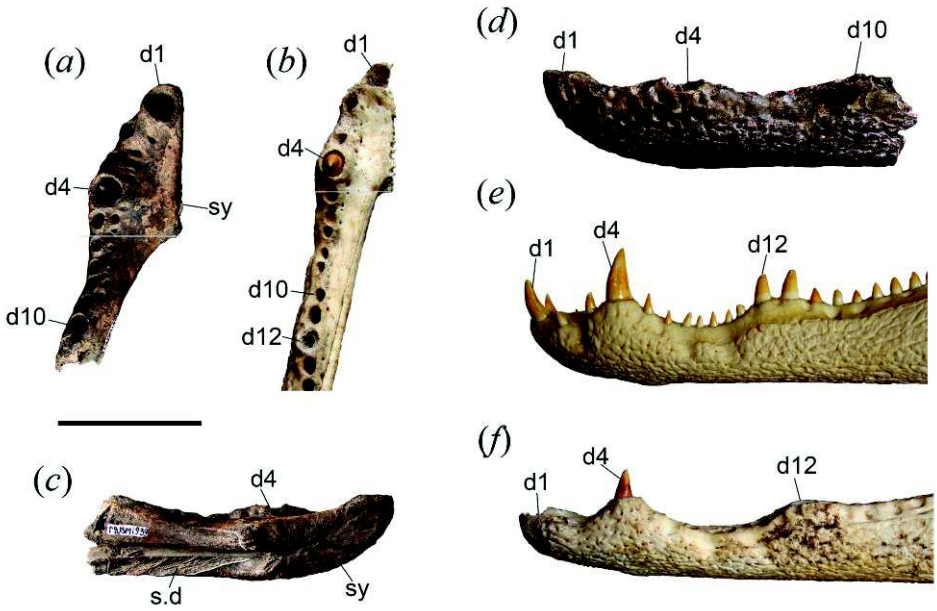

Figure IV.12. Dentary of *Paleosuchus*. (*a*, *c*, *d*,) Partial left dentary (MUSM 1939) in dorsal (*a*), medial (*c*), and lateral (*d*) view. (*b*, *f*) *Paleosuchus trigonatus* (MUSM DPV CR1) in dorsal (*b*) and lateral (*f*) view. *Paleosuchus palpebrosus* (MNHN n/n) in lateral (*e*) view. For anatomical abbreviations see Appendices. Scale bar, 5 cm.

The partial left dentary (MUSM 1939; Fig. IV.12) preserves the first eleven alveoli. First and fourth alveoli are the biggest and equal in size. Preserved alveoli are circular in cross section. Interalveolar spaces get progressively smaller backwards. The symphysis is relatively more robust and longer than extant *Paleosuchus* species. The posterior limit of the symphysis extends back to the level of the interalveolar space between the fifth and sixth dentary alveoli

(Fig. IV.12*a*). As extant *Paleosuchus* species, the dentary is not tranversally expanded at the fourth alveolus. A marked expansion in this position is observed in *Caiman crocodilus*. The dentary suture for the splenial almost contact the symphysis and, as in *Paleosuchus trigonatus*, ventral and dorsal processes of the splenial seem to have been equivalent in length. The dentary is gently curved between the fourth and the tenth alveoli differing from the deeply curved dentary in extant *Paleosuchus* species.

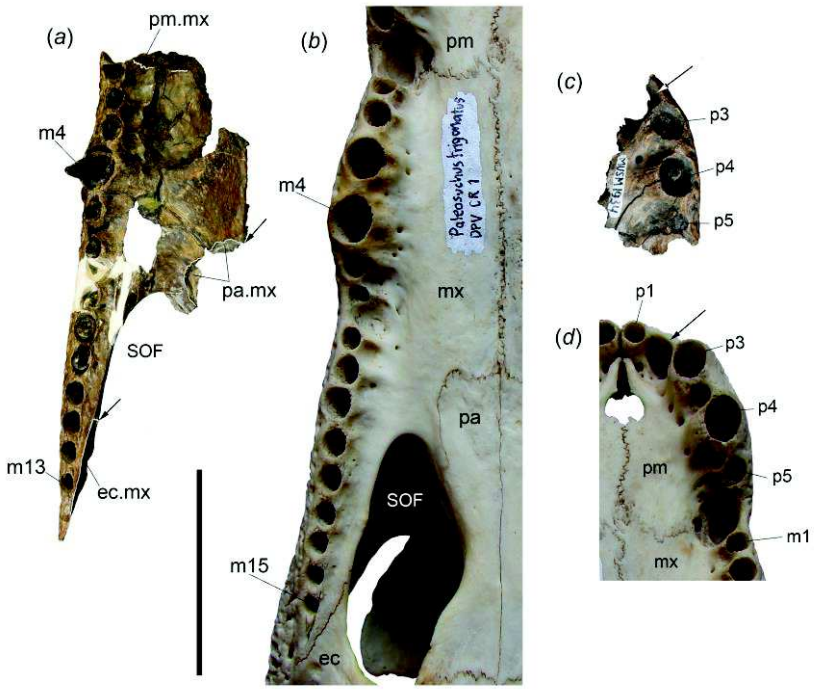

Figure IV.13. *Paleosuchus* sp. (*a*) Right maxilla (MUSM 1724) and (*c*) left premaxilla (MUSM 1934) compared with homologous parts (*b*, *d*) of extant *Paleosuchus trigonatus* (MUSM DPV CR1). Arrows in (*a*) show anterior limit of ectopterygoid and notched palatine**.** Arrows in (*c*) and (*d*) show alveolar space between p1 and p3 denoting the absence of p2 of other caimanines and consequently bearing just four premaxillary alveoli. For anatomical abbreviations see Appendices. Scale bar, 5 cm.

Dentition. The dental formula of the Pebasian *Paleosuchus* species is 4 + 13/?. Teeth are known from a number in the maxillae whereas only the fourth tooth is preserved in the dentary. The teeth are conical, slender, and sharply pointed. Crown teeth are straight with the fore and aft carinae dividing each crown tooth in two equivalent areas. The crown of the posterior teeth is slightly blunt. The crown teeth surface is smooth. In the maxilla, the eighth to thirteenth teeth are laterally compressed.

As in species of *Paleosuchus*, it has four premaxillary teeth (character 87-1) and a notched palatine anterior process (character 113-1). Although still poorly known, this fossil taxon (*Paleosuchus* sp.) differs from its extant relatives in having less maxillary teeth and a proportionally longer anterior process of the ectopterygoid running medially to posterior alveoli (Fig. IV.12*a*).

Purussaurus Barbosa-Rodrigues, 1892

Purussaurus neivensis (Mook, 1941)

Referred specimens and localities. From IQ26 (MZ8): MUSM 1731, left premaxilla (Fig. IV.14*a*, *b*); MUSM 1733, skull table (Fig. IV.14*d*); MUSM 1392, right dentary (Fig. IV.14*e*-*g*); MUSM 2413, skull table (Fig. IV.14*c*). From IQ114 (MZ8): MUSM 2075, tooth; MUSM 2076, tooth. From IQ116 (MZ8): MUSM 916, tooth. *Purussaurus* sp. from IQ125 (MZ9 or younger intervals): MUSM 2426, ten associated teeth (Fig. IV.18*b*).

Comparative description and remarks. Several isolated cranial, mandibular, and dental remains document the presence of *Purussaurus* within the Middle and Late Miocene Pebasian localities. Some cranial and mandibular bones (MUSM 1731, left premaxilla; MUSM 1733, skull table and; MUSM 1392, right dentary) from IQ26 might represent a single individual, slightly smaller in size than the type specimen of *Purussaurus neivensis* (UCMP 39704; Langston, 1965) from La Venta (Colombia). *Purussaurus* teeth are relatively common. Giant vertebrae were recovered from a number of localities and should belong to *Purussaurus*.

MUSM 1731 is a left premaxilla lacking the posterior dorsal process and the palatal surface medial to the fifth alveolus (Fig. IV.14*a, b*). The alveoli are distorted. The fourth premaxillary tooth is placed in its alveolus. The premaxilla is deep and wide. The external surface is decorated with pits and furrows. The narial opening flushes with the premaxillary surface. The premaxilla encircles the narial opening anteriorly, laterally and posterolaterally,

as other caimanines and *Purussaurus neivensis*, thus this opening is not elongated as in *P. brasiliensis* and *P. mirandai*. The palatal surface of the premaxilla is high relative to the alveolar margin. The premaxilla bears five alveoli, all of them relatively large. The biggest alveolus is the fourth. Deep pits for the recepcion of the anterior dentary teeth occur internal to the premaxillary alveoli. The margin of the incisive foramen is partially preserved. It seems to be teardrop-shaped. The anterior tip of the premaxillary foramen abuts the premaxillary tooth row.

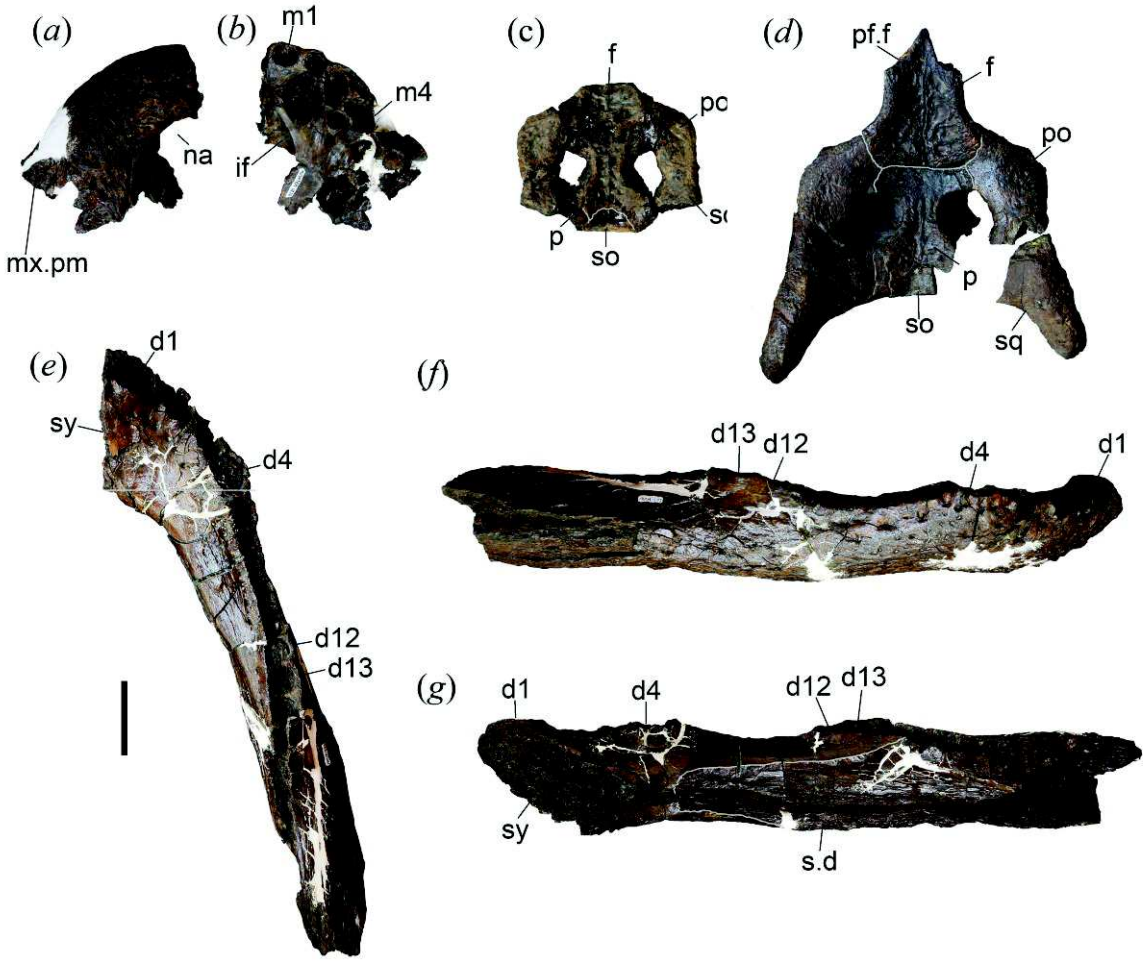

Figure IV.14. ***Purussaurus neivensis*.** Premaxilla (MUSM 1731) in dorsal (*a*) and ventral (*b*) view. (*c*) Skull table (MUSM 2413) in dorsal view. (*d*) Skull table (MUSM 1733) in dorsal view. (*e-g*) Right dentary (MUSM 1392) in dorsal (*e*), lateral (*f*), and medial (*g*) view. For anatomical abbreviations see Appendices. Scale bar, 5 cm.

The skull table (MUSM 1733) preserves frontal, postorbitals, parietal, and partially the supraoccipital and the squamosals (Fig. IV.14*d*). Within the skull table surface, the parietal and frontal are depressed medially whereas the squamosals form elevated posterior horn-like projections. The supratemporal fenestrae are slightly longer than wide and lack the overhanging rims typically observed in other caimanines. The frontal is shield-shaped. The anterior process of the frontal is short and triangular. The orbital margins are upturned. The frontoparietal suture is a straight line lying entirely on the skull table. Limits of the supraoccipital on the skull table are not well defined. In MUSM 2413, another partial skull table, the supraoccipital is trapezoidal in shape (Fig. IV.14*c*). The parietal is excluded from posterior edge of the skull table.

MUSM 1392 is a right dentary preserving several diagnostic features fairly known for *Purussaurus* (Fig. IV.14*e-g*). The posterior alveoli are incomplete and slightly distorted. The dentary is wide and massive at the level of the symphysis. The dentary bears 21 alveoli. The medial wall of the last three alveoli is lacking, probably because it was formed by the splenial. All the alveoli are closely spaced, exclusive of the first three alveoli. The symphysis is short, reaching posteriorly the level of the fourth alveolus (Fig. IV.14*e*). The four anterior alveoli are the biggest of the whole dentary. The dentary is expanded laterally at the level of the fourth alveolus. Posterior to the fourth alveolus, the biggest alveolus probably is the thirteenth, as can be observed in DGM 527-R, a mandible from Jurua River assigned to *Purussaurus brasiliensis* (Price, 1967; Aguilera et al., 2006). The dorsal edge of the dentary is modestly festooned. Medially, the dentary preserves the surface of contact for the splenial. The anterior limit of the splenial ends far behind the posterior limit of the symphysis, at the level of the sixth alveolus. The dorsal and ventral anterior processes of the splenial were equivalent in size and shape. The splenial reaches the medial alveolar margin behind the fourteenth alveolus. No tooth crowns are preserved. Alveoli are roughly circular. In dorsal view, posterior to the

fourth tooth locus, the lateral wall of the dentary is bowed medially and the alveolar row shifts medially. UCMP 38827 is an incomplete left dentary from La Venta, Colombia (Langston, 1965; figure 46). Here, this specimen is assigned to *Purussaurus* based on the presence of short symphysis, big anterior four alveoli, position of the anterior process of the dentary, and moderate dorsal festooning.

Teeth. Isolated *Purussaurus* teeth are relatively common remains in the Amazonian basin (Spillmann, 1949; Willard, 1966; Aguilera et al., 2006; Aureliano et al., 2015). However, few teeth were documented in their alveolar position, thus variation of tooth morphology is partially known along upper and lower quadrants. MUSM 916 is a big tooth measuring around 70 mm from the tip to the base of the crown. MUSM 3190 is similar in shape and proportions, but smaller in size. Its crown length is 45 mm. These teeth are massive and conical. The crown is circular in section at the base and roughly lentoid upper to it due to the strong carinae dividing the internal and external portions of the crown. The carinae bear pseudoziphodont ridges (Aureliano et al., 2015). The tip of the tooth is blunt. The blunt-point bears longitudinal ridges and striae. In MUSM 916 the crown surface is relatively smooth although longitudinal ridges are usually observed (i.e., MUSM 2262: Fig. IV.18*b*). MUSM 916 might represent the general morphology of the anterior teeth of upper and lower quadrants.

MUSM 2075, MUSM 2076, MUSM 3189 are similar to MUSM 916, but much blunter and smaller. The crown measures about 45-50 mm. They might belong to intermediate positions within upper and lower quadrants.

Mourasuchus atopus (Langston, 1965)

Referred specimens and localities. From IQ26 (MZ8): MUSM 1726, partial left maxilla; MUSM 1734, partial left maxilla (Fig. IV15*m*, *n*); MUSM 1735, left jugal (Fig.

IV19*e*); MUSM 1762, partial left maxilla; MUSM 1933, left premaxilla (Fig. IV.15*e-h*); MUSM 1984, partial right maxilla (Fig. IV.15k, l); MUSM 2077, posterior left maxilla; MUSM 2378, skull table and quadrates (Fig. IV.15*a-d*); MUSM 2379, jaw elements (Fig. IV.16), humerus, cervical vertebra, and scapula; MUSM 2496, right jugal (Fig. IV19*f*) From IQ114 (MZ8): MUSM 1966, right quadrate; MUSM 2074, right jugal.

Comparative description and remarks. The material includes isolated cranial bones and one specimen comprising associated elements of a single individual. Rostral bones document individuals of different sizes and probably major modifications occuring during the ontogeny.

Here, we document the first complete skull table and quadrates (MUSM 2378) belonging to *Mourasuchus atopus* (Fig. IV.15*a-d*). The laterosphenoids are incomplete. The transversal diameter at the level of the lateral articular condyle of the quadrates is 172 mm. Compared to other caimanines, the skull table is reduced in size, bear strong "eminences" (*sensu* Bona et al., 2012), and articular condyles of the quadrates are displaced posterolaterally. The supratemporal fenestrae are extremely reduced and slit-eyed in shape. The anterior process of the frontal is extremely short on the dorsal surface of the skull, but it continues anteriorly to underlap the prefrontals, probably beyond the anterior limit of the orbit. The interobital bridge is narrow. The margins of the orbits are markedly everted. The eversion of the orbital margin also comprises the postorbitals. The frontoparietal suture is linear and lies entirely of the skull table. The postorbitals limit the anterior margin of the supratemporal fenestrae. In MUSM 2378, the eminences are a half-ring-torus structure that strongly protrudes up the skull table. The existence of squamosal eminences was unknown for *Mourasuchus atopus*. This structure resembles more closely in shape and proportions to eminences of UFAC 1424, a specimen from the Late Miocene of Acre (Brasil) assigned to *Mourasuchus nativus* (Bocquentin-Villanueva & Souza Filho, 1990; Bona et al., 2012). we

recognized a squamosal eminence from LaVenta identical in shape and size to that of the Iquitos specimen, in old La Venta collections at the MNHN of Paris (Fig. IV.15*i*, *j*), suggesting that this morphology pertains also to *Mourasuchus atopus*.

Other *Mourasuchus* species show lesser degree of development or this structure is restricted to a transverse ridge confined to the posterior margin of the skull table (see Bona et al., 2012). In MUSM 2378, the eminences occupy the posterior half of the skull table and largely overlap its lateral and posterolateral margin. As described by Bona et al. (2012), the eminences are composed by the parietal, supraoccipital, and squamosals. The parietal surface is vertical since this bone takes part of the anterior wall of the eminences. The supratemporal fenestrae face anteriorly and the parietal borders it dorsally. The supraoccipital briefly contacts the parietal anteriorly but has extensive contact with the squamosals laterally. The squamosals comprise most of the eminences volume. The squamosals bear putative vascular channels that lead to the supratemporal fenestrae (Bona et al., 2012). The squamosal groove for the ear flap musculature is wide, shallow, and particularly large. Although this groove is restricted to the lateral side of the skull table in all crocodylians, in MUSM 2378 the groove continues dorsomedially to the skull table surface, between the emerged posterior orbital margins and the base of the eminences. The occipital plate is a vertical, tall and wide, concave surface (Fig. IV.15*c*). The occipital plate is roughly triangular to trapezoid in shape, with the eminences capping it. On this plate, although the supraoccipital is tall, it is excluded from the foramen magnum by the exoccipitals. The postemporal fenestrae are limited ventrally and dorsally by the supraoccipital and the squamosals, respectively. The postemporal and supratemporal fenestrae are equivalent in size. The processes postoccipitales (sensu Kälin, 1933) are not prominent. The squamosals extend posterolaterally to form a long and thin crest that limits the occipital plate laterally. This crest is placed along the paraoccipital process of the exoccipitals and the quadrate rami.

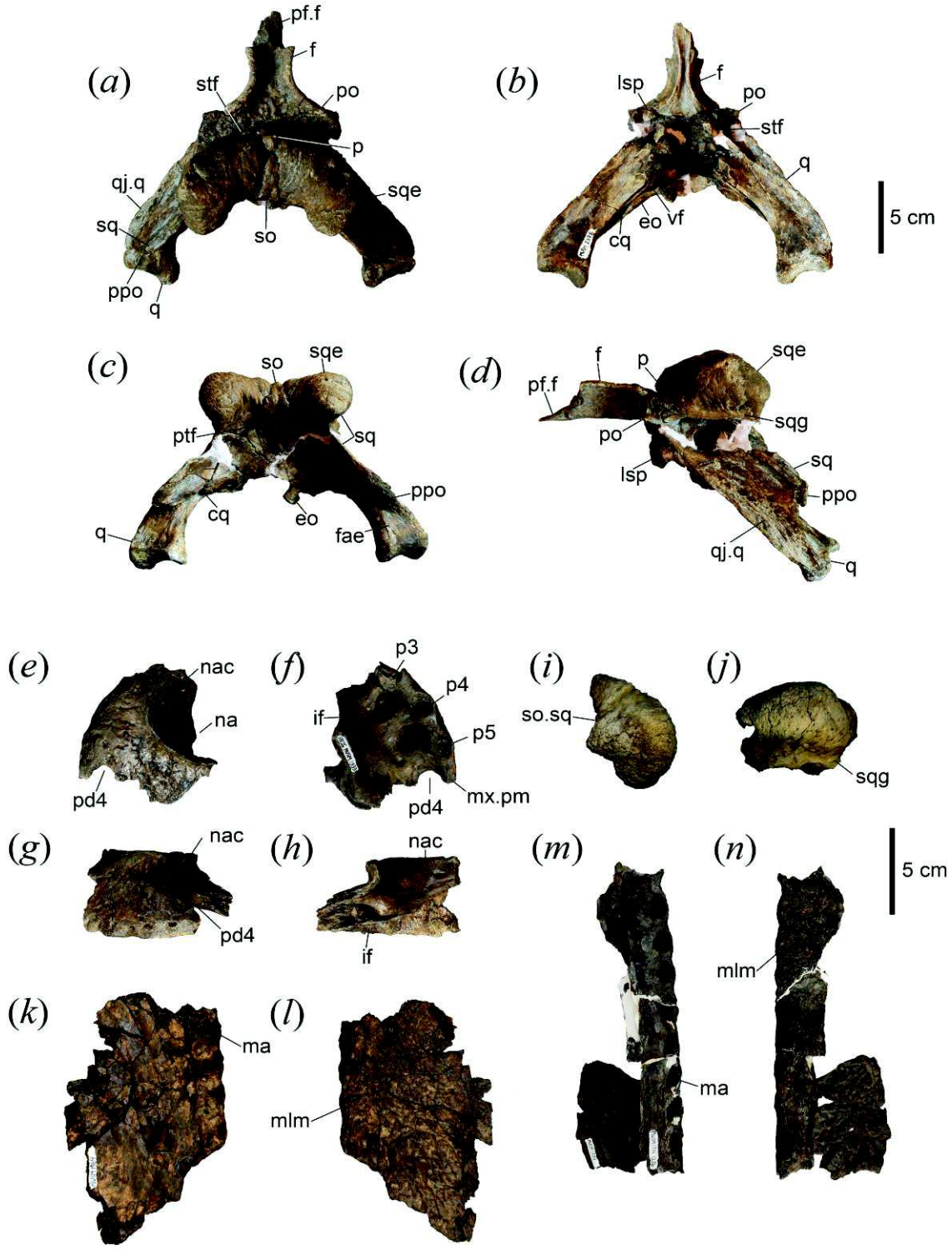

Figure IV.15. ***Mourasuchus atopus.*** (*a-d*) Skull table and quadrates (MUSM 2378) in dorsal (*a*), ventral (*b*), posterior (*c*), and left lateral (*d*) view. (*e-h*) Partial left premaxilla in dorsal (*e*), ventral (*f*), lateral (*g*), and posteromedial (*h*) view. (*i, j*) squamosal eminences (MNHN n/n) from La Venta in dorsal (*i*) and lateral (*j*) view. (*k-n*) Portions of maxilla. MUSM 1984 in ventral (*k*) and dorsal (*l*) view. MUSM 1734 in ventral (*m*) and dorsal (*n*) view. For anatomical abbreviations see Appendices. Scale bar, 5 cm.

The quadrate rami and the paraoccipital processes are both elongated compared with other crocodylians. On the dorsal surface of the quadrate, the foramen aerum is shift medially. The articular condyles of the quadrate are robust. The main axis of articulation is oblique, with the medial hemicondyle positioned higher and posterior relative to the lateral hemicondyle. On the ventral surface of the quadrate, crest A' and B (*sensu* Iordansky, 1976) are observed. The laterosphenoids are thick. The contact surface of the frontal bone for the laterosphenoid is wide and denticulated.

MUSM 1933 (Fig. IV.15*e-h*) is a partial left premaxilla similar in size and shape to the type of *Mourasuchus atopus* (UCMP 38012; Langston, 1965: figure 15). The premaxilla lacks the first and fifth alveoli, as well as its posterior dorsal process. This bone is characterized its light construction and thin walls. The alveoli are located within a low, collar-like rim. Internal to this rim, the palatal surface is elevated to almost reach the level of the dorsal surface of the premaxilla, denoting the typical flat snout morphology of *Mourasuchus*. As *Mourasuchus atopus*, the narial opening bears a high and sharp narial margin. Medial to this margin, a smooth convex lip-like surface descends into the opening. Ventrally, the premaxilla presents deep pits for the first to third dentary teeth and half of a notch for the fourth dentary teeth, at the premaxillary-maxillary suture. The fourth and the fifth alveoli are complete whereas the third is only partially preserved. The alveoli are roughly circular. The fourth alveolus is slightly bigger than the other preserved ones. The shape of the incisive foramen is not discernable. The dorsal surface of the premaxilla is irregular but relatively smooth. The sculpture comprises disperse grooves and foramina.

Pieces of the maxillae correspond to individuals of disparate sizes as well as portions of different regions within the snout. Identification of most of the maxillae portions is inferred from the alveolar series pattern. The maxilla is flat and wide. The alveolar margin is straight and paraxial. MUSM 1984 is an intermediate portion of the right maxilla preserving four

alveoli and the actual transverse diameter of the maxilla on the palate (Fig. IV.15*k*, *l*). This specimen is flattened by post mortem compression. The alveoli are circular and widely spaced. The interalveolar distance is larger than the alveolar diameter and is shorter in between the last two preserved alveoli. Medial to the interalveolar space, the palatine surface of the maxilla bears distinct cavities for the reception of dentary teeth. These cavities are shallower anteriorly. The lateral margin bears gentle depressions between alveoli. The sculpture consists of abundant shallow furrows.

MUSM 1734 (Fig. IV.15*m*, *n*) and MUSM 1762 are contiguous portions of the left maxilla probably belonging to a single individual. Both specimens preserve the lateral margin with several alveoli and should correspond to areas right in front the suborbital fenestra. The alveoli in these specimens are twice the size of those in MUSM 1984 and about one-third bigger than those of the type of *Mourasuchus atopus* (UCMP 3812; Langston, 1965: figure 16). Contrary to what is observed in MUSM 1984, the interalveolar space is smaller than the alveolar diameter, possibly because MUSM 1734 corresponds to a more posterior area within the maxilla than MUSM 1984. The alveoli are circular in MUSM 1734 and laterally compressed in MUSM 1762. The most posterior alveoli in *M. atopus* are laterally compressed. MUSM 1734 presents gentle undulations along the lateral margin. The dorsal and lateral surfaces of the maxilla are distinct, flat planes forming a right angle. The lateral surface is low, vertical, and perforated by a number of vascular foramina. The dorsal surface of the maxilla is flat and horizontal. This surface is relatively smooth. No surface contact for adjacent bones is observed.

MUSM 1726 and MUSM 2077 correspond to mostposterior portions of the left maxilla, lateral to the suborbital fenestra. Alveoli in this position are laterally compressed and closely spaced. The maxilla has a lineal medial margin adjacent to the suborbital fenestra. Dorsally, a wide maxillary surface contact for the overlapping jugal is preserved. The anterior

limit of this surface and that of the suborbital fenestra reach the level of the ninth maxillary alveolus counting from the last alveolus.

The jugal is flat anteriorly and oval in section posteriorly. MUSM 2074 preserves the anterior process of the jugal and the ascending process for the postorbital pillar. The ascending process of the jugal is inset from the jugal horizontal ramus. The jugal orbital margin bears an uptuned rim. The medial contact of the jugal with the lacrimal is long and straight. The contact surface with the lacrimal also includes a triangular smooth facet of the ventral side of the bone. Lateral to this facet, a big flat surface to overlap and contact the maxilla comprises most of the anterior process of the jugal. Posteriorly, a small contact with ectopterygoid is denticulated and extends to the ascending process of the postorbital pillar.

From IQ26, two jugals lacking the anterior portion that overlaps the maxilla were recovered (Fig. IV.19*e*, *f*). These bones preserve the massive posterior process of the jugal that constitute most of the lower bar of the infratemporal fenestra. The horizontal bar of the jugal is high at the level of the postorbital bar. Posterior to it, the bar is low, thick, and roughly oval in section. The bar is bowed outward as is typical in *Mourasuchus atopus*. In *M. amazonensis* (Price, 1964) and *M. nativus* (Bocquentin-Villanueva & Souza Filho, 1990), this bar bears an angular lateral margin due to the abrupt expansion of the postorbital region of the skull. The postorbital process of the jugal is relatively flat. Medially, the contact surface for the ectopterygoid is demarcated by vertical grooves. On the horizontal ramus, the ectopterygoid bore a posterior pointed process. A small foramen is located at the posterior base of the postorbital pillar. The lower bar of the infratemporal fenestra is excavated medially for the reception of the quadratojugal. From IQ26, associated bones of *M. atopus* include a well-preserved partial mandible (Fig. IV.16). It comprises the right dentary and splenial, including the first nineteen alveoli. The mandible is long and slender. The whole preserved portion is tubular-shaped and presents an invariable oval section.

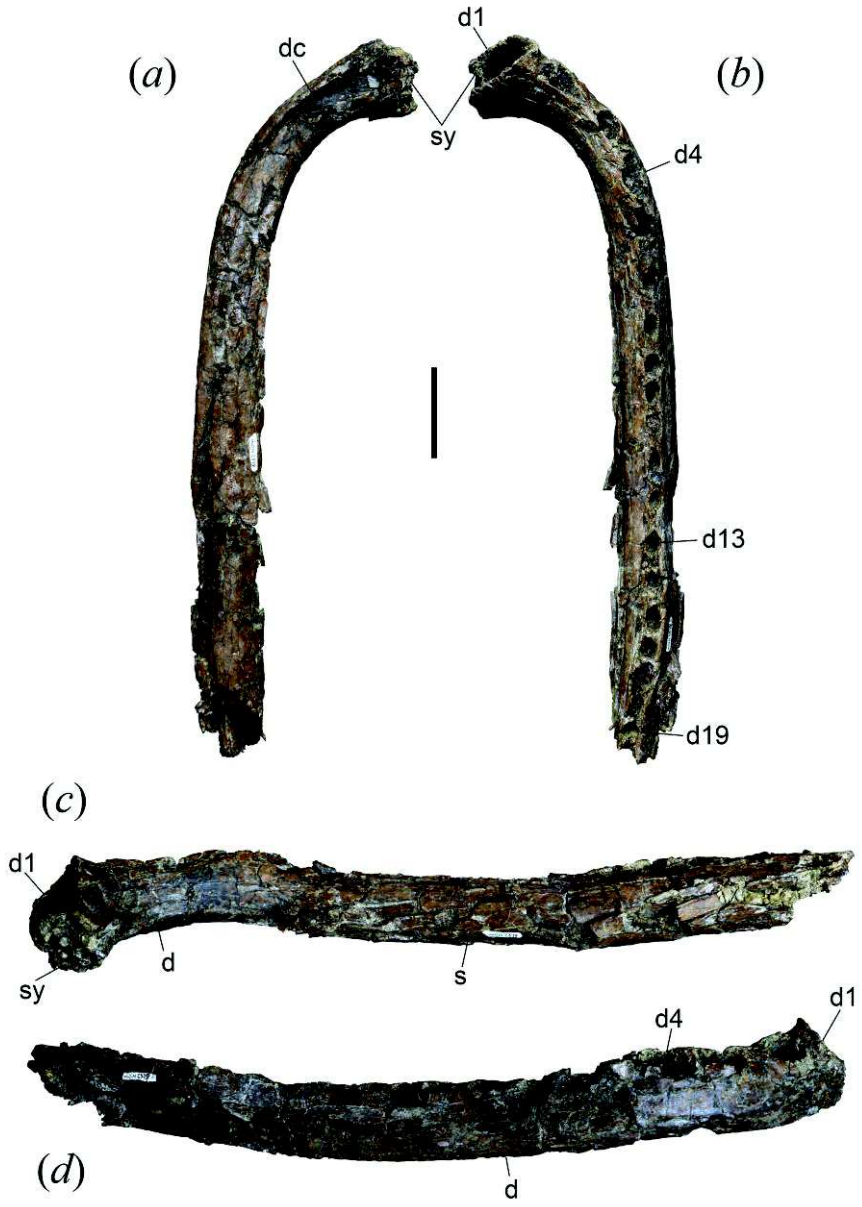

Figure IV.16. ***Mourasuchus atopus*.** Right dentary (MUSM 2379) in ventral (*a*), dorsal (*b*), medial (*c*), and lateral (*d*) view. For anatomical abbreviations see Appendices. Scale bar, 5 cm.

The symphysis is extremely short, comprising only the length of the first alveolus. The mandible reaches the symphysis plane at a right angle and, from this position it describes a broad curvature to become parallel to the longitudinal axis behind the fifth alveolus. The anterior limit of the splenial is obscured by cracks, but probably reaches anteriorly beyond the eighth dentary alveolus. The biggest alveolus is the first one. It seems to be that this alveolus diameter is more than twice the diameter of the second, third, and fourth alveoli, and all these latters of similar size. These four first alveoli are the biggest in the mandible. The first and

second alveoli are oriented anterodorsally; other alveoli face dorsally. Posteriorly to the fourteenth alveolus, the interalveolar distances are reduced. Exclusive of the first alveolus, all the alveoli are slightly laterally compressed. No teeth are preserved. The Meckel's groove is not identified. The ventral surface of the dentary is transversally rounded. In this surface, posterolateral to the symphysis, Langston (1965) described for *Mourasuchus atopus* a wide longitudinal trough. More than a longitudinal trough, in MUSM 2379 this surface bears a distinct longitudinal crest bordering the lower margin of the external wall of the dentary until the level of the fifth alveolus.

C.2 Nueva Unión caimanines

Alligatoroidea Gray, 1844

Globidonta Brochu, 1999

Caimaninae Brochu, 1999.

Gnatusuchus pebasensis Salas-Gismondi et al., 2015a

Material. MUSM 2393, posterior half of the right mandibular ramus (Fig. IV.17*a*, *c*, *e*), Locality IQ125 (Chapter II.A; Fig. II.1).

Comparative description and remarks. The specimen is the posterior portion of a right mandible comprising the surangular, the angular, the articular, and the wall of the dentary anterior to the external mandibular fenestra (Fig. IV.17*a*, *c*, *e*). The lateral surface of the ramus is smashed and distorted. Most sutural limits in this side are hidden by cracks. The size and general shape of this specimen is equivalent to MUSM 1979 (Fig. IV17*b*, *d*, *f*), a complete right mandible from IQ114 (MZ8). The total length of this latter mandible is 308 mm (Salas-Gismondi et al., 2015a).

The external mandibular fenestra is large and ovoid in shape. The dentary that borders anteriorly the external mandibular fenestra is thin-walled. The ventral posterior process of the

dentary is restricted to the anterior half of the fenestral margin. The dorsal posterior process is much longer but apparently fails to reach the rear angle of the fenestra. As described for *Gnatusuchus*, the angular and the surangular are massive bones (Salas-Gismondi et al., 2015a). The surangular bridge above the external mandibular fenestra is wide and bears an eaves-like medial projection that embraces dorsally the adductor fossa. This condition is typical of *Gnatusuchus* and is related with a wider and more capacious adductor fossa than usually in crocodylians (Salas-Gismondi et al., 2015a). The lateral wall of the glenoid fossa is high and confines a deep, concave articular surface for the lateral hemicondyle of the quadrate.

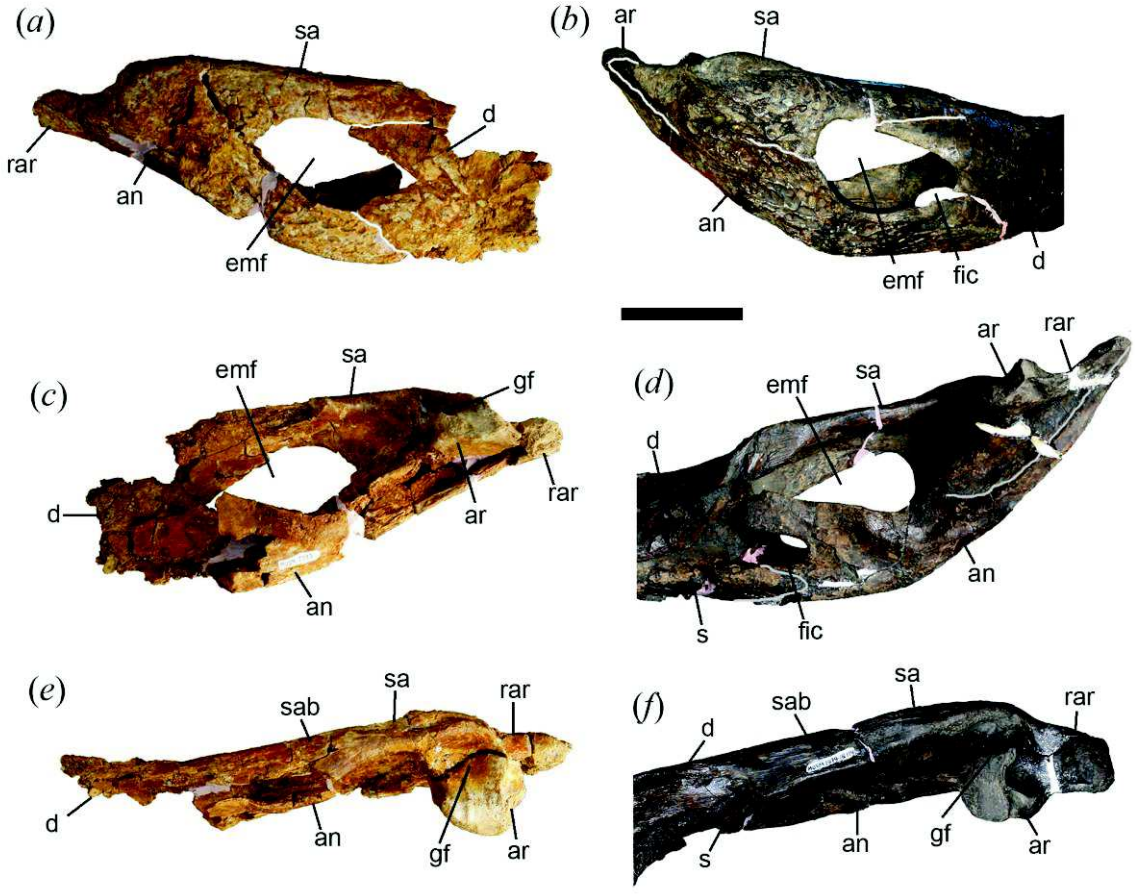

Figure IV.17. *Gnatusuchus pebasensis* from Nueva Unión. Posterior mandibular rami from Nueva Unión (MUSM 2393) in lateral (*a*), medial (*c*), and dorsal (*e*) view. For comparison, the anatomical area in MUSM 1979 from Iquitos in lateral (*b*), medial (*d*), and dorsal (*e*) view. For anatomical abbreviations see Appendices. Scale bar, 5 cm.

The articular-surangular contact within the genoid fossa is anteromedially oriented (i.e., oblique), thus the surangular has a larger articular surface for the lateral quadrate hemicondyle than the articular. The surangular extends to the posterior end of the retroarticular process.

Purussaurus Barbosa-Rodrigues, 1892

Purussaurus sp.

Material. MUSM 2262, large tooth (Fig. IV.18*a*), Locality IQ129; MUSM 2426, ten associated teeth (Fig. IV.18*b*), Locality IQ125 (Chapter II.A; Fig. II.1).

Comparative description and remarks. MUSM 2262 is the largest tooth found within the Iquitos and Nueva Unión area. The height of the tooth crown (measured from the tip to the base of the crown) is 92 mm. It is conical in shape and extremely robust, being bigger and more massive than other large teeth of *Purussaurus* from Acre (Aureliano et al., 2015: figure 5) and Urumaco (Aguilera et al., 2006: figure 4).

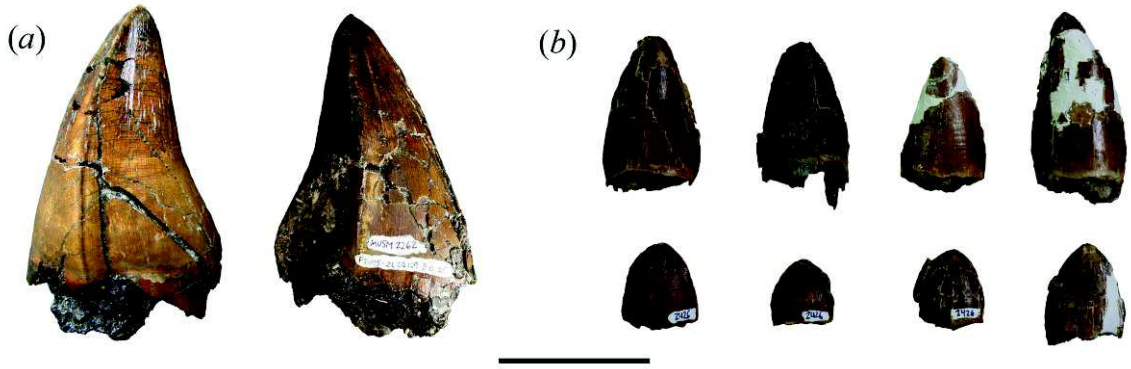

Figure IV.18. *Purussaurus* teeth from Nueva Unión. (*a*) MUSM 2262, isolated large tooth. (*b*) MUSM 2426, associated teeth showing morphological disparity within a single individual. Scale bar, 5 cm.

The transversal section of the crown is circular and roughly lentoid. Strong carinae divide the internal and external portions of the crown. The base of the crown is particularly expanded. The carinae bear pseudoziphodont ridges (Aureliano et al., 2015). The tip of the tooth is blunt. In this tooth, the crown surface is relatively smooth at the base and presents longitudinal

ridges towards the tip. This tooth might correspond to the anterior tooth loci of upper or lower quadrants.

We found ten associated teeth regarded as belonging to a single individual in Nueva Unión locality IQ125 (Fig. IV.18*b*). These teeth include the characteristic robust, conical teeth of *Purussaurus* as well as other smaller, blunt teeth with a constricted neck at the base of the crowns. This assemblage also includes teeth with intermediate morphologies. The crown height of the conical teeth ranges from 30 to 45 mm. Blunt teeth average height is 20 mm. The latter teeth might belong to intermediate or posterior positions within jaws.

Mourasuchus Price, 1964

Mourasuchus sp.

Material. From Locality IQ125: MUSM 2427, partial left jugal (Fig. IV.19*a*, *c*); MUSM 2477, partial left jugal (Fig. IV.19*b*, *d*); MUSM 3191, large osteoderm (Fig. IV.19*g*); MUSM 2428, small osteoderm (Fig. IV.19*g*).

Comparative description and remarks. Two posterior portions of jugals (MUSM 2427 and MUSM 2477: Fig. IV.19*a*-*d*) were recovered from IQ125. The size of these specimens is about twice larger than those from IQ26. The horizontal bar of these jugals bears an angular lateral margin as in *Mourasuchus amazonensis* (Price, 1964) and *M. nativus* (Bocquentin-Villanueva & Souza Filho, 1990).

MUSM 2428 and MUSM 3191 are isolated osteoderms here referred to *Mourasuchus* based on the presence of high, "plump", cornuted spikes (Langston, 2008;
Scheyer & Moreno-Bernal, 2010). In specimens from Nueva Unión, the spike constitutes most of the osteoderm since the base of the osteoderm is restricted to the base of the spike. The height of the MUSM 2428 is around 40 mm whereas this measure is MUSM 3191 is 54 mm. The spike of MUSM 2428 is more slender than that of specimen MUSM 3191.

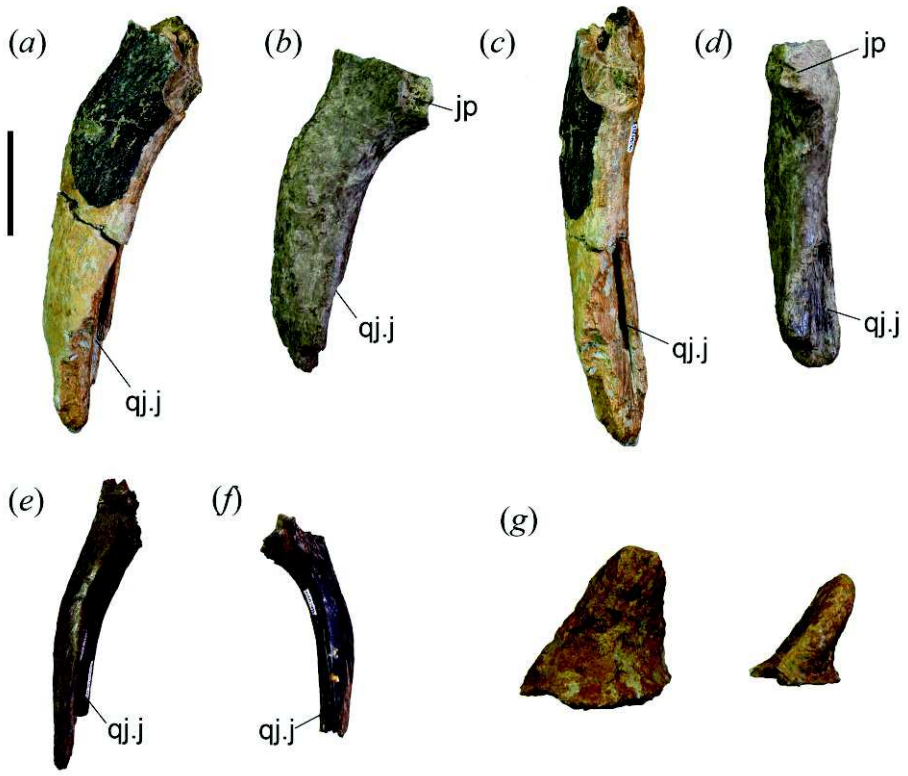

Figure IV.19. *Mourasuchus* from Nueva Unión. Partial jugals: Left ramus (MUSM 2427) in dorsal (*a*) and medial (*c*) view. Left ramus (MUSM 2477) in dorsal (*b*) and medial (*d*) view. For comparison, from Iquitos: (*e*) left ramus (MUSM 1735) in dorsal view; (*f*) right ramus (MUSM 2496). (*g*) Isolated osteorderms from Nueva Unión. For anatomical abbreviations see Appendices. Scale bar, 5 cm.

D. Results of the phylogenetic analysis

The analysis retained 70 equally optimal trees with a minimum length of 677 steps. The strict consensus tree (figure S6) calculated from them provided the following statistics: length = 695; consistency index (CI) = 0.377; retention index (RI) = 0.797. This strict consensus tree (Fig. IV.20) is the base for the simplified phylogeny of Fig. IV.24) We performed other analyses using the same parameters but excluding relatively incomplete and problematic taxa from the heuristic search, such as *Necrosuchus ionensis* and *Allognathosuchus wartheni* (see below). These parsimony analyses recover *Gnatusuchus pebasensis* within the Caimaninae clade (Figs. IV.20 and IV.24), supported by the presence of small supratemporal fenestrae with overhanging rims, surangular extending to the posterior end of the retroarticular process, maxilla with a broad shelf extending into the suborbital

fenestra, parietal excluded from posterior edge of skull table, and a slender process of exoccipital ventrally to basioccipital tubera.

Gnatusuchus pebasensis is the most basal caimanine and *Globidentosuchus brachyrostris* is the next outgroup to all remaining caimanines; these two taxa reveal unknown character states ancestrally present within the caimans (i.e., long splenial symphysis, posterior globular teeth) and their inclusion influenced the topology of relationships within the caimanine clade. Character support provides a novel sister-grouped relationship between the South American caimans and the North American Cretaceous globidontan alligatoroids (i.e., *Brachychampsa*, *Albertochampsa*, and *Stangerochampsa*), whereas prior analyses showed either the monophyly of Alligatoridae (Caimaninae + Alligatorinae) exclusive of Cretaceous globidontans (Brochu, 1999; Brochu, 2010) or, more recently, a polytomy within the globidontan alligatoroids (Caimaninae + [alligatorines and Cretaceous globidontans]; Brochu, 2011; Scheyer et al., 2013). Here, this polytomy (dotted lines in figure IV.24) is obtained when the alligatorine *Allognathosuchus wartheni* is excluded from the analysis. Results also suggest an early diversification of major groups within the Caimaninae dating back to the end of the Cretaceous or Paleeocene interval.

This analysis shows low support for relationships within the globidontans alligatoroids, mainly due to the fragmentary condition on some taxa and the inclusion of new basal species. Based on this analysis, caimanines and the Cretaceous globidontans are sister clades and alligatorines lie outside the aforementioned association. Excluding *Necrosuchus ionensis* from the analysis provides the same topology but higher Bremer support for some clades within the Caimaninae. However, character support for this new arrangement is weak since it collapses in trees one step longer or when a problematic taxon, like *Allognathosuchus wartheni*, is excluded from the analyses (dotted lines in figure IV.20).

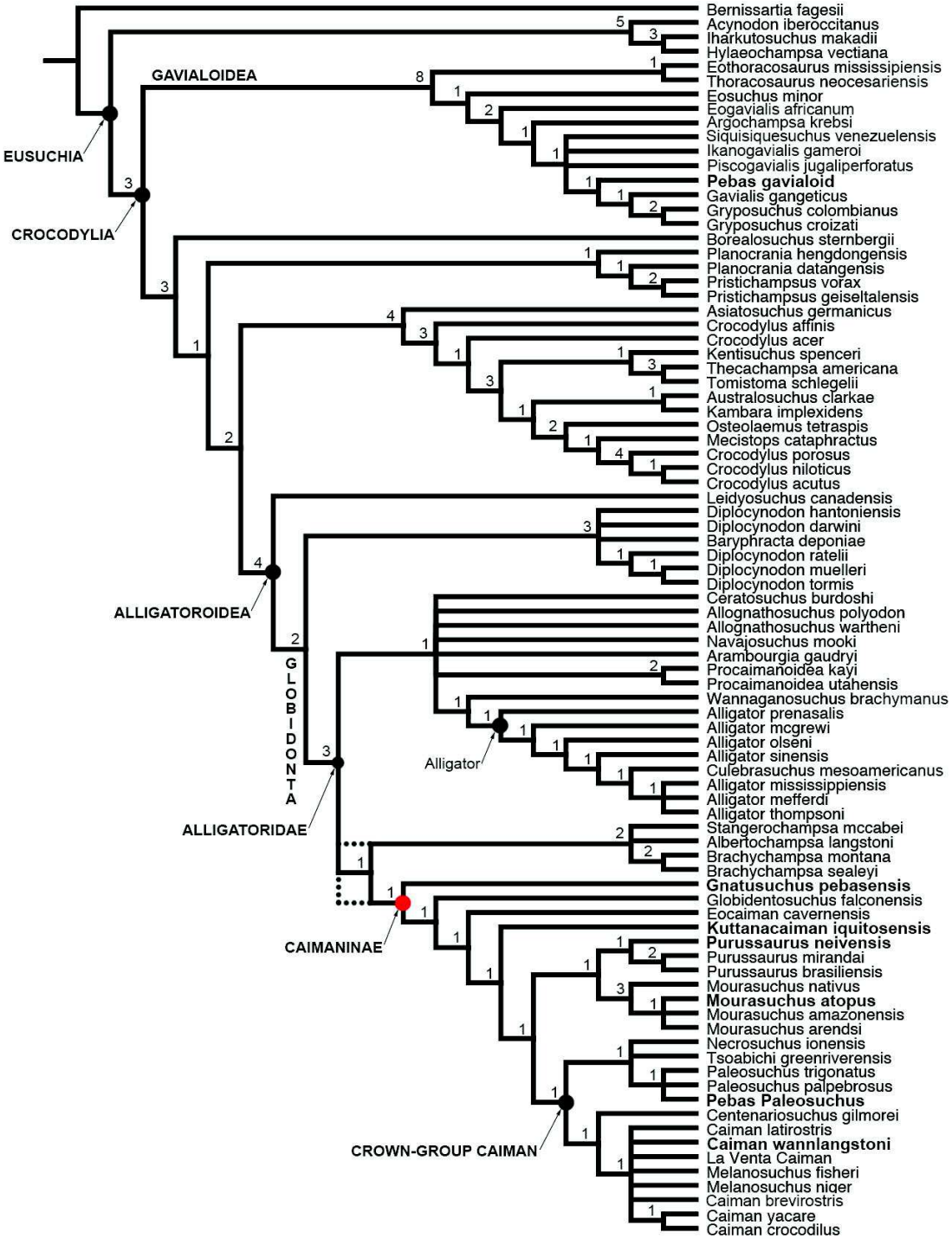

Figure IV.20. Strict consensus tree of 70 Most Parsimonious Trees. Tree Length = 695 Consistency Index = 0.377; Retention Index = 0.797. The analysis excluding *Necrosuchus ionensis* yielded the same topology. Numbers at nodes indicate Bremer support values. Dotted lines indicate collapse of the node supporting sister relationships between Cretaceous alligatoroids and caimanines when *Allognathosuchus wartheni* is excluded from the analyses. Pebas taxa are bold typed.

The clade formed by caimanines and the Cretaceous globidontans is only supported by two ambiguous synapomorphies: proatlas lacks anterior process (Character 3, state 1) and surangular does not extend dorsally beyond anterior end of foramen intermandibularis

caudalis, anterior tip blunt (character 65, state 1). As a consequence of this tree rooting, Globidonta and Alligatoridae are taxonomically redundant (Fig. IV.20).

Culebrasuchus mesoamericanus is based on a damaged skull from the Lower Miocene Culebra Formation of Panama (Hastings et al., 2013). This taxon was considered as the basal-most caimanine (Hastings et al., 2013), with that position supported by the presence of a large supraoccipital exposure in the skull table and the absence of a splenial symphysis. In our analysis, *Culebrasuchus mesoamericanus* is deeply rooted within the *Alligator* genus as the sister taxon of the clade consisting of *A. thompsoni* + *A. olseni* + *A. mississippiensis* (Fig. IV.20). *Culebrasuchus mesoamericanus* lacks both the overhanging rims within the supratemporal fenestrae and the slender ventral process of the exoccipital that characterises caimanines. As a morphologically advanced representative of the *Alligator* clade instead of a basal caimanine, it possesses an external mandibular fenestra enlarged so much that the foramen intermandibularis caudalis is visible laterally. However, character support for this newly hypothesised systematic position is still weak: *Culebrasuchus* jumps back to the caimanines (as the sister taxon of *Necrosuchus ionensis* within an early divergent clade) when excluding *Gnatusushus* and *Globidentosuchus* from the analysis. In this analysis, the non-South American taxa *Tsoabichi greenriverensis* (+ *Necrosuchus ionensis*) and *Centenariosuchus gilmorei* are the sister species of *Paleosuchus* and jacareans, respectively. Previous phylogenetic approaches showed similar results (Brochu, 2010; Hastings et al., 2013). Although character support is weak, this tree also provides evidence for a relationship between *Paleosuchus* + *Tsoabichi* + *Necrosuchus* and *Centenariosuchus* + jacareans, with the consequent exclusion of the *Purussaurus*-*Mourasuchus* clade from crown-group caimans. The same analysis, exclusive of *Gnatusuchus* and *Globidentosuchus*, recovers the *Purussaurus*-*Mourasuchus* clade within the crown-group, as was suggested by previous researches.

E. Discussion and conclusions

E.1 Diversity and dominant ecology of the caimanine assemblage

The crocodylian assemblage of the Iquitos bonebeds is extraordinary in representing both the highest taxonomic diversity and the widest range of snout morphotypes ever recorded in any crocodyliform community, recent or extinct.

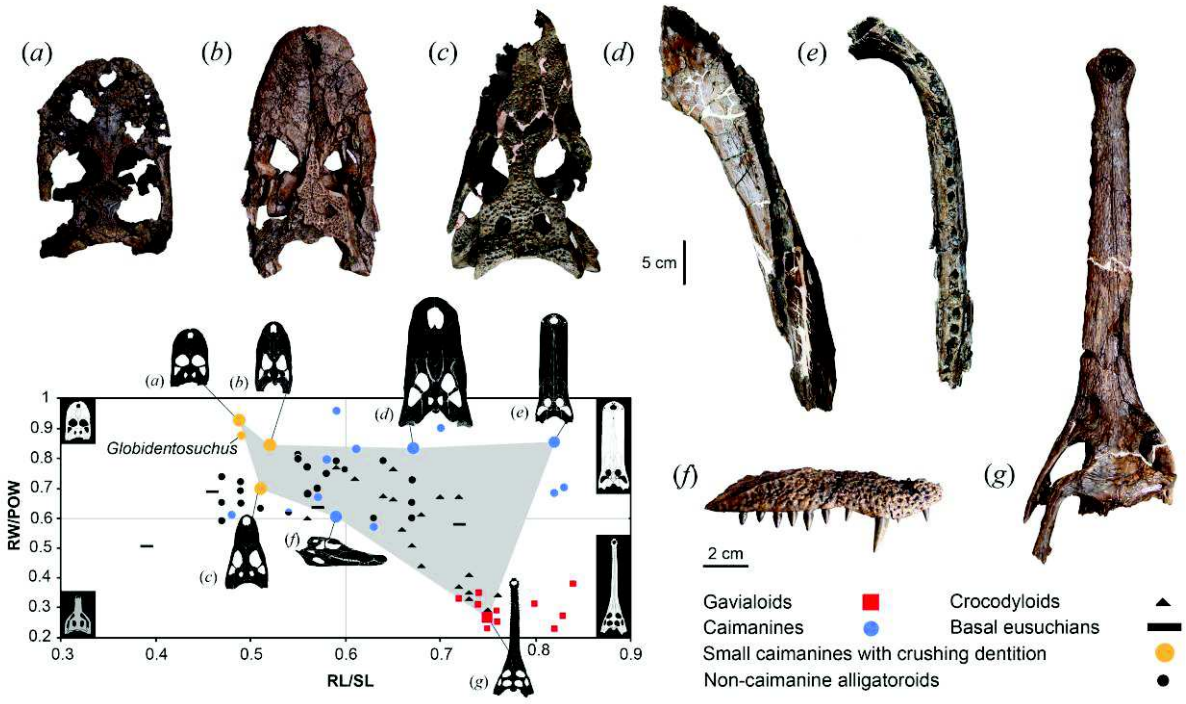

Figure IV.21. Pebasian crocodylian diversity and snout morphotypes. Positions of the six caimanines (*a-f*) and the sole gavialoid (*g*) from Iquitos are indicated in a plot of relative snout width and length within the Eusuchia. (*a*) *Gnatusuchus pebasensis*, (MUSM 990) skull. (*b*) *Kuttanacaiman iquitosensis* (MUSM 1490), skull. (*c*) *Caiman wannlangstoni* (MUSM 2377), skull. (*d*) *Purussaurus neivensis* (MUSM 1392), right dentary. (*e*) *Mourasuchus atopus* (MUSM 2379), right dentary. (*f*) Pebas *Paleosuchus* sp. (MUSM 1985) right maxilla in lateral view. (*g*) Pebas gavialoid (MUSM 1981), skull. Bivariate plot modified from Busbey (1995). Quadrants correspond to the four potential combinations of the bi-dimensional snout-shaped morphospace. RW/POW, rostral width-postorbital width index; RL/SL, rostral length-skull length index.

Other previously proposed peaks in sympatric diversity (e.g. in Late Miocene faunas of Venezuela and Brazil) are based on material from correlated strata of various localities and multiple horizons within basins rather than from a single site (Cozzuol, 2006; Scheyer et al., 2013). The hyperdiverse Iquitos assemblage (six caimanines and one gavialoid; Fig. IV.21) includes five new taxa that form the endemic Pebasian crocodylian fauna of the long-lived

proto- Amazonian lakes that occupied most of western Amazonia during the Middle Miocene. Taxonomic distinctions from coeval assemblages within the same Neotropical realm, such as La Venta, Colombia (Langston, 1965) and Fitzcarrald, Peru (Salas-Gismondi et al., 2015a), probably represent more fluvial-dominated palaeoenvironments. The extraordinary heterogeneity of snout shapes at Iquitos covers most of the morphospace range known for the entire Crocodylia clade (Fig. IV.21), reflecting the combined influences of long-term evolution, resource abundance and variety, and niche partitioning in a complex ecosystem.

Small caimanines with posterior globular teeth were conspicuous components of the Pebasian crocodylian assemblage (Fig. IV.22). These posterior teeth resemble those of the extant teiid lizard *Dracaena*, which has a strictly malacophagous diet (Dalrymple, 1979). In addition to the globular dentition, these taxa share several other distinctive traits (i.e. massive jaws, long symphysis, blunt snouts) of particular ecological relevance in the context of the peculiar Pebas palaeoenvironment as they together strongly suggest durophagy (Abel, 1928; Carpenter & Lindsey, 1980). We propose that this array of crushing-toothed caimans predominantly fed on endemic molluscs that were copious in this time interval (MZ8; Fig. IV.23). Within the diverse fauna of approximately 85 co-occurring endemic species (Wesselingh et al., 2006a; Wesselingh & Salo, 2006), corbulid pachydontine bivalves were especially abundant (Wesselingh et al., 2002). These bivalves display high morphological disparity and distinct anti-predatory adaptations, including thick shells, profuse ornamentation, overlapping valves, globose shape and a rostrum projecting siphons (Wesselingh, 2006). Successful and unsuccessful (i.e. healed) crushing predation scars are common and the proportion of shell fragments with sharp edges typical of this kind of damage reach up to 93% in valves of some molluscan samples (Fig. IV.22*h*–*l*). This extremely intense predation had been attributed to fishes and decapod crustaceans (Wesselingh, 2006), but the Pebasian ichthyofauna does not differ significantly from its

modern Amazonian counterpart (Monsch, 1998), which lacks large-shell crushing fishes and is poor in molluscan species (Fittkau, 1981).

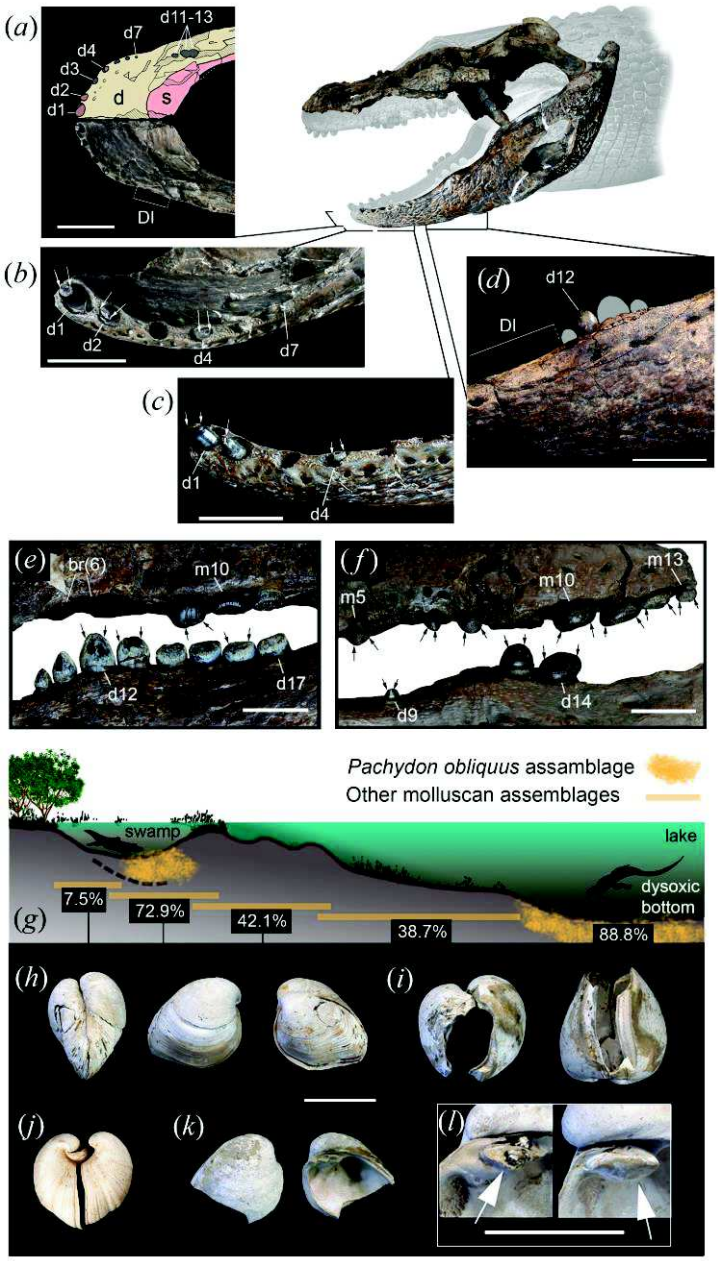

Figure IV. 22. Crushing-dentition caimanines and co-occurring pachydontine molluscs. (*a-d*) *Gnatusuchus pebasensis*. MUSM 662, anterior mandibular anatomy in dorsal (*a*), anterodorsal (*b*), and lateral view (*c*). (*d*) MUSM 2040, posterior mandibular dentition in lateral view. (*e*) *Kuttanacaiman iquitosensis*, MUSM 1942, posterior dentition. (*f*) *Caiman wannlangstoni*, MUSM 1983, posterior dentition. (*g*) Inferred distribution of molluscan assemblages within the typical depositional environments of the Pebas System (after Wesselingh et al., 2002). Percentage values correspond to the estimated average abundance of the *Pachydon* group within each assemblage. Thick-shelled *Pachydon obliquus* (*h, i, k, l*) and *Pachydon cuneatus* (*j*) with convex outline making them well capable to withstand external pressure. (*h*,*i*) Crushing type predation scars in specimens that survived and then resumed growth. (*k*) Sharp edges typical of this type of predation. (*l*) Detail of cardinal tooth with (left) and without (right) crushing damage. See Wesselingh et al. (2002) and Wesselingh et al. (2006a) for molluscan data and localities. Arrows in (*b*, *c*, *e*, *f*) indicate severe crown tooth wear. Scale bars: 5 cm for (*a*), 2 cm for (*b-f*), and 1 cm for (*h-l*).

Instead, an array of crushingdentition Pebasian caimans co-evolved with and exploited this trophically distinct, long-lasting, proto-Amazonian episode of increasing molluscan diversity and abundance, resulting in the high mollusc predation intensity observed. Consistent with these predator–prey interactions, the crocodylian 'crusher' morphotype exhibits anterior and posterior teeth with severe wear (Fig. IV.22*e*, *f*). The Iquitos bonebeds are also rich in isolated globular caiman teeth that were worn flat, suggesting active crushing or grinding during normal feeding activity. Small globidontan crocodylians from the Cretaceous and Palaeogene of the Great Plains of United States were interpreted as shell crushers owing to similar feeding-related traits and heavy surface wear pattern (Abel, 1928; Carpenter & Lindsey, 1980). At least during the Paleocene epoch, the huge freshwater systems of the Great Plains hosted three genera of corbulid bivalves that also occurred in the Pebasian Mega-Wetland System (*Pachydon*, *Ostomya* and *Anticorbula*), possibly indicating a much longer corbulid-globidontan interaction (Brochu, 1999; Anderson et al., 2006). Similar interactions are hypothesized for molluscs and durophagous freshwater stingrays, co-occurring in early Paleogene deposits of both the Great Plains (Paleocene) and Western Amazonia (Middle Eocene-onward; Adnet et al., 2014).

Besides the blunt-snouted caimanines with crushing dentition and stout jaws, we also recovered the first unambiguous fossil of the extant smooth-fronted caiman *Paleosuchus*, which possesses a relatively more generalist snout shape (Figs. IV.11, IV.12, and IV.21). It bears a lightly built maxilla with vertically oriented walls, and distinctive sharply pointed teeth. Although still poorly known, this fossil taxon (*Paleosuchus* sp.) differs from its extant relatives in having less maxillary teeth and a proportionally longer anterior process of the ectopterygoid running medially to posterior alveoli. Large caimanines are represented by *Purussaurus neivensis* and *Mourasuchus atopus*, the only two Pebasian taxa previously known from Miocene localities in the region (Langston, 1965). *Purussaurus* possessed a

hulking skull and a mandible with large robust anterior teeth and smaller blunt posterior teeth (Figs. IV.14 and IV.21). The "duck-faced" taxon *Mourasuchus* occupies one extreme of crocodylian snout morphotypes, with an exceptionally long and wide rostrum (Figs. IV.15, IV.16, and IV.21). Its feeding habits are controversial, although it was considered to eat small organisms (e.g., fishes) by some kind of filtering strategy (Langston, 1965).

E.2 Potential preys of crushing-dentition, durophagous caimanines

The Pebas Mega-Wetlands System hosted taxonomically diverse and abundant molluscan life that would form suitable prey for the diversity of crushing-dentition caimanine species. Especially abundant were pachydontine bivalves, a group of endemic species partially adapted to dysoxic lake floor settings (Wesselingh, 2006). The most common species in the Pebas Formation is the highly inflated and thick-shelled *Pachydon obliquus*. This species typically makes up ca. 40-70% of shell numbers in Pebas lacustrine samples; in the Santa Rosa de Pichana site, it represents 47% of the total number of counted shells (Wesselingh et al., 2006a).

Shell damage as a result of both successful and unsuccessful (healed) crushing predation is common in many samples in the Pebas Formation. Unsuccessful damage is found in a few samples, where specimens of *Pachydon obliquus* survived severe crushing and then resumed growth (Fig. IV.22*h*-*l*). In sample F539 from Santa Rosa de Pichana, representing a shallow lacustrine floor assemblage (Wesselingh et al., 2006a), 93% of valves and fragments with hinge remains have sharp edges typical of predation (Fig. IV.22*i*, *k*, *l*). These edges are not the result of compaction, as accompanying gastropods in the same sample were not affected. Neither are they the result of breakage during collecting, as many of the sharp edged surfaces show similar post-depositional etching and discoloration of the shell's outer- and

inner surfaces. In another sample (F74) (see Wesselingh et al. 2006a for locality data), 77% of the counted *P. obliquus* specimens contained signs of crushing.

Not only crushing-type of predation by crocodylians can cause sharp-edged fragments; attacks by decapod crustaceans, that also were large and plentiful in the Pebas System, might have caused similar damage. Yet, the characteristic decapod pattern of a scissor-edge is entirely lacking in this sample (and in many others). Thus, the F539 *Pachydon obliquus* sample is severely affected by a non-crustacean, crushing type of predation. As postulated here, based on their craniodental anatomy *Gnatusuchus pebasensis*, *Kuttanacaiman iquitosensis*, and *Caiman wannlangstoni* are all considered to have been durophagous crushing predators, although other potential crushing-type feeders were present in the Pebas System. These include sciaenid fish that were common in the Pebas System, and piranhas, the remains of which are found only very rarely. The pharyngeal jaw system of the former must have had great difficulty dealing with prey that were typically quite large (1/2 to 2 cm across), while the saw-like dentition of the latter is not adapted to durophagy. Given the obliteration of the massive cardinal tooth of the bivalve *Pachydon obliquus* in many instances (In Fig. IV.22*l*, compare cardinal tooth with [left] and without damage [right]), the crushing force for this damage must have been formidable, which is consistent only with the strong adductor musculature estimated for crushing-dentition caimanines among potential predators in the Pebas System. Other *Pachydon* species show similar breakage.

Several morphological characters in species of *Pachydon*, and especially in *P. obliquus*, are well suited to defend against crushing predators. These are: (a) very thick shell, (b) massive, tightly interlocking hinge, (c) convex shape of paired valves, (d) smaller left valve fitting well within the larger right valve, and (e) ability of the animal to live well within the shell away from the edges, as indicated by the deep location of the pallial line (Wesselingh, 2006). Although we cannot confirm a causal relationship, these characters may

well have evolved in conjunction with increased adaption to molluscivory in Miocene Pebas predators such as blunt-snouted crushing-dentition caimans, potamotrygonid rays, and caiman lizards (i.e., *Paradracaena*, *Dracaena*).

In general, *Pachydon* specimens are thickest shelled and largest in shallow lacustrine settings with little dysoxia and become smaller and thinner-shelled in deeper dysoxic lake floor settings (Wesselingh, 2006) Predation pressure may have been highest in the shallow lacustrine-wetlands settings from which *Gnatusuchus pebasensis, Kuttanacaiman iquitosensis*, and *Caiman wannlangstoni* have been recovered.

In summary, *Pachydon* bivalves may have been the dominant prey of choice for most crushing-dentition caimanines, and particularly for the highly specialized and anatomically distinctive new taxon *Gnatusuchus pebasensis*. These bivalves were extremely abundant on the shallow floors of the Pebasian lakes, and signs of both successful and failed crushing predation are plentiful. The severity of shell damage indicates extremely powerful predators, such as caimans with strong adductor musculature, massive jaws, and posterior globular teeth.

E.3 Feeding ecology of *Gnatusuchus pebasensis*

Even though correlations between morphotype and ecology cannot be stated with certainty in extinct taxa, the singular *Gnatusuchus pebasensis* anatomy not only further supports durophagy but also reveals other distinctive aspects of its feeding strategy. Unique among crocodyliforms, *Gnatusuchus* possesses a dentary bearing a large edentulous gap between the seven procumbent anterior and four globular posterior teeth. This mammal-like diastema of about 30 mm results from the evolutionary loss of most of the alveoli lying between the dual (anterior and posterior) regions of maximum alveolar diameter of most crocodylians (Brochu, 2011). Mandibular rami are firmly sutured, yielding the longest symphysis observed within globidontan alligatoroids, and a stable shovel-like structure for the lower jaws (Fig. IV.22*a*-*c*). Posteriorly, the mandibular ramus is high and robust. In this

region, the entire ramus is tilted lateroventrally and houses a wider and more capacious adductor fossa (Fig. IV.3*b*). In *Gnatusuchus*, strong adductor muscles and robust mandibular joints might have facilitated any feeding activity involving powerful dislocating jaw forces. This distinctive dental and craniomandibular anatomy is consistent with a durophagous diet, as well as with head burrowing activity in search of prey. Infaunal pachydontine bivalves (length ~7-25 mm) were diverse and abundant in unconsolidated bottoms of dysoxic lakes of the Pebas System (Fig. IV.22*h-l*; Wesselingh et al., 2002; Wesselingh, 2006). *Gnatusuchus* likely fed on them by "shoveling" with the jaw and the procumbent anterior teeth, then crushing shells with the globular, tightly packed posterior teeth. During durophagy, traumatic tooth avulsion and severe damage involving tooth replacement might provide explanations for cases of bone resorption of posterior tooth loci in *Gnatusuchus* mandibles. Alveolar remodelling is also observed in one specimen of *Kuttanacaiman iquitosensis* (Figs. IV6*d* and IV.22*e*). Although this condition is common among crushing-dentition Pebasian caimans, it is unusual among extinct or extant reptiles (Xing et al., 2013). Oxygen-stressed environments might be adverse for many potential predators feeding on mud bottoms (e.g., benthic fishes or crustaceans) but not for air-breathing caimans.

E.4 Rise and demise of the dysoxic lacustrine ecosystems and the evolution of caimans

This new fauna highlights co-occurrence at approximately 13 Ma of every phylogenetic lineage currently recognized within the Caimaninae, emphasizing the role these proto-Amazonian mega-wetlands played in fostering the persistence of basal lineages simultaneously with the initial diversification of their modern relatives (Fig. IV.23). Phylogenetic analysis of a morphological dataset (Salas-Gismondi et al., 2015a: electronic supplemental material) positions *Gnatusuchus* as the most basal caiman, suggesting that a blunt-snouted rostrum with crushing dentition could have been the ancestral condition for the

entire clade, while the more generalized morphology of the caiman crown-group is derived (Fig. IV.23). A long mandibular splenial symphysis also might be associated with early stages of caimanine evolution (Scheyer et al., 2013). An evolutionary pattern in which generalist taxa, such as the extant species of *Caiman*, originated from blunt-snouted "crushers" was similarly proposed for a different crocodylian clade: the alligatorines (Brochu, 2004b). This distinctive caimanine morphotype, closer to that of Cretaceous alligatoroids, was unknown prior to the discovery of the Miocene taxa *Gnatusuchus* and *Globidentosuchus*, probably due to the scarce Paleogene fossil record in tropical South America. Similarly, Paleocene or even Cretaceous origins and diversification of some caimanine groups consequently are expressed as long ghost lineages within the time-calibrated phylogenetic tree (Fig. IV.23), predicting currently unrecovered high morphotypic and taxonomic diversity continuously along caimanine evolutionary history until the Late Miocene. Regarding the evolution of globular dentitions, results of this analysis also suggest that a reversal occurred later within jacarean caimanines. Posterior globular teeth of the new crushing-dentition taxon *Caiman wannlangstoni* would have evolved from a generalized dental pattern as an opportunistic adaptation to the increasing abundance and diversity of molluscs throughout the Middle Miocene (Fig. IV.23).

The Pebas fossil record further underlines the occurrence of a key ecological turnover in western Amazonia around the Middle-Late Miocene transition, providing new insights on establishment of modern ecosystems. The Iquitos bonebeds immediately underlie strata documenting episodes of marine incursions and the first decline in endemic mollusc diversity (Hoorn et al., 2010a; Wesselingh et al., 2006a). This stage (MZ9, ca. 12 Ma) represents the initial demise of dysoxic lacustrine Pebas environments (Wesselingh et al., 2006a), and coincides with events of intense Andean uplift that dissected proto-Amazonia into the modern Magdalena, Orinoco, and Amazonian river basins. Major reorganization of drainage patterns

at approximately 10.5 Ma included initiation of the transcontinental Amazon River drainage (Fig. IV.23; Hoorn et al., 2010b; Figueiredo et al., 2010; Shephard et al., 2010).

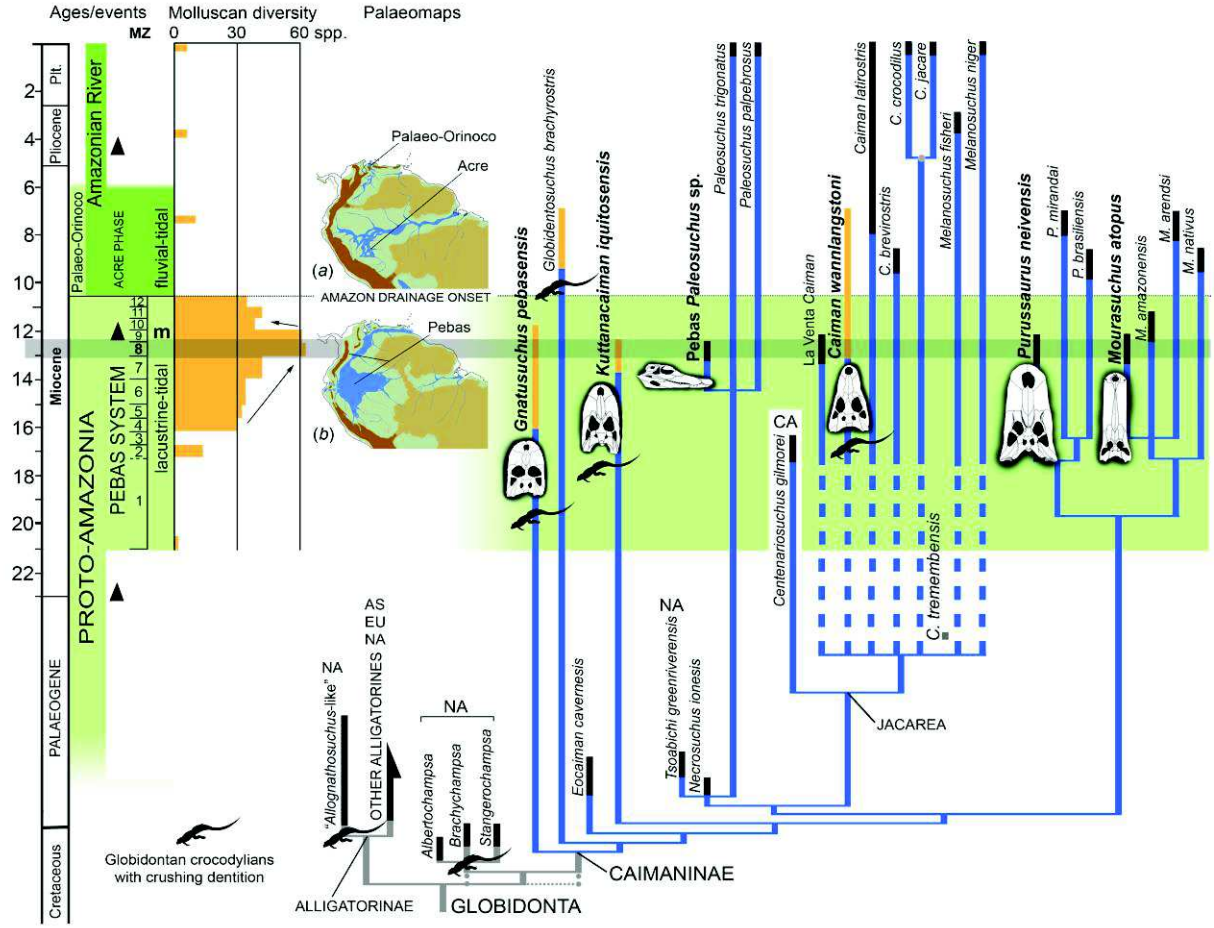

Figure IV.23. Phylogenetic position of the Pebasian caimanines within the Alligatoroidea. Time-calibrated, strict consensus cladogram of 70 most parsimonious trees (see figure IV.20). *Gnatusuchus pebasensis* is the most basal caimanine and *Globidentosuchus brachyrostris* is the next outgroup to all remaining caimanines; these two taxa reveal unknown character states ancestrally present within the caimans (i.e., long splenial symphysis, posterior globular teeth) and their inclusion influenced the topology of relationships within the caimanine clade. Character support provides a novel sister-grouped relationship between the South American caimans and the North American Cretaceous globidontan alligatoroids (i.e., *Brachychampsa*, *Albertochampsa*, and *Stangerochampsa*). Here, this polytomy (dotted lines) is obtained when the alligatorine *Allognathosuchus wartheni* is excluded from the analysis. Results also suggest an early diversification of major groups within the Caimaninae dating back to the end of the Cretaceous or Palaeocene interval. (*a*) The Acre Phase (ca. 9 Ma) after intense Andean uplift and onset of the transcontinental Amazon River System. (*b*) The Pebas Mega-Wetland System in northwestern South America during MZ8 (ca. 13 Ma). Stratigraphic distribution of taxa (yellow bars for crushing-dentition caimanines, black lines for other taxa) relative to major Neogene stages and events in Amazonia. Paleogeographical reconstructions, andean uplift peaks (black triangles) and marine incursions (m) are from Hoorn et al. (2010b). Molluscan Zones and diversity for the Pebas System (MZ1-12) are from Wesselingh et al., 2006a. When suitable, internal nodes were time-calibrated with molecular data from Oaks (2011). Darker gray remarks MZ8. Alligatoroids are from South America, Africa (AF), Asia (AS), Central America (CA), Europe (EU), or North America (NA).

Lignite-poor outcrops just above MZ9 (see Chapter II; Rebata et al., 2006) in the Nueva Unión area south of Iquitos yield the youngest record of *Gnatusuchus* (Fig. IV.17*a*, *c*, *e*), but do not contain other crushing-dentition caimanines. Giant caimans like *Purussaurus* and *Mourasuchus* are common at Nueva Unión (Figs. IV.18 and IV.19), as is also characteristic in the Late Miocene Solimões Formation of Acre that represents the fluvio-tidal Acre Phase, when a transcontinental river system first became established (Hoorn et al., 2010a). Contrary to the Pebas System, small to medium-sized caimanines in Acre are represented by two *Caiman* species, including only one short-snouted species (i.e., *C. brevirostris*) with blunt posterior teeth considered ecologically similar to the extant *Caiman latirostris* (Fortier et al., 2014; Cozzuol, 2006). Relatively depauperate fluvial mollusc assemblages dominate the Acre Phase (Wesselingh et al., 2006b), resembling modern Amazonian faunas. In northern South America, the Urumaco Formation (coeval with the Late Miocene Solimões Formation) documents life in the palaeo-Orinoco basin, including at least three "crushers" among both basal (i.e., *Globidentosuchus brachyrostris*) and advanced caimanines, such as the Pebasian *Caiman wannlangstoni* (Sánchez-Villagra & Aguilera, 2006; Scheyer et al., 2013). Freshwater molluscs have not been described there yet, but shells are abundant throughout the Urumaco Formation (Quiroz & Jaramillo, 2010). As a whole, Acre and Urumaco crocodylian faunas are highly similar (i.e., several longirostrine crocodylians, giant taxa among gavialoids and caimanines; Cozzuol, 2006), although evidence suggests that an equivalent array of the Pebas crushing-dentition caimanines persisted during the late Miocene within the palaeo-Orinoco (Scheyer et al., 2013) whereas they decayed in the Amazonian Acre Phase, suggesting faunal provincialism and persistence of Pebas-like ecosystems throughout the Late Miocene only in the northernmost Neotropics.

Morphological diversification of "crusher" crocodylians during the Pebas System, including the singular anatomy of the shoveling caiman *Gnatusuchus pebasensis*, appears to

have been largely driven by adaptation to molluscan food sources abundance in dysoxic lake bottom habitats (Fig. IV.24). Crocodylian peak diversity was reached near the end of the MMCO, prior to fragmentation of these proto-Amazonian wetlands. Central and northern Andean uplift at approximately 12 Ma (Middle-Late Miocene transition) not only contributed to retreat of the Pebasian system to northernmost South America, but also fostered the origin of the transcontinental flow of the modern Amazon River (Hoorn et al., 2010b; Mora et al., 2010). This transition ultimately led to the development of early Amazonian-type trophic dynamics that favored fluvial faunas, including the initial replacement of more archaic, dietarily-specialized crocodylians by the more generalist-feeding caimans that dominate modern Amazonian ecosystems.

Figure IV.24. Reconstruction of the crushing-dentition caimanines *Kuttanacaiman iquitosensis* (left), *Caiman wannlangstoni* (right), and *Gnatusuchus pebasensis* (below) within the swamps of the Pebas System. Painting by Javier "Canelita" Herbozo.

CHAPTER V – CROCODYLIAN COMMUNITY FROM THE LAKES AND SWAMPS OF THE PEBAS SYSTEM, IQUITOS AREA (GAVIALOIDEA)

CHAPTER V – CROCODYLIAN COMMUNITY FROM THE LAKES AND SWAMPS OF THE PEBAS SYSTEM, IQUITOS AREA (GAVIALOIDEA)

A NEW MIOCENE GAVIALOID CROCODYLIAN FROM PROTO-AMAZONIAN MEGA-WETLANDS REVEALS PARALLEL EVOLUTIONARY TRENDS IN SKULL SHAPE LINKED TO LONGIROSTRY

This chapter section corresponds to the extended version of the following article:

Salas-Gismondi, R., Flynn, J., Baby, P., Tejada-Lara, J. V., Claude, J., Antoine, P.-O.

A new Miocene gavialoid crocodylian from proto-Amazonian mega-wetlands reveals parallel evolutionary trends in skull shape linked to longirostry. Submitted to PLoS ONE

Abstract

Gavialoid crocodylians are the archetypal longirostrine archosaurs and, as such, understanding their patterns of evolution is fundamental to recognizing cranial rearrangements and reconstructing adaptive pathways associated with elongation of the rostrum (longirostry). The living Indian gharial *Gavialis gangeticus* is the sole survivor of the group and is unique in providing evidence on the distinct biology of its fossil kin. Yet phylogenetic relationships and evolutionary ecology spanning ~70 million-years of longirostrine crocodylian diversification remain unclear. Analysis of cranial anatomy of the proto-Amazonian gavialoid, *Gryposuchus* nov. sp., from the Miocene lakes and swamps of the Pebas Mega-Wetland System reveals that acquisition of both widely separated and

protruding eyes (telescoped orbits) and riverine ecology within South American and Indian gavialoids is the result of parallel evolution. Phylogenetic and morphometric analyses show that, in association with longirostry, circumorbital bone configuration is highly plastic and may reflect habitat preferences and feeding strategy. Our results support a long-term and large-scale radiation of the South American forms, with taxa occupying either extreme of the gavialoid morphospace showing preferences for coastal marine versus fluvial environments. Early biogeographic history of South American gavialoids was strongly linked to the northward drainage system connecting proto-Amazonian wetlands to the Caribbean region.

Keywords: Miocene, gavialoid crocodylians, proto-Amazonia, telescoped orbits, parallel evolution, longirostry

A. Introduction

Numerous unresolved issues hinder understanding of the origin, time of divergence, and patterns of adaptive radiation of gavialoid crocodylians. Whereas molecular data sets favor a close relationship and an Eocene (Harshman et al., 1992) or even Neogene (Hass et al., 1992; Gatesy et al., 2003; Oaks, 2011) divergence between the Indian gharial *Gavialis gangeticus* and the Indonesian false gharial *Tomistoma schlegelii*, morphological phylogenies suggest that these two extant longirostrine species are much more distantly related, that their elongated skulls are convergently evolved, and that the oldest fossil gavialoid dates back to the Cretaceous Period in North America, Europe, and Africa (Brochu, 2004a; Jouve et al., 2008). In fact, analyses of extant *Gavialis* and its nearest fossil relatives do not provide strong support for their phylogenetic affinities with any other crocodylian clade, probably as part of what Clark (1994) called the "longirostrine problem". Clark (1994) identified several cranial features related to longirostry in crocodyliforms that might have appeared independently, such

as possessing widely separated and protruding eyes, namely "telescoped" orbits. The evolution of this distinctive cranial morphotype in gavialoids not only obscured which is the ancestral anatomical condition of the clade, but also created a challenge for deciphering ingroup affinities. For example, Indian *Gavialis* and South American *Gryposuchus* species are extremely similar in cranial morphology and both have fully "telescoped" orbits (Langston & Gasparini, 1997; Riff & Aguilera, 2008). Whether this distinctive pattern results from common or independent origin has been uncertain and debated (e.g. Jouve et al., 2008, Brochu & Rincón, 2004).

As an island-continent since the beginning of the Paleogene, gavialoid sudden appearance in South America is explained either by marine dispersals or by the incompleteness of the fossil record (see Brochu & Rincón, 2004; Jouve et al., 2008). The oldest South American gavialoid, *Siquisiquesuchus venezuelensis*, is known so far from early Miocene units of Venezuela (Brochu & Rincon, 2004). The existence of a deltaic-coastal Oligocene Caribbean taxon, *Aktiogavialis puertoricensis* (Velez-Juarbe et al., 2007), having putative affinities with South American gavialoids favors the marine dispersal hypothesis. Certainly, *Siquisiquesuchus*, *Aktiogavialis*, and *Piscogavialis jugaliperforatus*, the later from the Miocene and Pliocene of Peru (Kraus, 1998), were found in coastal marine deposits and show a mixture of primitive and derived cranial characters. Whereas remains of *Ikanogavialis gameroi* from the Late Miocene of Venezuela have doubtful depositional data (Sill, 1970), other gavialoids were recovered from freshwater-dominated deposits, such as *Gryposuchus* species (i.e., *G. jessei*, *G. neogaeus*; *G. colombianus*, and *G. croizati*) and *Hesperogavialis cruxenti* (e.g., Langston, 1965 Gasparini, 1968; Buffetaut, 1982; Langston & Gasparini, 1997; Riff & Aguilera, 2008).

Here, we describe a gavialoid with "non-telescoped" orbits from the Middle Miocene of the Pebas Formation of northeastern Peru that provides evidence of early morphological

stages of the evolution of the *Gryposuchus* lineage in the Amazonian Neotropics. This new gavialoid is the only longirostrine species in the hyperdiverse crocodylian community that inhabited lakes, swamps, and deltas of the Pebas Mega-Wetland System (Salas-Gismondi et al., 2015a), a huge proto-Amazonian biome that appears to have played a crucial role for marine to freshwater transitions in many vertebrate groups occurring today in various river drainage systems of tropical South America (Wesselingh & Salo, 2006). Its lineage survived within the paleo-Orinoco drainage throughout the Late Miocene, providing further evidence for the persistence of Pebas-like mega-wetland conditions in aquatic environments of northernmost South America (Salas-Gismondi et al., 2015a). These records highlight the biogeographic role of the long-lasting drainage linking western proto-Amazonia with the Caribbean region prior to onset of the eastward flowing, transcontinental Amazonian River system. We analyze the phylogenetic relationships of this new Pebasian species to test whether parallel evolution occurred within adaptive radiation of Indian and South American gavialoids. Mapping our phylogenetic hypothesis onto a morphometric space, the remarkable taxonomic and anatomical diversification of South American forms provides novel insights into the ecological significance underlying circumorbital skull configurations throughout gavialoid history.

B. Material and methods

B.1 Phylogenetic analysis

To determine the phylogenetic relationships of the new Pebasian gavialoid species, we included it in a data matrix of morphological characters provided by Salas-Gismondi et al. (2015a). This data matrix builds on characters developed by Brochu (1999, 2011) and Jouve et al., (2008), as well as additional characters compiled from other contributions (Appendices). Relative to Salas-Gismondi et al., (2015a), three characters (i.e., 202-204) are

new. The present analysis focuses on the phylogenetic relationships of gavialoid crocodylians rather than more broadly across all Crocodylia as in the former analyses. Character codings published by Salas-Gismondi et al. (2015a) have been revised and updated, particularly for gavialoids. The complete data matrix consists of 206 morphological characters for 42 eusuchian taxa, with *Bernissartia fagesii* as an outgroup and including most members of the gavialoid clade but only representative taxa of Brevirostres. Ingroup taxa included in this analysis are *Acynodon iberoccitanus*, *Iharkutosuchus makadii*, *Hylaeochampsa vectiana*, *Borealosuchus sternbergii*, *Eothoracosaurus mississipiensis*, *Thoracosaurus neocesariensis*, *Eosuchus lerichei*, *Eosuchus minor*, *Eogavialis africanus*, Siwaliks *Gavialis*, *Gavialis bengawanicus*, *Gavialis gangeticus*, *Aktiogavialis puertoricensis*, *Argochampsa krebsi*, *Boverisuchus vorax*, *Planocrania hengdongensis*, *Leidyosuchus canadensis*, *Diplocynodon ratelii*, *Brachychampsa montana*, *Alligator mississippiensis*, *Navajosuchus mooki*, *Purussaurus neivensis*, *Mourasuchus atopus*, *Caiman crocodilus*, *Paleosuchus trigonatus*, *Culebrasuchus mesoamericanus*, *Globidentosuchus brachyrostris*, *Gnatusuchus pebasensis*, *Crocodylus niloticus*, *Crocodylus acutus*, *Crocodylus acer*, *Crocodylus affinis*, *Tomistoma schlegelii*, *Thecachampsa americana*, *Kentisuchus spenceri*, *Asiatosuchus germanicus*, the new Pebasian gavialoid *Gryposuchus* nov. sp., and most South American gavialoids.

South American gavialoids are represented in this matrix by *Ikanogavialis gameroi* Sill, 1970, *Piscogavialis jugaliperforatus* Kraus, 1998, *Siquisiquesuchus venezuelensis* Brochu & Rincón, 2004, *Gryposuchus colombianus* (Langston 1965), and *Gryposuchus croizati* Riff & Aguilera, 2008. We also include score coding of the Caribbean taxon *Aktiogavialis puertoricensis* based on Vélez-Juarbe et al. (2007). *Aktiogavialis* was codable only for 13.1% of the proposed characters (i.e., 27 of 206) and considering that water abrasion affected preservation of the holotype and only specimen (Vélez-Juarbe et al., 2007), we cautiously scored it as unknown for prootic exposure around the trigeminal foramen (i.e.,

character 164-?). Although *Gryposuchus neogaeus* (Burmeister, 1885) and *Gryposuchus jessei* Gürich, 1912 are referred for anatomical comparisons through this contribution, these taxa are not included in current analyses because their precarious scoring is redundant with other *Gryposuchus* species. New material of *Piscogavialis jugaliperforatus*, comprising well-preserved partial skull and mandibles (MUSM 439; MUSM 2528), was used to complement scores provided by Delfino et al. (2005) based on the type specimen (SMNK 1282 PAL). Our matrix also includes new scorings for the non-South American taxon *Eogavialis africanus* based on direct examination of original material (AMNH 5067, AMNH 5069, AMNH 5071, AMNH 5073, AMNH 5074, AMNH 5075, SMNS 11785, SMNS 50.734). To assess nodal support, branches with a minimum length of 0 were collapsed and Bremer support values (decay indices) were calculated and shown on the strict consensus phylogeny.

B.2 Cranial circumorbital morphospace analysis and phylogenetic mapping

In order to understand morphological evolution linked to longirostry, we applied a geometric morphometric approach on circumorbital anatomy of 22 species of crocodylians, including extant and extinct species (Appendices). As circumorbital region has shown minor intraspecific variation within extant adult crocodylians (Mook, 1921c), all taxa are represented by one fully adult specimen, each preserving in dorsal view: (1) rostral sutures, (2) orbital shape pattern, and (3) no significant postmortem distortion. Morphometric analyses require complete datasets for all landmarks, thus MUSM 1981 was partially reconstructed from the morphology of the complete left side via geometric reflection (Claude, 2008), and included in the analysis. We selected twenty discrete landmark loci considering their availability, relative co-planarity, and clear demarcation within images (Appendices; Fig. V.1). Two-dimensional landmark digitization, Procrustes superimposition (Appendices), and principal component analyses (PCA) were performed with the Geomorph package in R software (R Development Core Team, 2011; Adams et al., 2014). The 22 landmark

configurations were superimposed and scaled to unit centroid size following the generalized procrustes method (Rohlf, 1999). The coordinates of the superimposed configurations were later sent to the Euclidean tangent shape space for allowing subsequent statistical analysis (Rohlf, 1999). In order to obtain component of shape variation, the 22 principal components from that analysis were obtained by applying a principal component analysis (PCA) on the variance covariance of the projected coordinates. Principal component axes (PCs) 1 and 2 (estimated cumulative variance = 70.6%) were plotted in principal components space. A simplified version of the parsimony-based phylogenetic hypothesis unweighted for branch length was mapped in the circumorbital morphospace with MorphoJ software (Klingenberg, 2011).

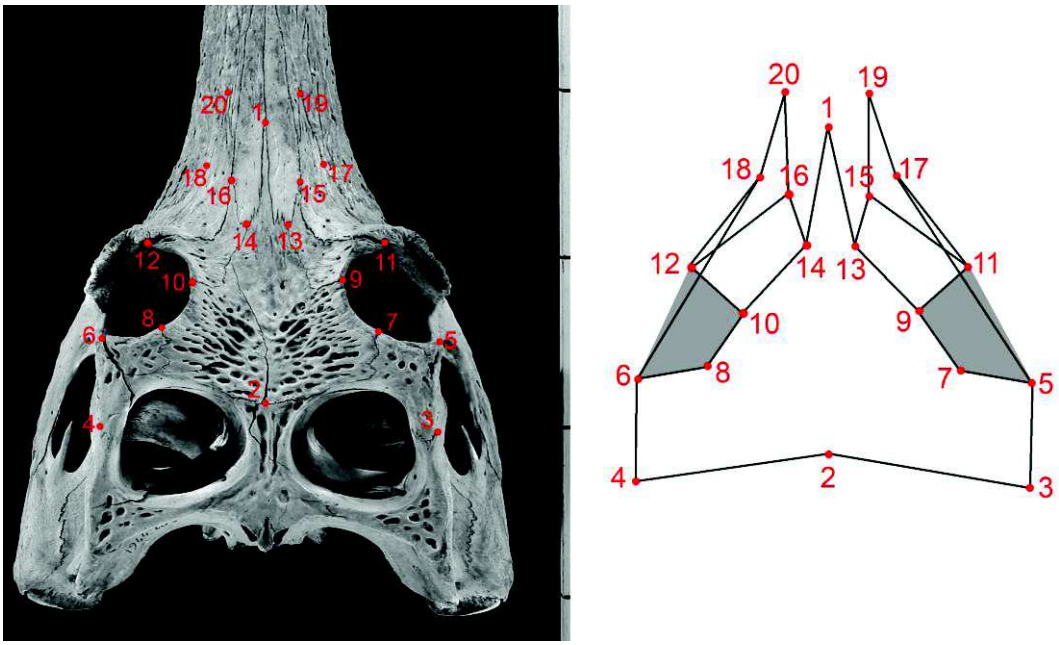

Figure V.1. Landmarks of the circumorbital region of *Gavialis* and its schematic representation. Landmarks are labeled from 1 to 20. Gray area symbolizes orbits defined by landmarks 5-7-9-11 and 6-8-10-12 on the right and left sides, respectively.

C. Systematic Paleontology

C.1 Iquitos gavialoid material

Crocodyliformes Hay, 1930

Eusuchia Huxley, 1875

Crocodylia Gmelin, 1789

Gavialoidea Hay, 1930.

Gryposuchus Gurich, 1912

Gryposuchus nov. sp.

Holotype: Vertebrate Paleontology Collection of the Natural History Museum of San Marcos University, Lima, Peru (MUSM) 1981, nearly complete skull (Figs. V.2*a*-*c* and V.4*h*; Table V.1).

Locality and Horizon: Locality IQ114 (Chapter II.A; Fig. II.1), Iquitos area, Peru; Pebas Formation, late Middle Miocene, approx. 13 Ma; Mollusc Zone 8 (MZ8; Wesselingh et al., 2006a).

Referred specimens: MUSM 987, right mandible (Figs. V.2*d*, V.5*a*, *b*, and V.4*i*), Locality IQ101 (MZ6); MUSM 900, skull without anterior half of the snout (Figs. V.2*e* and V.3*b*), Locality IQ116 (MZ8); MUSM 1439, juvenile mandibular symphysis (Fig. V.6*f*), IQ26 (MZ8); MUSM 1440, posterior portion of right mandible (Fig. V.4f, g), Locality IQ26 (MZ8); MUSM 1681, partial skull (Fig. V.2*f* and V.4*a, c, d*; Tables V.1 and V.2), Locality IQ136 (MZ5); MUSM 1682, juvenile mandibular symphysis (Fig. V.6*g*), Locality IQ126 (MZ5).

Diagnosis. *Gryposuchus* nov. sp. is a long-snouted crocodylian diagnosed by the following unique combination of characters: dental formula consisting of four premaxillary and 22 maxillary and mandibular teeth; ventral margin of postorbital bar inset from lateral jugal surface; frontoparietal suture between supratemporal fenestrae strongly concavoconvex; splenial with anterior perforation for mandibular ramus of cranial nerve V posterior to symphysis; splenial constricted within symphysis; surangular-dentary suture intersecting external mandibular fenestra at posterodorsal corner; surangular-articular suture bowed strongly laterally within glenoid fossa. Differs from *Gr*. *croizati* and *Gr*. *colombianus* in having nasals and premaxillae in extensive contact (character 82-2), narial opening longer

than wide (character 83-0), posterior orbital margin not upturned (character 137-1), ventral margin of the orbit gently circular (character 138-0), and narrow interorbital bridge (character 190-0).

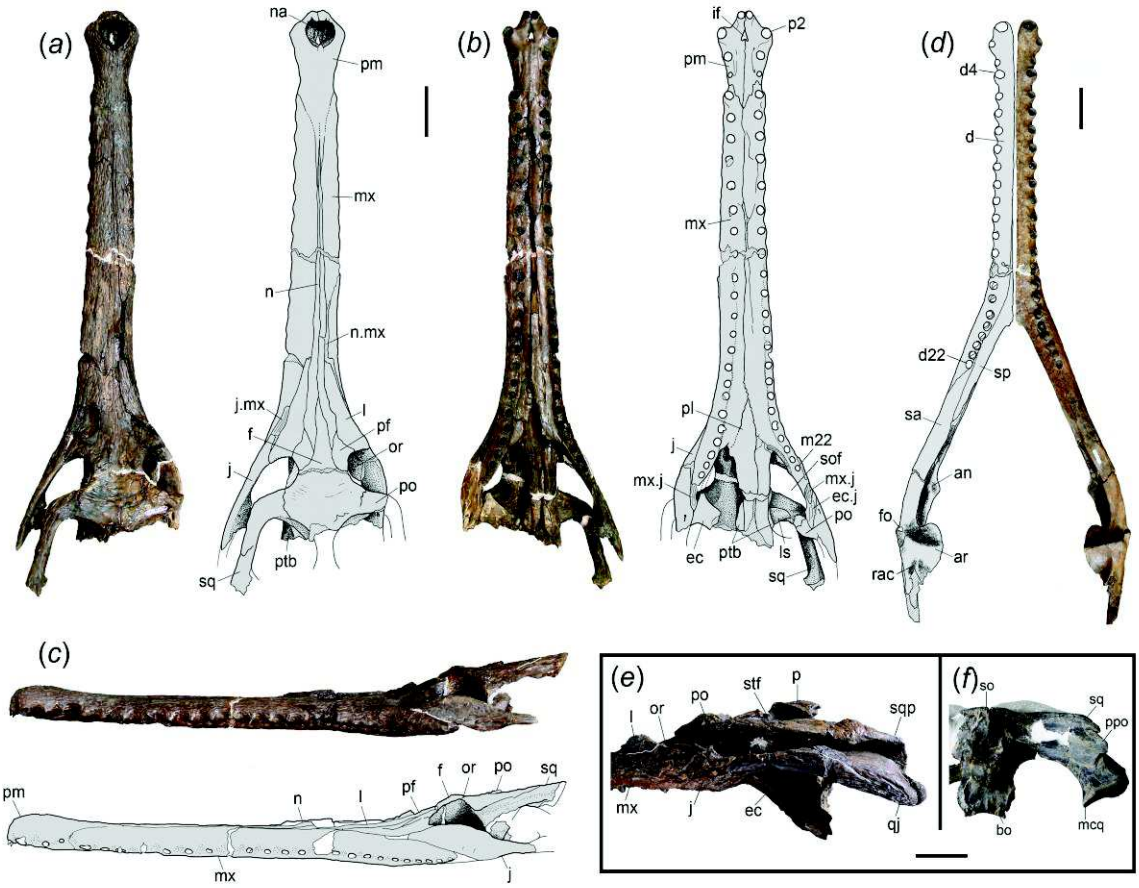

Figure V.2. *Gryposuchus* nov. sp. Photograph and schematic drawing of the skull (holotype, MUSM 1981) in dorsal (*a*), ventral (*b*), and lateral (*c*) view. (*d*) Photograph of the right mandible (MUSM 987) and schematic drawing in dorsal view. Details of the skull (*e*, *f*). (*e*) MUSM 900 in lateral view. (*f*) MUSM 1681 in occipital view. For anatomical abbreviations see Appendices. Scale bars, 5 cm.

General Description. Within the Iquitos bonebeds we recognized cranial and mandibular remains of a longirostrine crocodylian among the diversified caimanine assemblage composed of at least six taxa (Salas-Gismondi et al., 2015a). The material includes different size individuals whose morphology is consistent with ontogenetic stages of a single new taxon (see below). The type of *Gryposuchus* nov. sp. (MUSM 1981) is a well-preserved skull slightly distorted at the right orbital region. It lacks most of the temporal and

occipital bones, as well as the pterygoid wings (Figs. V.2*a-c* and V.4*h*). The skull table is incomplete in the holotype, but well preserved in MUSM 1681 (Fig. V.3*a*), MUSM 2032 (Fig. V.3*c*), and partially distorted in MUSM 900 (Fig. V.3*b*). The type skull preserved length (from tip of the snout to the posterior angle of left supratemporal fenestra) is 623.2 mm. Other specimens, including cranial and mandibular remains, represent individuals of equivalent size (MUSM 1440; MUSM 987, MUSM 2032 MUSM 1428, MUSM 1681, MUSM 2407, MUSM 2472; MUSM 1435, MUSM 2470, and MUSM 2471; Fig. V.3*a, c*) with the exception of MUSM 900, a bigger skull lacking the anterior half of the snout (Figs. V2*e*, V.3*b*). MUSM 1439, MUSM 1727, MUSM 1993, MUSM 1682, and MUSM 1988 comprise specimens sensibly smaller in size with features associated to juvenile morphology and herein referred to *Gryposuchus* nov. sp. (Fig. V.6). The description of the mandible is mainly based on MUSM 987 (Figs. V.2*d*, V.4*i*, and V.5*a, b*), a complete right mandible corresponding to an individual of equivalent size to the holotype. This specimen only lacks the coronoid bone and posterior end of the retroarticular process. Parts of the posterior lamina of the splenial in contact with the surangular are missing or collapsed. Postcranial material was not identified. Two specimens, MUSM 1681 and MUSM 1682, were found in locality IQ136, probably corresponding to MZ5 (Middle Miocene; ca. 16-15 Ma). These are the oldest gavialoids known from the Amazon basin. An additional specimen, MUSM 987 was unearthed at IQ101, in the Momón River banks and might correspond to MZ6 (ca. 15-14 Ma). Pebas deposits in these localities represent lacustrine-dominated paleoenvironments with marine influence (Nuttall, 1990; Hoorn, 1994; Wesselingh et al., 2002; Boonstra et al., 2015). Dysoxic muddy bottoms within lakes and swamps were common in the Pebas System. Other gavialoid bones, including a diagnostic postorbital bone (MUSM 2430; Fig. V.7*a*) belonging to *Gryposuchus colombianus* or *Gr. croizati*, were found in IQ125 at Nueva Unión area.

Gryposuchus nov. sp. has a long and slender skull. The snout is parallel-sided and tubular in cross section. The anterior maxillary snout has slightly sinuate margins. Proportions of the rostrum correspond to those of *Gavialis gangeticus*: the rostral length/skull length index is 0.75 (0.76 in *G. gangeticus*) and the rostral width/postorbital width index is 0.27 (0.25 in *G. gangeticus*). In front of the orbits, the initial lateral expansion of the skull occurs at the level of the sixteenth maxillary alveolus and continuous to widen gradually posteriorly. In dorsal view, the postrostral skull outline is roughly triangular and the skull table is wide, trapezoidal in shape, and perforated by large supratemporal fenestrae. The supratemporal fenestrae are irregular in outline and wider posteriorly. The orbits are markedly smaller than the supratemporal fenestrae and roughly circular. The infratemporal fenestra is roughly ellipsoid in shape. The narial opening is heart-shaped, and its narial rim surface is interrupted anteriorly and anterolaterally by distinctive grooves, but no plateau-like shelf typical of *Gavialis* male adults is observed. The incisive foramen forms a slender, elongated isosceles triangle. The occipital plate is posteriorly inclined but appears to be at a lesser degree than in other South American gavialoids. Suborbital fenestrae are proportionally longer than those of *Gryposuchus colombianus* and *Gavialis gangeticus*, with the anterior end acute and the posterior margin broadly rounded. Pterygoid bullae are located laterodorsal to the posterior half of the palatine bridge. The mandibular rami (MUSM 987; Fig. V.2*d*) are sutured anteriorly, through a long rostral symphysis, to form a Y-shaped structure. Although long, the symphyseal region is proportionally shorter than in *Gavialis*, *Ikanogavialis*, *Siquisiquesuchus*, and *Piscogavialis*. The mandible is low along the symphysis and posteriorly its height progressively increases until the level of the glenoid fossa. The external mandibular fenestra is small, eye-shaped and occurs comparatively closer to the articular region than in *Gavialis*. The upper dentition formula is 4 premaxillary + 22 maxillary. This count is similar to other *Gryposuchus* species (Langston & Gasparini, 1997; Riff & Aguilera, 2008) but much less

than that of *Piscogavialis* (Kraus, 1998) and *Ikanogavialis* (Sill, 1970). The number of tooth loci in the lower jaw is 22.

Skull. The premaxillae are expanded at the level of the anterior end of the external naris but not as much as in *Gavialis* or *Gryposuchus colombianus*. Long and slender posterior processes of the premaxillary reach the level of the fifth maxillary alveolus. Thin anterior processes of nasals are in large contact medially with the posterior processes of the premaxillae. Although the extension of these processes is not precisely symmetrical, their contact length roughly equals the narial opening length, a condition also observed in *Eogavialis africanus*. As in all South American gavialoids, each premaxilla bears four alveoli and not five as in *Gavialis*, *Eogavialis*, and *Eothoracosaurus*, most probably by the loss of the second tooth loci of these later taxa (Brochu, 2004a). In *Gryposuchus* nov. sp. and other South American gavialoids where known, the first premaxillary alveoli are closed together and separated by large gaps from the second alveoli. First and second tooth loci bear alveolar collars projected ventrally relative to the palatal plate. Second alveoli are the biggest in the premaxilla whereas the fourth premaxillary alveoli are the smallest, as in *Gryposuchus* species (Fig. V.4*c*, *d*). Relatively big foramina are located medial to third and fourth premaxillary alveoli. The foramina are connected by shallow and bowed grooves. As other *Gryposuchus* species, posterior ventral processes of premaxillae are relatively short, reaching the level of the second maxillary alveoli. In *Piscogavialis*, they reach the level of the fifth maxillary alveoli. Ventrally, the premaxilla bears two anterior medial processes that are projected into the incisive foramen and the premaxillary-maxillary suture is stepwise and not linear as all other gavialoids.

The maxillae are long and tubular resembling those of *Eogavialis*, and not dorsoventrally flattened as in *Gryposuchus colombianus* and *Piscogavialis*. Dorsally, maxillae are not in contact due to the presence of the nasals and the slender posterior processes of the

premaxillae. As other *Gryposuchus* species, modest alveolar salients are observed along most of the maxillary margins. Each maxilla bears 23 tooth positions, all of them subequal in size, exclusive of the last two maxillary alveoli that are the only sensibly smaller alveoli. Ventrally, the intermaxillary suture is extended posteriorly until the level of the fifteenth tooth position. prefrontals. The edge of the maxillary tooth alveoli is higher than the palatal space between both tooth rows.

Table V.1 – Measurements (mm) of the holotype (MUSM 1981) and referred cranial specimens (MUSM 1681 and MUSM 900) of *Gryposuchus* nov. sp. Measurements after Langston & Gasparini (1997). Measurements with missing data are omitted. Abbreviations: e, estimate; l, left; r, right.

	MUSM 1981	MUSM 1681	MUSM 900
Basal length of the skull	--	--	--
Greatest width	--	--	291.8
Width of the rostrum, posterior	125.2e	--	160.5e
Length of the snout, medial axe	463.1	--	--
Length of skull, dorsal	--	--	--
Interorbital distance	51.2	42.1	59.0
Orbit length	44.3e	34.0e	58.3e
Skull table width, anterior	149.0e	144.8	171.3
Skull table length, lateral	--	129.5	172.4
Skull table width, posterior	--	207.9	262.1
Skull width across postorbital bars	--	--	231.6
Occipital condyle width	--	34.5	36.3
Occipital condyle height	--	24.3	28.3
Orbits width	56.8(l)	54.0e(l)	63.6(r)
Nares width	28.3	--	--
Nares length	29.5	--	--
Choana width	--	--	42e
Choana length	--	--	29e
Skull table length, medial	--	96.1	133.9
Snout length, to posterior nares	412.1	--	--
Quadrate condyle width	--	43.2(r)	56.3(l)
Supratemporal fenestra width	--	70.9(l)	86.4(r)
Supratemporal fenestra length	--	66.6(l)	75.5(r)
Suborbital fenestra length	--	96.5(l)	119.1(l)
Suborbital fenestra width	42.0e	41.9e(l)	59.8
Pterygoid wings width	--	--	208.8
Incisive foramen length	21.1	--	--
Rostrum width at fourth maxillary alveoli	48.6	--	--
Rostrum width at notch for fourth mandibular tooth	37.7	37.3	--
Tooth row length	495.2e	--	--
Palatine bar width	33.0e	--	48.0e
Skull length	--	--	--
Skull height	--	70e	--

Palatal surface is relatively convex. Anterior interalveolar length is notably larger than the diameter of adjacent alveoli. This length decreases progressively posteriorly to be equal to alveoli diameter at fifteenth tooth position and even smaller posterior to it. Dorsally, at the level of thirteenth tooth position the maxillae contact the anterior extension of the lacrimals. The initiation of the posterolateral orientation of the maxilla at this position is consequence of the increasing width of the lacrimals considering that the maxilla maintains its transversal diameter. There is no posterior process of the maxilla between the lacrimal and jugal as in *Gryposuchus colombianus*. The maxillae have a long edentulous posterior process that reaches the level of the postorbital bar (e.g., MUSM 900). Maxillae have no contact with

The nasals are extremely long, slender bones with intimate extensive anterolateral contact with the premaxillae. Additionally, the nasals contact the maxillae and lacrimals laterally, the prefrontals posteriorly, and the frontal posteromedially. Nasals are in contact along the sagittal axe for most of their length. Posteriorly, they are separated by the pointed anterior process of the frontal, almost at the level of the anterior extension of the jugals. Lateral margin of the nasals slightly diverge posteriorly, reaching their largest transversal diameter just ahead of the anterior processes of the prefrontals. Nasals posterior end reach the level of the anterior margin of the orbits, resembling in this aspect to *Eogavialis* and *Gryposuchus colombianus*, and distinguishing from *Piscogavialis* and *Ikanogavialis* in which nasals posterior end is located far anterior to this position. The condition in *Gavialis* is intermediate in this aspect. Whereas posterior process of the nasal is pointed in all South American gavialoids where known including *Gryposuchus* nov. sp., in *Gavialis* it is strongly denticulated.

The lacrimals are large and roughly triangular in shape. They contact the maxillae and jugals laterally and the nasals and prefrontals medially. Posteriorly, they form the anterior margin of the orbits. Anterior process of the lacrimal exceeds that of the frontal and

prefrontal. A small, discrete knob occurs at the orbital margin, lateral to the prefrontal-lacrimal suture.

The jugals form the orbit and infratemporal fenestra ventral margins. In *Gryposuchus* nov. sp. this bone differs from other *Gryposuchus* species and most gavialoids, and more closely resembles to the general pattern of non-gavialoid crocodylians. Gavialoids, such as *Gr. colombianus, Gr. croizati*, *Ikanogavialis*, *Gavialis,* and in lesser degree *Siquisiquesuchus*, present a deep notch immediately anterior to the postorbital pillar. However, in non gavialoid crocodylians and some gharials such as *Gryposuchus* nov. sp., *Eothoracosaurus*, *Eosuchus*, and *Piscogavialis*, the jugal orbital rim progressively descends lateral to the postorbital pillar, thus the ventral margin of the orbit is gently circular. Additionally, in these taxa as well as in *Siquisiquesuchus*, the postorbital pillar reaches the horizontal bar of the jugal medially and, between these structures, a longitudinal sulcus is present. This latter condition also differs from the distinctive feature observed in gavialoids such as *Gavialis* and other *Gryposuchus* species, in which the postorbital bar flush with the lateral jugal surface.

The prefrontals are short and rhomboid in shape. They are separated from each other by the frontal and nasals and take part of the anterodorsal orbital margin. From the orbit, the prefrontal-frontal suture follows a gentle semicircular path until its anterior end. In *Gavialis* and *Gryposuchus colombianus*, this suture is sharply angulated, a condition probably allied to fully "telescoped orbits" of these latter taxa.

The frontal bears a long anterior process that largely exceeds the prefrontal and the anterior orbital rim. Posteriorly, the main surface of the frontal is slightly concave and poorly sculptured. Laterally, along the fronto-postorbital suture the skull table is markedly higher than surrounding areas. Frontal participation in the orbital rim is reduced to the posteromedial corner. The frontal in the skull table is anteroposteriorly short due to the large size of the supratemporal fenestrae. Frontal sutures on skull table are not discernible in the holotype but

are well preserved in MUSM 1681 and MUSM 2032 (Fig. V.3*a*, *c*). The fronto-parietal suture is markedly concavoconvex (i.e., M-shaped) between the supratemporal fenestra and linear laterally. It runs along the anterior border of and only briefly enters to the supratemporal fenestra as in *Gryposuchus colombianus*. In MUSM 900 the suture runs on the dorsal surface of the skull table just grazing the margin of the fenestra. The frontal bone and skull table are not elevated relative to the rostrum. The skull table presents an uneven surface, being depressed between the orbits but higher along the postorbital-frontal suture and parietal-supraoccipital region.

The postorbital bones on skull table are relatively flat and weak. They form the anterior corner of the skull table and lack the anterolateral postorbital process characteristic of *Gavialis*, *Gryposuchus colombianus*, *and Gryposuchus neogaeus*. The development of this feature is variable in *Gryposuchus croizati* and incipient in *Siquisiquesuchus* and *Piscogavialis*. The postorbital contacts medially the frontal and briefly the parietal at the rim of supratemporal fenestra. The postorbital takes part of the dorsal portion of the postorbital bar. As other gavialoids, the postorbital bar is robust and longer than wide in cross section. On the lateral side of the postorbital bar, there is an anteroposteriorly crest-like bump, similar to that of *Gr. colombianus* and *Piscogavialis*. This structure lies entirely on the postorbital. In MUSM 900, the largest specimen, the bump presents an anterolateral spine similar to that of *Gavialis* (Norell, 1989). The suture with the jugal is placed lower in the postorbital bar although its precise pattern is not recognized. The lowermost descending process of the postorbital is located posteriorly; it reaches the level of the horizontal bar of the jugal, and contacts the ectopterygoid medially. The postorbital bar is inset from the anterolateral margin of the skull table. Under this margin, on the excavated lateral surface, most specimens present generally two big foramina although their size, number, and position are variable. It is not possible to determine if the postorbital contacts the quadratojugal medially.

The squamosals are incomplete in the holotype but well preserved in MUSM 1681, MUSM 2032, and particularly in MUSM 900. They occupy the posterolateral corner of the skull table. Posterior lateral squamosal processes are shorter than those of most South American gavialoids and *Argochampsa*, but the characteristic prong-like extension of the squamosals is still present (Fig. V.2*e*; Brochu & Rincón, 2004; Jouve et al., 2008; Riff & Aguilera, 2008). In *Gryposuchus colombianus*, this region is not well preserved, but seems to be that long "prongs" were present as well (Langston & Gasparini, 1997). Posterior bar surface is relatively thin (MUSM 1681: Fig. V.3*a*), similar to that of *Gavialis* and *Gr. colombianus*, but in a lesser degree than in *Piscogavialis* and *Gr. neogaeus* (Gasparini, 1968; Kraus, 1998); in *Eogavialis*, it is comparatively wider. The anterior process of the squamosal lateral to the skull table runs anteroventrally and reaches the posterodorsal end of the postorbital pillar.

The parietal forms the medial and posteromedial margins of the supratemporal fenestrae. Anteriorly, the parietal surface between the supratemporal fenestrae is horizontal and relatively even. Backwards, the parietal surface gently ascends, thus its main body slopes anteriorly and also laterally as usual in gavialoids. Posteriorly, it contacts with the supraoccipital on the sagittal axis. The parietal interfenestral bar is comparatively thinner than that of *Gavialis* and *Siquisiquesuchus* (see Brochu & Rincón, 2004).

The supraoccipital forms an inverse triangle in the occipital plate excluded from the foramen magnum. It also bears a small rhomboid-shaped dorsomedial projection on the cranial roof that points posteriorly. Along with the parietal, this posterior extension becomes into a prominent vertical medial crest on the occipital plate (observed in MUSM 1681). The postemporal fenestrae are hardly discernable in any of the specimens and they seem to be reduced in size. Available specimens show asymmetrical development of the postoccipital processes (processus postoccipitales of Kälin, 1933) and surrounding area of the

supraoccipital, although the so-called “nuchal crest” is not hypertrophied as in *Gr. colombianus* (Langston & Gasparini, 1997).

The quadratojugal forms the posterior margin and corner of the infratemporal fenestra. The anterior process of the quadratojugal comprises a robust spine as usually observed in gavialoids. Dorsomedially, the ascending process that bounds most of the posterior margins of the infratemporal fenestra is very thin and long; its dorsal end is not discernible. Sutural contacts with the jugal and the quadrate are not parallel as in *Piscogavialis*.

The quadrates are robust and relatively short. The quadrate bounds ventrally the otic aperture and, although incomplete, it seems to occupy part of its posterior margin, thus the quadrate-squamosal suture might have reached the otic aperture along the posterior wall. The small foramen aerum is located on the mediodorsal surface of the quadrate. The axe of mandibular condyles is oblique as generally in gharials. Medial and lateral condyles are clearly discernable with the medial one reflected ventrally as in South American gharials where known, such as *Piscogavialis*, *Siquisiquesuchus*, and *Gryposuchus croizati*.

The laterosphenoids are partially preserved in the holotype as well as in MUSM 2032 and MUSM 1681. Anterior dorsal margin of the laterosphenoids, as well as the capitate process are oriented lateromedially. The dorsal capitate process is massive. The whole anterior portion is relatively flat.

The palatine bones cover the whole ventral surface of the bridge between the suborbital fenestrae. They are roughly parallel-sided and transversally convex along this bridge. From the anterior limit of the suborbital fenestrae, the lateral margins of the palatine bones converge to a point at the level of the fifteenth maxillary alveolus. The anterior limit of the suborbital fenestra is located at the level of the nineteenth maxillary alveolus. The palatine-pterygoid suture is anterior to the rear margin of the suborbital fenestra.

The ectopterygoids are incomplete and badly damaged, preserved regions are informative though. The anterior process of the ectopterygoid is thin and long, resembling that of *Piscogavialis*. It comprises the posterior half margin of the suborbital fenestra. The anterior tip runs medially to the maxillary tooth row until the level of the anterior limit of the penultimate alveolus as in *Piscogavialis*. The distance between the tooth row and the anterior process of the ectopterygoid is reduced relative to that of *Gavialis*. In ventral view, *Gryposuchus* nov. sp. and *Piscogavialis* bear large contact between ectopterygoid and jugal whereas this contact is reduced in the extant gharial. Current evidence concerning the same anatomical area is not clear in other South American gharials. Revised *Eogavialis* specimens do not preserve details of this region other than a large ectopterygoid-jugal contact. As no other gavialoids, in *Argochampsa* the ectopterygoid stops far behind the tooth row (Jouve et al., 2006). Posterior process of ectopterygoid is short, thus actual contact with the pterygoid flanges is reduced.

The pterygoid widely separates de ectopterygoids from the palatines. In the holotype, pterygoid bullae in intimate contact with the palatines are observed dorsal to the posterior portion of the palatal bridge (Fig. V.4*h*). The bullae are neither ovoid in shape nor smooth in surface; instead they are brain-like in shape with irregular prominences and depressions. They are relatively small, flat, and projected laterally just slightly into the suborbital fenestrae as in the type specimen of *Gr. colombianus*. The choana is distorted in MUSM 900 but is not preserved in any other specimen.

The exoccipitals are better preserved in MUSM 1681. Although they are exposed in dorsal view (Fig. V.3*a*), this condition is attenuated compared with *Piscogavialis*, *Gryposuchus colombianus*, and *Gryposuchus croizati*. The paraoccipital processes are long and encompass a ventral plate-like expansion that completely covers the cranioquadrate foramen. Dorsal to the foramen magnum, exoccipitals and the supraoccipital are collapsed,

thus relations with these bones are obscured. The ventral extension of the exoccipitals embraces laterally the basioccipital tubera. They are robust and anteroposteriorly extended (Fig. V.2*f*). The basioccipital is typically gavialoid in being low and laterally expanded ventral to the condyle producing two pendulous tuberae (Fig. V.2*f*).

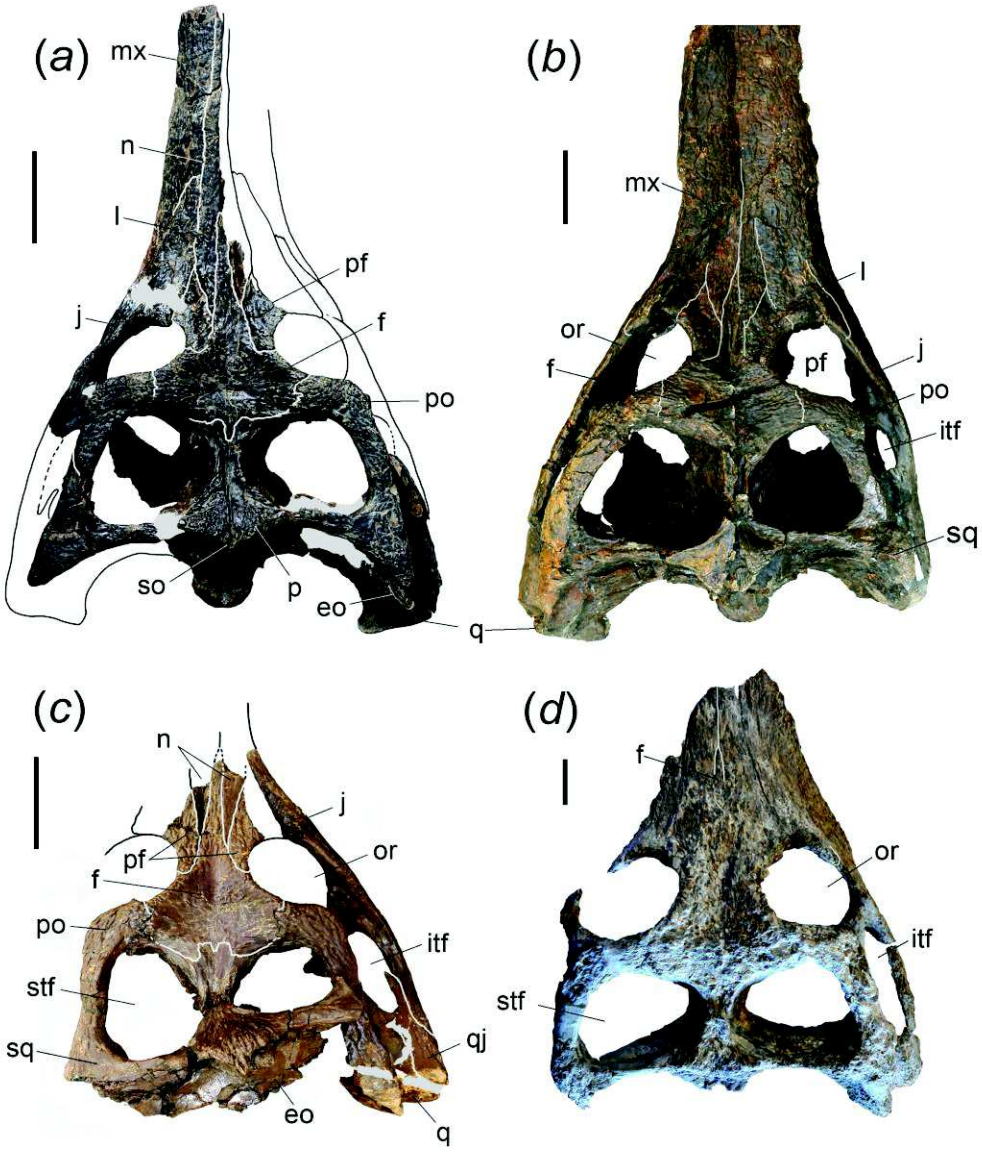

Figure V.3. Comparisons between selected cranial materials referred to *Gryposuchus* nov. sp. Skulls in dorsal view of: (*a-c*) *Gryposuchus* nov. sp. from the Middle Miocene of the Pebas Formation, Peru and (*d*) *Gryposuchus* nov. sp. from the Late Miocene of Urumaco, Venezuela. (*a*) MUSM 1681, adult specimen, MZ5; (*b*) MUSM 2032, adult specimen, MZ8; (*c*) MUSM 1988, juvenile specimen, MZ8; (*d*) AMU CURS 12, adult specimen. For anatomical abbreviations see Appendices. Scale bars, 5 cm.

The basioccipital plate is smooth exclusive of the lateral and ventral margins, where tuberosities are well developed. Medially, the ventral margin is excavated. Anterior to the bassioccipital, the basisphenoid is anteroposteriorly wide.

The braincase region is badly damaged around the prootic in all the specimens.

Anatomical remarks of the circumorbital region: Circumorbital bones include the frontal, prefrontals, lacrimals, jugals, and postorbitals. The orbits are slightly wider than long, closer in shape to those of *Eogavialis africanus* than to the circular orbits of *Gavialis* and other *Gryposuchus* species (Fig. V.2*a*). In contrast to the adult condition, the orbital shape and proportions of a juvenile specimen (MUSM 1988; Fig. V.6*a*) resemble those of *Piscogavialis* and *Eothoracosaurus*, in which the orbits are comparatively longer anteroposteriorly. Although variable, the interorbital bridge diameter (i.e., frontal bone width) is essentially equivalent to the width of the orbit and consistently more slender than that of *Gavialis* and other species of *Gryposuchus*. The dorsal and anteroventral orbital margins are upturned, but to a lesser degree than in *Gavialis* and other *Gryposuchus* species. The anterior orbital margin (i.e., lacrimal bones) lies flush with the rostral surface and bears two sulci. The lacrimals are large and roughly triangular in shape. The prefrontals are short and rhomboid in shape, separated from each other by the frontal and nasals, and form part of the anterodorsal orbital margin (Fig. V.2*a*). The jugals differ from those of other *Gryposuchus* species and of most gavialoids; they more closely resemble the general pattern of non-gavialoid crocodylians. Gavialoids, such as *Gryposuchus colombianus*, *Gryposuchus croizati*, *Ikanogavialis*, *Gavialis*, and to a lesser degree *Siquisiquesuchus*, present a deep notch immediately anterior to the postorbital pillar. However, in non-gavialoid crocodylians and some gavialoids such as *Gryposuchus* nov. sp., *Eothoracosaurus*, *Eosuchus*, and *Piscogavialis*, the jugal orbital rim progressively descends lateral to the postorbital pillar, thus the ventral margin of the orbit is gently circular (Fig. V.2*c*). Additionally, in these taxa as well as in *Siquisiquesuchus*, the

postorbital pillar reaches the horizontal bar of the jugal medially and, between these structures, a longitudinal sulcus is present. This latter condition also differs from a distinctive feature observed in many gavialoids, such as *Gavialis* and other *Gryposuchus* species, in which the postorbital bar lie flush with the lateral surface of the jugal. Postorbital bones on skull table are relatively flat and weak. They form the anterior corner of the skull table and lack the anterolateral postorbital process characteristic of *Gavialis*, *Gr. colombianus*, and *Gr. neogaeus*.

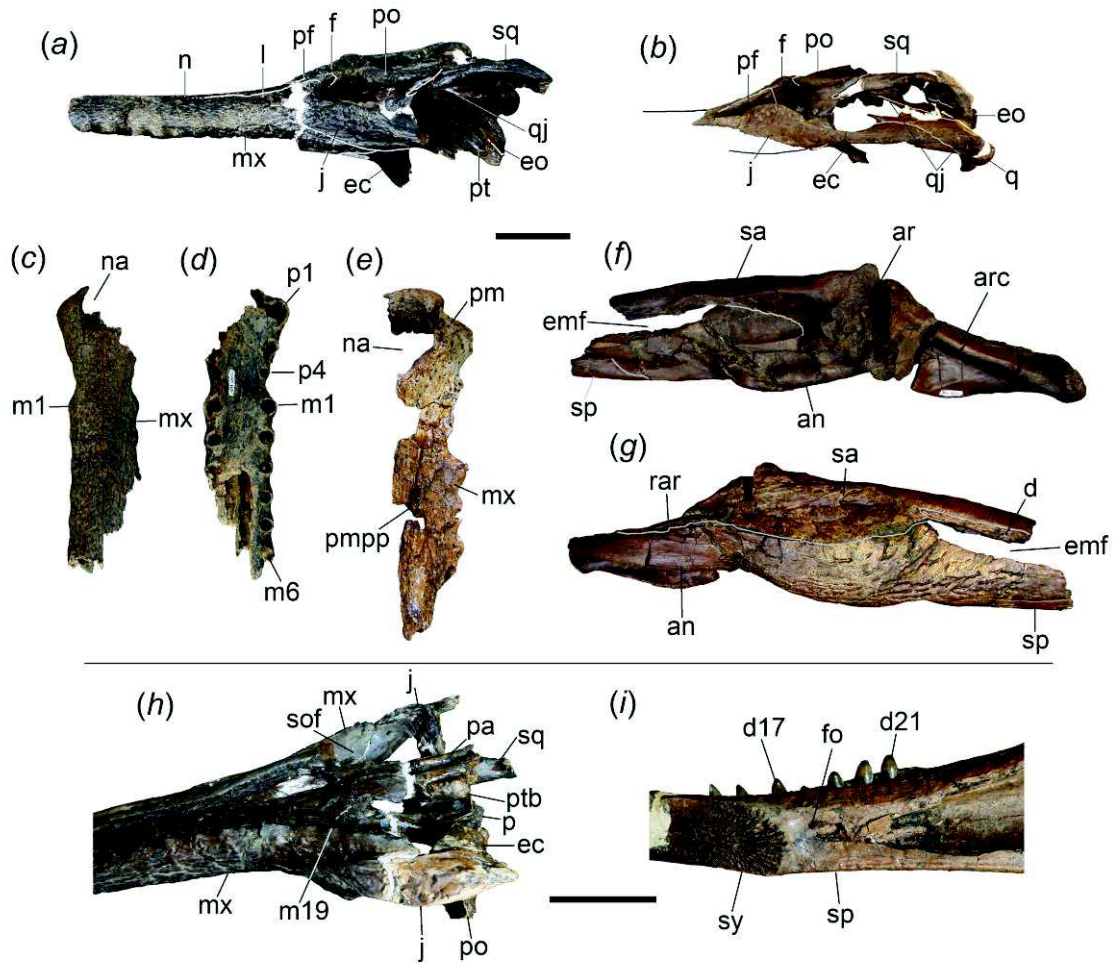

Figure V.4. Anatomical details of *Gryposuchus* nov. sp. (*a*) MUSM 1681, skull in left lateral view. (*b*) MUSM 2032, skull in left lateral view. (*c*, *d*) MUSM 1681, partial snout in dorsal (*c*) and ventral (*d*) view. (*e*) UFAC 1272, partial snout in dorsal view. (f, g) MUSM 1440, posterior right mandibular ramus in medial (*f*) and lateral (*g*) view. (*h*) MUSM 1981, detail of the palatine region in ventrolateral view. (*i*) MUSM 987, detail of the foramen (fo) located behind the mandibular symphysis. For anatomical abbreviations see Appendices. Scale bars, 5 cm.

In summary, the general configuration of this area in *Gryposuchus* nov. sp. depicts weak development of "telescoped" orbits. This is interpreted as an incipient condition for more extensive telescoping of the orbits in later diverging relatives, based on ancestral state transformations determined from the maximum parsimony phylogeny.

Mandible. The dentary bone is long, expanded at the level of the second alveolus and restricted to the lateral wall of the mandibular ramus behind the level of the tooth series. It reaches posteriorly the rear margin of the external mandibular fenestra (EMF). Up to the fifteenth tooth position, alveoli are implanted within salients along the lateral border of the dentary and provide a sinuate profile to this margin. The dentary (MUSM 987; Fig. V.2*d*) bears 22 alveoli, all of them sub-equal in size, exclusive of the first and fourth of bigger diameter, and the second and third being the smallest of the whole series. *Gryposuchus colombianus* and *Gr*. *croizati* present similar alveolar count (i.e., 22-23) and general dental pattern. Differences relative to these species include: proportionally higher and tubular dentary, stronger alveolar salients, and no sensible constriction between the fourth and fifth alveoli (this late character only compared to *Gr*. *colombianus*). Posterior to the level of the mandibular symphysis we count at least four tooth positions as in *Piscogavialis*, whereas other gavialoids generally present no more than three. These last alveoli are located along the medial limit of the dentary and their lingual wall is completed either by the splenial (i.e., nineteenth and twentieth) or the surangular (i.e., twenty first and twenty second).

The splenials wedge out between the dentaries at the level of the twelfth dentary alveolus (Fig. V.2*d*). As recognized for South American gavialoids which splenial is known, the anterior process is long, slender, and constricted between dentaries along the symphysis. Its lateral margin is bowed medially. In MUSM 1428, a right mandible, the medial surface of the splenial within the symphysis shows no perforation of the foramen intermandibularis oralis. Although absent in *Tomistoma schlegelii*, the presence of this foramen was recognized

within the symphysis of *Gavialis* at the level of the twenty-second alveolus (Norell, 1989). Interestingly, we identified in *Gryposuchus* nov. sp. and *Eogavialis africanus* (AMNH 5069) a foramen – probably homologous to that of *Gavialis* – just behind the symphysis, in the medial divergent walls of the splenial at the level of the twentieth alveolus. Posterior to the symphysis, the splenial occupies the internal half of the rami.

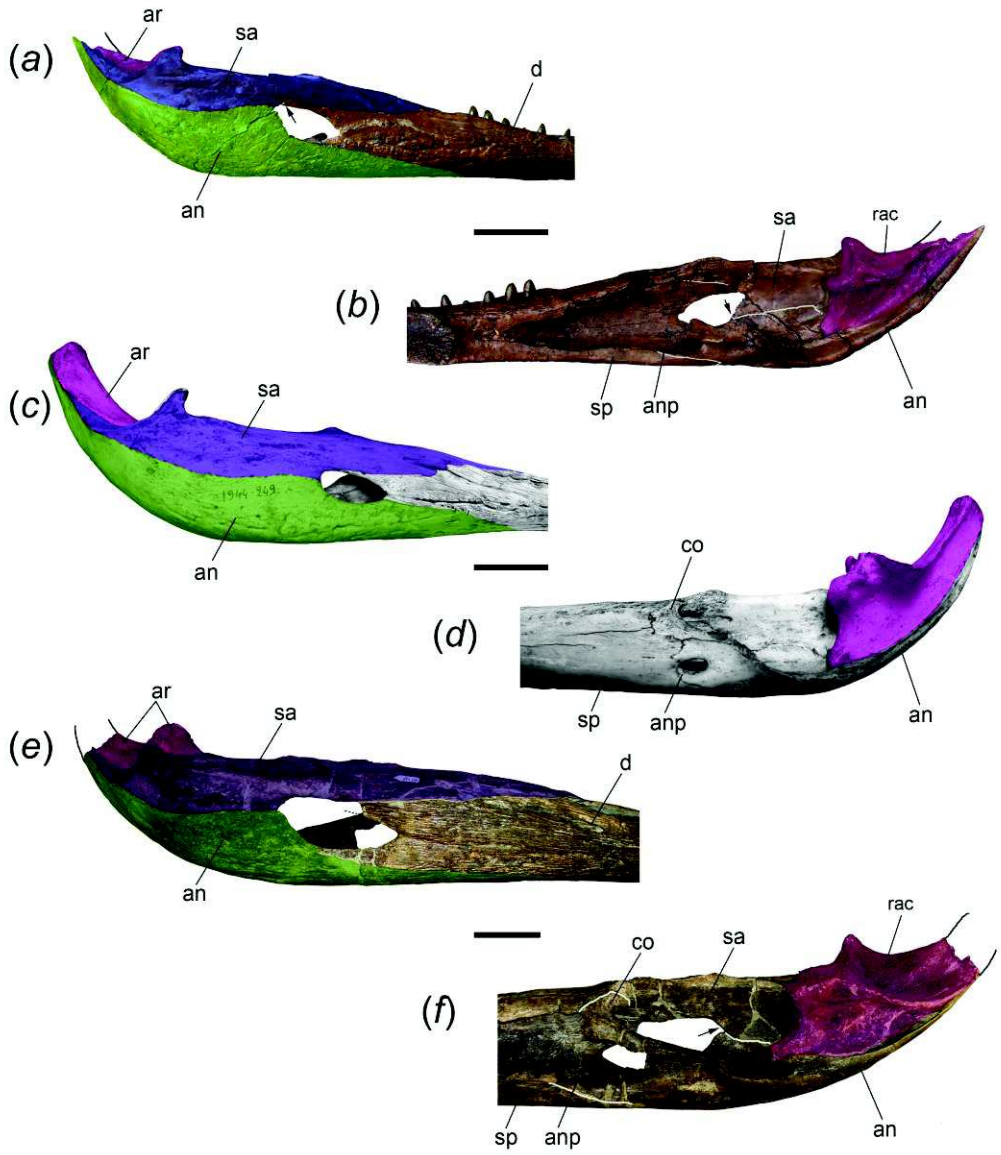

Figure V.5. Post-symphyseal anatomy of gharial mandibles. (*a*, *b*) *Gryposuchus* nov. sp. (MUSM 987) in lateral (*a*) and medial (*b*) views. (*c*, *d*) *Gavialis gangeticus* (MNHN A-5312) in lateral (*c*) and medial (*d*) views. (*e*, *f*) *Piscogavialis jugaliperforatus* (MUSM 449) in lateral (*e*) and medial (*f*) views. For anatomical abbreviations see Appendices. Scale bars, 5 cm.

It seems that the splenial is excluded from the margins of the foramen mandibularis caudalis whereas its ventral posterior process largely surpasses the rear limit of this foramen (Fig. V.5*b*). Other details of the splenial anatomy relative to the angular or coronoid are missing.

Table. V.2 – Measurements (mm) of mandibles of *Gryposuchus* nov. sp. MUSM 987, right mandible; MUSM 1428, partial right mandible. Mandible width at the end of the symphysis was estimated by duplicating the minimum width measurement of the preserved mandibular ramus. Measurements modified from Langston & Gasparini (1997). Abbreviations: e, estimate, l, left; r, right.

	MUSM 987	MUSM1428
Mandible length	698.0e	--
Symphysis length	369.2	398.3
Tooth row length	414.5	479.3e
External fenestra length	49.0	--
External fenestra height	21.0	--
Glenoid fossa length	24.9	--
Retroarticular process length	85.7e	--
Mandible height	25.8	--
Mandible width at fourth tooth	24.7 (x 2)= 49.4	29.5 (x2)= 59.0
Mandible width at the end of the symphysis	46.0 (x 2)= 92.0	51.1 (x2)=102.2
Splenial length in symphysis	133.9	145.0

The surangular extends from the medial anterior border of the twentieth alveolus to the lateral surface of the retroarticular process. Within this process, the surangular is partially preserved in MUSM 987, but fully preserved in MUSM1440 (Fig. V.5*g*). This latter specimen shows that the surangular fails to reach the posterior tip of the retroarticular process. In lateral view the surangular is low. It is restricted to the posterior angle of the EMF due to the rear expansion of the dentary and remarkable depth of the angular that embraces this fenestra posteriorly (Fig. V.5*a*). Probably this condition also pertains to *Piscogavialis* (Fig. V.5*f*) and *Gr. colombianus* (Langston & Gasparini, 1997). Externally, at the level of the glenoid fossa there is a big foramen facing anterodorsally. Among gavialoids, a similar foramen is only observed in *Eogavialis africanus* (SMNS 11785). Just behind this foramen, the surangular cover the postglenoid process of the articular, therefore this process is hardly seen in lateral view as in *Gavialis* (Fig. V.5*a*, *c*) contrary to *Piscogavialis* in which surangular ascending

lamina is relatively small (Fig. V.5*e*). Medially, the surangular almost reaches the lower margin of the EMF as observed in most crocodylians and South American gharials known so far (Gasparini, 1968; Langston & Gasparini, 1997), but *Piscogavialis* (Fig. V.5*e*). Posteriorly, the surangular-angular suture reaches the articular at ventral tip. Proportions of the foramen mandibularis caudalis are similar in *Gryposuchus* nov. sp. and *Piscogavialis*, with this foramen being relatively longer than in *Gavialis*.

The angular is excluded from the ventral margin of the EMF being only restricted to its posterior margin, a feature also observed in the new material of *Piscogavialis* (MUSM 449; Fig. V.5*e*). Other gavialoids such as *Gavialis*, *Gr. neogaeus*, and *Gr. colombianus* (Gasparini, 1968; Langston & Gasparini, 1997) typically present a reduced posterior process of the dentary; therefore the angular borders most of the EMF ventrally. The angular approaches dorsally to the posterior process of the dentary but fails to contact it. An angular-dentary contact in this position is described for *Gr*. *colombianus*, but to our knowledge this area is damaged in referred specimens and this condition is best seen as unknown in this taxon. The angular forms the ventral section of the retroarticular process. Its posterior tip is not preserved.

The articular bone is lying down over the angular. It is posteriorly and medially inclined compared to *Gavialis* (Fig. V.5*d*). The articular is also inclined in *Piscogavialis*, a condition probably correlated with the ventromedial projection of the medial hemicondyle of the quadrate. As a consequence, the medial fossa of the retroarticular dorsal surface can be observed in medial view. A prominent longitudinal crest on the dorsal surface of the retroarticular process limits this fossa laterally. This crest is also well developed in *Piscogavialis*, other South American gharials, such as *Gr. colombianus*, and *Siquisiquesuchus* (Brochu & Rincón, 2004). Within the glenoid fossa, the articular-surangular suture runs diagonally from its concave anterior margin to the lateral limit of the postglenoid crest.

Teeth. Teeth crowns are conical in shape and inclined posterolingually in the plane formed by the fore and aft carinae. Within this general morphology, proportions vary substantially relative to loci position in both upper and lower jaws. Although anterior teeth are long and slender, they do not show the sigmoid-shaped crown of other gavialoids. Posterior teeth are short, robust, and slightly blunt. Although weak longitudinal striae are observed, the surface can be described as virtually smooth.

Juvenile specimens. Specimens of relative smaller sizes are referred here as juvenile individuals of *Gryposuchus* nov. sp. (Fig. V.6). MUSM 1988 is an incomplete skull without the snout (Fig. V.6*a-c*). The width of the skull across the postorbital bars is 90.5 mm whilst in the holotype this diameter is around 178.0 mm. It preserves the skull table as well as the orbital and occipital regions. Medial portion of the posterior skull table has been pressed down due to compression, thus the foramen magnum is collapsed and occipital plate partially distorted.

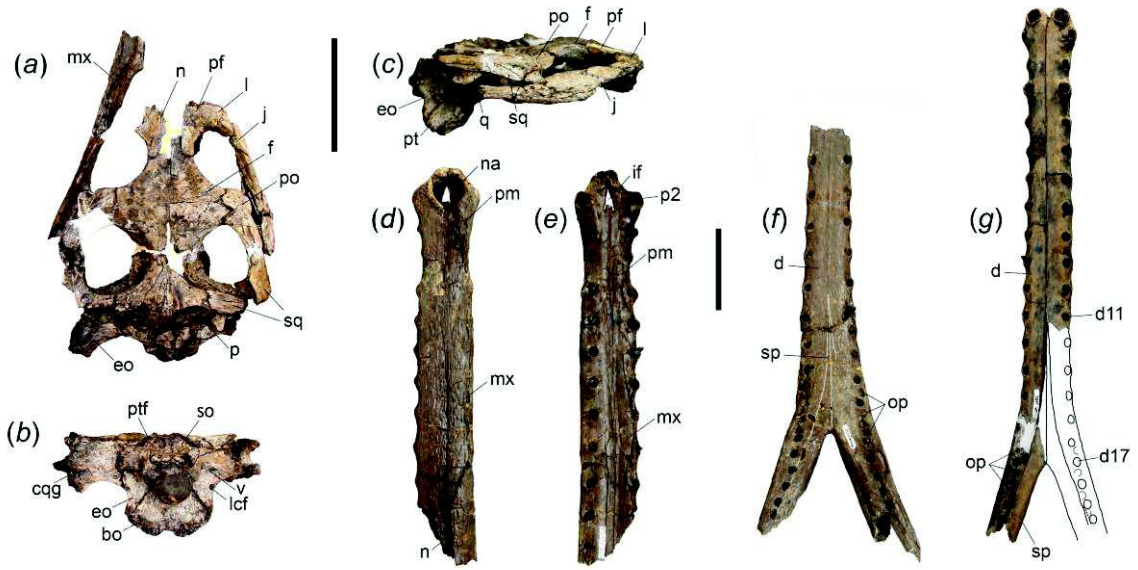

Figure IV.6. Juvenile specimens of *Gryposuchus* nov. sp. (*a-c*), MUSM 1988, partial skull in dorsal (*a*), occipital (*b*), and right lateral (*c*) views. (*d*, *e*) MUSM 1727, snout in dorsal (*d*) and ventral (*e*) views. (*f*) MUSM 1439, symphyseal mandible in dorsal view. (*g*) MUSM 1682, symphyseal mandible in dorsal view. For anatomical abbreviations see Appendices. Scale bars, 5 cm; smaller scale bar for (*d*)-(*g*).

Compared with specimens described here as possessing the adult morphology of *Gryposuchus* nov. sp., MUSM 1988 has a slender postrostral skull due to the less degree of posterior divergence of the jugal lateral margins.

The orbits are elongated and equivalent in size to the supratemporal fenestrae. The adult morphology shows short, wide orbits, and large supratemporal fenestrae, suggesting that an allometric development between the orbital and postorbital skull region occurred during ontogeny. Juvenile fenestral shape and proportions resemble those of the holotype of *Piscogavialis jugaliperforatus*. The fronto-parietal suture lies entirely on the skull table without grazing the margin of the supratemporal fenestra. Posterior process of the nasals surpasses the anterior margin of the orbits. The interorbital bridge is equivalent to the orbit transverse diameter as in adult individuals. The basioccipital plate and tubera are well preserved in MUSM 1988 (Fig. V.6*b*). The basioccipital plate is wider and dorsoventrally shorter than the adult condition represented in MUSM 1681 (Fig. V.2*e*). The lateral carotid foramen is well exposed in posterior view, next to the lateral margin of the exoccipital ventral processes. These processes are robust and reach the tubera. The tubera is separated medially by a depression posterior to the medial Eustachian foramen. Lateral margins of basioccipital plate are parallel and composed entirely by the exoccipitals. In adult specimens (Fig. V.6*e*), lateral margins become divergent ventrally and a significant portion of the tubera is extended ventral to the exoccipital, providing to the basioccipital-exoccipital structure a pendulous shape.

MUSM 1727 comprises a partial snout preserved until the level of the ninth maxillary alveolus (Fig. V.6*d*, *e*). As the posterior skull, the juvenile snout is comparatively more slender than in specimens representing the adult morphology. Major differences regard the relative smaller size of the alveoli and, consequently the larger diastemata between adjacent tooth loci within the juvenile specimens in both upper and lower quadrants (Fig. V.6*e*). Partial

mandibles comprising the symphyseal region are recovered from IQ 136 (MUSM 1682: MZ5; Fig. V.6*g*) and IQ 26 (MUSM 1439: MZ8; Fig. V.6*f*). The time span separating these localities is estimated in around 3 million years. They represent animals of equivalent size, although smaller alveoli in the specimen coming from the younger outcrops are probably depicting an earlier ontogenetic stage and a bigger adult size. Other features, such as the extension of the splenial symphysis and the postsymphyseal tooth loci, seem to be consistent with those of adult individuals.

Gryposuchus *specimen from Venezuela*. Among the copious gavialoid material from the Late Miocene Urumaco Formation, we identified a taxon consistent in morphology with the new Pebasian gavialoid. Here, we tentatively refer it as *Gryposuchus* nov. sp. The Urumaco Formation consists of complex intercalation of sandstone, organic-rich mudstone, coal, shale, and thick-bedded coquinoidal limestones with abundant mollusc fragments (Quiroz & Jaramillo, 2010). The specimen comprises a partial skull (AMU CURS 12; Fig. V.3*d*) collected within the Upper Member, at the Domo de Agua Blanca Locality (Sánchez-Villagra & Aguilera, 2006). This member is characterized by organic-rich, dark-gray laminated mudstone and shale, and abundant vertebrate fragments (Quiroz & Jaramillo, 2010). The upper member of the Urumaco Formation was deposited in a delta plain.

Other than differences in size, the anatomical traits of AMU CURS 12 from the Late Miocene Urumaco Formation of Venezuela are essentially identical to those of *Gryposuchus* nov. sp. (Fig. V.3*d*). As in the Peruvian specimens, AMU CURS 12 bears a trapezoidal skull table vastly perforated by supratemporal fenestrae, and circular and only moderately "telescoped" orbits. Additionally, the Venezuelan specimen resembles *Gryposuchus* nov. sp. and also differs from other *Gryposuchus* species in having its interorbital bridge width equalling the transverse diameter of the orbit, and a postorbital pillar contacting the horizontal bar of the jugal medially. Bone sutures are not discernable on the Venezuelan specimen.

C.2 Nueva Union gavialoid material

Gryposuchus Gurich, 1912

Gryposuchus cf. *colombianus* Langston, 1965

Material. MUSM 2430, left postorbitary (Fig. V.7*a-c*).

Locality and Horizon. Locality IQ125 (Chapter II.A; Fig. II.1), Nueva Unión area, Peru; "Uppermost Pebas" Formation, early Late Miocene, ca. 11 Ma (MZ9 or younger intervals (Rebata et al., 2006; Wesselingh et al., 2006*a*; Salas-Gismondi et al., 2015a).

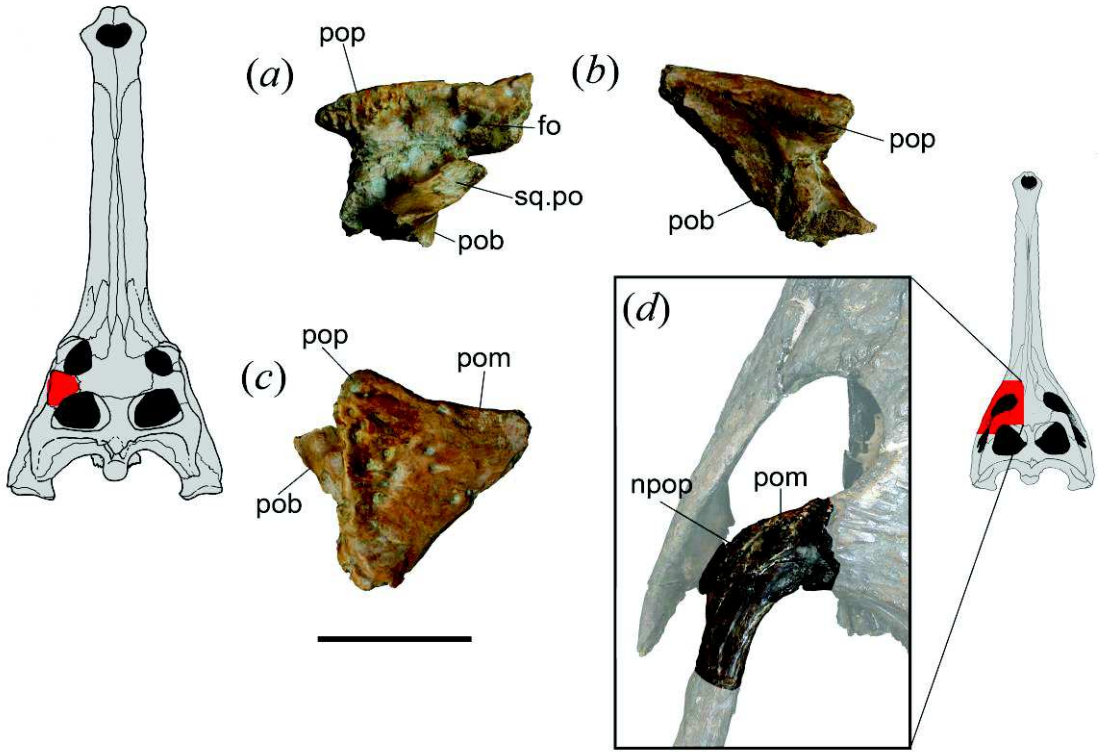

Figure V.7. *Gryposuchus* cf. *colombianus* from Nueva Unión. (*a-c*) MUSM 2430, partial left postorbital bone in lateral (*a*), anterior (*b*), and dorsal (*c*) view. For comparison, close-up of the postorbital bone in dorsal view of *Gryposuchus* nov. sp. (MUSM 1981) from Iquitos (IQ26). npop in (*d*) indicates the absence of postorbital process. For anatomical abbreviations see Annexes. Scale bars, 5 cm.

Comparative description and remarks. The left postorbitary preserves portions of the skull table and dorsal section of the postorbital bar broken at the level of the anteroposterior crest.

The skull table surface is relatively flat and virtually lacks of ornamentation. Based on the orientation of the postorbital bar, we presume that the postorbital skull table surface faced laterodorsally as in *Gryposuchus colombianus*. The orbital margin of the postorbital is concave, thus the anterior corner of the skull table was strongly proyected anterolaterally. Its lateral margin is linear. It strongly overhangs the postorbital bar. The postorbital bar is massive and large in cross section. As described for *Gryposuchus colombianus* (Langston & Gasparini, 1997), below the overhanging lateral margin of the skull table is an excavation with big foramina. The postorbital bar bears a sutural trough for the reception of the anterior process of the squamosal as in *Gryposuchus colombianus*. In *Gryposuchus* nov. sp., the anterior process of the squamosal abuts the postorbital pillar but fails to invade it. The contact with the squamosal in the skull table is denticulated. Other bone contacts are not preserved.

D. Results

D.1 Results of the phylogenetic analysis

Our first parsimony analysis retained 45 equally optimal trees with a minimum length of 538 steps. The strict consensus phylogeny (Figs. V.8 and V.10*a*; Appendices) calculated from those trees provided the following statistics: length = 553; consistency index (CI) = 0.461; retention index (RI) = 0.743. Our strict consensus tree shows general coincidence with previous morphological and molecular analyses for major relationships within crocodylian clades (Brochu, 1999, 2004a; Jouve et al., 2008; but as in other morphological analyses, it differs markedly from results based only on molecular data in the hypothesized affinities between *Gavialis* and *Tomistoma* (e.g., Gatesy et al., 2003; Oaks, 2011). Thus, we found strong Bremer support for the monophyly of Gavialoidea, with *Gavialis* having much closer relationships with Cretaceous gavialoid taxa such as *Eothoracosaurus*, than with extant *Tomistoma*, the latter being closely allied with *Crocodylus* within the Crocodyloidea. Within

the Alligatoroidea, *Culebrasuchus mesoamericanus* is closer to *Alligator mississippiensis* than to *Caiman crocodilus* (Salas-Gismondi et al., 2015a).

Figure V.8. First strict consensus phylogenetic tree. The strict consensus phylogeny calculated from the complete data matrix: length = 553; consistency index (CI) = 0.461; retention index (RI) = 0.743.

The new Pebasian species, *Gryposuchus* nov. sp., is recovered within gavialoids as the sister taxon of the *Gr. colombianus* + *Gr. croizati* clade. Thus, our results suggest that all known Amazonian gavialoids belong to a single, monophyletic taxon (the inclusive species of

Gryposuchus) characterized by association with riverine and lacustrine-tidal paleoenvironments. On the other hand, relationships among South American taxa usually associated with coastal marine paleoenvironments show no resolution: *Siquisiquesuchus*, *Piscogavialis*, and *Ikanogavialis* lie in a polytomy together with Amazonian *Gryposuchus* and Indo-Asian *Gavialis* (Figs. V.8 and V.10*a*). As a consequence, this first analysis finds no support for the monophyly of a clade comprising South American gavialoids as was suggested by previous contributions (Brochu & Rincón, 2004; Brochu, 2006; Vélez-Juarbe et al., 2007). This clade, namely Gryposuchinae as proposed by Vélez-Juarbe et al., (2007), was usually associated only by weak support or collapsed when the analysis included *Argochampsa* (Riff & Aguilera, 2008). It is noteworthy that we found support, although low, for a novel association between African *Argochampsa* and the Caribbean taxon *Aktiogavialis*, with this clade found as most closely related to the clade of South American gavialoids and Indo-Asian *Gavialis*, and with *Eogavialis* as the nearest outgroup to all of the others. Therefore, African *Argochampsa* is more closely related to Indo-Asian *Gavialis* as was previously suggested by other contributions (Jouve et al., 2008; Riff & Aguilera, 2008), than it is to African *Eogavialis*. In fact, both Paleogene African taxa, *Argochampsa* and *Eogavialis*, share key characters with more anatomically-derived gavialoids like *Gavialis*. The clade encompassing this subset of late-diverging gavialoids is here termed "gharials" (Figs. V.8-V.10) and it is characterized by a posteriorly pointing supraoccipital (character 160-1), anteroposteriorly wide basisphenoid (character 172-1), robust exoccipital ventral process to basioccipital tubera (character 176-1), and basioccipital plate with ventrally divergent sides (character 196-1). Paleocene *Eosuchus* and Cretaceous "thoracosaurs" from the northern hemisphere are identified in this analysis as the first and second basalmost branches among gavialoids, respectively.

To better understand morphological transformations, we performed a second analysis, this time excluding individual characters revealed as highly homoplastic, since results suggested that they were acquired independently up to three times among later-diverging gavialoids, including *Gryposuchus* and *Gavialis*. In addition, this analysis collapsed states of character 138 and deleted state 2 from character 137, both of which describe morphology of the orbital margin associated with "telescoped" orbits, which clearly evolved multiple times independently with gavialoids (see Chapter V.E).

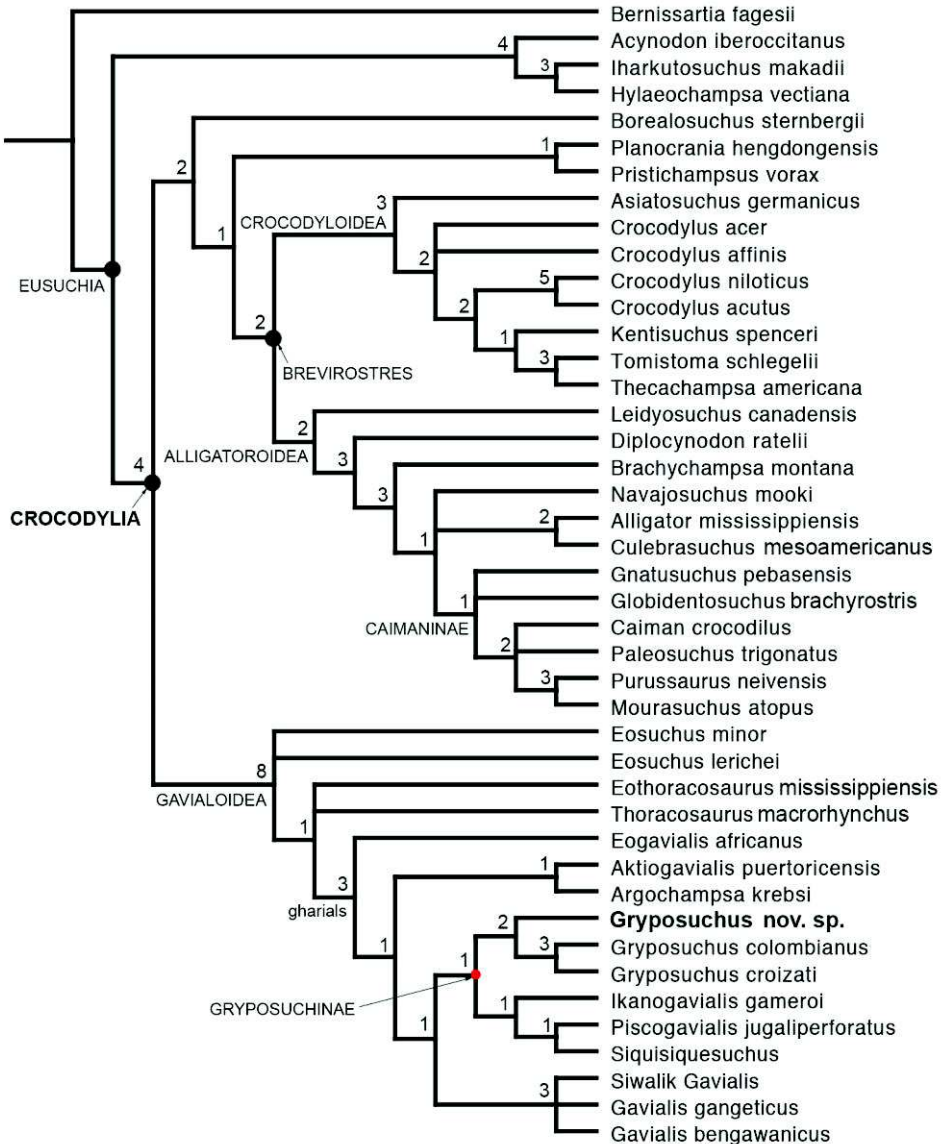

Figure V.9. Second strict consensus phylogenetic tree. Second approach after removing character state 137-2 and character 138. Numbers at nodes indicate Bremer support values. Phylogenetic hypothesis followed here.

Regarding character 138, all taxa previously coded as having state 2 (i.e., 138-2: dorsal and posterior orbital edges upturned) were recoded as 1 (i.e., 138-1: dorsal edges of orbits upturned). This search retained 24 equally optimal trees, with a length of 533 steps. The corresponding strict consensus tree is 542 steps-long (CI = 0.467; RI = 0.750; Figs. V.9 and V.10*b*).

Compared to the first analysis, this approach substantially increased resolution of South American gavialoid relationships. The monophyly of gryposuchines, exclusive of the Caribbean taxon *Aktiogavialis*, is recovered and *Gavialis* is identified as its sister clade. Within gryposuchines, there is low support for a clade comprising *Ikanogavialis*, *Siquisiquesuchus*, and *Piscogavialis*. Other gavialoid relationships were unaffected relative to the initial analysis. Discussions below are based on this second phylogenetic analysis, unless otherwise noted.

D.2 Results of the morphospace analisis

PC1 correlates mainly with the width of the pre- and post-orbital regions, and orbit length. Species on the positive extreme of PC1 present slender skull tables and interorbital bridge, long orbits and prefrontals, and laterally oriented anterior processes of the jugals, whereas those on the negative extreme bear broad skull tables, wide posterior portion of the interorbital bridge and orbits, short orbits, short prefrontals, and medially oriented anterior processes of the jugals. PC2 correlates with the relative length of the pre-orbital bones, involving mostly the frontal and lacrimals and the width of the prefrontals. Species with higher PC2 scores have comparatively longer and more slender frontals and a narrow interorbital bridge. Taxa with lower scores present short frontal and lacrimal bones and short and wide anterior portion of the interorbital bridge. The phylogenetic morphospace of orbital and circumorbital region in Miocene South American gavialoids covers most of the variation of the whole clade.

E. Discussion

E.1 Phylogenetic relationships

The phylogenetic analyses indicate that *Gryposuchus* nov. sp. is a gavialoid crocodylian sharing several basicranial synapomorphic traits that are not yet fully developed in "thoracosaurs" (basal gavialoids) but were integrated into the typical gharial anatomy at least since the Paleocene (Brochu, 2006; Hua & Jouve, 2004; Jouve et al., 2006), including features also retained from the ancestral gharial condition in Indo-Pacific, South American, Caribbean and African taxa (Figs. V.10 and V.12). *Gryposuchus* nov. sp. and most gavialoids including *Gavialis*, exhibit significant rearrangements in the skull table relative to brevirostrines and non-crocodylian eusuchians, revealed in the laterally oriented capitate process of the laterosphenoid, larger and comparatively wide supratemporal fenestra, and a fronto-parietal suture grazing or modestly entering these fenestrae. Although some of these traits might be attributed to longirostry, they are exclusive to gharials among long-snouted crocodylians. Other conspicuous features of gavialoid temporal region present in *Gryposuchus* nov. sp., such as ovoid infratemporal fenestra and anteriorly flaring squamosal groove, are also observed in the tomistomine *Thecachampsa americana* and might represent independent acquisitions. As most crocodylians, the infratemporal fenestra is triangular in *Gavialis* and is most parsimoniously regarded as a reversal in this latter taxon.

Gryposuchus *monophyly*. The species *Gryposuchus jessei* Gürich, 1912 was based on a rostral tip including both premaxillae and the anterior portion of maxilla and nasals from the Miocene-Pliocene of Amazonas, Brazil (Buffetaut, 1982). Although fairly incomplete, this specimen was crucial to recognize affinities between some South American gharials originally assigned to different taxa and now widely accepted as *Gryposuchus* species (see Buffetaut, 1982; Langston & Gasparini, 1997). Indeed, distinctive characters historically identified in the Amazonian rostral tip are recognized as diagnostic for *Gryposuchus* in this research. As in

other *Gryposuchus* species, the premaxillary alveoli (exclusive of the first alveolus) of *Gryposuchus* nov. sp. are aligned and, the left and right series separate from each other anteriorly (i.e., anteriorly diverging series). Particularly noteworthy is that in *Gryposuchus* the second alveolus (apparently homologous to the third of *Gavialis* and other gavialoids) is considerably bigger than the third (apparently homologous to the fourth of *Gavialis* and other gavialoids), here termed the "*Gryposuchus* pattern". Character 201 of our phylogenetic analysis (modified from Jouve et al., 2008) deals with the configuration and relative size of these premaxillary alveoli. In most gavialoids including *Gavialis*, *Eogavialis*, and *Piscogavialis*, the intermediate premaxillary alveoli show no significant difference in size, whereas in Cretaceous *Eothoracosaurus*, most brevirostrines, and basal eusuchians the fourth alveolus (apparently homologous to the third of *Gryposuchus*) is much bigger than the two adjacent anterior tooth loci. Riff & Aguilera (2008) showed that the rostral tip of *Gryposuchus* might vary within a single species since the "*Gryposuchus* pattern' is well developed in some specimens of *Gryposuchus croizati* (i.e., type MCN-URU-2002-77; AMU-CURS-133) but virtually unrecognizable in one same-sized individual (AMU-CURS-58). As stated by these authors, such intraspecific variation precludes the use of solely rostral tip characters to discriminate species, although the presence of distinctive features, probably related to sexual dimorphism (Riff & Aguilera, 2008), is still suitable for other systematic purposes. In *Gryposuchus* nov. sp., this region is preserved in two adults and one juvenile specimen (i.e., type MUSM 1981, MUSM 1681, and MUSM 1727), all of them consistently showing the "*Gryposuchus* pattern" in close agreement with the types of *Gr. jessei*, *Gr. croizati*, and specimen MLP 26-413 referred to *G. neogaeus* (Gasparini, 1968). Known material of *Gr. colombianus* either lacks of the rostral tip or this region is not fully accessible in ventral view (Langston, 1965). This latter situation pertains to IGM 184696, a complete skull and articulated mandibles from La Venta (Langston & Gasparini, 1997), in which the

wide external naris and widest expansion at level of second premaxillary alveolus might be indicative of possessing the distinctive "*Gryposuchus* pattern" since these traits occur associated in *G. croizati* and *G. jessei* (type and UFAC 1272). Unfortunately, the premaxillary alveolar pattern of other South American taxa, such as *Siquisiquesuchus* and *Ikanogavialis*, is currently partially known and, although it was coded in *Piscogavialis* as no possessing the "*Gryposuchus* pattern" based in the sole material where the rostral tip is preserved, its presence cannot be fully falsified. Additionally, the species of *Gryposuchus* all possess a dentary-surangular suture contacting the external mandibular fenestra at posterodorsal corner (character 64-1), from 18 to 22 maxillary teeth (character186-1), and a smooth frontal plate surface (character 202-1).

Among gavialoids, *Gryposuchus* bears a relatively small number of maxillary teeth. Tracking evolutionary history of maxillary teeth number in this phylogenetic hypothesis reveals that having between 19 (*Gr. croizati*) and 21-22 (*Gryposuchus* nov. sp. and *Gr. colombianus*) teeth is most parsimoniously seen as a secondary loss of tooth loci and a derived condition for *Gryposuchus* (Character 186-1). Adjacent relatives, including *Gavialis*, and immediate outgroup taxa (i.e., *Argochampsa*) bear no less than 23-24 maxillary tooth loci. In fact, all other South American taxa display proportionally longer rostra and the largest number of maxillary tooth loci among gharials, reaching up to 28 in *Piscogavialis* (Kraus, 1998).

In *Gryposuchus* nov. sp. and *Gr. colombianus*, the dentary-surangular suture contacts the external mandibular fenestra at the posterodorsal corner (Character 64-1). It represents an ambiguous synaphomorphy for *Gryposuchus* in our analysis, since this region is unknown in *Gr. croizati* and most South American gharials. Although this condition is not observed in *Ikanogavialis*, it might diagnose a more comprehensive clade considering that we recognized it in *Eogavialis* (i.e., SMNS 11785).

New support for *Gryposuchus* monophyly lies in the sculpture and morphology of the frontal bone. We observed that in *Gryposuchus* nov. sp., *Gr. colombianus*, and *Gr. croizati* the frontal plate surface is relatively smooth (i.e., character 202-1) and not sculpted with deep pits and furrows as is usual in other gavialoid and brevirostrine crocodylians. Although a smooth frontal surface is consistently documented in most individuals of *Gryposuchus* (Langston, 1965; Langston & Gasparini, 1997; Riff & Aguilera, 2008), a skull table referred to *Gr. colombianus* (uncataloged specimen, IGM) indicates that some anastomosing furrows might be present in some individuals. The precise significance of this discrepancy needs further evaluation since similar surface irregularities uniformly distributed on the entire frontal plate are seen in *Gryposuchus neogaeus* (i.e., MLP 26-413). Regarding the bone shape of this region, *Gryposuchus* bears an interorbital bridge broader than the adjacent diameter of the orbit (character 190-1), with the orbits particularly separated from each other in *Gr. croziati* and *Gr. colombianus*. *Gryposuchus neogaeus* present a wide interorbital bridge, probably of equivalent dimensions to *Gryposuchus* nov. sp. Although broad interorbital bridge is also present in *Gavialis* among derived gavialoids, our analysis results regard the acquisition of these traits as independent evolutionary events in *Gryposuchus* and *Gavialis* (Fig. V.10).

A clade comprising the remaining South American forms was recovered as the nearest relatives of the *Gryposuchus* clade in the phylogenetic hypothesis of this study. That clade is characterized by a relatively longer snout and probably marine habitus preferences (Kraus, 1998; Brochu & Rincón, 2004). In this clade, the frontoparietal suture traced entirely on the skull table (character 150-2) represents only a weak support, as this feature is highly variable across gavialoids and unknown in *Siquisiquesuchus* (Brochu & Rincón, 2004).

Are gryposuchines monophyletic? The clade Gryposuchinae (Vélez-Juarbe et al., 2007) was recovered only after removing the two characters regarded as highly homoplastic

(Analysis 2; Figs. V.9 and V.10*b*). Character support for the gryposuchines, exclusive of *Aktiogavialis*, includes having four premaxillary alveoli (character 87-1), lack of exposure of the prootic on external braincase wall (character 164-1), a quadrate with ventromedially projected medial hemicondyle (character 181-4), and a retroarticular longitudinal crest (character 203-1). This last character is present in all South American gharials preserving this region (Brochu & Rincón, 2004; Riff & Aguilera, 2008), including an unnamed Late Oligocene gavialoid from Pirabas, Brazil (Moraes Santos et al., 2011). The distinctive long

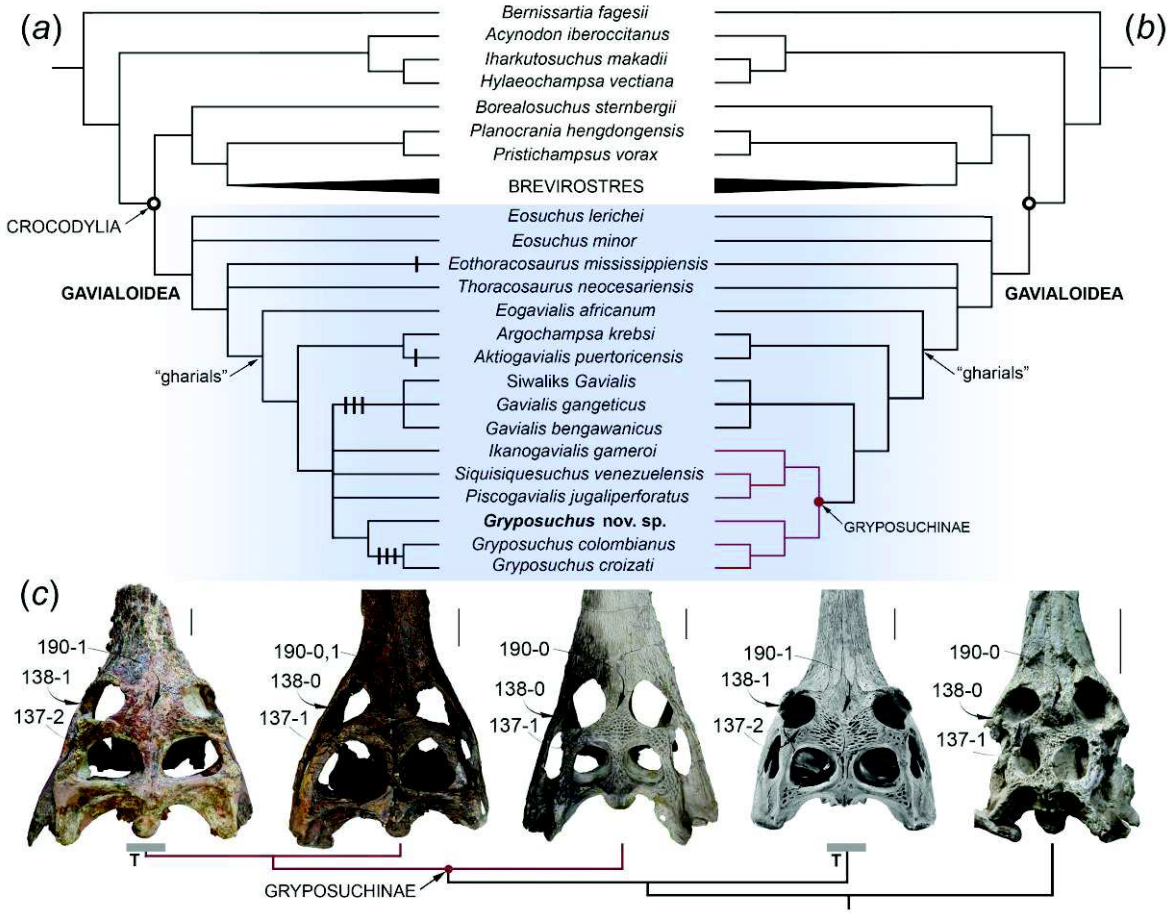

Figure V.10. Phylogenetic position of *Gryposuchus* nov. sp. within crocodylians. (*a*) Strict consensus cladogram of 45 most parsimonious trees based on analysis of the complete data matrix (Appendices). Apomorphic character states associated with a "telescoped" orbit condition are plotted on the cladogram as black lines (i.e., 137-2, 138-1, and 190-1). (*b*) Strict consensus cladogram of 24 optimal trees in a second analysis performed after removing character state 137-2 and character 138 from the data matrix. (*c*) Parallel acquisition of a fully "telescoped" orbit condition (TO) in advanced South American *Gryposuchus* and Indian *Gavialis*. Selected character states of the circumorbital region are indicated with arrows. From left to right: *Gryposuchus colombianus* (IGM 184696), *Gryposuchus* nov. sp. (MUSM 900), *Piscogavialis jugaliperforatus* (SMNK 1282 PAL), *Gavialis gangeticus* (MNHN A5321), and *Argochampsa krebsi* (OCP DEK-GE 333). Scale bars, 5 cm.

posterior or posterolateral projections of the squamosal, (i.e., squamosal prongs) no longer diagnose Gryposuchinae as had been hypothesized previously (Brochu & Rincón, 2004), as *Argochampsa* clearly possesses this feature (Jouve et al., 2008). *Eogavialis* displays long posterior projections, but the dorsal margin of these structures is ventrally inclined in this taxon. The length of these "prongs" varies among gryposuchine taxa, being shorter in *Gryposuchus* (Riff & Aguilera, 2008). *Gavialis* bears inclined and short posterior projections.

E.2 The evolutionary ecology of gavialoids: evidence from Amazonia

Gryposuchus nov. sp. inhabited the heart of the proto-Amazonian mega-wetlands ecosystem during the Middle Miocene, from around 16 to 13 Ma, and it represents the oldest known record of a gavialoid from this area. Remains belonging to this new taxon were consistently recovered from deposits depicting shallow lacustrine paleoenvironments (see Chapter II). As the basalmost species of the *Gryposuchus* clade, it provides essential evidence for accurately reconstructing the ancestral anatomy and ecology of this clade and provides evidence of parallel evolution in gavialoids. These phylogenetic analyses reconstruct the acquisition of widely separated orbits as independent evolutionary events in Asian *Gavialis* and later-diverging *Gryposuchus* species (*Gr. colombianus* + *Gr. croizati*) in South America. As a consequence, the comparatively slender interorbital bridge of *Gryposuchus* nov. sp. is primitive for all gavialoids (Fig. V.10*c*). A wide interorbital bridge is associated with possessing "telescoped" orbits. Traits associated with fully "telescoped" orbits, as is observed in *Gavialis* and advanced *Gryposuchus* species (but absent in *Gryposuchus* nov. sp.) include: postorbital bar flush with lateral jugal surface (character 135-1), upturned dorsal and posterior orbital margins (character 137-2), and ventral orbital margin with a prominent notch (character 138-1). Parsimony analyses also suggests parallel development for two of these character states, indicating that the "telescoped" orbit condition is homoplastic in gavialoids

and occurred independently in advanced South American *Gryposuchus* and Asian *Gavialis* species.

By mapping the phylogenetic tree onto the 2 first axes of the PCA analysis, we examined ecological associations of circumorbital bone arrangements throughout gavialoid evolution (Fig. V.11). Higher PC1 and PC2 scores define a morphospace of gavialoids found

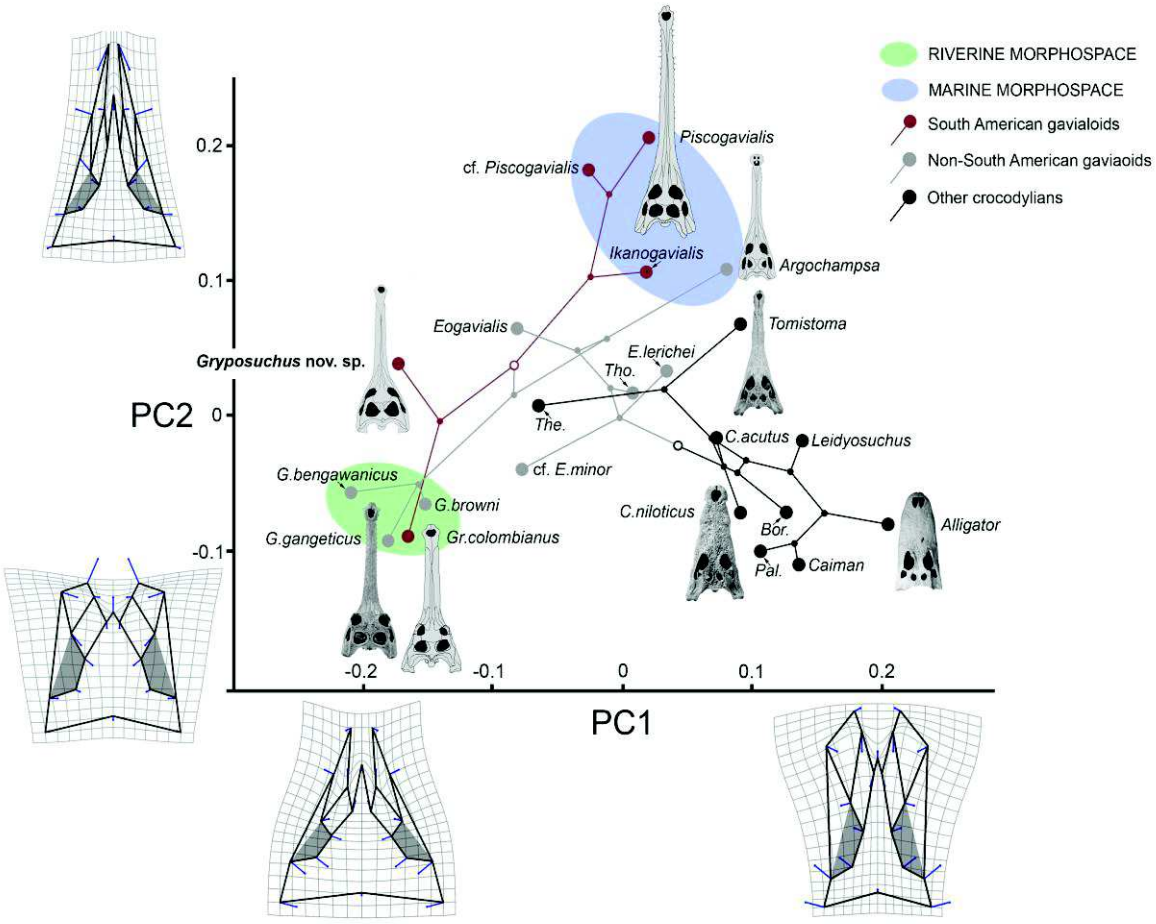

Figure V.11. Phylogenetic relationships of the Crocodylia mapped on the circumorbital morphospace defined by PC1 and PC2. Deformation grids depict extreme values along each axis and blue vectors indicate the position of the mean relative to the landmark variation. PC1 correlates mainly with the width of the pre- and post-orbital regions, and orbit length. Species on the positive extreme of PC1 present slender skull tables and interorbital bridge, long orbits and prefrontals, and laterally oriented anterior processes of the jugals, whereas those on the negative extreme bear broad skull tables, wide posterior portion of the interorbital bridge and orbits, short orbits, short prefrontals, and medially oriented anterior processes of the jugals. PC2 correlates with the relative length of the pre-orbital bones, involving mostly the frontal and lacrimals and the width of the prefrontals. Species with higher PC2 scores have comparatively longer and more slender frontals and a narrow interorbital bridge. Taxa with lower scores present short frontal and lacrimal bones and short and wide anterior portion of the interorbital bridge. The phylogenetic morphospace of orbital and circumorbital region in Miocene South American gavialoids covers most of the variation of the whole clade. Taxon abbreviations: *Bor*., *Borealosuchus Pal*., *Paleosuchus*; *The*., *Thecachampsa*, *Tho*., *Thoracosaurus*.

in coastal marine deposits, such as *Piscogavialis* and *Argochampsa*, whereas lower scores along these PC axes correspond to the morphospace including taxa with fully "telescoped" orbits. Lacustrine *Gryposuchus* nov. sp. and *Eogavialis africanus*, the latter lacking definite data on paleoenvironmental provenance, exemplify the intermediate morphospace. The fully "telescoped" orbit morphospace is represented by *Gavialis* and *Gryposuchus colombianus*; since they are distantly related, this morphospace depicts the parallel evolution of this distinctive cranial anatomy, apparently associated with convergent specialization for a freshwater habitat and visually enhanced feeding strategies.

Distinct features of this morphotype include: upturned anterior, dorsal, and posterior orbital margins; ventral orbital margin with a prominent notch; postorbital pillar laterally displaced; and orbits widely separated. Gavialoids display different degrees of the "telescoped" condition, depending on whether they possess all or only some of these features. The feeding strategy of the extant gharial *Gavialis gangeticus* seems to involve active use of the telescoped eyes and integumentary sense organs in capturing fishes in streams (Thorbjarnarson, 1990), as its habitat is confined to freshwater settings of the Indian subcontinent, notably restricted to riverine environments (Whitaker & Basu, 1983). Fossil gharials with well-developed "telescoped" orbits are usually found in depositional settings documenting fluvial-dominated paleoenvironments. This similar habitat association in the extant and extinct convergent taxa offers further support for the adaptive value of possessing "telescoped" orbits and suggests that this morphotype in fossil gavialoids typically is correlated with riverine ecosystems. Plio-Pleistocene fossil *Gavialis* species inhabited, and might have dispersed geographically via, fluvial systems then occurring between Indo-Pakistan and Southeast Asia (Martin et al., 2012). In South America, late Middle Miocene *Gryposuchus colombianus* is restricted to fluvial-influenced settings of the Pebas Mega-Wetland System at La Venta (Colombia; Langston, 1965; Langston & Gasparini, 1997) and

Fitzcarrald (Peru; Salas-Gismondi et al., 2007; Tejada-Lara et al., 2015a; Chapter VI), close to the rapidly rising Andes, whereas this species is absent from coeval deposits depicting brackish, dysoxic lakes, swamps and deltas of the same biome at Iquitos (Peru) where *Gryposuchus* nov. sp. consistently occurs. This latter species not only is the sole gavialoid in the Iquitos fauna, but the sole longirostrine crocodylian within a highly diversified community dominated by small caimans with a malacophagous diet (Salas-Gismondi et al., 2015a). In younger beds at Nueva Unión (southern Iquitos; Molluscan Zone MZ9 or younger: Wesselingh et al., 2006a), a "telescoped" orbit gavialoid was only recovered from one locality (IQ125; Fig. V.7*a*-*c*) in the "Uppermost Pebas" Formation (Rebata et al., 2006), at a time corresponding to development of new regional fluvial-dominated conditions, attributable to a peak in Andean uplift and the onset of the Amazon River System (Salas-Gismondi et al., 2015a). Within this wider environmental context, the demise of the Pebas Mega-Wetland System and subsequent establishment of the fluvio-tidal Acre Phase in the Amazonian Basin at around 10.5 Ma seems to have promoted diversification, size increase, and specialization in gharials (Fig. V.12) compared with the presence of only one species per Pebasian-aged crocodylian fauna (i.e., Iquitos, La Venta, and Fitzcarrald). In contrast, Late Miocene assemblages of Acre (Brazil) contain four gavialoid taxa (Cozzuol, 2006), including the conspicuous record of forms with "telescoped" orbits (pers. obs). Although the same number of taxa is observed in the Late Miocene Urumaco Formation, matches between the dominant environment and specific morphotypes are far more complicated to assess. The Urumaco Formation preserves several aquatic environments that were potential habitats for crocodylians within the Paleo-Orinoco Basin, such as delta plains, swamps, rivers, and marginal marine embayments, all with a marine influence from the Caribbean (Quiroz & Jaramillo, 2010).

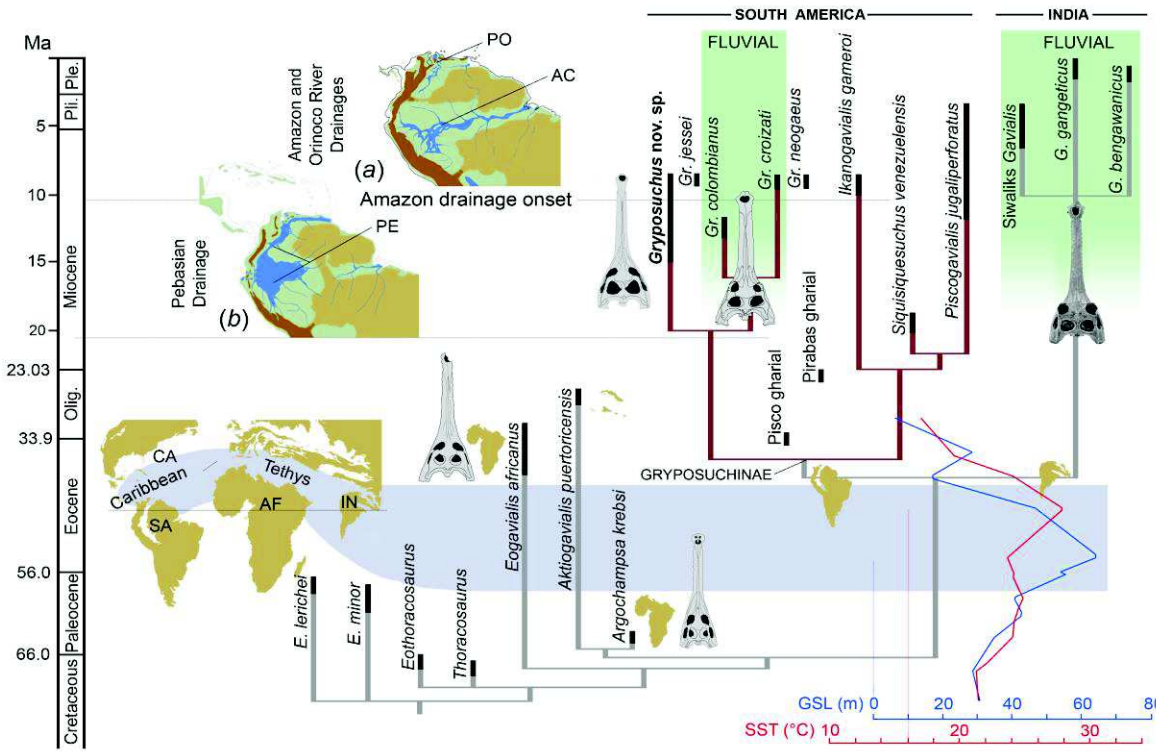

Figure V. 12. Time calibrated phylogenetic tree of the Gavialoidea and relevant paleogeographic distributions associated with the evolution and diversification of gavialoids in marine and freshwater settings. During the Late Paleocene-Early Eocene interval, peaks of sea surface temperature (SST) and global sea surface level (GSL) occurred together with tropical marine connections through the Tethys Ocean and Caribbean Sea (Martin et al., 2014; Blakey, 2008). During the Neogene, distinct biomes dominated tropical South America: (*a*) Acre Phase, after the onset of the eastern-draining Amazon and northward-draining Orinoco river systems; and (*b*) Pebas Mega-Wetland System, with its drainage northward to the Caribbean Sea. Abbreviations: AC, Acre Phase; Olig., Oligocene; PE, Pebas System; PO, paleo-Orinoco, Ple., Pleistocene; Pli., Pliocene. Global and South American paleogeographic maps from Blakey (2008) and Hoorn et al. (2010b), respectively.

Consistent with this patchwork of environments, the Urumaco gavialoid species exhibit a disparate array of cranial circumorbital configurations (Sill, 1970; Sánchez-Villagra & Aguilera, 2006; Riff & Aguilera, 2008). In Urumaco the telescoped orbit specialization was fully attained by the giant *Gryposuchus croizati*, most likely a dweller in fluvial settings. Based on its paleoenvironmental preference in the Iquitos fauna, *Gryposuchus* nov. sp. instead might have occupied relicts of the brackish lacustrine ecosystems once widely distributed in proto-Amazonia (Boonstra et al., 2015). Therefore, the record of this gavialoid at Urumaco adds evidence for the persistence of Pebasian aquatic conditions during the Late Miocene in

northernmost South America, where the lower course of the Pebasian proto-Amazonian System drainage was formerly situated (Salas-Gismondi et al., 2015a).

Inasmuch as gharials were inhabitants in the Caribbean region at least since the Late Oligocene (Vélez-Juarbe et al., 2007), the Caribbean Portal, at the mouth of the proto-Amazonian aquatic system might have played an important role for the invasion of gavialoids into the inland areas. *Siquisiquesuchus* was an early Miocene Caribbean inhabitant of present-day Venezuelan coasts (Brochu & Rincón, 2004). Other marine and fresh water units in the region documented numerous remains of gharials throughout the Miocene (Sánchez-Villagra & Aguilera, 2006; Riff & Aguilera, 2008; Moreno et al., 2015), showing persistent faunas living close to the Caribbean Portal. Either by means of marine transgressions or via riverine drainage systems, a continuous aquatic corridor united the Caribbean Sea with western proto-Amazonia for most of the Paleogene and early Neogene (Wesselingh et al., 2006a; Hoorn et al., 2010b; Boonstra et al., 2015). The heart of proto-Amazonia during the extensive and persistent Pebas Mega-Wetland System was continuously connected with the Caribbean Portal by a northward flowing trunk drainage (Hoorn et al., 2010b; Boonstra et al., 2015). Although not coeval, evidence of the prevailing aquatic connections that linked both areas through the Llanos (Colombia) until the Late-Middle Miocene boundary is founded on the record of *Gryposuchus* nov. sp. from both Urumaco and Iquitos, as well as other biotic indicators (Nuttal, 1990; Hoorn, 1993; Lovejoy, 1998; Lundberg, 1998; Wesselingh & Macsotay, 2006; Salas-Gismondi et al., 2015a). Specific environmental conditions fostering high diversity of Late Miocene Urumaco gavialoids remain elusive.

E.3 The origin of Caribbean and South American gharials

Our phylogenetic analyses propose sister-group relationships of Caribbean *Aktiogavialis* and African *Argochampsa* (Figs. V.10 and V.12). This clade is supported by the

presence of long supratemporal fenestrae (character 191-0), a character state that implies a reversal within these gavialoids. This might be considered problematic since *Argochampsa*, as an early representative of the clade, could have retained the ancestral condition for Crocodylia if character polarization based on the phylogenetic position of "thoracosaurs" is erroneous. Nevertheless, further comparisons between *Argochampsa* and *Aktiogavialis* allows us to recognize other similarities not yet included in phylogenetic analyses, but potentially supporting their close relationship, such as the relative proportions of the skull table in dorsal view and the presence of a distinctive shallow fossa in the anterior margin of the supratemporal fenestra. This fossa has not been identified in any other crocodylian species at any ontogenetic stage (Vélez-Juarbe et al., 2007) but it is clearly visible in the holotype of both species, although barely discernable in other individuals of the African taxon (Jouve, pers. comm.). In the context of our time-calibrated phylogenetic tree, this association would suggest an African origin for the Caribbean gavialoid, probably by western transatlantic dispersal as suggested by Vélez-Juarbe et al. (2007). *Argochampsa*, *Aktiogavialis*, and the oldest records of South American gharials all were found in deposits from coastal marine settings (Brochu & Rincón, 2004; Vélez-Juarbe et al., 2007; Hua & Jouve, 2004; Moraes-Santos et al., 2011). Whether fossil gharials were strictly marine or not, distinct lines of evidence indicate that gavialoids flourished during high sea surface level and temperatures (SST) of the Paleocene and Eocene epochs (Martin et al., 2014). During this time interval (~60-45 Ma), paleogeographic reconstructions depict a tropical marine connection from India and Africa to the Caribbean and northern South America through the Tethys Ocean and Caribbean Sea (Blakey, 2008). Although the fossil record is far from complete in these areas, our time-calibrated phylogenetic tree and the occurrence of advanced gavialoids along both the Tethys and Caribbean coasts and islands, suggest that this marine realm could have served as a preferred habitat and dispersal system for gavialoids during the Paleogene (Fig. V.12).

The presence of gharials in South America most likely resulted from a single transoceanic colonization event and subsequent diversification in South America, distinct from the one that gave rise to the Caribbean taxon *Aktiogavialis*.

F. Conclusions

Gavialoid history exhibits independent acquisitions of the "telescoped" orbits condition. Analyses of the new Pebasian species *Gryposuchus* nov. sp. and other South American gavialoids document high plasticity in orbital anatomy, which appears to have been strongly correlated with feeding strategy and environmental circumstances. Morphospaces occupied by fluvial and coastal marine specialists are identified by statistical analysis of orbital and circumorbital shape variation. In light of the phylogenetic history, a fluvial habitus in South American gharials is derived from ancestral lacustrine-deltaic forms with incipient development of protruding eyes or telescoped orbits. Circumorbital region of coastal marine gavialoids is closer in morphology to that of brevirostrine crocodylians. Identifying morphological steps of parallel evolution and ancestral ecological habitus in gavialoids provide models for reconstructing puzzling phylogenetic histories and adaptive radiation within extinct crocodyliform clades with elongated rostrum, such as thalattosuchians, dyrosaurids, and pholidosaurids (Wilberg, 2015). Proto-Amazonian connections with the Caribbean Sea to the north, and the subsequent onset of the Amazon River System draining eastward, provided multiple habitats and conditions for gavialoid colonizations of new areas and extensive morphological diversification in South America throughout the mid-late Cenozoic.

CHAPTER VI – CROCODYLIAN COMMUNITY FROM THE FLUVIAL-INFLUENCED ENVIRONMENTS OF THE PEBAS SYSTEM, FITZCARRALD ARCH

CHAPTER VI – CROCODYLIAN COMMUNITY FROM THE FLUVIAL-INFLUENCED ENVIRONMENTS OF THE PEBAS SYSTEM, FITZCARRALD ARCH

LIVING ON THE EDGE OF THE PEBAS SYSTEM: LATE MIDDLE MIOCENE CROCODYLIFORMS FROM THE FITZCARRALD ARCH, PERUVIAN AMAZONIA

This chapter section corresponds to the following article:

Salas-Gismondi, R., Antoine P.-O., Baby, P. and Tejada-Lara J. V.

Living on the edge of the Pebas System: late Middle Miocene crocodyliforms from the Fitzcarrald Arch, Peruvian Amazonia. In preparation.

Abstract

Under the influential role of the Andean mountains, western Amazonia develoved distinctive environmental conditions that ultimately lead to high and divergent biodiversity. Although this intimate geologic-biotic interaction might have produced similar phenomena in the past, our knowledge about the tropical biotic evolution occurring in close proximity to these rapid growing mountains is poorly documented. Here, we study the Middle Miocene mesoeucrocodylians from the Fitzcarrald Arch (Peruvian Amazonia) to outline patterns of evolution and biogeography within paleoenvironments of the western proto-Amazonian ecosystems. As the highly heterogeneous mesoeucrodylian community recorded in the Colombian locality of La Venta, the Fitzcarrald fauna inhabited fluvial-dominated paleoenvironments of the Pebas Mega-Wetland System on the eastern flanks of the tropical Andean reliefs about 13 of the Mya. Both assemblages document the last representatives of

deep-snouted sebecids, one gavialoid species with protruding eyes, and generalized caimanines of small body size. These faunas show little taxonomic and phylogenetic morphotype similarities with the coeval lacustrine faunal community of the Iquitos bonebeds, the latter dominated by small caimanines with crushing dentition, providing evidence about the different ecological and environmental conditions coexisting within the Pebas Mega-Wetland System. Based on the "giant mandible" discovered by Matthiessen in the Fitzcarrald Arch, we describe a new species of *Purussaurus* that point to a proto-Amazonian origin for the clade comprising giant *Purussaurus* species. Prior to the fluvial-dominated Acre System, the Pebas System marks the last record of basal *Eocaiman*-like morphotype in Amazonia and the first appearance of the smooth-fronted caiman *Paleosuchus*. As a whole, this evidence provides further support for the instrumental role of the proto-Amazonian Pebas System in the survival and diversification of basal forms as well as for the origin of the extant linages dwelling modern Amazonian ecosystems. The initial loss of morphotype snout and ecological diversity in Amazonia occurred with the dissapearence of the long-lasting, lacustrine-dominated environments of the Pebas Mega-Wetland System, ca. 10 million years ago. Most of these morphotypes persisted in northernmost South America during the Late Miocene.

Keywords: Miocene, mesoeucrocodylians, proto-Amazonia, Fitzcarrald Arch, Pebas Mega-Wetland System

A. Introduction

Before the establishment of the fluvial-dominated environments of the Amazonian System, a distinctive aquatic biome –the Pebas Mega-Wetland System– prevailed in western proto-Amazonia during most of the Miocene (Wesselingh et al., 2002; Hoorn et al., 2010a). As no other stage in the evolution of the Neotropics, this long-lasting and large-scale biome

was characterized by the develvopment of brackish, dysoxic lacustrine environments centered in present-day boundary areas of Peru, Colombia, and Brazil (Wesselingh et al., 2002; Wesselingh & Salo, 2006). The proliferation of lakes and swamps favored the extensive adaptive radiation of molluscs, in which cochliopid snails reached high diversity whereas *Pachydon* bivalves underwent further in abundance (Wesselingh et al., 2002; Wesselingh et al., 2006a). As shown by the rich late Middle Miocene bonebeds of the Pebas Formation in the Iquitos area (Peru), this resource was notably exploited by at least three taxa of small blunt-snouted caimanines with globular dentition (Salas-Gismondi et al., 2015a). Intriguingly, coeval fossiliferous sites of La Venta (Colombia) representing different areas of the same large proto-Amazonian biome, include at least six mesoeucrocodylian taxa, being none of them small crushing-dentition caimanines (Langston, 1965; Langston & Gasparini; 1997).

In 2005 and 2007, our geological and paleontological team followed old maps and directions of early explorers (Matthiessen, 1961; Willard, 1966; Buffetaut & Hoffstetter, 1977) to reach into emblematic fossiliferous areas within the Fitzcarrald Arch in Peruvian Amazonia. During these expeditions we documented around 14 in-situ vertebrate-bearing localities (Antoine et al., 2007), including the original site of the "giant mandible" found by Peter Matthiessen (1961) in Quebrada Grasa. We focused on surveying for fossil vertebrates in Miocene outcrops of the Inuya, Mapuya, and Sepa Rivers, in the northwestern flank of the Fitzcarrald Arch. Sedimentary, geomorphological, and geochronological data gathered from the Fitcarrald arch indicate that Ipururo Formation rocks outcropping in that area are coeval with those of the Pebas Mega-Wetland System in the Iquitos and La Venta area, roughly 13 million years old (late Middle Miocene; Espurt et al., 2007, 2010; Tejada-Lara et al., 2015a). Paleontological approaches based on mammals (Salas-Gismondi et al., 2006; Antoine et al., 2007; Negri et al., 2010; Goillot et al, 2011; Pujos et al., 2013) and a preliminary study on its mesoeucrocodylian assemblage (Salas-Gismondi et al., 2007) confirmed the same general age

for all the vertebrate sites surveyed in the area (Tejada-Lara et al., 2015a). Initial observations on the mesoeucrocodylian faunal diversity from Fitzcarrald found expectable closer affinities with coeval La Venta faunas (Colombia) than with later assemblages, such as Acre (Brazil) and Urumaco (Venezuela), both from the Late Miocene (Cozzuol, 2006; Sánchez-Villagra & Aguilera, 2006; Salas-Gismondi et al., 2007).

In this research, we describe the mesoeucrocodylians from the Fitzcarrald localities, a diversified assemblage of distantly related taxa considered pertaining to the Pebas Mega-Wetland System (Salas-Gismondi et al., 2007; Tejada-Lara et al., 2015a). Contrasting with the fossiliferous deposits typically representing contemporary lacustrine paleoenvironments, Fitzcarrald mesoeucrocodylians were recovered from bonebeds corresponding to conglomeratic storm deposits in tidally-influenced, fluvially dominated settings (Baby et al., 2005; Espurt et al., 2006; Tejada-Lara et al., 2015a). We provide comparisons regarding taxonomic and phylogenetic composition of Middle and Late Miocene mesoeucrocodylian communities in tropical South America to recognize regional and ecological faunal discrepancies within the Pebas Mega-Wetland System.

B. Material and methods

The cranial and mandibular specimens described here correspond to our own survey in the Inuya (IN008), Mapuya (DTC20, DTC32, DTC34, Quebrada Grasa), and Sepa River (SEP002, SEP006) localities during Fitzcarrald Expeditions 2005 and 2007, as well as two previous remarkable discoveries, namely a "giant mandible" (Matthiessen, 1961) and a "maxilla of *Sebecus* cf. *huilensis*" (Buffetaut & Hoffstetter, 1977). Details regarding these latter specimens are given below.

B.1 Phylogenetic analysis.

To determine the phylogenetic position of the new species of *Purussaurus* from Fitzcarrald, we included it in the data matrix of morphological characters of Salas-Gismondi et al. (2015a). This data matrix includes 200 characters and 86 eusuchian taxa, with *Bernissartia fagessi* as a formal outgroup. The characters for *Gryposuchus colombianus* were scored based on both the holotype and referred specimens from La Venta, Colombia (Langston, 1965; Langston & Gasparini, 1997). In our phylogenetic analysis *Kuttanacaiman iquitosensis* and *Paleosuchus* sp. were score thanks to the Iquitos specimens (Salas-Gismondi et al., 2015a). Phylogenetic relationships of *Barinasuchus arveloi* and *Sebecus huilensis* within the Sebecosuchia follow the analysis of Pol & Powell (2011).

Characters 200 and 201 of Salas-Gismondi et al. (2015a) are not included in this analysis. Instead, we included a new character, as follows:

Character 200. Postnarial fossa absent (0) or present (1).

Character coding for the new species of *Purussaurus*:

```
????? ????? ????? ????? ????? ????? ????? ????? ????? ?????
????? ????? ????? ????? ????? ???00 112?0 0021? 10000 1?01?
????? ????? ?00?0 00??? ????? ????? ????? ????? ????? ?????
????? ????? ????? ????? ????? ????? ?0??0 ????? ????? ????1
```

B.2 Faunal similarity analysis.

To test similarities between mesoeucrocodylian faunas of Fitzcarrald and other Miocene proto-Amazonian and Amazonian faunas we used Simpson Coefficient (SC; Simpson, 1960). We performed two analyses to provide evidence based on a taxonomic and phylogenetic morphotype perspective. These analyses include data from Iquitos (Late Middle Miocene; Salas-Gismondi et al., 2015a), La Venta (Late Middle Miocene; Langston, 1965; Langston & Gasparini, 1997), Nueva Unión (Late Miocene; Chapters IV and V), Acre (Late Miocene; Bocquentin-Villanueva et al., 1989; Souza-Filho & Bocquentin-Villanueva, 1989;

Souza-Filho, 1993; Cozzuol, 2006; Riff et al., 2010; Fortier et al., 2014; Aureliano et al., 2015), and Urumaco (Late Miocene; Aguilera et al., 2006; Sánchez-Villagra & Aguilera, 2006; Scheyer & Moreno-Bernal, 2010; Scheyer et al., 2013). For the first analysis, taxa are represented basically by species of mesoeucrocodylians recovered from these tropical localities. However, due to doubtful taxonomic identifications, we found convenient to group some closely related species (that were poorly represented by fragmentary fossil evidence) using a shared diagnostic, manifest feature that can be easily verified in the available material. Thus, we grouped *Purussaurus brasilensis*, *P. mirandai*, and *Purussaurus* new species in "large *Purussaurus*", based on its giant size. Similarly, we grouped *Mourasuchus amazonensis* and *M. nativus* in "large *Mourasuchus*" based on the same feature. A third group includes *Gryposuchus colombianus* and *G. croizati*, namely "telescoped *Gryposuchus*" and grounded on the presence of fully telescoped orbits (see Chapter V). Finally, we included all Miocene *Charactosuchus* forms in *C. fieldsi* because current diagnostic features to discriminate them are weakly supported (see Souza-Filho & Bocquentin-Villanueva, 1989; Souza-Filho, 1993). In this analysis, the taxonomic composition of the Fitzcarrald fauna is compared with that of other aforementioned localities. Faunal similarities were assessed using Simpson minimum (SC_{min}) and maximum similarity (SC_{max}) following the protocol of Croft (2007), in order to deal with doubtful record of taxa. SC_{min} includes shared taxa confirmed to be present in the locality by diagnostic material. SC_{max} was calculated including these shared taxa plus those suspected to be present based on less diagnostic material. In this latter case, we assumed that those taxa belonged to the species recorded in other faunas (Croft, 2007). Results are provided in table VI.1.

The criteria for the second analysis are based on the relevance of phylogenetic hypoteses for understanding fundamentals of adaptive radiation (Losos & Miles, 1994; Larson & Losos, 1996; Brochu, 2001). Under this scope, we intend to recognize morphotypes

associated with their phylogenetic histories. Results are expected to provide clues about the evolution of phylogenetic morphotypes across space and time in proto-Amazonia. Rostral shape, tooth morphology, orbital configuration, and size are features with presumed ecological value (Brochu, 2001; Salas-Gismondi et al., 2015a; Chapter V) and central characteristics for defining eco-morphotypes in crocodylians (Busbey, 1995; Brochu, 2001). Therefore, based on these features and the proposed phylogenetic history, we set up ten "phylogenetic morphotype" groups for Miocene mesoeucrocodylians, as follows: (1) Sebecidae (high rostrum non crocodylians, probably terrestrial; Langston, 1965), (2) basal caimanines (paraphyletic association: *Gnatusuchus*, *Globidentosuchus*, *Kuttanacaiman*, and *Eocaiman*; small size, blunt-snouted; Scheyer et al., 2013; Salas-Gismondi et al., 2015a), (3) *Purussaurus* (generalized top predator, large size; Brochu, 2001; Aureliano et al., 2015), (4) *Mourasuchus* (duck-faced, micro-feeder; Langston, 1965; Brochu, 2001) (5) *Paleosuchus* (small size, generalized high rostrum caimanine; Brochu, 2001), (6) crushing-dentition jacarean (blunt-snouted with crushing dentition; Salas-Gismondi et al., 2015a), (7) generalized jacarean (small to medium size, generalized teeth; Brochu, 2001), (8) non "telescoped" *Gryposuchus* (long snout, not protruding eyes gavialoid; chapter Chapter V), (9) "telescoped" *Gryposuchus* (long snout, protruding eyes gavialoid; Chapter V), and (10) *Charactosuchus* (slender snout crocodyloid; Langston, 1965). In this analysis, we compared pairs of localities. Results are provided in tables VI.2 and VI.3.

C. Systematic paleontology

Crocodyliformes Hay, 1930

Mesoeucrocodylia Whetstone & Whybrow, 1983 (sensu Clark, 1986)

Sebecosuchia Simpson, 1937

Sebecidae Simpson, 1937

Sebecus Simpson, 1937

Sebecus cf. *huilensis*

Material. MUSM 912, tooth, Locality IN008; MUSM 1665, tooth, Locality Inuya River (on surface); MUSM 1266, tooth, Locality Quebrada Grasa; MUSM 2421, tooth with broken tip, Locality DTC32; MUSM 2422, tooth, Locality IN008 (Chapter II; Fig. VI.1*a-c*).

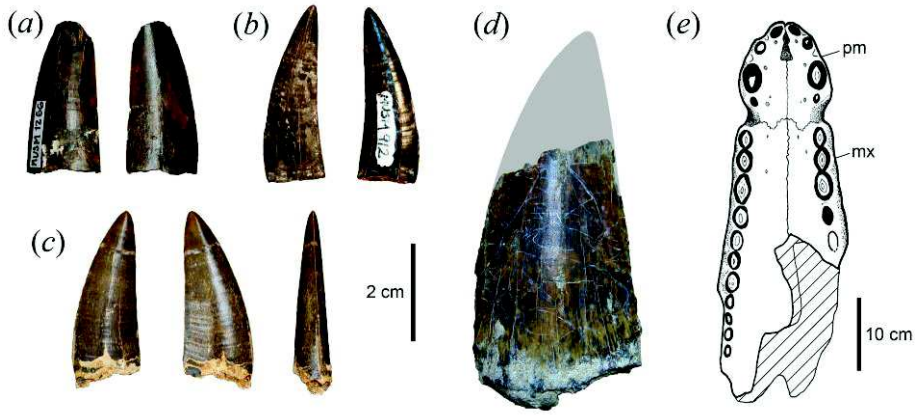

Figure VI.1. Sebecidae. (*a-c*) *Sebecus huilensis*. (*a*) MUSM 1266, tooth. (*b*) MUSM 912, tooth. (*c*) MUSM 2422, tooth. (*d*) MNHN n/n, tooth of a large Sebecidae. (*e*) Ventral view of *Barinasuchus arveloi* from the Mapuya River, specimen currently lost. For anatomical abbreviations see Appendices.

Comparative description and remarks. The record of this taxon is limited to several isolated teeth having the same crown height (~35-40 mm). As stated for *Sebecus huilensis* (Langston, 1965), teeth are long and slender. The slenderness is emphasized by a strong transversal compression that produces a lanceolate cross section. Sharp anterior and posterior borders are finely serrated. Variation among teeth is mainly in the degree of the backward curvature. MUSM 2421 lacks of its tip, probably broken during biting activity (Fig. VI.*a*).

Previous record of *Sebecus huilensis* is restricted to the late Middle Miocene of La Venta, Colombia. This taxon is inadequately known due to the fragmentary condition of all skeletal remains recovered so far (Langston, 1965; Busbey, 1986; Langston & Gasparini,

1997). A composite image of the skull indicates that most of the rostrum was very narrow, quite deep, poorly sculpted, and with almost vertical walls. Alveoli were laterally compressed and separated with long diastemas. In the jaw, the symhyseal region was long, reaching posteriorly beyond the level of the sixth dentary alveolus. Although the fourth dentary alveolus is hypertrophied, this area is not laterally expanded but markedly high compared with the anterior symphysis. Most of the retroarticular process is straight exclusive of the medial distal portion that sweeps downward. Specific features present in the premaxilla and dentary referred to *S. huilensis* by Langston & Gasparini (1997; IGM 250816: Fig. 8.1A-D) made us suspect that either this might be a case of mistaken identity or presumed diagnostic characters are not inherent to *Sebecus huilensis*. In overall, IGM 250816 bear an external surface more rugose compared to that consistently attributed to *S. huilensis* (Langston, 1965; Busbey, 1986). Additionally, the ventral border of the anterior dentary is markedly convex, whereas the holotype of *S. huilensis* presents a gently concave margin (Langston, 1965: Fig. 3). Besides its smaller size, IGM 250816 resembles the anatomy of *Barinasuchus arveloi*, a species currently known from the middle Miocene of Venezuela and Peru (Paolillo & Linares, 2007). However, as in *Sebecus huilensis*, the dentary is not laterally expanded at the level of the fourth alveolus in contrast to that area in the holotype of *B. arveloi*, in which there is a marked lateral expansion. Although a single sebecid taxon was reported from La Venta, unpublished material belonging to old collections (MNHN s/n; IGM s/n 85-181) includes isolated teeth of a giant form (Fig. VI.1*d*). These teeth are both twice the height and more robust than those known for *Sebecus huilensis* (Langston, 1965: Pl. 1a-c), depicting the existence of two sebecids in La Venta, the second being a *Barinasuchus*-sized species.

Barinasuchus Paolillo & Linares, 2007

Barinasuchus arveloi Paolillo & Linares, 2007

Material. Snout (Fig. VI.1*e*) collected by J. Pérez-Vásquez at Quebrada Grasa of the Mapuya River (Buffetaut & Hoffstetter, 1977). Specimen currently lost.

Comparative description and remarks. The Mapuya specimen described by Buffetaut & Hoffstetter (1977) comprised most of the snout of a large-sized sebecid. This fossil, now identified as belonging to *Barinasuchus arveloi* (Paolillo & Linares, 2007), shows a long, deep, straight, and robust snout. In spite of its robustness, the rostrum is particularly compressed laterally. The surface of the snout is heavily sculptured with ridges and furrows. The third premaxillary and maxillary alveoli are the biggest in the upper quadrants. Although the nasals and the narial opening end anteriorly at the same level, the later is completely surrounded by the premaxilla. In the holotype of *Barinasuchus arveloi* from the Middle Miocene of Venezuela (Paolillo & Linares, 2007), the rostrum is further characterized by a slightly concave dorsal profile, depressed lateral walls of the posterior maxilla, and a lateral expansion of the symphysis at the level of the fourth dentary alveolus. Although for Paolillo & Linares (2007) the homology of the premaxillary teeth is doubtful, it seems to be certain that there were four premaxilary alveoli, with the third being the biggest as has been recognized in the Mapuya specimen (Buffetaut & Hoffstetter, 1977; Fig. VI.1*e*) and in *Sebecus icaeorhinus* (Colbert, 1946). The pit-like alveolus located at the back of the premaxilla is actually homologous to the fourth alveolus of *S. icaeorhinus*. In this latter taxon, Colbert (1946) identified a pit inside the fourth alveolus for the reception of the third dentary tooth.

Although relationships within Sebecidae are far from resolved (Pol & Powell, 2011; Kellner et al., 2014), recent phylogenetic analyses show that *Barinasuchus* and *Sebecus huilensis* are not closely allied, with the former representing an early offshoot of the clade. These taxa are the latest-occurring members of the Sebecosuchia, so far.

Mesoeucrocodylia Whetstone & Whybrow, 1983 (sensu Clark, 1986)

Crocodylia Gmelin, 1789

Gavialoidea Hay, 1930

Gryposuchus Gurich, 1912

Gryposuchus colombianus (Langston, 1965)

Material. MUSM 650, symphyseal region of a mandible (Fig. VI.2*a*, *c*), Locality DTC20; MUSM 906 (incorrectly denoted as MUSM 609 as in Salas-Gismondi et al., 2007), partial symphysis (juvenile; Fig. VI.2*e*, *f*), Locality DTC32; MUSM 2630, partial frontal bone (Fig. VI.2*g*), Locality DTC32 (Chapter II).

Comparative description and remarks. MUSM 650 is a partial mandible bearing the symphyseal region of both rami. Only the right ramus is preserved behind the symphysis, until the level of the twenty-first dentary alveolus. The symphyseal region is flat as in *Gryposuchus colombianus* and *Gryposuchus croizati* (Riff & Aguilera, 2008). In the new *Gryposuchus* species from Iquitos bonebeds this region is higher and tubular in cross section (Fig. VI.2*b*,*d*; see Chapter V). The symphysis reaches posteriorly the level of the 19th alveolus. The tip of the rostral symphysis is separate by a medial cleft and expanded at the level of the second alveolus, as is characteristic in *Gryposuchus* species (Langston & Gasparini, 1997; Riff & Aguilera, 2008). The first alveolus is apparently the biggest in the jaw. Remaining alveoli are much smaller and similar in size, besides the fourth alveolus that is slightly bigger. Parallel margins along the symphysis are modestly sinuate. The interalveolar space is larger than the adjacent alveolar diameters. These proportions are present in similar size specimens of *Gr. colombianus* (IGM 250480) whereas bigger individuals present strong alveolar salients and shorter interalveolar spaces (see Langston &

Gasparini, 1997). As most gavialoids, the alveolar row is depressed compared to the palatal surface of the dentary. The same general features are observed in MUSM 906, a notably smaller specimen preserving the rostral symphysis with the first fifteen alveoli. However, whereas in MUSM 650 the dorsal tip of the splenial within the symphysis reaches anteriorly the level of the twelfth alveolus as is generally seen in *Gr. colombianus* (i.e., twelve-thirteen, not to the level of the eighteen alveolus as stated by Brochu & Rincón, 2004), in MUSM 906 it reaches the level of the fourteenth alveolus, a fact that might be related with changes during the ontogenetic process (Langston & Gasparini, 1997; Salas-Gismondi et al., 2007).

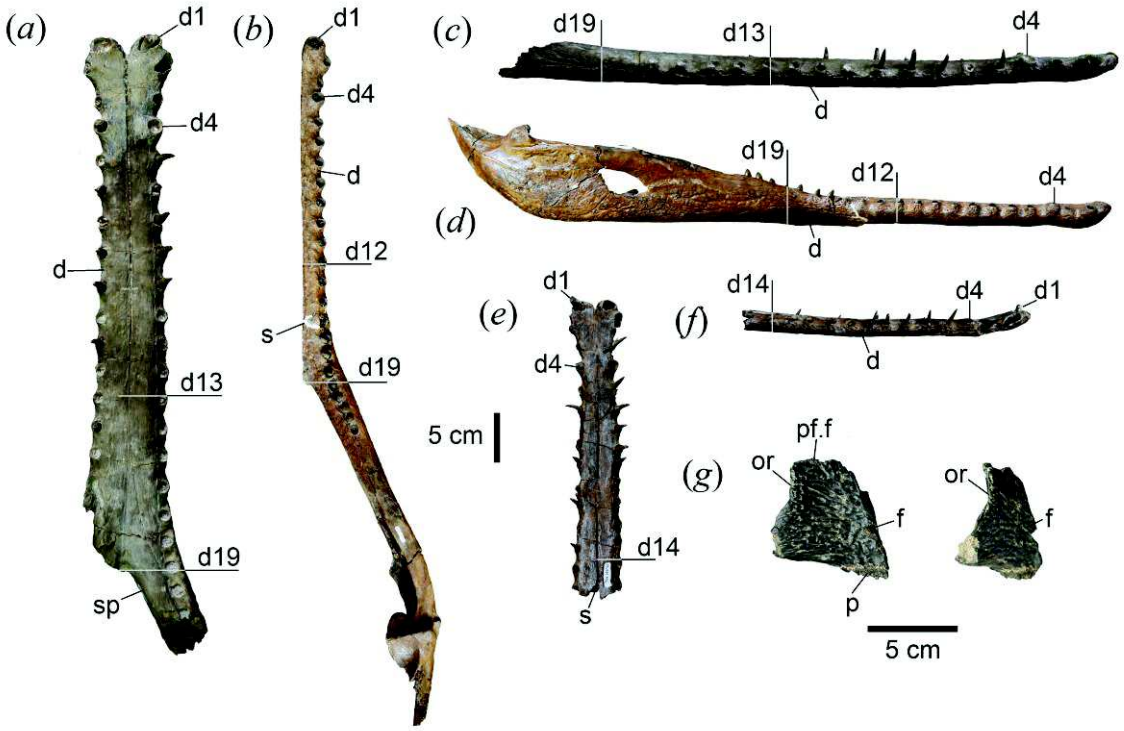

Figure VI.2. *Gryposuchus colombianus*. (*a*, *c*) MUSM 650, symphyseal region of the mandible in dorsal (*a*) and right lateral (*c*) view. For comparison, right mandible of *Gryposuchus* nov. sp. (MUSM 987) from Iquitos (IQ26) in dorsal (*b*) and right lateral (*d*) view. MUSM 906, partial symphysis of a juvenile in dorsal (*e*) and right lateral (*f*) view. MUSM 2630, partial frontal bone in dorsal (*g*) and dorsolateral (*h*) view. For anatomical abbreviations see Appendices.

In MUSM 650, lateral margins of the dentary are parallel posteriorly until the level of the 16th alveolus, well posterior the anterior apex of the splenial, as in La Venta specimens of *Gryposuchus*, and contrary to the condition of *G. croizati* in which the level of the splenial apex coincides with the initial divergence of the lateral margins (Riff & Aguilera, 2008). The

forward extension of the wedge-like splenial symphysis is constricted; posterior to the 18th tooth alveolus, the splenial-dentary suture runs more laterally to become in contact with the lingual border of 20th and 21th tooth alveoli. At this level, behind the symphysis, the splenial is transversally wider than dentary bone on the dorsal surface of the ramus. This pattern might be characteristic of South American gavials (Brochu & Rincón, 2004).

Both specimens show preserved anterior teeth positioned in their alveoli (Fig. VI.2*c*, *f*). They are slender, conical and slightly sigmoid. These teeth present a marked posteromedial curvature, with the sharp carinae not aligned with the parasagittal plane of the mandible. The crown surface is delicately fluted.

MUSM 2630 is a portion of a frontal bone preserving the left orbital margin (Fig. VI.2*g*). The orbital margin is sharp and elevated relative to the frontal plate as in gharials with fully-telescoped orbits, such as *Gryposuchus colombianus*, *Gryposuchus croizati*, and the Indian *Gavialis* (see Chapter V).

In recent phylogenetic analyses, *Gryposuchus* species and *Gavialis gangeticus*, the extant Indian gharial, are shown to be close relatives (Jouve et al., 2008; Salas-Gismondi et al., 2015a). These results point to a biogeographic conundrum in which gavialoid interchange might have happened at least twice between South America and other continental masses. However, further morphological studies on new Pebasian gavialoid provided evidence for parallel evolution between *Gavialis* and *Gryposuchus* in India and South America, respectively (Chapter V).

Alligatoroidea Gray, 1844

Globidonta Brochu, 1999

Alligatoridae Gray, 1844

Caimaninae Brochu 2003

Eocaiman Simpson, 1933

Eocaiman sp.

Material. MUSM 2082, anterior portion of right dentary (Fig. VI.3*a*, *b*), Locality Quebrada Grasa of the Mapuya River, Fitzcarrald Arch, Ucayali Department.

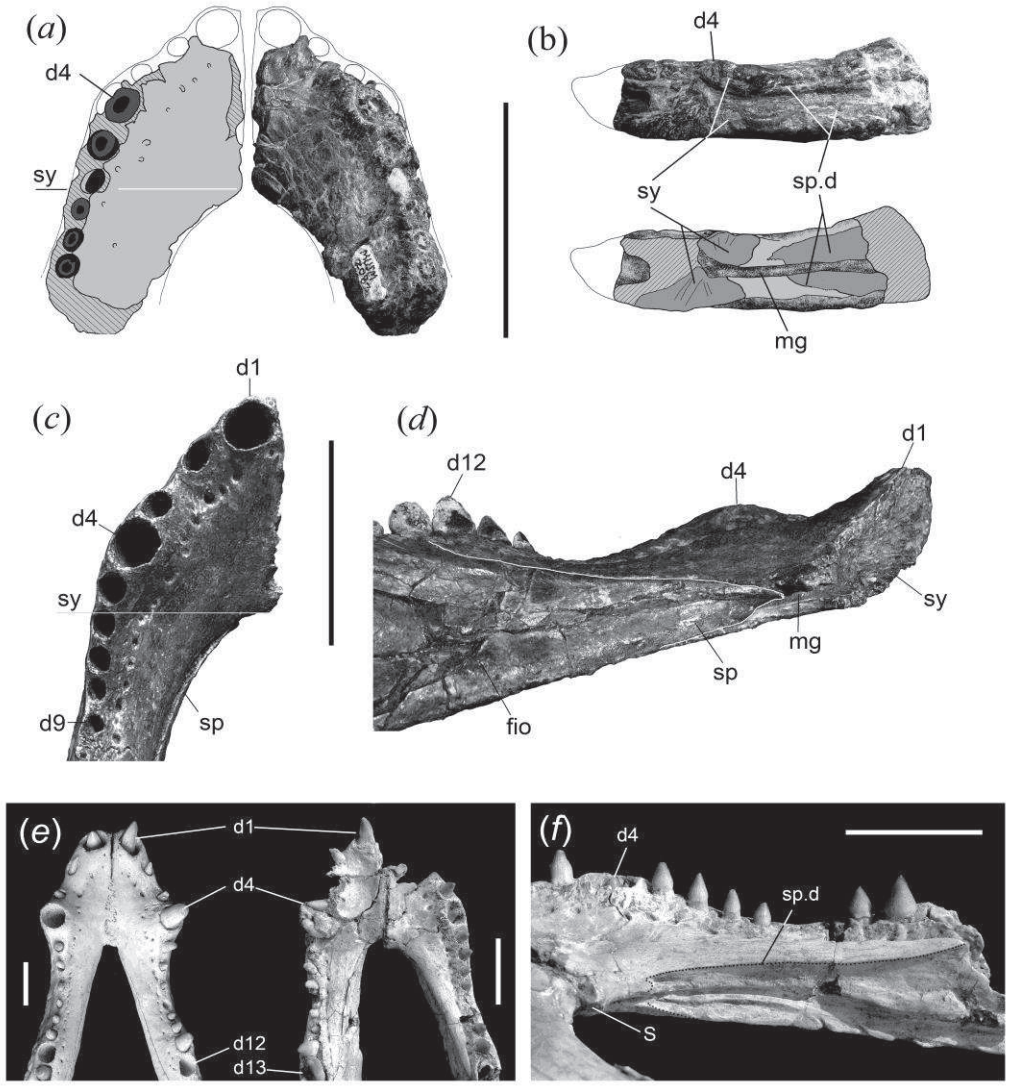

Figure VI.3. *Eocaiman* and allies. (*a*, *b*) MUSM 2082, fragment of right dentary in dorsal (*a*) and medial (*b*) view. (*c*, *d*) *Kuttanacaiman iquitosensis* (MUSM 1942), details of the anterior symphyseal region in dorsal (*c*) view and splenial in posteromedial (*d*) view. (*e*, *f*) *Eocaiman cavernensis* (holotype, AMNH 3158) Comparison between the anterior symphyseal region of *Caiman crocodilus* (left) and *E. cavernensis*. (*f*) Detail of the dentary contact for the splenial. For anatomical abbreviations see Appendices. Scale bars, 5 cm.

Comparative description and remarks. This small, badly weathered right dentary is preserved posteriorly up to the ninth alveolus. It bears a broad and relatively flat symphyseal area. The symphysis is entirely composed by the dentary bone, which reaches posteriorly the level of the sixth tooth alveolus. Although the first alveolus is not complete, it might be similar in size to the fourth. The size of these alveli is not markedly different relative to the fifth alveolus, resembling the condition of *Eocaiman cavernensis* (Fig. VI.3*e*) and contrasting the alveolar size pattern observed in *Kutanacaiman* (Fig. VI.3*c*), *Caiman* species (Fig. VI.3*e*), and *Melanosuchus niger*, in which the fourth alveolus diameter is hypertrophied, being twice (or more) as large as the diameter of the fifth dentary alveolus. Additionally, the fourth tooth alveolus is neither expanded laterally nor dorsally in both MUSM 2082 and *E. cavernensis* (Simpson, 1933). The splenial is not preserved, but its contact surface with the dentary indicates that the dorsal anterior process of the splenial was just slightly longer than the ventral one, as can be similarly established for *Eocaiman cavernensis* (Fig. VI.3*f*). They differ from *Kuttanacaiman*, in which the dorsal anterior process is much longer (Fig. VI.3*d*). Preserved alveoli (i.e., fourth to tenth) are positioned closely. The alveolar shape is not discernable due to distortion of their borders.

MUSM 2082 display several features recognized in the mandible of the holotype of *Eocaiman cavernensis*, such as long and flat symphysis and fourth alveolus not hypertrophied relative to the fifth alveolus. This morphology is further characterized by the lack of a prominent enlargement of the dentary at the level of the fourth alveolus. In fact, aforementioned features are consistently present in most poorly known Paleogene caimanines (e.g., *Eocaiman* species: Simpson, 1933; Bona, 2007; Pinheiro et al., 2013; *Notocaiman stromeri*: Rusconi, 1937), suggesting that they represent a condition ancestrally distributed within the clade rather than a specific taxonomic identity. Other proto-Amazonian basal caimanines from Iquitos Miocene bonebeds retained such primitive features (*Gnatusuchus*

and *Kuttanacaiman*: Salas-Gismondi et al., 2015a) and UCMP 38878, a fragmentary dentary from La Venta, Colombia (Langston, 1965). This latter material is almost undistinguishable from the Fitzcarrald specimen, thus they are likely co-specific.

Purussaurus Barbosa-Rodrigues, 1892

Taxonomic remarks. *Purussaurus* is a genus of large caimans restricted to the Middle and Late Miocene of South America, although distinct *Purussaurus*-like isolated teeth have been reported from the early Miocene of Panamá (Hastings et al., 2013). Recent phylogenetic analyses support a close relationship between *Purussaurus* and *Mourasuchus* (e.g., Brochu, 1999, 2011; Scheyer et al., 2013; Salas-Gismondi et al., 2015a), both taxa sharing a relative short symphysis and large anterior teeth. After a long history of naming new taxa on fragmentary material with vague (or not) locality data (Gervais, 1876; Mook, 1921a, 1921b), *Purussaurus* has been recognized as a valid taxon comprising three species: *Purussaurus neivensis* (Mook, 1941) from the late Middle Miocene of La Venta (Colombia; Langston, 1965), *Purussaurus brasiliensis* Barbosa-Rodrigues, 1892 from the Late Miocene of Acre (Brazil; Bocquentin-Villanueva et al., 1989), and *Purussaurus mirandai* Aguilera, Riff, and Bocquentin-Villanueva, 2006 from the Late Miocene of Urumaco (Venezuela; Sánchez-Villagra & Aguilera, 2006).

Purussaurus nov. sp.

Holotype: Museo regional de Ucayali (MRU) 17, complete snout (Fig. VI.4, VI.5*a*-*c*).

Locality and Horizon. Locality Quebrada Grasa of the Mapuya River, Atalaya Province, Ucayali Department, Peru; Late Middle Miocene beds of Ipururo Formation (Chapter II).

Brief history of the specimen. Peter Matthiessen (1961), in his classic book "The Cloud Forest: A Chronicle of the South American Wilderness" detailed the discovery of a "giant mandíbula" (in fact a cranial snout) in Quebrada Grasa (Grease Creek) of the Mapuya River (Fig. VI.4*a*):

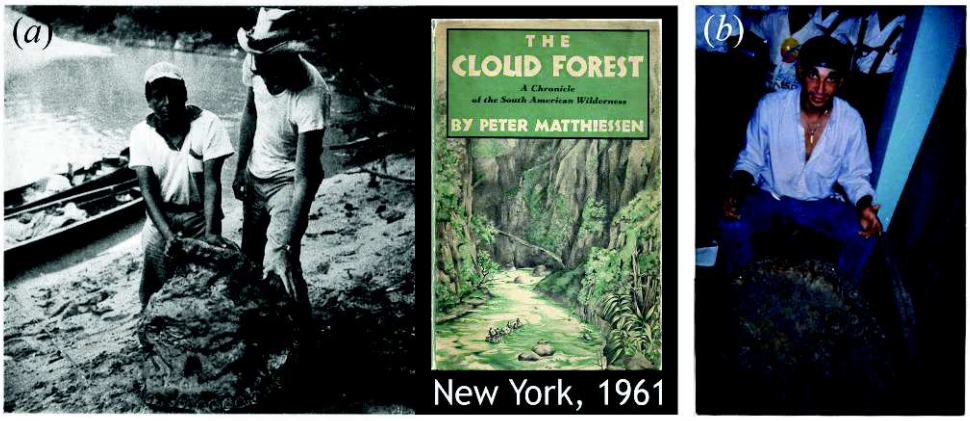

Figure VI.4. Crucial events. (*a*) Matthiessen and Vargaray with the snout of *Purussaurus* at Quebrada Grasa. Photograph published in "The Cloud Forest" by Peter Matthiessen, 1961. (*b*) In the 80's, Mario Urbina rediscovers in Pucallpa the snout of *Purussaurus* from Mapuya at the house of Ulyses Reategui.

"But there it was, sunk in the mud of the Mapuya bank, and it is almost everything Vargaray said it was: a *mandible* so large and heavy that it takes, if not six men, at least four strong men to lift it. Its great weight, which must exceed two hundred pounds, is less a consequence of its size than of its matter: beneath the smears of petrified clay which have adhered to it lies a solid block of petrified marble-like stone" (Matthiessen, 1961, p. 236).

He canoed with the 120-kilogram-fossil for about 300 km down the Ucayali River to the Pucallpa city, where the specimen was retained in the police station and subsequently lost for many years. Back in New York, Matthiessen showed photographs of the specimen to Charles Mook and Edwin Colbert of the American Museum of Natural History. Both decidedly identified this animal as an unknown giant Miocene crocodile (Matthiessen, 1961). From the images published in the book (Fig. VI.4*a*), Langston (1965) presumed the fossil could belong either to *Purussaurus* Barbosa-Rodrigues, 1892 or *Brachygnatosuchus* Mook,

1921a. By that time, none well preserved cranial material of enormous neogene alligatorids was found in the Amazon Basin.

In the early 1980s, paleontologist and fossil hunter Mario Urbina found Matthiessen's specimen of *Purussaurus* in Pucallpa, at the house of a private collector and prominent physician, Ulises Reátegui (Fig. VI.4*b*; Salas-Gismondi et al., 2014a). In 1997, the Gobierno Regional of Ucayali acquired this invaluable specimen of *Purussaurus* and currently it is stored in the *Museo Regional de Ucayali* (MRU), city of Pucallpa. A preliminary review of the material found differences with known *Purussaurus* species (Salas & Urbina, 2003). Removing the hard matrix covering the dorsal surface of the rostrum revealed peculiar features that phylogenetically ally this animal with the Late Miocene *P. brasiliensis* and *P. mirandai* (Salas-Gismondi et al., 2014b).

Diagnosis. A giant-sized *Purussaurus* species diagnosed by the following combination of characters: narial opening reaching posteriorly the level of the fifth maxillary alveolus (outreaching the level of the eight maxillary alveolus in *P. brasiliensis* and *P. mirandai*); no longitudinal depression behind the narial fossa; narial aperture irregular in shape, with sinuous profile, and displaced anteriorly; anterior margin of the narial aperture close to the tip of the snout. Contrary to *P. neivensis*, it shares with *P. brasiliensis* and *P. mirandai* an enlarged narial aperture with a postnarial fossa, short V-shaped nasal bones, and giant size.

General description. Based on its size, the snout (MRU 17) might belong to an adult individual (maximum width: 670 mm; length from the tip of the snout to the anterior end of the suborbital fenestrae: 540 mm). MRU 17 includes premaxillae, maxillae, anterior portion of the palatines, and nasals. Ventrally, the alveoli, incisive foramen, and anterior margins of infraorbital fenestrae are preserved. Dorsally, the narial opening is stuffed with hard matrix whereas its antero-lateral rim is covered with bone fragments, although most narial rims and

adjacent bones, including nasals, were exposed after preparation process. The proximal ends of these bones are weathered.

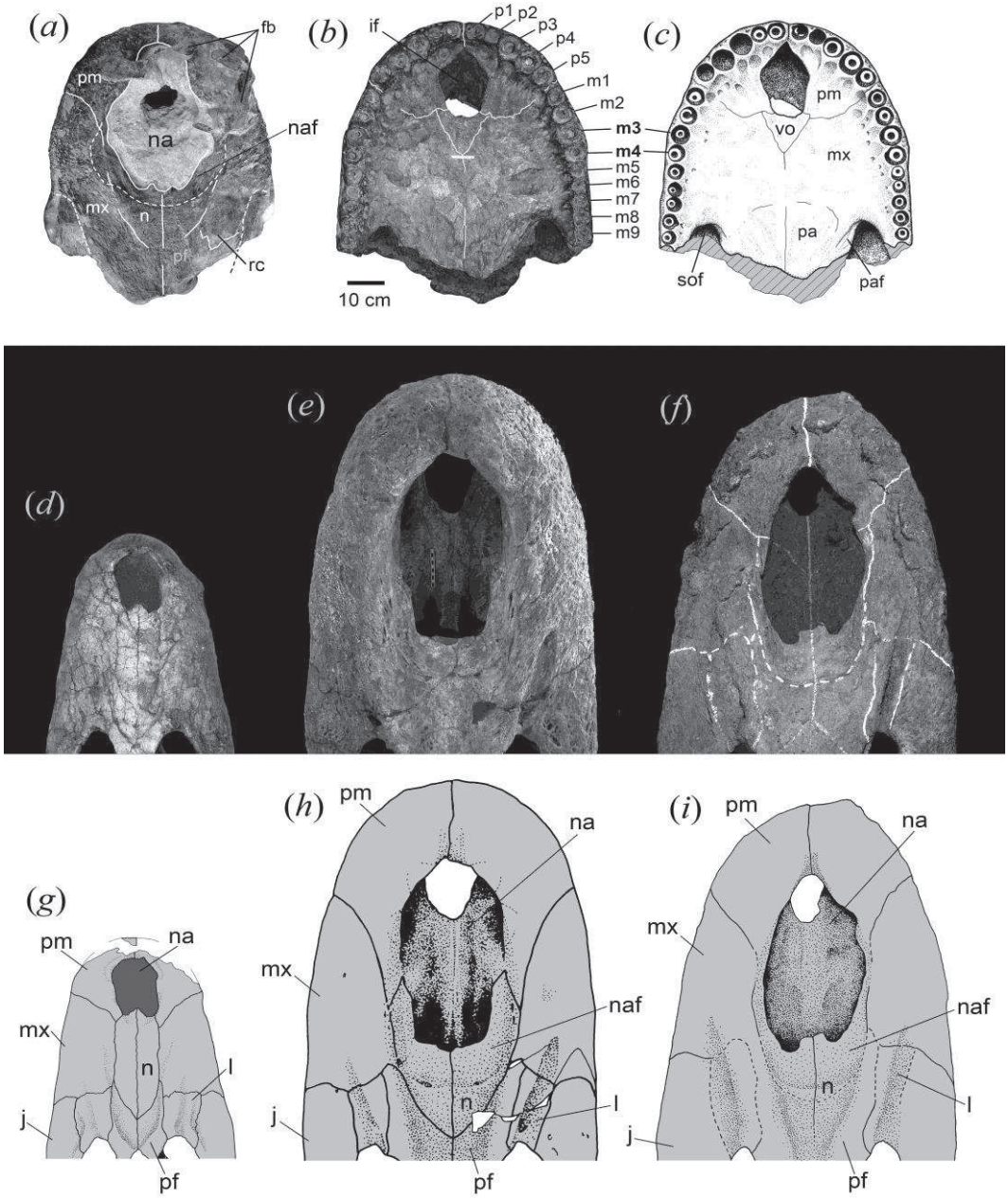

Figure VI.5. *Purussaurus.* (*a*-*c*) *Purussaurus* nov. sp., snout (MRU 17) in dorsal (*a*), and ventral (*b*, *c*) view. Rostra of *Purussaurus neivensis* (*d*, *g*), *Purussaurus brasiliensis* (*e*, *h*), and *Purussaurus mirandai* (*f*, *i*). For anatomical abbreviations see Appendices.

MRU 17 denotes a short rostrum relative to its width, slightly bowed lateral margins, and steep-sided. The ratio of the palatal length to the maximum width of the maxilla is 0.87, as in *Purussaurus brasiliensis* (UFAC 1403), whereas in *P. neivensis* (UCMP 39704) and

Purussaurus mirandai (UNEFM 1369) it is about 1.00. The rostrum ends in a bluntly rounded snout remarkably deeper than its proximal region. In lateral view, the dorsal surface of the rostrum is ventrally inflected.

The premaxillae and maxillae are heavily sculpted anterior and lateral to external naris. The maxillae participate in the postero-lateral rims of the external naris, as in *P. brasiliensis*. The external naris is greatly enlarged as is typical in representatives of *Purussaurus*, and it extends posteriorly to the anterior margin of the sixth maxillary alveolus. The external naris is composed by the big narial aperture and, at least posteriorly, by a narial fossa. This latter feature observed in *P. brasiliensis* and *P. mirandai* (Bocquentin-Villanueva et al., 1989; Aguilera et al., 2006; Fig. VI.5*e*, *f*, *h*, *i*). *Purussaurus neivensis* shows no evidence of narial fossa (Fig. VI.5*d*, *g*). The narial aperture is longer than wide and has an unusual sinuous profile. A constricted projection of the narial aperture extends anteriorly between the premaxillae farther beyond any other specimen of *Purussaurus*. The nasal bones essentially make up the narial fossa. The surface of the latter is irregular but symmetrical transversally, with a medial bifurcated spine and, laterally to it, an oblique longitudinal dome-like crest. The dorsal surface behind the external naris, delimited by the massive rostral canthi, is virtually flat.

MRU 17 possesses five premaxillary and ten maxillary alveoli, being the tenth of each maxilla (i.e., left and right) broken in its anteriormost area (Fig. VI.5*b*, *c*). The third and fourth premaxillary alveoli are the largest in this specimen. In the maxilla, the third maxillary alveolus is bigger than the fourth as seems to be typical of *Purussaurus* (Salas-Gimondi et al., 2014b). All the alveoli are very close together, excluding the last premaxillary and first maxillary alveoli, which are separated by a diastema. The premaxillary-maxillary suture on the palatal surface is winding and essentially transverse, whereas dorsally it is mostly hidden by the sculpture. The incisive foramen is located behind the first two premaxillary alveoli. It

is diamond-shaped and extends all the length of the premaxillae in the palatal surface. The incisive foramen is limited posteriorly by a triangular exposure of the vomer on the palate, as we suspect is characteristic of *Purussaurus*. The vomer and the fan-like anterior extension of the palatine bone restrict contact of the maxillae in the midline to a short distance between the third and seventh maxillary alveoli. The anterior and anterolateral borders of the suborbital fenestrae are limited by the maxillae. The anterior end of the suborbital fenestrae reaches the level of the eighth maxillary alveoli.

Mourasuchus Price, 1964

Mourasuchus sp.

Material. MUSM 930, portion of right dentary including third and fourth alveoli (Fig. VI.6*a-d*), Locality DTC32; MUSM 931, partial left premaxilla (Fig. VI.6*f, g, j-l*) Locality DTC32; left MUSM 1672, associated postcranial elements, including vertebrae, ribs, ilium, and multiple osteoderms, Locality SEP006.

Comparative description and remarks. The fragmentary condition of the Fitzcarrald material referable to *Mourasuchus* impedes any assignment at the species level. In general, these specimens belong to individuals similar in size to those documented in coeval localities of the Iquitos area (Fig. VI.6*e*, *h*, *i*). MUSM 931 is a partial left premaxilla including a portion of the narial rim, the interpremaxillary suture and, the first and second alveoli (Fig. VI.6*f*, *g*, *j-l*). The premaxilla is deep and relatively robust. As usual in *Mourasuchus*, a high crest circumscribes anterolaterally the external naris. Anterior to this crest, a huge pit for the reception of the first dentary tooth perforates the premaxillary roof. Ventrally, the palate surface is steepy vaulted and is higher anteriorly. Preserved alveoli are nearly circular. Interalveolar spaces are smaller than diameter of adjacent alveoli. The first alveolus is bigger

than the second one. The third alveolus is partially preserved and probably similar in size to the second one. The anterior margin of the incisive foramen is almost linear and posterolaterally oriented. It denotes a relatively large incisive foramen. The incisive foramen probably abuts the premaxillary tooth row.

MUSM 930 is a fragment of a mandible represented by a curved section of the dentary (Fig. VI.6*a-d*). Albeit not conclusive, this portion might pertain to the left mandible, probably comprising the second and third alveoli and only remnants of the first and fourth ones.

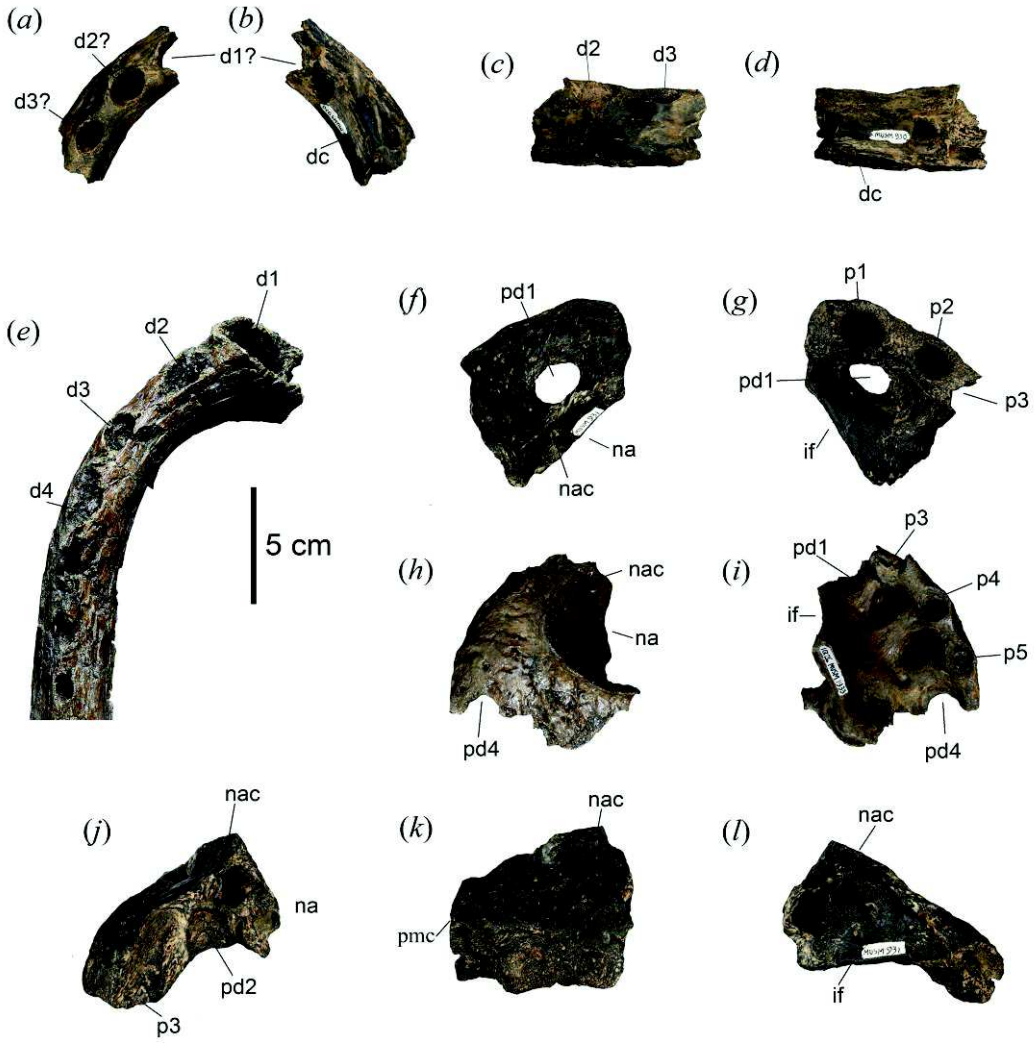

Figure VI.6. ***Mourasuchus*.** (*a-d*) MUSM 930, fragment of dentary in dorsal (*a*), ventral (*b*), lateral (*c*), and medial (*d*) view. (*e*) Anterior portion of the dentary of *Mourasuchus atopus* (MUSM 2379) from Iquitos (IQ26). (*f*, *g*, *j-l*) MUSM 931, partial left premaxilla in dorsal (*f*), ventral (*g*), posterior (*j*), lateral (*k*), and medial (*l*) view. (*h*, *i*) Left premaxilla of *Mourasuchus atopus* (MUSM 1933) in dorsal (*h*) and ventral (*i*) view. For anatomical abbreviations see Appendices.

Based on this premise, the second alveolus is slightly bigger than the third one. The dentary is oval in section and higher anteriorly. Ventrally, the lateral wall of the dentary projects a longitudinal crest similar to that identified in a well-preserved mandible (MUSM 2379: Fig. VI.6*e*) from IQ26 (Iquitos bonebeds, late Middle Miocene). Additionally, this area is traversed by irregular furrows and probably by a shallow longitudinal trough, as was described for *M*. *atopus* (Langston, 1965). Other details were hidden away by the erosion.

Paleosuchus Gray, 1862

Paleosuchus sp.

Material. MUSM 929, portion of right dentary (Fig. VI.7*a*, *b*, *f*), Locality DTC20; MUSM 1673, portion of right dentary (Fig. VI.7*d*, *e*, *g*), Locality DTC32 (Chapter II).

Comparative description and remarks. These fragmentary portions of dentaries show clear morphological affinities with extant *Paleosuchus* species. Specimens denote animals of slightly larger size than MUSM DPV CR 1, a skull with mandibles of an extant *Paleosuchus trigonatus* and measuring 260 mm in dorsal length. This modern specimen belonged to an individual of about 1,760 mm of total body length.

MUSM 929 comprises an intermediate portion of a right dentary with five fairly complete alveoli, most probably representing the 13th to 17th ones (Fig. VI.7*a*, *b*, *d*). Three alveoli are partially preserved in front of them and one behind. MUSM 1673 corresponds to a smaller portion of the same region (Fig. VI.7*c*). In the latter, four alveoli are preserved. The dentary at this position is relatively low and straight. On the medial side, dentary surface for the splenial is slightly convex and smooth. The Meckelian groove is relatively narrow. These specimens lack evidence of mandibular festooning.

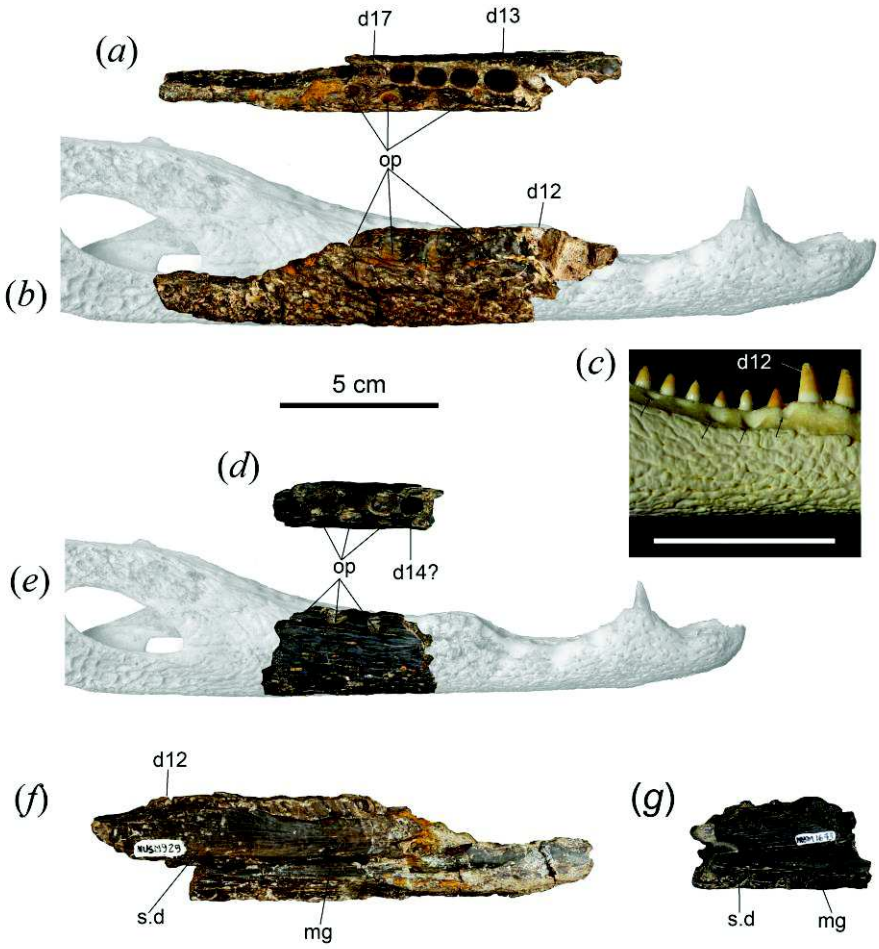

Figure VI.7. *Paleosuchus.* (*a*, *b*, *f*) MUSM 929, portion of right dentary in dorsal (*a*), lateral (*b*), and medial (*f*) view. (*d*, *e*, *g*) MUSM 1673, portion of right dentary in dorsal (*d*), lateral (*e*), and medial (*g*) view. (*c*) Homologous anatomical region in *Paleosuchus palpebrosus*. Arrows indicate the position of occlusal pits (op). For anatomical abbreviations see Appendices. Scale bar, 5 cm

Alveoli are laterally compressed. Interalveolar partitions are narrow. In MUSM 929, alveolar diameter decreases posteriorly whereas in MUSM 1673 alveoli bear equal size. The sculpture of the lateral face of these specimens consists mainly of sinuous furrows and small, irregular holes. In both specimens, the most conspicuous feature is located higher on the lateral wall of the dentary, in a relatively smooth area next to the alveolar margins. Here, this area bears deep pits for the reception of pointed maxillary fangs. Identical pits are also observed in the mandibular rami of extant *Paleosuchus palpebrosus* (Fig. VI.7*c*). This condition might reflect the tight fit between upper and lower dental quadrants as produced by the large overlapping jaws within *Paleosuchus* species.

D. Results

D.1 Results of the phylogenetic analysis

Our phylogenetic analysis retained 50 most parsimonious trees with a minimum length of 677 steps. The strict consensus phylogeny (Fig. VI.8) calculated from those trees yielded the following statistics: length = 695; consistency index (CI) = 0.377; retention index (RI) = 0.797. *Purussaurus* is monophyletic, with *P. neivensis* being sister group to *Purussaurus* nov. sp., *P. mirandai*, and *P. brasiliensis*. The large-sized *Purussaurus* clade is further characterized by the presence of rostral canthi (character 96-1) and postnarial fossa (character 200-1). Other phylogenetic relationships are in accordance with those as proposed by Salas-Gismondi et al., (2015a).

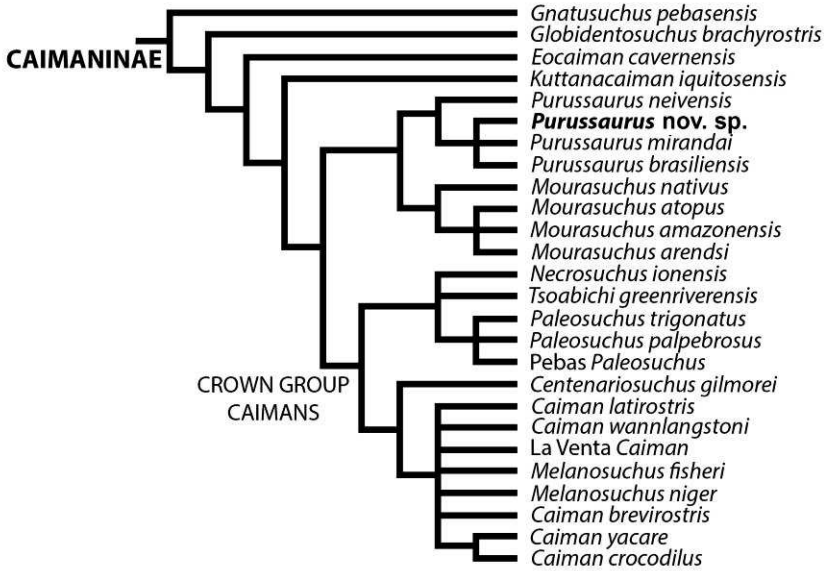

Figure VI.8. Phylogenetic position of *Purussaurus* nov. sp. within the caimanines. Strict consensus phylogeny from 50 most parsimonious trees.

D.2 Results of the similarity analyses

Results of the first analysis, although not conclusive, indicate that the Fitzcarrald mesoeucrodylian fauna (FZ) might have significant resemblance with Nueva Unión (NU) and La Venta faunas (LV; Table VI.1). SC values of FZ-NU are 50 for minimum and maximum similarity, since NU shares two taxa of four for both calculations. Although Simpson's index

shows little influence from the sample size (Nakaya & Tsujikawa, 2006), these relatively high results have been driven partially by the smaller number of taxa recorded within the Nueva Unión fauna (see Simpson, 1960). Two taxa are also shared between FZ and Acre (AC) and FZ and Urumaco (UR), but lower values were obtained (33.3 and 28.6, respectively) due to the higher number of taxa in the smaller fauna (i.e., five and seven taxa, respectively). FZ-LV SC_{min} of 28 is comparatively low as well, but the SC_{max} equals 71.4, i.e. the highest similarity value of this analysis. This value is recording the probability of sharing five out of seven species between coeval Fitzcarrald and La Venta faunas. On the other hand, comparisons between coeval Fitzcarrald and Iquitos faunas resulted in the lower values, with SC_{min} of 14.3 and SC_{max} of 28.6. In summary, Fitzcarrald might have the highest faunal similarity with La Venta and Nueva Unión, a preliminary assumption already proposed for mammals by Tejada-Lara et al. (2015*a*), at least regarding Fitzcarrald and La Venta localities. Yet, although representing the same time interval (late Middle Miocene), Fitzcarrald and Iquitos crocodile faunas are significantly different.

Regarding the second analysis based on phylogenetic morphotypes, general results agree with the previous analysis of similarity, with Fitzcarrald fauna having high values when compared with Nueva Unión and La Venta (Tables VI.2 and VI.3), although most comparisons made with Nueva Unión have high values as well. The SC values for most Iquitos comparisons are relatively lower than those of other pairs not comprising Iquitos. IQ-AC value is the lowest for any pair of faunas whereas Iquitos highest similarity is with UR. Late Miocene faunas show high similarity, with Acre possessing the same (but not all) phylogenetic morphotypes present in Urumaco. As a whole, the analysis suggests that Middle Miocene faunas encompass less homogeneity in terms of phylogenetic morphotypes than Late Miocene faunas. Nueva Unión fauna is highly similar to both Middle and Late Miocene faunas. Similarly, Urumaco shows similarities with Iquitos and Acre.

Table VI.1. Shared taxa of mesoeucrocodylians from fossiliferous localities of tropical South America. Faunal similarities were calculated using the Simpson Coefficient (SC). Locality faunal data is from Sánchez-Villagra & Aguilera (2006), Cozzuol (2006), Salas-Gismondi et al. (2015a), and personal observation.

Miocene mesoeucrocodylian fauna		Late Middle Miocene			Late Miocene		
		Fitzcarrald	La Venta	Iquitos	Nueva Union	Acre	Urumaco
Sebecosuchia	*Sebecus huilensis*	x	x				
	Barinasuchus arveloi	x	*				
Crocodylia							
Caimaninae	*Gnatusuchus pebasensis*			o	o		
	Kuttanacaiman iquitosensis			o			
	Globidentosuchus brachyrostris						o
	Miocene *Eocaiman*	*	*				
	Purussaurus neivensis		o	o			
	Large *Purussaurus* ssp.	x			x	x	x
	Mourasuchus atopus	*	*	*			
	Mourasuchus arendsi						o
	Large *Mourasuchus* spp.				o	o	o
	Caiman wannlangstoni			o			o
	Caiman brevirostris					o	o
	La Venta *Caiman*		o				o
	Miocene *Paleosuchus*	x		x			
Gavialoidea	*Gryposuchus* nov. sp.			o			o
	"Telescoped" *Gryposuchus* spp.	x	x		x	x	x
?Crocodyloidea	*Charactosuchus fieldsi*		o			o	o
Minimum number of shared species/forms			2	1	2	2	2
Maximum number of shared species/forms			5	2	2	2	2
Minimum (SC_{min}) and maximum (SC_{max}) value od faunal similarity			28.6/71.4	14.3/28.6	50.0/50.0	33.3/33.3	28.6/28.6

x, taxa present in Fitzcarrald and shared with other localities; *, taxa with doubtful record in Fitzcarrald and shared with other localities; o, taxa with no occurrence data in Fitzcarrald.

Table VI.2. Occurrence of selected groups of mesoeucrocodylians in Middle and Late Miocene well-documented South American localities.

Miocene mesoeucrocodylian fauna		Late Middle Miocene			Late Miocene		
		Fitzcarrald	La Venta	Iquitos	Nueva Union	Acre	Urumaco
Sebecosuchia	Sebecidae	x	x				
Crocodylia							
Caimaninae	Basal caimanines	x	x	x	x		x
	Purussaurus	x	x	x	x	x	x
	Mourasuchus	x	x	x	x	x	x
	crushing dentition *Caiman*			x			x
	generalized *Caiman*		x			x	x
	Paleosuchus	x		x			
Gavialoidea	non "telescoped" *Gryposuchus*			x			x
	"Telescoped" *Gryposuchus*	x	x		x	x	x
?Crocodyloidea	*Charactosuchus*		x			x	x

x, representative of the group present.
For grouping criteria see Material and Methods.

Table VI.3. Indices of faunal resemblances (Simpson Coefficients) within pairs of Middle and Late Miocene localities of tropical South America. Second analysis.

	Fitzcarrald	La Venta	Iquitos	Nueva Unión	Acre	Urumaco
Fitzcarrald	-	83.3	66.7	100	60	66.7
	La Venta	-	50.0	100	80	85.7
		Iquitos	-	75	40	83.3
			Nueva Unión	-	75	100
				Acre	-	100

E. Discussion

E.1 *Purussaurus* evolution and biogeography

Phylogenetic analysis indicates that the new Middle Miocene species of *Purussaurus* from Fitzcarrald is closer to *P. mirandai* and *P. brasiliensis* than to *P. neivensis* (Fig. VI.9). Thus, striking giant size and narial opening characteristic of Late Miocene species was already acquired during proto-Amazonian times, at least since the late Middle Miocene. By the time the new taxon was dwelling in the tidally-influenced, fluvially dominated settings of Fitzcarrald, *Purussaurus neivensis* was still the dominant predator in the northern La Venta and Iquitos areas of the Pebas Mega-Wetland System (Langston, 1965; Salas-Gismondi et al., 2015a).

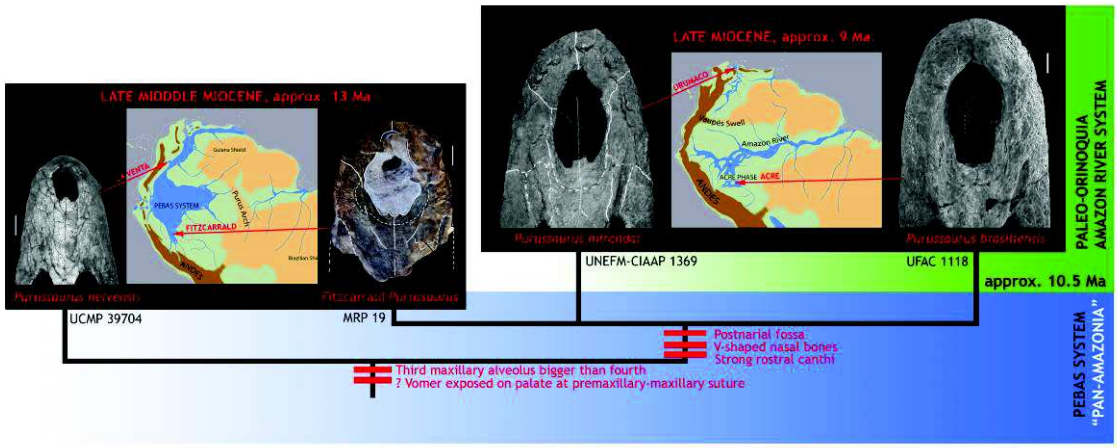

Figure VI.9. Evolution of *Purussaurus*. Paleogeographic reconstructions of the Pebas System and Acre phase (including paleo-Orinoco area), prior and after Middle-Late Miocene boundary Andean uplift, respectively. Paleogeographic maps modified from Hoorn et al. (2010b) and Figueiredo et al. (2010).

In Nueva Unión locality, southern Iquitos, outcrops of the lignite-rich late Middle Miocene Pebas Formation show a gradational transition into those of the lignite-poor channelized early Late Miocene units of the "uppermost Pebas" Formation, depicting environmental changes associated with the final phases of the Pebas Mega-Wetland System (Rebata et al., 2006; Salas-Gismondi et al., 2015a). Fragmentary specimens from the younger deposits document the presence of giant forms of *Purussaurus* and *Mourasuchus* (Figs. IV.18*a* and IV.19*a-d*;

Salas-Gismondi et al., 2015a). This record suggests that the onset of regional environmental changes at the Middle-Late Miocene boundary is associated with the prevalence of the giant-sized species, that would last throughout the Late Miocene interval in the Amazonian and paleo-Orinoco basins (Aguilera et al., 2006; Cozzuol, 2006).

E.2 Did *Balanerodus logimus* exist?

Relatively large bulbous teeth were found within the Fitzcarrald mesoeucrodylian fauna and subsequently referred to *Balanerodus logimus* Langston 1965 (Salas-Gismondi et al., 2007: Fig. 1f). This taxon was originally erected on the basis of scattered dental material from contemporaneous Middle Miocene La Victoria and Villavieja Formations from Colombia (Langston, 1965). Additionally, Langston & Gasparini (1997) described new material comprising a fragment from the middle part of the right maxilla bearing two teeth with the same typical shape (IGM 250668). *Balanerodus logimus* teeth have a bulb-shaped crown with radiating crenulations and a coronal coarse ridge (Langston, 1965; Langston & Gasparini, 1997). Crown height is around 20-30 mm. Due to the poorly diagnostic fragmentary condition of *Balanerodus* material, some authors raised doubts about its taxonomic validity (Scheyer & Moreno-Bernal, 2010).

Among a set of teeth unambiguously referable to *Purussaurus* from Nueva Unión locality (Fig. VI.10*a*), we recognized teeth with bulb-shaped crowns that are virtually indistinguishable from those assigned to *Balanerodus logimus* in La Venta and Fitzcarrald (Fig. VI.10*b*), suggesting that material of this latter species might pertain instead to intermediate or posterior regions of *Purussaurus* jaws, undermining recognition of it as a distinct taxon. Accordingly, the anatomy of the intermediate portion of a maxilla from La Venta assigned to *Balanerodus* (i.e., IGM 250668) is consistent with posterior maxillary region of *Purussaurus* species.

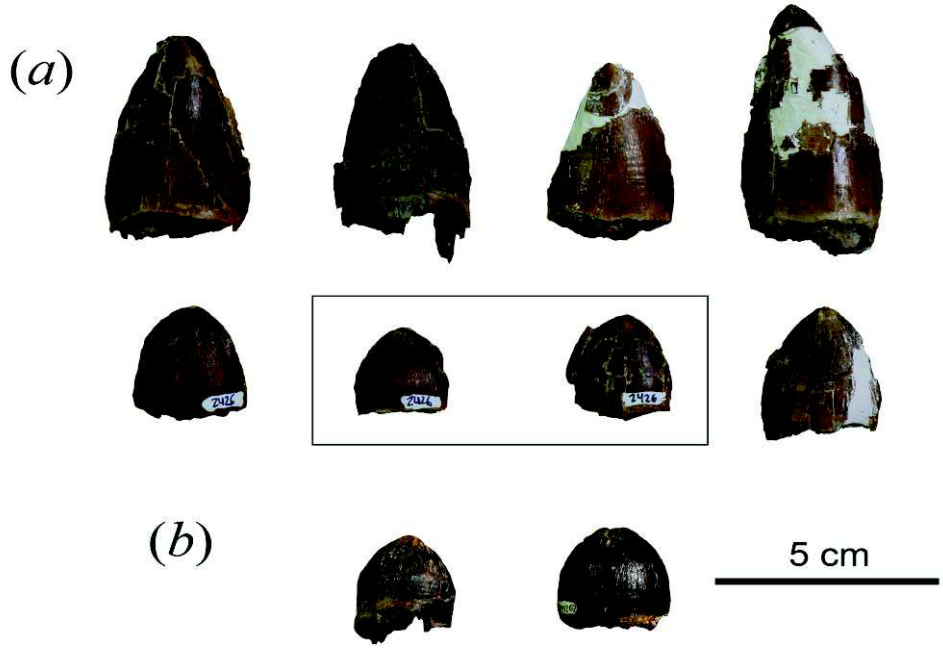

Figure VI.10. *Purussaurus* teeth. (*a*) MUSM 2426, associated teeth from Nueva Unión (IQ125). In the box, selected teeth bearing bulbous-shaped crown with radiating crenulations. (*b*) MUSM 1261 (left) and MUSM 1262 (right), teeth assigned to originally to *Balanerodus logimus* by Salas-Gismondi et al., (2007).

E.3 Mesoeucrocodylian Fitzcarrald faunal assemblage

Mesoeucrocodylians from Fitzcarrald remarks the extraordinary diversity of snout morphotypes occuring within the Pebas System (Figs. VI.11 and VI.12). They are represented by two sebecid notosuchians and five crown-grouped crocodylians. The sebecid component of the Fitzcarrald fauna, i.e. *Sebecus huilensis* and *Barinasuchus*, probably also pertains to the La Venta assemblage. Besides the medium-sized *Sebecus huilensis* identified in La Venta (Langston, 1965), a second larger sebecid species, comparable in size with *Barinasuchus*, roamed this region. High faunal similarities obtained from SC_{max} values of FZ-LV comparison notably rely on the share presence of sebecids in both localities among Miocene Neotropical assemblages analyzed (Table VI.1). The rich record of fossil vertebrates from the coeval Iquitos bonebeds lacks of remains belonging to sebecid mesoeucrocodylians (Fig. VI.12), a fact that might be related with the distinct aquatic conditions of Iquitos paleoenvironments (Wesselingh et al., 2002).

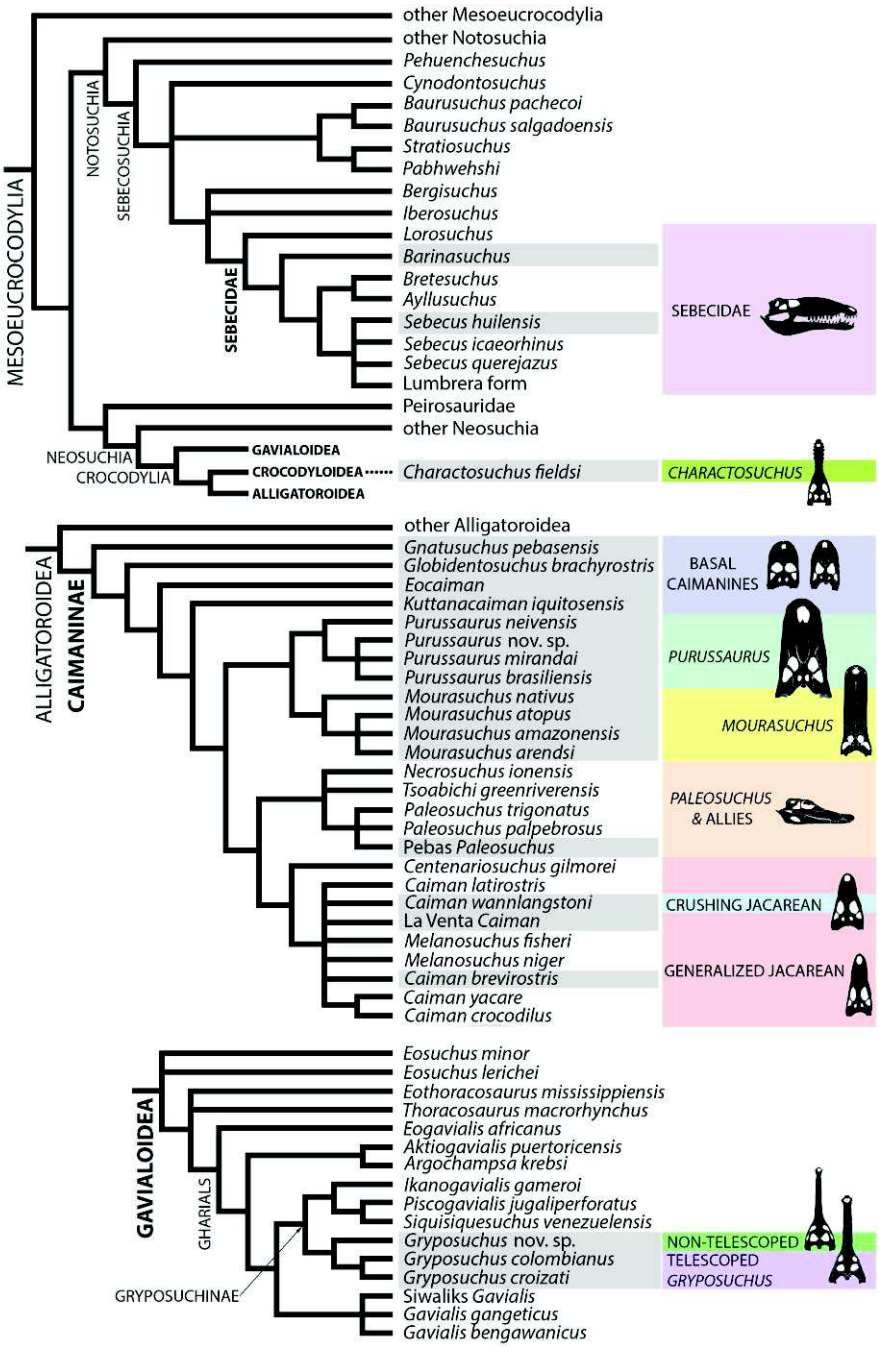

Figure VI.11. Phylogenetic snout morphotypes of mesoeucrocodylians of the Pebas System. Phylogenetic hypotheses are from Pol & Powell (2011; Notosuchia), chapter V (Gavialoidea).

In turn, these settings were dominated by crushing-dentition caimanines and one gavialoid (Salas-Gismondi et al., 2015a). Current knowledge of sebecid ecology based on conspicuous cranial and appendicular features suggests more terrestrial habits than those of modern crocodylians (Pol et al., 2012).

As other late Middle Miocene faunas in tropical South America, such as La Venta and Iquitos, Fitzcarrald mesoeucrocodylians are further composed by several caimanine species and only one gavialoid form (Langston, 1965; Langston & Gasparini, 1997; Salas-Gismondi et al., 2015a). To date, this fossil record is only a cursory glance to this faunal community since most taxonomic identifications are based on fragmentary material. However, an initial outline allows recognizing typically Miocene caimanines, such as *Purussaurus* and *Mourasuchus* species, as well as small forms with poorly known fossil documentation. Among them, *Eocaiman* sp. is for the first time reported within the Fitzcarrald fauna. Although this taxon is consistently referred to Paleogene forms from Patagonia (Simpson, 1933; Bona, 2007; Pinheiro et al., 2013), Langston (1965) identified its distinctive morphology in two dentaries from La Venta (UCMP 38878 and UCMP 39023). Fitzcarrald specimen (MUSM 2032: Fig. VI.3*a*, *b*) and UCMP 38878 (Langston, 1965: Fig. 31, left) are decidedly indistinguishable, whereas UCMP 39023 resembles more the anatomy of *Caiman wannlangstoni* from Iquitos (Salas-Gismondi et al., 2015a). Phylogenetic analyses suggest that *Eocaiman* encompasses several features of the caimanine ancestral condition, including long and flat mandibular symphysis and lack of enlargement of the dentary at the level of the fourth alveolus. This morphotype was definitely present in proto-Amazonia until the initial establishment of the transcontinental drainage system as documented in Nueva Unión (Salas-Gismondi et al., 2015a; Chapter IV). During the Late Miocene, basal caimanines exclusively survived in the Paleo-Orinoco basin; small to medium-sized caimans in Acre are restrited to advanced jacarean caimanines (Cozzuol, 2006). Here, we also reaffirm the initial identification of *Paleosuchus* in Fitzcarrald (Salas-Gismondi et al., 2007), now a record shared with the crocodylian assemblage from Iquitos (Salas-Gismondi et al., 2015a). On the other hand, we reject previous report of *Caiman* species in Fitzcarrald solely based on isolated teeth (*contra* Salas-Gismondi et al., 2007).

Gryposuchus colombianus seems to be confined to the Middle Miocene interval, although it was not ubiquitous in coeval sites of tropical South America. This species is known so far only within Fitzcarrald and La Venta localities (Langston, 1965; Langston & Gasparini, 1997; Salas-Gismondi et al, 2007) whereas it is absent among the copious material of crocodylians found in the Pebas Formation of the Iquitos area. In these deposits, a single gavialoid representing a new *Gryposuchus* species was reported (Salas-Gismondi et al., 2015a; Chapter V). At first glance, the vacancy of *Gr. colombianus* in the late Middle Miocene Pebas Formation is intriguing since Iquitos area is geographically intermediate between La Venta and Fitzcarrald sites. However, within the vast Pebas Mega-Wetland System, environmental segregation might have played an important role in the distribution of the taxa (Antoine et al., 2013; Tejada-Lara et al., 2015a, 2015b).

E.4 Ecological and paleoenvironmental implications

Fitzcarrald fauna shows the highest and lowest similarity with coeval Neotropical late Middle Miocene faunas, namely La Venta and Iquitos (Fig. VI.12), respectively. Results are even odder considering that Iquitos is located in the midway between Fitzcarrald and La Venta. This conundrum suggest that, besides contemporaneity, taxonomic similarities between Fitzcarrald and La Venta are not driven by geographic proximity; instead sedimentologic, tectonic, and taphonomic data (Kay & Madden, 1997; Espurt et al., 2006; Roddaz et al., 2010) point to the decisive role of regional environmental conditions and ecological segregation (Antoine et al., 2013; Tejada-Lara et al., 2015a). Paleogeographic reconstructions depict the existence of continental Andean reliefs and fluvially influenced paleo-environments in La Venta and Fitzcarrald during the late Middle Miocene, with these areas corresponding to the western peripheric Andean riverine and estuarine environments of the Pebas Mega-Wetland System (Kay & Madden, 1997; Guerrero, 1997; Espurt et al., 2006). To the east, Iquitos deposits from this time interval consistently document lacustrine

environments recording endemic adaptive radiations of bivalves, gasteropods, and ostracods (Muñoz-Torres et al., 2006; Wesselingh et al., 2006a). The evolutionary radiation of crocodylians shows high levels of endemicity as well (Salas-Gismondi et al., 2015a).

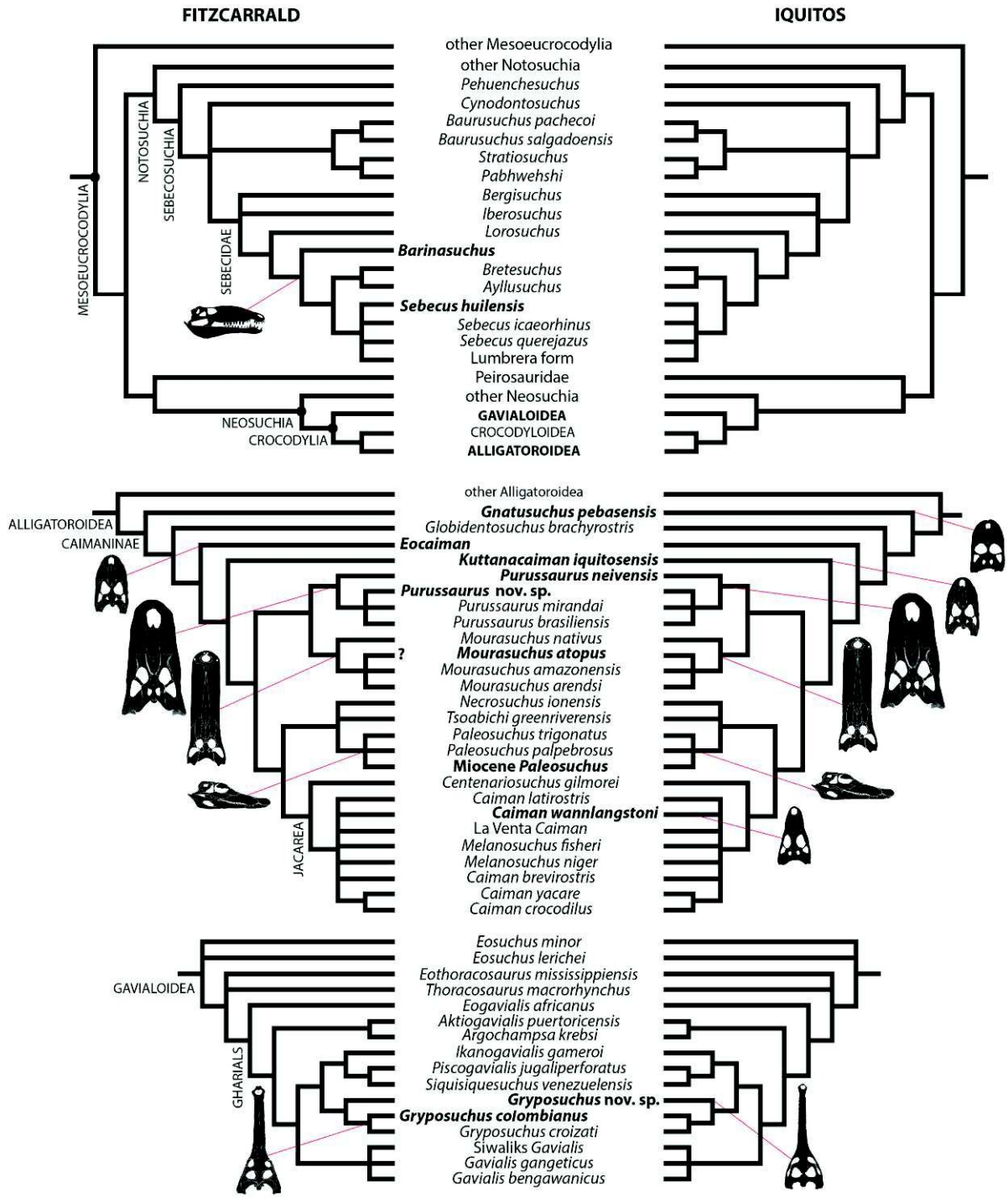

Figure VI.12. Comparison between of the phylogenetic and morphotypic diversity between Fitzcarrald and Iquitos, both representing different environmental conditions within the Pebas Mega-Wetland System.

The widespread dysoxia and muddy lake bottoms seem to be linked to this typical association (Wesselingh et al., 2002; Salas-Gismondi et al., 2015a), providing peculiar ecological conditions and therefore, limiting the distribution of these and other aquatic organisms across the Pebas biome. High levels of endemicity and extensive evolutionary radiations like those of the lakes and swamps of the Pebas System are characteristic of long-lived lakes, often located in tectonically active areas (Wesselingh et al., 2002). The analyses of taxonomic similarity consequently reflect the heterogeneous character between lacustrine and fluvially-influenced Pebasian faunas.

The end of the Pebas Mega-Wetland System notably resulted in the reduction of phylogenetic and morphotype mesoeucrocodylian diversity, particularly in the Amazonian basin, designating the beginning of the modern Amazonian faunas. Fitzcarrald and La Venta local faunas document the latest record of the long-lasting sebecid clade. Considering the putative terrestrial preferences allocated to the high and slender snout morphotype of the sebecids, their extinction might not be related with the demise of the aquatic environments of the Pebas System, yet causes remain obscure. Within crocodylians, stem caimanines were apparently common in South America until the Middle-Late Miocene transition, since they are represented in La Venta, Fitzcarrald, Iquitos, and Nueva Unión. The latter assemblage probably represents a transitional stage from the Pebas System to the so-called Acre phase in Nauta area, when the transcontinental drainage of the Amazon River became established (Rebata et al., 2006; Hoorn et al., 2010). The Acre phase in the Late Miocene Amazonian basin lacks of stem caimanine lineages (Cozzuol, 2006). The sole Late Miocene survivor of these old lineages, *Globidentosuchus brachyrostris*, is recorded within the abundant and diversified fauna of Urumaco (Scheyer et al., 2013). Our analyses indicate that Urumaco assemblages condense most faunal phylogenetic morphotypes of the Pebasian faunas as well as those represented in Acre (Table VI.3). This is further supported by the presence of the

new Iquitos gavialoid among Urumaco crocodylians (Chapter V). This astounding faunal composition suggests that Urumaco encompasses multiple environments, notably including Pebasian-like conditons (Salas-Gismondi et al., 2015a). Additionally, this suggests that conspicuous faunal elements of the Amazonian basin documented in the Acre vertebrate community were already roaming proto-Amazonia by the Middle Miocene times.

F. Conclusions

As other localities documenting Pebasian mesoeucrocodylian faunas, Fitzcarrald documents high phylogenetic and morphotype diversity. This fauna also allow us to recognize different ecological and environmental conditions coexisting within the Pebas Mega-Wetland System. Contrary to the coeval lacustrine faunal community of the Iquitos bonebeds, Fitzcarrald and La Venta represent the characteristic assemblages living of the Andean edge of the Pebas Mega-Wetland System. These assemblages, composed by sebecids, basal caimanines, giant caimanines (*Purussaurus*, *Mourasuchus*), and a gavialoid species with protruding eyes, might correspond to more riverine and continental conditions. Miocene proto-Amazonian ecosystems included archaic clades as well as most advanced caimanine lineages characteristic of living Amazonian biotas, hence an unparalleled specific diversity. The initial step to the depauperate Amazonian morphotype crocodylian diversity as documented today occurred at the end of the Pebas Mega-Wetland System, ca. 10 million years ago.

CHAPTER VII – CONCLUSIONS AND PERSPECTIVES

CHAPTER VII – CONCLUSIONS AND PERSPECTIVES

Mesoeucrocodylians from the Pebas Mega-Wetland System exemplify the extraordinary phylogenetic and ecological diversity having occurred within western proto-Amazonian ecosystems around 13 million years ago. These Miocene biotas included a variety of archaic and advanced clades with multiple snout morphotypes, emphasizing the role proto-Amazonian ecosystems played in fostering the persistence of basal lineages simultaneously with the origin and initial diversification of their modern relatives. Therefore, evidence suggests that major evolutionary processes regarding the adaptive radiation of mesoeucrocodylians and living Neotropical caimans have preceded the onset of transcontinental Amazonian River System.

Bonebeds of the Iquitos area documents both the highest taxonomic diversity and the widest range of snout morphotypes ever recorded in any crocodyliform community, recent or extinct. The hyperdiverse Iquitos assemblage comprises six caimanines (*Gnatusuchus pebasensis*, *Kuttanacaiman iquitosensis*, *Caiman wannlangstoni*, *Paleosuchus* sp., *Purussaurus neivensis*, and *Mourasuchus atopus*) and one gavialoid (*Gryposuchus* nov. sp.). Five among them are new taxa documenting the endemic Pebasian crocodylian fauna of the long-lived proto-Amazonian lakes that occupied most of western Amazonia during the Middle Miocene. Indeed, results indicate that multiple environmental conditions coexisted within the Pebas Mega-Wetland System, producing ecological isolation and favoring the existence of high snout morphotype disparity. As snout morphotypes are associated with feeding strategies and ecologies, this remarkable proto-Amazonian diversity reflects the combined influences of long-term evolution, resource abundance and variety, and niche partitioning in a complex ecosystem.

Gnatusuchus pebasensis, *Kuttanacaiman iquitosensis*, and *Caiman wannlangstoni* were small blunt-snouted caimanines, bearing robust jaws and conspicuous posterior globular

dentition, which inhabited the dysoxic lakes and swamps of the Pebas Mega-Wetland System. This array of crushing-toothed caimans predominantly fed on the abundant and diversified endemic molluscs that florished in the lacustrine settings during this time interval. Among them, the distinctive craniomandibular and dental anatomy of *Gnatusuchus pebasensis* indicate that this caiman was unique among crocodyliforms in having a malacophagous diet via head burrowing within swampy muddy bottoms. *Gnatusuchus* likely fed on infaunal *Pachydon* bivalves by "shoveling" with its jaw and procumbent anterior teeth, then crushing shells with the globular, tightly packed posterior teeth.

Considering the long-lasting conditions of the proto-Amazonian paleoenvironments, the crushing-dentition caimanines and the endemic species of molluscs acquired durophagous feeding strategies and distinct anti-predatory features, respectively. Ultimately, this reciprocal effect gave rise to the trophically distinct, lacustrine Pebasian ecosystem. The high predation intensity observed in the molluscan shells and the worn-to-flat teeth are lively marks of these quotidian interactions. The phylogenetic analysis positions *Gnatusuchus* as the most basal caiman, depicting blunt-snouted rostrum with crushing dentition as the ancestral condition for the entire clade, while the more "generalized" morphology of the living caimans should be derived. This distinctive blunt snout morphotype with crushing dentition of basal caimanines, such as *Gnatusuchus* and *Globidentosuchus*, is closer to that of Cretaceous alligatoroids. Possibly, globidontan-molluscan contends are part of a longer history datable back to the Paleocene epoch of the Great Plains of North America (Fig. VII.1). Accordingly, posterior globular teeth of the new crushing-dentition taxon *Caiman wannlangstoni* would have evolved from a generalized dental pattern seen on living relatives.

The only long-snouted crocodylian documented at several localities of the Pebas Formation of the Iquitos area represents the oldest gavialoid record in the Amazonian basin thus far. Remains belonging to this new taxon were consistently recovered from the typical

lacustrine deposits of the Pebas System. The general configuration of the circumorbital cranial region in *Gryposuchus* nov. sp. is intermediate in morphology between the fully "telescoped" riverine modern gharial *Gavialis gangeticus* and those gharials found in coastal marine paleoenvironments, such as *Piscogavialis* and *Argochampsa*. The phylogenetic analysis depicts independent, parallel evolution of the fully "telescoped" orbit condition of *Gavialis* in India and *Gryposuchus colombianus* or *Gryposuchus croizati* in South America. In the light of the phylogenetic analysis, South American gharials with a fluvial habitus have derived from ancestral lacustrine-deltaic forms with incipient development of protruding eyes or telescoped orbits; therefore *Gryposuchus* nov. sp. typifies an ancestral morphology. The evolution of the fully "telescoped" orbits or protruding eyes is correlated with visually enhanced feeding strategies in riverine environments. Such an anatomical-ecological association should be tested in other longirostrine archosaurs with tubular, long and slender snouts.

The clade of South American gharials, namely Gryposuchinae, was recovered only after removing features of the circumorbital region regarded as highly homoplastic. The monophyly of gryposuchines implies that all South American species known so far might result from a single transoceanic dispersal. The high taxonomic and ecological diversity of South American gharials depict a long-term evolution within the continent, predicting an early Tertiary arrival for the clade. To date, the fragmentary condition of the type and only specimen of the Caribbean taxon *Aktiogavialis* is not evidence for its affinities to gryposuchines.

The mesoeucrocodylian fauna from Fitzcarrald includes deep-snouted sebecids (*Sebecus* and *Barinasuchus*), a *Gryposuchus* species with protruding eyes (*Gr. colombianus*), and the caimanines *Purussaurus*, *Mourasuchus*, *Paleosuchus*, and *Eocaiman*.

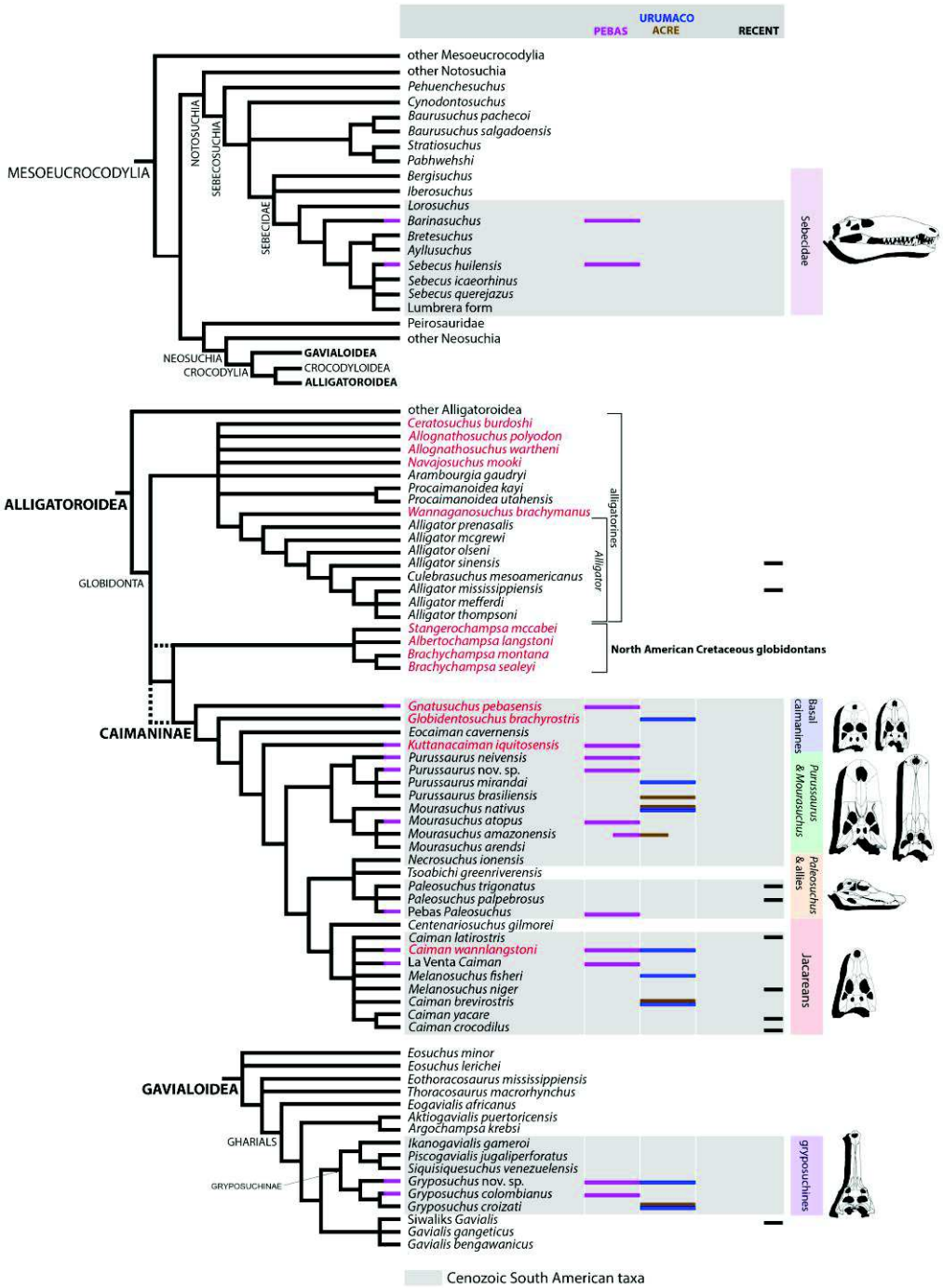

Figure VII.1. Phylogenetic relationships of South American mesoeucrocodylians and the occurrence of snout morphotypes in the Middle Miocene Pebas and Late Miocene Urumaco and Acre localities.

This fauna also allows us to recognize different ecological and environmental conditions coexisting within the Pebas Mega-Wetland System; contrary to the coeval lacustrine faunal community of the Iquitos bonebeds, Fitzcarrald and La Venta represent the characteristic assemblages having lived at the Andean edge of the Pebas Mega-Wetland

System. These two fluvially-dominated local faunas document the latest record of the long-lasting sebecid clade. Basal caimanine lineages with *Eocaiman* affinities roamed in proto-Amazonia until the late Middle Miocene, just before the initial establishment of the Amazonian drainage system. During the Late Miocene, basal caimanines exclusively survived in the Paleo-Orinoco basin; small to medium-sized caimans in Acre are restricted to advanced jacarean caimanines. *Balanerodus* is regarded as a junior synonym of *Purussaurus* species. *Gryposuchus colombianus* seems to be confined to the Middle Miocene interval and to riverine paleoenvironments. At least two notably different *Purussaurus* species inhabited proto-Amazonia, one of them bearing giant size and a complex external naris. Thus, striking giant size and complex narial region characteristic of Late Miocene species was already acquired during proto-Amazonian times. Although not conclusive, *Culebrasuchus mesoamericanus* is best seen as an *Alligator* species.

Evidence underlines the occurrence of a key ecological turnover in western Amazonia during the earliest Late Miocene (~10.5 Mya), providing new insights on establishment of modern ecosystems. A major Andean uplift episode recorded by that time not only fostered the origin of the transcontinental flow of the modern Amazon River, but also contributed to the retreat the Pebasian System to northernmost South America (Fig. VII.2). The record of *Caiman wannlangstoni* and *Gryposuchus* nov. sp. at Urumaco adds evidence for the persistence of Pebasian aquatic conditions during the Late Miocene in northernmost South America, where the lower course of the proto-Amazonian System drainage was formerly situated (Hoorn et al., 2010b). The demise of the Pebas Mega-Wetland System promoted diversification, increase in size, and specialization in gharials. Late Miocene Urumaco assemblages of the Paleo-Orinoco basin condense most faunal phylogenetic morphotypes of the older Pebasian community as well as those of the coeval Amazonian faunas represented in Acre. In the Amazon basin, the end of the Pebas Mega-Wetland System notably resulted in

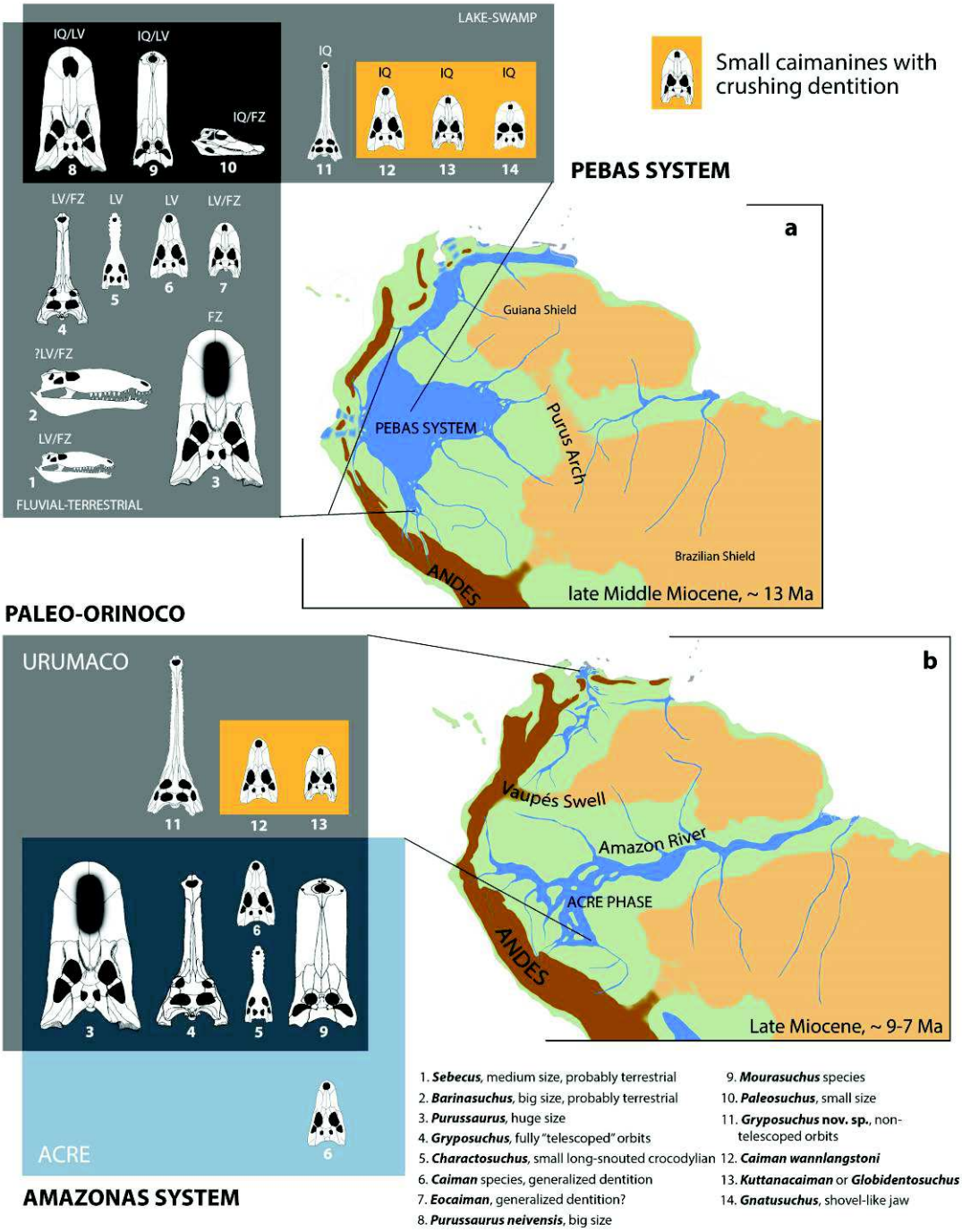

Figure VII.2 Crocodylian diversity prior to and after the Middle-Late Miocene Amazonian ecological turnover. (*a*) The climactic Pebas Mega-Wetland System in northwestern South America during MZ8 (ca. 13 Ma). Pebas crocodylians are from lake-swamp (Iquitos: IQ) and fluvial-terrestrial (Fitzcarrald: FZ; La Venta: LV) paleoenvironments. (*b*) The Paleo-Urumaco and Amazonian Acre Phase (ca. 9 Ma) after intense Andean uplift, establishment of the Vaupés Swell, and onset of the transcontinental Amazon River System. Shared taxa are located in the darker gray areas. Palaeogeographic reconstructions based on Hoorn et al. (2010a, 2010b) and Figueiredo et al. (2010).

the reduction of phylogenetic and morphotype mesoeucrocodylian diversity. Events occurring at after the Middle-Late Miocene transition favored fluvial faunas, including the initial

replacement of more archaic, dietarily-specialized crocodylians by the more generalist-feeding caimans that dominate modern Amazonian ecosystems.

This research has allowed me to explore not only the conspicuous evolution of mesoeucrocodylians in the Neotropics but also the potentialities of these largely diversified groups for inferring paleoenvironmental conditions and hypothesizing paleogeographical reconstructions (Fig. VII.2). These archosaurs occupied multiple ecological niches in aquatic and possibly terrestrial habitats throughout the Cenozoic. These cold-blooded organisms were particularly susceptible to environmental changes, such as temperature fluctuations, basin features, the dynamics of aquatic settings, mountain building, long-term droughts, marine incursions, or food resource fluctuation. Therefore, mesoeucrocodylian anatomy and distribution are good proxies for reconstructing defining events of the landscape evolution. To date, most studies have been focused in the cranio-mandibular-dental elements since these skeletal structures seem to concentrate most of the morphological disparities within mesoeucrocodylians. However, postcranial anatomy is poorly known to *a priori* discard its discriminant ecological value. For example, recent studies on the axial and appendicular skeleton of sebecids have provided further evidence for their terrestrial habitus (Pol et al., 2012).

Decidedly, before starting to use mesoeucrocodylians as environmental proxies, it is essential to have a better understanding of their phylogenetic relationships and ecologies, a real challenge considering that most clades and morphotypes are exclusively known from the scarce fossil record. Some of the questions that remain unresolved are for example, how are the relationships between Cretaceous globidontans, alligatorines, and caimanines? Our phylogenetic analyses show no resolution on this topic, but predict the existence of crushing-caimanines throughout the Cenozoic. Were they restricted to the tropical areas of South America during all this time frame? Do the caimanine clade itself originated in South

America? Considering the record of caimanines in the Eocene of North America (Brochu, 2010), no conclusive answer can be reached yet.

Current knowledge of the phylogenetic relationships of several groups of mesoeucrocodylians is based on weak character support or show contradictory affinities due to the inclusion or exclusion of key taxa (Wilberg, 2015). This is the case for gavialoid relationships, probably due to the rearrangement of cranial bones associated with longirostry. Fundamental pieces of evidence for recognizing phylogenetic relationships and patterns of adaptive radiation of the group might be found in South America. Recent discoveries of South American gavialoid remains in Paleogene rocks of Peru will give new clues about early gavialoid evolution. During the Neogene, the highest diversity of gharials occurred in northernmost South American locality of Urumaco, in close proximity to the Caribbean Sea (Sánchez-Villagra & Aguilera, 2006). This site records gharials with different snout length proportions, alveolar pattern, and circumorbital configuration. Considering predictions of our circumorbital morphospace analysis, these dissimilar morphologies might represent the existence of multiple habitats and ingroup feeding specializations.

Current record of mesoeucrocodylians of the Pebas Mega-Wetland System is restricted to the late Middle Miocene, when this distinctive biome reached its peak in size and complexity. But, how did all this amazing history start? How was the anatomy of *Gnatusuchus* (Fig. VII.3) at the origin of the defining features of the Pebas System? How was the composition of the mesoeucocodylian community? We might have some opportunities to assess this fascinating topic thanks to the currently unexplored, earliest lignite levels of the Pebas Formation located in far-off northern tributaries of the Amazon River (Wesselingh et al., 2006a) and in the early-middle Miocene Pebasian deposits recently unveiled near Contamana in eastern Peru (Antoine et al., submitted). The original faunal composition of the

Pebas System is primordial to have a more comprehensive view of the evolution of diversity in western Amazonia.

Figure VII.3. Life reconstruction of the shovel-like jaw, head-burrower caiman *Gnatusuchus pebasensis*. Model by Kevin Montalván-Rivera.

The Pebas Mega-Wetland System was connected with the Caribbean Sea by an aquatic pathway for most of the Paleogene and the early Neogene. The impact of this long-

lasting communication needs to be further explored, considering the large debate regarding the origin of Caribbean island biotas and the marine-fresh water transition of several groups living in the modern Amazonian basin (Iturralde-Vinent & MacPhee, 1999; Wesselingh & Salo, 2006). Little is known about the mesoeucrocodylian faunas during this time frame in the Caribbean Portal. What was the level of biotic integration between the Caribbean and the proto-Amazonian domains? Tidally- and wave-influenced deposits document marine incursions from the Caribbean that affected episodically the peculiar Pebasian conditions through most of the Miocene (Hovikoski et al., 2010; Boonstra et al., 2015). Were aquatic environments ecologically unified between these biomes during marine incursions? Are there clues of an early "Great American Biotic Interchange" in Neotropical mesoeucrocodilyan communities? We know that advanced caimans were present during the early-middle Miocene of Panama (Hastings et al., 2013). No matter which biogeographic history we prefer, a sea barrier between Panama and northwestern South America was still present at that time. Thus, did continuous marine incursions in the proto-Amazonian aquatic environments favored the development of osmoregulatory capabilities of caimans?

The snout morphotypes of mesoeucrocodylians might even offer more information than usually regarded. But, how to decipher the ecologies of fossil mesoeucrocodylians without extant relatives? For example, how to assess the ecology and feeding strategies of the distinct caiman *Mourasuchus*? We need to perform new integrative morphometric-phylogenetic analyses and probably carefully look for ecological analogous in distantly related taxa. For instance, innovative approaches revealed parallel evolutionary trajectories in the morphology of the feeding apparatus of giant suspensory fishes and cetaceans (Friedman, 2011). There might be few anatomical solutions for a precise ecology (Borchu, 2001). The time has come to work it out!

CHAPTER VIII – RÉSUMÉ ÉTENDU / EXTENDED ABSTRACT / RESUMEN EXTENDIDO

CHAPTER VIII – RÉSUMÉ ÉTENDU / EXTENDED ABSTRACT / RESUMEN EXTENDIDO

RÉSUMÉ ÉTENDU

Notamment sous l'influence des Andes, des conditions environnementales particulièrement favorables existent aujourd'hui en Amazonie occidentale, qui ont permis le développement d'une biodiversité inégalée à l'échelle des Néotropiques (Hoorn et al., 2010b). Il est probable que de telles interactions (géologie-climat-biocénoses) aient également prévalu dans le passé, mais le caractère très lacunaire du registre fossile à proximité des Andes, et en particulier dans le temps profond, a longtemps empêché de le vérifier. Toutefois, le Miocène semble être une période clé pour l'émergence des écosystèmes amazoniens modernes : une phase majeure de la surrection andine a en effet remodelé les paysages du bassin d'avant-pays et déclenché la mise en place du drainage transcontinental actuel de l'Amazone, il y a environ 10,5 millions d'années (Ma; Figueiredo et al., 2010). Acquérir une meilleure connaissance des biomes proto-amazoniens immédiatement antérieurs à cet épisode apparaît donc crucial pour mieux caractériser les origines de la biodiversité néotropicale. Malheureusement, le registre fossile était jusqu'alors extraordinairement restreint, en particulier pour ce qui est des vertébrés. Le présent volume a pour objet de dépeindre une instantanée de la vie florissante de la proto-Amazonie occidentale, en étudiant l'évolution, l'écologie et la biogéographie des mésoeucrocodiliens fossiles (sébécidés, gavials et caïmaninés) découverts dans de nouvelles localités très riches d'Amazonie occidentale, à l'est du Pérou. Ces communautés de mésoeucrocodiliens vivaient dans le Méga-système Pebas (« *Pebas Mega-Wetland System* »), un immense domaine constitué d'une complexe mosaïque d'environnements aquatiques documenté pendant la majeure partie du Miocène (Wesselingh et al., 2002). Ces

environnements aquatiques avaient la particularité d'être connectés par intermittence à la Mer Caraïbe par l'intermédiaire d'un drainage méridien (Sud-Nord) au pied des Andes (Hoorn et al., 2010a, 2010b). Les environnements sédimentaires correspondants, très singuliers, coïncident avec des fonds de lacs et marécages dysoxiques et boueux (Wesselingh et al., 2002, 2006a). L'ampleur exceptionnelle de la radiation adaptative des mésoeucrocodiliens dans les écosystèmes proto-amazoniens de l'époque (Langston 1965 ; Salas-Gismondi et al., 2015a) offre une occasion inespérée pour explorer les modalités de diversification et l'histoire évolutive d'un clade néotropical.

Les mésoeucrocodiliens des paléoenvironnements lacustres

Dans la région d'Iquitos, les gisements du Miocène moyen sont rapportés à la Formation Pebas/Solimões. Le contexte temporel de cette formation est contraint par biostratigraphie, grâce au pollen (Hoorn, 1993), aux ostracodes (Muñoz-Torres et al., 2006) et aux mollusques, abondants et diversifiés pendant toute la période considérée (cochliopinés et pachyodontinés ; Wesselingh et al., 2006a). Les mésoeucrocodiliens sont seulement représentés par des espèces appartenant au groupe apical (Crocodylia). Les restes correspondants, principalement mis au jour dans des chenaux ligniteux (« *bonebeds* ») datés d'environ 13 Ma (fin du Miocène moyen), constituent la faune crocodilienne typique des lacs et marécages dysoxiques du Méga-système Pebas (Salas-Gismondi et al., 2015a). L'assemblage en question est extraordinaire en ce qu'il représente à la fois la plus grande diversité taxonomique (jusqu'à sept espèces associées) et la plus grande variété de morphotypes du rostre connues pour une communauté donnée de crocodyliformes (actuels-fossiles). L'hétérogénéité des formes de rostre dans les localités de la région d'Iquitos recouvre la majeure partie du morpho-espace connu pour le clade des crocodyliformes dans son ensemble. Cette hyperdiversité reflète les influences conjointes d'une évolution à long

terme, d'une grande abondance/variété de ressources alimentaires, et d'une ségrégation de niches dans un écosystème complexe et plutôt stable, sans équivalent actuel à l'échelle du globe. Outre les caïmans géants *Purussaurus neivensis* et *Mourasuchus atopus*, tous les autres crocodiliens d'Iquitos sont des taxons nouveaux et de taille réduite, parmi lesquels un caïman basal—*Gnatusuchus pebasensis*—possédant une mandibule massive en forme de pelle, des dents antérieures proclives et postérieures globuleuses et un diastème à la façon des mammifères. La symphyse mandibulaire est de loin la plus longue à l'échelle des alligatoroïdes, et elle inclut les os dentaires et spléniaux. La présence de crêtes puissantes sur l'os latérosphénoïde et celle d'une crête B en forme de bouton sur l'os carré témoignent d'une grande puissance des muscles adducteurs. Cette anatomie dentaire et crânio-mandibulaire unique est compatible avec un régime alimentaire durophage, avec une quête de nourriture par fouissage de la tête dans les sédiments. *Gnatusuchus* se nourrissait probablement de bivalves pachydontinés endobenthiques en « pelletant » le fond meuble des marécages dysoxiques avec la mâchoire et les dents antérieures proclives, puis en brisant les coquilles avec les dents postérieures globuleuses et resserrées. Les mêmes dépôts fossilifères incluent deux autres caïmans putativement malacophages, avec des museaux courts et plats et des dents globuleuses, *Kuttanacaiman iquitosensis* et *Caiman wannlangstoni*. Cette radiation de petits caïmans à dents globuleuses témoigne de stratégies alimentaires coïncidant avec un pic dans l'abondance et la diversité des mollusques aquatiques en Amazonie occidentale, en plein coeur du Méga-système Pebas. La forte pression de prédation observée sur les coquilles de mollusques et l'extrême usure de nombreuses dents globuleuses des individus de *Gnatusuchus* témoignent de telles interactions quotidiennes. Par ailleurs, plusieurs maxillaires isolés et un dentaire attestent de la présence d'un proche parent du caïman gris (*Paleosuchus*) dans ces niveaux lacustres miocènes. Finalement, cette faune d'Iquitos inclut au moins un représentant de tous les clades couramment reconnus au sein des caïmaninés, soulignant en

cela la particularité du Méga-système Pebas, au sein duquel coexistaient les derniers survivants des clades basaux, en association avec les premiers représentants des taxons actuels. Une analyse phylogénétique fondée sur des données morpho-anatomiques place *Gnatusuchus* en position de groupe-frère de tous les autres caïmans, suggérant qu'un museau court et plat avec une denture globuleuse pourrait avoir été le morphotype ancestral du clade, cependant que la morphologie plus « généraliste » du groupe apical des caïmans serait alors dérivée. *Gryposuchus* nov. sp. est à la fois le seul crocodilien longirostre et non-caïmaniné de cette communauté et le gavialoïde le plus basal connu en Amazonie. Cette nouvelle espèce apporte des informations cruciales pour reconstituer de manière argumentée l'anatomie et l'écologie ancestrales du clade des Gavialoidea. *Gryposuchus* nov. sp. diffère des autres représentants de *Gryposuchus* par le faible télescopage des orbites. Les résultats de l'analyse de parcimonie réalisée à l'échelle des gavialoïdes indiquent que le télescopage, beaucoup plus marqué chez des gavials divergeant plus tardivement, comme *Gryposuchus colombianus* et *Gryposuchus croizati*, est un trait dérivé. L'inclusion de cette nouvelle espèce dans des analyses phylogénétiques-morphométriques suggère que l'apparition de patrons similaires chez les gavialoïdes d'Amérique du Sud et d'Inde résulte de phénomènes de convergence liés à des adaptations au milieu fluviatile. Par conséquent, il semblerait que le patron circumorbitaire télescopé et la longirostrie soient des traits hautement labiles, qui reflèteraient des préférences écologiques et des stratégies alimentaires analogues plutôt qu'une parenté entre les gavialoïdes de l'Ancien et du Nouveau Mondes. Les résultats viennent à l'appui d'une radiation précoce et explosive des formes sud-américaines, avec des taxons occupant les antipodes du morpho-espace des gavialoïdes et montrant des préférences pour des environnements marins côtiers ou purement fluviatiles. L'histoire biogéographique ancienne des gavialoïdes sud-américains apparaît de ce fait comme ayant été étroitement liée au

drainage méridien (Sud-Nord) du Méga-système Pebas, qui connectait les zones humides proto-amazoniennes à celles du domaine caraïbe (Venezuela et Colombie).

Les mésoeucrocodiliens des paléoenvironnements fluviatiles

Situées à la périphérie du biome pébasien et contemporaines des assemblages d'Iquitos, les localités de l'Arche de Fitzcarrald (13-12 Ma) correspondent à une influence plus marquée des Andes, en termes d'environnements. Les gisements de la faune locale de Fitzcarrald sont situés dans le Département d'Ucayali et correspondent à des dépôts conglomératiques de tempête, dans des milieux fluviatiles sous l'influence de marées, à la marge du Méga-système Pebas. A l'instar de la faune de La Venta (fin du Miocène moyen ; Colombie) qui lui est contemporaine, cette communauté de crocodiliens inclut à la fois les derniers représentants des sébécidés (Sebecosuchia) au crâne comprimé latéralement et un gavialoïde dérivé aux yeux proéminents. Cette association particulière suggère la prédominance des milieux terrestres et fluviatiles dans la région à l'époque. Ces faunes présentent très peu de similitudes avec la communauté lacustre d'Iquitos, que ce soit en termes de taxonomie ou pour ce qui est des morphotypes du rostre. Cependant que les caïmaninés à dents globuleuses dominaient la faune d'Iquitos, aucun indice de leur présence n'est attesté à ce jour à Fitzcarrald ou à La Venta. Le registre fossile disponible laisse donc supposer que des conditions écologiques et environnementales très distinctes coexistaient dans le Méga-système Pebas, en tout cas à son apogée (fin du Miocène moyen). Une nouvelle espèce de *Purussaurus* est décrite, sur la base de la « mandibule géante » découverte par Matthiessen (1961) dans l'Arche de Fitzcarrald. L'anatomie de cette espèce indique une origine proto-amazonienne pour le clade incluant les formes géantes de *Purussaurus*. En définitive, le Méga-système Pebas a vu coexister les derniers représentants des caïmaninés basaux de type *Eocaiman* et les premiers représentants du caïman actuel *Paleosuchus*, que ce

soit à Iquitos ou à Fitzcarrald.

Le déclin du Méga-système Pebas

Tous les indices concordent à souligner l'importance du bouleversement écologique enregistré au début du Miocène supérieur, il y a environ 10,5 millions d'années. Cela est en particulier documenté par la faune de crocodiliens mise au jour à Nueva Unión, au sud d'Iquitos. Cet assemblage fournit de nouveaux éléments cruciaux, permettant de mieux caractériser les modalités de mise en place des écosystèmes ouest-amazoniens actuels. Si les affleurements pauvres en matière organique du sommet de la Formation Pebas à Nueva Unión (base du Miocène supérieur) ont bien livré les spécimens les plus récents de *Gnatusuchus*, ils ne contiennent en revanche aucun autre caïman à dents globuleuses. A l'instar des faunes fluvio-tidales du Miocène supérieur plus tardif de l'Acre (Brésil ; « Phase Acre », environ 8 millions d'années), Nueva Unión inclut des représentants géants de *Purussaurus* et de *Mourasuchus*. Ces deux localités livrent également un gavialoïde aux orbites complètement télescopées. Les données géologiques et paléontologiques de Nueva Unión suggèrent que des changements environnementaux cruciaux sont intervenus à l'échelle du bassin d'avant-pays, en réponse à un épisode majeur de surrection andine enregistré à l'époque (Hoorn et al., 2010b). Cette activité tectonique a non seulement engendré la mise en place du drainage transcontinental moderne de l'Amazone (Ouest-Est), mais aussi contribué au retrait du Méga-système Pebas vers les zones les plus septentrionales de l'Amérique du Sud (Salas-Gismondi et al., 2015a). Les faunes hautement endémiques d'Iquitos se sont développées au sein des lacs et marécages du Méga-système Pebas entre la fin du Miocène inférieur et le début du Miocène supérieur. Elles ont ensuite décliné avec l'émergence du drainage amazonien moderne, qui a par ailleurs favorisé la diversification des crocodiliens longirostres et des caïmans généralistes actuels. La présence de *Caiman wannlangstoni* et de *Gryposuchus* nov.

sp., deux espèces décrites dans le Miocène moyen d'Iquitos, dans la faune d'Urumaco (Venezuela, Miocène supérieur), confirme la persistance de conditions environnementales « pébasiennes » pendant la « Phase Acre » dans l'extrême Nord de l'Amérique du Sud, là même où l'embouchure du système de drainage proto-amazonien était située jusqu'alors (Hoorn et al., 2010b). Les assemblages crocodiliens d'Urumaco, attribués au « Paléo-Orénoque », rassemblent la majeure partie des morphotypes et des clades représentés dans les faunes contemporaines de l'Acre (environ 8 millions d'années) et les derniers représentants des communautés « pébasiennes », plus anciennes. La fin du Méga-système Pebas a en particulier eu pour conséquence la réduction dramatique de la diversité phylogénétique et morphotypique des mésoeucrocodiliens proto-amazoniens, préfigurant en cela les faunes crocodiliennes modernes d'Amazonie. Plus généralement, l'essor, la persistance, puis le déclin de ces écosystèmes aquatiques miocènes à forte productivité et sans équivalent actuel ont laissé une empreinte durable – et encore perceptible – sur la biodiversité amazonienne.

RESUMEN EXTENDIDO

Bajo el influyente dominio de las montañas Andinas, se originaron condiciones ambientales muy peculiares en la Amazonía occidental que decididamente condujeron al desarrollo de mayor biodiversidad en esta región que en el resto del Neotrópico (Hoorn et al., 2010b). Aunque la íntima interrelación entre componentes bióticos y geológicos debe haber producido fenómenos similares en el pasado, nuestro conocimiento sobre la evolución ocurrida próxima a los Andes tropicales durante sus millones de años de sostenido crecimiento es poco conocida. Un intervalo temporal de gran trascendencia para el origen de los ecosistemas Amazónicos modernos se produjo durante la época Mioceno, cuando el crecimiento de las montañas Andinas remodeló el paisaje de la cuenca de antepaís y propició el establecimiento inicial del Sistema del Río Amazonas, hace aproximadamente unos 10.5 millones de años (Ma; Figueiredo et al., 2010). Las biotas proto-Amazónicas justo antes de este episodio son sustanciales para entender los orígenes de la biodiversidad Neotropical; sin embargo, la evidencia fósil, principalmente de vertebrados, ha sido muy escasa hasta ahora. Esta investigación está dedicada a brindar una mirada a la floreciente vida del Mioceno en la proto-Amazonía occidental a través del estudio de la evolución, ecología y biogeografía de los mesoeucocodrilos fósiles (sebécidos, gaviales y caimanes) registrados en nuevas localidades paleontológicas del oriente peruano. Estas comunidades de mesoeucocodrilos habitaron el Sistema de Mega-Humedales Pebas, un enorme y duradero bioma que estuvo constituido por un complejo mosaico de ambientes acuáticos (Wesselingh et al., 2002). Una de las características más destacables de este bioma era su conexión con el Mar Caribe mediante un drenaje que corría de sur a norte (Hoorn et al., 2010a, 2010b). Los característicos depósitos sedimentarios del Sistema Pebas representan lagos y pantanos de poca profundidad de fondos fangosos y con poco oxígeno (Wesselingh et al., 2002, 2006a). Considerando que los

mesoeucocodrilos alcanzaron un enorme radiación adaptativa en estos ecosistemas proto-Amazónicos (Langston, 1965, Salas-Gismondi et al,, 2015), ellos ofrecen la oportunidad de explorar los patrones de la ecología evolutiva y diversificación que se produjo en el Neotrópico Sudamericano.

Los Mesoeucrocodylia de los paleo-ambientes lacustres

En el área de Iquitos, los sitios fosilíferos pertenecientes al Mioceno medio pertenecen a la Formación Pebas/Solimões. El contexto bioestratigráfico de esta formación está basado en la evidencia palinológica, en los ostrácodos, y particularmente en la abundancia y diversidad faunística de moluscos (Cochliopinae y Pachydontinae) preservados en todos los niveles de la unidad (Hoorn, 1993; Muñoz-Torres et al., 2006; Wesselingh et al., 2006a). Los fósiles de mesoeucocodrilos pertenecen únicamente al grupo corona (i.e., Crocodylia) y han sido descubiertos en niveles de lignita pletóricos en huesos (capas osíferas) que datan de unos 13 Ma (parte tardía del Mioceno medio). Ellos caracterizan la fauna de los lagos y pantanos con poco oxígeno que predominaron durante el Sistema de Mega-Humedales Pebas (Salas-Gismondi et al., 2015a). El ensamble de cocodrilos de las capas osíferas de Iquitos es extraordinario por representar tanto la más alta biodiversidad taxonómica (con siete especies encontradas en la misma localidad) y el más amplio rango de morfotipos rostrales jamás registrado en cualquier comunidad de Crocodryliformes, viviente o extinta. La heterogeneidad de las formas rostrales documentada en las localidades miocénicas del Perú abarca casi la totalidad del morfo-espacio conocido para todo el clado, reflejando así las influencias combinadas de una evolución prolongada, variedad y abundancia de recursos y, además partición de nichos en un complejo sistema ecológico sin equivalente moderno. Fuera de los grandes caimanes *Purussaurus neivensis* y *Mourasuchus atopus*, todos los otros Crocodylia son taxones nuevos para la ciencia, incluyendo un caiman basal –*Gnatusuchus pebasensis*– que posee una mandíbula muy robusta con forma de pala, dientes anteriores procumbentes y

posteriores globulares, y un espacio sin dientes (diastema) similar al que poseen algunos mamíferos. La sínfisis mandibular es de lejos la más larga entre los Alligatoroidea e incluye tanto el hueso dentario como el esplenial. Los lateroesfenoides masivos y la cresta B del hueso cuadrado con una protuberancia en forma de ampolla son indicadores de que *Gnatusuchus* poseía músculos aductores proporcionalmente mayores que los de otros cocodrilos. Esta distintiva anatomía dentaria y craneomandibular es consistente con una dieta durófaga y hábitos excavadores durante la búsqueda de alimento que involucraban el uso activo de la cabeza. *Gnatusuchus* probablemente se alimentaba de bivalvos paquidontinos infaunales "paleando" con sus mandíbulas los fondos fangosos de los pantanos; luego trituraba las conchas con su batería de dientes globulares. Los mismos depósitos fosilíferos incluyen otros dos caimanes de presumibles hábitos malacófagos, con los característicos hocicos romos y dientes "trituradores", llamados *Kuttanacaiman iquitosensis* y *Caiman wannlangstoni*. Esta radiación de pequeños caimanes con dientes "trituradores" revela peculiares estrategias alimenticias y relacionadas con un pico en la abundancia y diversidad de moluscos acuáticos en el Sistema Pebas, en lo profundo de la proto-Amazonia. Dientes desgastados hasta el nivel de la raíz y conchas mostrando altos niveles de depredación son vívidas marcas de sus interacciones cotidianas. En estos ambientes lacustres, el caimán enano de frente lisa *Paleosuchus* está representado por varios huesos, entre maxilares y una porción de mandíbula. Esta composición faunística destaca la coexistencia de cada linaje filogenético de caimaninos conocido hasta la fecha, enfatizando el rol decisivo que jugaron estos humedales proto-Amazónicos en favorecer la supervivencia de clados basales de caimanes mientras se producía la diversificación inicial de sus parientes modernos. Los análisis filogenéticos basados en datos morfológicos ubican a *Gnatusuchus* como el más basal de los caimanes y sugieren que la morfología de rostro romo con dentición "trituradora" pudo haber sido la condición ancestral de todo el grupo, mientras que la morfología considerada más

generalista de los caimanes pertenecientes al grupo corona, es derivada. *Gryposuchus* nov. sp. difiere de otras especies de *Gryposuchus* por poseer orbitas oculares poco "telescopadas" (i.e., huesos circumorbitarios solo levemente proyectados dorsalmente). Basado en las transformaciones del estado ancestral reveladas por el análisis filogenético de máxima parsimonia, esta condición ha sido interpretada como incipiente relativa al marcado "telescopaje" orbital propio de sus parientes que habrían evolucionado posteriormente, como *Gryposuchus colombianus* y *Gryposuchus croizati*. Al incluir esta nueva especie en análisis filogenéticos y morfométricos, los resultados sugieren que la similitud de los patrones rostrales de gavialoides sudamericanos e indios fue consecuencia de procesos evolutivos paralelos e independientes en hábitats fluviales de Sudamérica e India, respectivamente. Como consecuencia, es probable que en asociación con la tenencia de un rostro largo y delgado (i.e., longirrostría), la configuración circumorbitaria sea altamente plástica en términos evolutivos y como tal, podría reflejar preferencias de hábitat y estrategias de alimentación. Los resultados sustentan una radiación de larga data y a gran escala para los gaviales sudamericanos, los cuales ocupan ambos extremos del morfo-espacio del clado Gavialoidea con formas que indican preferencias por ambientes marinos en un extremo y fluviales en el otro. La biogeografía histórica de los gavialoides en Sudamérica desde sus estadios más tempranos estuvo fuertemente ligada al sistema de drenaje sur-norte que conectaba los humedales proto-Amazónicos con el Caribe.

Los Mesoeucrocodylia de los paleo-ambientes con influencia fluvial

La localidades de Iquitos y Fitzcarrald representan paleoambientes contemporáneos dentro del mismo gran Sistema Pebas (parte tardía del Mioceno medio), con Fitzcarrald situado más próximo a la influencia Andina. Las capas fosilíferas del Arco de Fitzcarrald están ubicadas en el Departamento de Ucayali y corresponden a depósitos conglomeráticos de tormentas, en ambientes con influencia fluvial y de mareas. Tal como en el caso de la

localidad de La Venta, la comunidad de mesoeucrocodylia en Fitzcarrald es altamente heterogénea y documenta (además de varios caimaninos) los más recientes representantes entre los sebécidos y una especie de gavial con órbitas oculares fuertemente proyectadas dorsalmente, reafirmando la presencia tanto de ambientes terrestres como fluviales. Estas faunas (i.e., Fitzcarrald y La Venta) muestran pocas similitudes taxonómicas y de morfotipos filogenéticos (basados en el rostro) con las faunas lacustres de las capas osíferas de Iquitos. Mientras que en Iquitos la comunidad estaba dominada por caimanes "trituradores", en La Venta y Fitzcarrald por el momento éstos no han sido identificados plenamente. La evidencia supone la existencia de diferentes condiciones ecológicas y ambientales dentro mismo Sistema de Mega-Humedales Pebas. En base a la "mandíbula gigante" descubierta por Matthiessen (1961) en la Quebrada Grasa del Arco de Fitzcarrald, se propone una nueva especie de *Purussaurus*. La anatomía de esta especie indica que el clado formado por formas gigantes del taxón *Purussaurus* se originaron en proto-Amazonia. En localidades del Sistema Pebas (Iquitos y Fitzcarrald), se produce el último registro de caimanes emparentados con *Eocaiman* de la región Amazónica y la primera aparición como fósil del caimán enano *Paleosuchus*.

El comienzo del final del Sistema de Mega-Humedales Pebas

La evidencia disponible destaca la existencia de un cambio ecológico en la Amazonia occidental durante la fase temprana del Mioceno tardío (~10.5 Ma), como lo indica la localidad de Nueva Unión al sur de Iquitos pues documenta indicios sobre el establecimiento de los ecosistemas modernos. Los afloramientos rocosos pobres en lignita de la Formación "Pebas Superior" en Nueva Unión (inicio del Mioceno tardío) han brindado el registro más reciente de *Gnatusuchus*, pero hasta la fecha no contienen otros caimanes "trituradores". Como en las faunas del Mioceno tardío de Acre (Brazil; Fase fluvio-mareica Acre), en Nueva Unión los caimanes *Purussaurus* and *Mourasuchus* eran gigantes; el registro también incluye

un gavialoide con “telescopaje” orbitario. Los datos geológicos y paleontológicos sugieren cambios ambientales a nivel regional en Nueva Unión en coincidencia con un importante episodio de crecimiento Andino (Hoorn et al., 2010b). Esta actividad tectónica no solo propició el origen del flujo transcontinental del Río Amazonas, sino que también contribuyó a la retracción del Sistema Pebas hacia la parte más septentrional de Sudamérica (Salas-Gismondi et al., 2015a). Las faunas altamente endémicas de Iquitos evolucionaron en los pantanos y marismas con poco oxígeno del duradero Sistema de Mega-Humedales Pebas (Mioceno temprano al inicio del Mioceno tardío) y declinaron con el inicio del drenaje Amazónico moderno, favoreciendo la diversificación de cocodrilos longirrostros y de los linajes evolutivamente avanzados de caimanes con hábitos alimenticios generalistas. El registro de *Caiman wannlangstoni* y *Gryposuchus* nov. sp. en Urumaco añade pruebas a hipótesis sobre la persistencia de condiciones del tipo Pebas en los ambientes acuáticos del área más nórdica de Sudamérica durante el Mioceno tardío, en el lugar donde el curso bajo del drenaje proto-Amazónico estuvo situado previamente (Hoorn, 2010b). Ciertamente, los ensambles de cocodrilos de la cuenca del Paleo-Orinoco condensan tanto los morfotipos filogenéticos de las faunas Amazónicas representadas en Acre, así como la mayor parte de aquellos de las comunidades del Sistema Pebas que les precedieron. El fin del Sistema de Mega-Humedales Pebas resultó en una reducción notable de los morfotipos rostrales de mesoucocodrilos proto-Amazónicos, marcando el inicio de las faunas y ecosistemas Amazónicos modernos. El origen y final de estos distintivos biomas acuáticos, todos tremendamente productivos, influenciaron sustancialmente la evolución de la alta biodiversidad de cocodrilos y otros organismos durante todo el Neógeno.

EXTENDED ABSTRACT

Under the influential role of the Andean mountains, western Amazonia developed distinctive environmental conditions that ultimately led to divergent, higher biodiversity within the Neotropics (Hoorn et al., 2010b). Although this intimate geologic-biotic interaction might have produced similar phenomena in the past, our knowledge about the tropical biotic evolution occurring in close proximity to these rapid growing mountains is poorly documented in the deep time. A pivotal stage for the emergence of the modern Amazonian ecosystems occurred during the Miocene, when major Andean uplift remodeled the landscape of the foreland basin and fostered the onset of the Amazon River System, at about 10.5 million years ago (Ma; Figueiredo et al., 2010). Proto-Amazonian biotas just prior to this episode are integral to understanding origins of Neotropical biodiversity, yet vertebrate fossil evidence was extraordinarily rare thus far. This research is devoted to provide a snapshot of the flourishing Miocene life of western proto-Amazonia by studying the evolution, ecology, and biogeography of fossil mesoeucrocodylians (sebecids, gharials, and caimanines) documented in new rich paleontological sites of eastern Peru. These mesoeucrocodylian communities inhabited the Pebas Mega-Wetland System, a huge long-lasting biome constituted by a complex mosaic of aquatic environments (Wesselingh et al., 2002). As a prominent feature, the aquatic environments were connected to the Caribbean Sea through a drainage of northern flow (Hoorn et al., 2010a, 2010b). The distinctive Pebasian sedimentary deposits indicate that dysoxic muddy bottoms within shallow lakes and swamps were prevalent (Wesselingh et al., 2002, 2006a). Since mesoeucrocodylians underwent large adaptive radiations within proto-Amazonian ecosystems (Langston 1965; Salas-Gismondi et al., 2015a), they offer a unique opportunity to explore patterns of the evolutionary ecology and diversification in the Neotropics.

Mesoeucrocodylians of the lacustrine-dominated paleoenvironments

In the Iquitos area, Middle Miocene fossiliferous sites are attributed to the Pebas/Solimões Formation. The biostratigraphic framework of this formation is based on pollen, ostracods, and particularly on the abundant and diverse molluscan faunas (cochliopines and pachydontines) preserved throughout the entire unit (Hoorn, 1993; Muñoz-Torres et al., 2006; Wesselingh et al., 2006a). The mesoeucrocodylians are only represented by species of the crown group (Crocodylia) and were discovered mainly in lignitic bonebed levels of about 13 Ma (late Middle Miocene), depicting the peculiar fauna of the dysoxic lakes and swamps of the Pebas Mega-Wetland System (Salas-Gismondi et al., 2015a). The crocodylian assemblage of the Iquitos bonebeds is extraordinary in representing both the highest taxonomic diversity (with up to seven associated species) and the widest range of snout morphotypes ever recorded in any crocodyliform community, recent or extinct. The heterogeneity of snout shapes at the Peruvian Miocene localities covers most of the morphospace range known for the entire crocodyliform clade. This reflects the combined influences of long-term evolution, resource abundance and variety, and niche partitioning in a complex ecosystem, with no recent equivalent. Besides the large-bodied *Purussaurus neivensis* and *Mourasuchus atopus*, all other crocodylians in Iquitos are new taxa, including a stem caiman—*Gnatusuchus pebasensis*—bearing a massive shovel-shaped mandible, procumbent anterior and globular posterior teeth, and a mammal-like diastema. The mandibular symphysis is by far the longest among alligatoroids and includes the dentary and splenial bones. Thick-crested laterosphenoids and knob-like quadrate crest B depict comparatively larger adductor muscles. This distinctive dental and craniomandibular anatomy is consistent with a durophagous diet, as well as with head burrowing activity in search of prey. *Gnatusuchus* probably fed on infaunal pachydontine bivalves by ‘shoveling’ the swamp muddy bottoms with the jaw and the procumbent anterior teeth, then crushing shells with the globular, tightly packed posterior teeth. The same fossiliferous deposits include two other

putative malacophagous caimans bearing blunt snouts and crushing dentitions, namely *Kuttanacaiman iquitosensis* and *Caiman wannlangstoni*. This radiation of small caimans with crushing dentitions records peculiar feeding strategies correlated with a peak in aquatic proto-Amazonian molluscan diversity and abundance, deep in the Pebas Mega-Wetland System. The high predation intensity observed in the molluscan shells and the worn-to-flat teeth are lively marks of these quotidian interactions. Several isolated maxillae and one dentary record the presence of the extant smooth-fronted caiman *Paleosuchus* in these lacustrine settings. As a whole, this fauna highlights the co-occurrence of every phylogenetic lineage currently recognized within Caimaninae, emphasizing the role of these proto-Amazonian Mega-Wetlands played in fostering the persistence of basal lineages simultaneously with the initial diversification of their modern relatives. Phylogenetic analysis of a morphological dataset positions *Gnatusuchus* as the most basal caiman, suggesting that blunt-snouted rostrum with crushing dentition could have been the ancestral condition for the entire clade, while the more generalized morphology of the caiman crown-group is derived. *Gryposuchus* nov. sp. is the sole non-caimanine, long-snouted crocodylian in this community and the most basal gavialoid of the Amazonian basin. This new species offers critical evidence for accurately reconstructing the ancestral anatomy and ecology of this clade. *Gryposuchus* nov. sp. differs from other *Gryposuchus* species by possessing only a weak development of "telescoped" orbits. Based on the ancestral state transformations determined from the maximum parsimony analysis, this is interpreted as an incipient condition for more extensive telescoping of the orbits in later diverging relatives, such as *Gryposuchus colombianus* and *Gryposuchus croizati*. Including this new species in the phylogenetic-morphometric analyses suggests that the acquirement of similar rostral patterns between South American and Indian gavialoids results from parallel evolution in riverine habitats. As a consequence, it seems to be that in association with longirostry the circumorbital configuration is highly plastic and might reflect

habitat preferences and feeding strategies. Results support a long-term and large-scale radiation of the South American forms, with taxa occupying either extreme of the gavialoid morphospace showing preferences for coastal marine versus fluvial environments. Early biogeographic history of South American gavialoids was strongly linked to the northward drainage system connecting proto-Amazonian wetlands to the Caribbean region.

Mesoeucrocodylians of the fluvially-influenced paleoenvironments

As part of the same prevailing Pebas biome, Iquitos and Fitzcarrald localities represent coeval paleoenvironments (late Middle Miocene), the latter closer to the Andean influence. The fossil-bearing beds of Fitzcarrald are located in the Ucayali Department and correspond to conglomeratic storm deposits, in tidally-influenced but fluvially-dominated settings. As the highly heterogeneous mesoeucrocodylian community recorded in the Colombian locality of La Venta, Fitzcarrald documents the last representatives of deep-snouted sebecids and one gavialoid species with protruding eyes, further suggesting the presence of combined terrestrial and fluvial environments. These faunas show little taxonomic and phylogenetic snout morphotype similarities with the lacustrine faunal community of the Iquitos bonebeds. Whereas the crushing-dentition caimanines dominated the crocodylian community of Iquitos, these animals are not recorded yet in La Venta and Fitzcarrald. Current evidence reveals that different ecological and environmental conditions coexisted within the Pebas Mega-Wetland System. Based on the "giant mandible" discovered by Matthiessen (1961) in the Fitzcarrald Arch, a new species of *Purussaurus* is described. The anatomy of this species points to a proto-Amazonian origin for the clade comprising giant *Purussaurus* forms. The Pebas System records the last occurrence of basal *Eocaiman*-like caimanines in the Amazonian region and the first appearance of the smooth-fronted caiman *Paleosuchus* in both Fitzcarrald and Iquitos.

The initial demise of the Pebas Mega-Wetland System

Evidence underlines the occurrence of a key ecological turnover in western Amazonia during the earliest Late Miocene (~10.5 Ma), as it is documented by the Nueva Unión locality southern to Iquitos, providing new insights on establishment of modern ecosystems. Lignite-poor outcrops of the "Uppermost Pebas" Formation in Nueva Unión (early Late Miocene) yielded the youngest record of *Gnatusuchus*, but do not contain other crushing dentition caimans so far. Like in the Late Miocene faunas recovered from Acre (Brazil; fluvio-tidal Acre Phase), *Purussaurus* and *Mourasuchus* from Nueva Unión are giants. The record shared by these two localities includes a gavialoid species with fully "telescoped" orbits. Geological and paleontological data from Nueva Unión suggest that regional environmental changes might have occurred in the foreland basin as a consequence of an Andean uplift episode recorded by that time (Hoorn et al., 2010b). This tectonic activity not only fostered the origin of the transcontinental flow of the Amazon River, but also contributed to the retreat of the Pebasian System to northernmost South America (Salas-Gismondi et al., 2015a). The highly endemic Iquitos faunas evolved within the dysoxic marshes and swamps typical of the long-lived Pebas Mega-Wetland System (late early–early late Miocene) and declined with the inception of the modern Amazon drainage, favoring diversification of longirostrine crocodylians and modern generalist-feeding caimans. The record of *Caiman wannlangstoni* and *Gryposuchus* nov. sp. at Urumaco (Venezuela, late Miocene) adds evidence for the persistence of Pebasian aquatic conditions during the "Acre Phase" in northernmost South America, where the lower course of the proto-Amazonian System drainage was formerly situated (Hoorn et al., 2010b). Indeed, Late Miocene Urumaco crocodylian assemblages of the Paleo-Orinoco basin condense most phylogenetic morphotypes of the coeval Amazonian faunas represented in Acre as well as those of the older Pebasian communities. The end of the Pebas Mega-Wetland System notably resulted in reduction of the phylogenetic and morphotypical mesoeucrocodylian proto-Amazonian diversity, designating the beginning of

the modern Amazonian faunas. The rise and demise of distinctive, highly productive aquatic ecosystems substantially influenced evolution of Amazonian biodiversity hotspots of mesoeucrocodylians and other organisms throughout the Neogene.

REFERENCES

REFERENCES

Abel, O. (1928). *Allognathosuchus*, ein an die cheloniphage Nahrungsweise angepaßter Krokodiltypus des nordamerikanischen Eozäns. *Paläontologische Zeitschrift*, *9*(4), 367-374.

Adams, D. C. & Otárola-Castillo, E. (2014). Geomorph: an R package for the collection and analysis of geometric morphometric shape data. *Methodsin Ecology and Evolution, 4*, 393-399.

Adnet, S., Salas-Gismondi, R., & Antoine, P.-O. (2014). Comparisons of dental morphology in river stingrays (Chondrichthyes: Potamotrygonidae) with new fossils from the middle Eocene of Peruvian Amazonia rekindle debate on their evolution. *Naturwissenschaften*, *101*(1), 33-45.

Aggarwal, R. K., Majumdar, K. C., Lang, J. W., & Singh, L. (1994). Generic affinities among crocodilians as revealed by DNA fingerprinting with a Bkm-derived probe. *Proceedings of the National Academy of Sciences*, *91*(22), 10601-10605.

Aguilera, O. A., Riff, D., & Bocquentin- Villanueva, J. (2006). A new giant *Purussaurus* (Crocodyliformes, Alligatoridae) from the upper Miocene Urumaco Formation, Venezuela. *Journal of Systematic Palaeontology*, *4*(3), 221-232.

Albert, J. S., Lovejoy, N. R., & Crampton, W. G. (2006). Miocene tectonism and the separation of cis-and trans-Andean river basins: Evidence from Neotropical fishes. *Journal of South American Earth Sciences*, *21*(1), 14-27.

Anderson, L. C., Hartman, J. H., & Wesselingh, F. (2006). Close evolutionary affinities between freshwater corbulid bivalves from the Neogene of western Amazonia and Paleogene of the northern Great Plains, USA. *Journal of South American Earth Sciences*, *21*(1), 28-48.

Antoine, P.-O., De Franceschi, D., Flynn, J. J., Nel, A., Baby, P., Benammi, M., Calderón, I., Espurt, N., Goswami, A. & Salas-Gismondi, R. (2006). Amber from western Amazonia reveals Neotropical diversity during the middle Miocene. *Proceedings of the National Academy of Sciences*, *103*(37), 13595-13600.

Antoine, P.-O., Salas-Gismondi, R., Baby, P., Benammi, M., Brusset, S., De Franceschi, D., Espurt, N. Goillot, C., Pujos, F., Tejada, J. & Urbina, M. (2007). The Middle Miocene (Laventan) Fitzcarrald fauna, Amazonian Peru. *Cuadernos del Museo Geominero*, *8*, 19-24.

Antoine, P.-O., Marivaux, L., Croft, D. A., Billet, G., Ganerød, M., Jaramillo, C., Martin, T., Orliac, M. J., Tejada, J. Altamirano, A. J., Duranthon, F., Fanjat, G., Rousse, S. & Salas-Gismondi, R. (2011). Middle Eocene rodents from Peruvian Amazonia reveal the pattern and timing of caviomorph origins and biogeography. *Proceedings of the Royal Society of London B: Biological Sciences*, rspb20111732.

Antoine, P.-O., Roddaz, M., Brichau, S., Tejada-Lara, J., Salas-Gismondi, R., Altamirano, A., Louterbach, M., Lambs, L., Otto, T. & Brusset, S. (2013). Middle Miocene vertebrates from the Amazonian Madre de Dios subandean zone, Peru. *Journal of South American Earth Sciences*, *42*, 91-102.

Antoine, P-O., Abello, M. A., Adnet, S., Altamirano-Sierra, A. J., Baby, P., Billet, G., Boivin, M., Calderón, Y., Candela, A., Chabain, J., Corfu, F., Croft, D. A., Ganerød, M., Jaramillo, C., Klaus, K., Marivaux, L., Navarrete, R. E., Orliac, M. J., Parra, F., Pérez, M. E., Pujos, F., Rage, J. C., Ravel, A., Robinet, C., Roddaz, M., Tejada-Lara, J. V., Vélez-Juarbe, J., Wesselingh, F. P., & Salas-Gismondi, R. (submitted) A 60-million year Cenozoic history of western Amazonian ecosystems in Contamana, Eastern Peru.

Aureliano, T., Ghilardi, A. M., Guilherme, E., Souza-Filho, J. P., Cavalcanti, M., & Riff, D. (2015). Morphometry, bite-force, and paleobiology of the Late Miocene caiman *Purussaurus brasiliensis*. *PloS ONE*, *10*(2), e0117944.

Baby, P., Hermoza, W., Navarro, L., Bolaños, R., Espurt, N., Roddaz, M., Brusset, S. & Gil, W. (2005). Geodinámica mio-pliocénica de las cuencas subandinas peruanas: un mejor entendimiento de los sistemas petroleros. *V International Seminar INGEPET, Lima, Peru*. Extended Abstracts CD.

Barbosa-Rodrigues, B. (1892). Les Reptiles fossiles de la vallée de l'Amazone. *Vellosia 2*, 41–46.

Benton, M. J., & Clark, J. M. (1988). Archosaur phylogeny and the relationships of the Crocodylia. In *The Phylogeny and Classification of the Tetrapods. Vol. 1: Amphibians, Reptiles, Birds* (M. J. Benton ed.), Oxford: Clarendon Press, 295-338.

Blakey, R. C. (2008). Gondwana paleogeography from assembly to breakup—A 500 my odyssey. *Geological Society of America Special Papers*, *441*, 1-28.

Blanco, R. E., Jones, W. W., & Villamil, J. (2015). The 'death roll' of giant fossil crocodyliforms (Crocodylomorpha: Neosuchia): allometric and skull strength analysis. *Historical Biology*, *27*(5), 514-524.

Bocquentin-Villanueva, J., Souza Fhilo, J. P., Buffetaut, E., & Negri, R. (1989) Nova interpretacão do genero *Purussaurus* (Crocodylia, Alligatoridae). *Anais do XI Congresso Brasileiro de Paleontologia*, *1*: 428-437.

Bocquentin-Villanueva, J. & Souza Filho, J. (1990). O crocodiliano *Carandaisuchus* como sinonímia de *Mourasuchus* (Nettosuchidae). *Revista Brasileira de Geociências, 20*: 230–233.

Bona P. (2007). Una nueva especie de *Eocaiman* Simpson (Crocodylia, Alligatoridae) del Paleoceno Inferior de Patagonia. *Ameghiniana. 44*: 435–445.

Bona, P., Degrange, F. J., & Fernández, M. S. (2013). Skull anatomy of the bizarre crocodylian *Mourasuchus nativus* (Alligatoridae, Caimaninae). *The Anatomical Record*, *296*(2), 227-239.

Bona, P., Riff, D., & Gasparini, Z. B. (2012). Late Miocene crocodylians from northeast Argentina: new approaches about the austral components of the Neogene South American crocodylian fauna. *Earth and Environmental Science Transactions of the Royal Society of Edinburgh*, *103*(3-4), 551-570.

Bona, P., Starck, D., Galli, C., Gasparini, Z., & Reguero, M. (2014). *Caiman* cf. *latirostris* (Alligatoridae, Caimaninae) in the Late Miocene Palo Pintado Formation, Salta Province, Argentina: Paleogeographic and Paleoenvironmental Considerations. *Ameghiniana*, *51*(1), 26-36.

Boonstra, M., Ramos, M. I. F., Lammertsma, E. I., Antoine, P.-O., & Hoorn, C. (2015). Marine connections of Amazonia: Evidence from foraminifera and dinoflagellate cysts (early to Middle Miocene, Colombia/Peru). *Palaeogeography, Palaeoclimatology, Palaeoecology*, *417*, 176-194.

Bravard, A. (1858). Monografía de los terrenos marinos terciarios del Paraná. *Diario Oficial de Gobierno: El Nacional*, Argentina.

Brochu, C. A. (1997). Morphology, fossils, divergence timing, and the phylogenetic relationships of *Gavialis*. *Systematic Biology*, *46*(3), 479-522.

Brochu, C. A. (1999). Phylogenetics, taxonomy, and historical biogeography of Alligatoroidea. *Journal of Vertebrate Paleontology*, *19*(S2), 9-100.

Brochu, C. A. (2001). Crocodylian snouts in space and time: phylogenetic approaches toward adaptive radiation. *American Zoologist*, *41*(3), 564-585.

Brochu, C. A. (2003). Phylogenetic approaches toward crocodylian history. *Annual Review of Earth and Planetary Sciences*, *31*(1), 357-397.

Brochu, C. A. (2004a). A new Late Cretaceous gavialoid crocodylian from eastern North America and the phylogenetic relationships of thoracosaurs. *Journal of Vertebrate Paleontology*, *24*(3), 610-633.

Brochu, C. A. (2004b). Alligatorine phylogeny and the status of *Allognathosuchus* Mook, 1921. *Journal of Vertebrate Paleontology*, *24*(4), 857-873.

Brochu, C. A. (2010). A new alligatorid from the Lower Eocene Green River Formation of Wyoming and the origin of caimans. *Journal of Vertebrate Paleontology*, *30*(4), 1109-1126.

Brochu, C. A. (2011). Phylogenetic relationships of *Necrosuchus ionensis* Simpson, 1937 and the early history of caimanines. *Zoological Journal of the Linnean Society*, *163*(s1), S228-S256.

Brochu, C. A. (2013). Phylogenetic relationships of Palaeogene ziphodont eusuchians and the status of *Pristichampsus* Gervais, 1853. *Earth and Environmental Science Transactions of the Royal Society of Edinburgh*, *103*(3-4), 521-550.

Brochu, C. A., & Rincón, A. D. (2004). A gavialoid crocodylian from the Lower Miocene of Venezuela. *Special Papers in Palaeontology, Fossils of the Miocene Castillo Formation, Venezuela: Contributions in Neotropical Palaeontology*, *71*(71), 61-79.

Brochu, C. A., Wagner, J. R., Jouve, S., Sumrall, C. D., & Densmore, L. D. (2009). A correction corrected: consensus over the meaning of Crocodylia and why it matters. *Systematic Biology*, *58*(5): 537-543.

Buckley, G. A., Brochu, C. A., Krause, D. W., & Pol, D. (2000). A pug-nosed crocodyliform from the Late Cretaceous of Madagascar. *Nature*, *405*(6789), 941-944.

Buffetaut, E. (1982) Systématique, origine et evolution des gavialidae Sud-américains. *Geobios, 6*, 127-140.

Buffetaut, E. & Hoffstetter R. (1977). Découverte du Crocodilien Sebecus dans le Miocène du Pérou oriental. *Comptes Rendus de l'Academie des Sciences. Paris*, 284 (Série D): 1663-1666.

Buffetaut, E., & Marshall, L. G. (1991). A new crocodilian, *Sebecus querejazus*, nov. sp. (Mesosuchia, Sebecidae) from the Santa Lucia Formation (Early Paleocene) at Vila Vila, southcentral Bolivia. *Fósiles y Facies de Bolivia*, *1*, 545-557.

Burmeister, G. (1883). Reprint of Bravard, 1858: Monografía de los terrenos marinos terciarios del Paraná. *Ann. Mus. Púb. Buenos Aires, 3* (Ent. 13), 45-94.

Burmeister, G. (1885). Exámen crítico de los mamíferos y reptiles fósiles denominados por D. Bravard. *Ann. Mus. Púb. Buenos Aires, 3*, 151-152.

Busbey, A. B. (1986). New material of *Sebecus* cf. *huilensis* (Crocodilia: Sebecosuchidae) from the Miocene La Venta Formation of Colombia. *Journal of Vertebrate Paleontology*, *6*(1), 20-27.

Busbey, A. B. (1989). Form and function of the feeding apparatus of *Alligator mississippiensis*. *Journal of Morphology*, *202*(1), 99-127.

Busbey, A. B. (1995). The structural consequences of skull flattening in crocodilians. *Functional morphology in vertebrate paleontology*, (J. J. Thomason ed.), Cambridge: Cambridge University, 173-192.

Buscalioni, A. D., Sanz, J. L., & Casanovas, M. L. (1992). A new species of the eusuchian crocodile *Diplocynodon* from the Eocene of Spain. *Neues Jahrbuch für Geologie und Paläontologie Abhandlungen*, *187*, 1-29.

Buscalioni, A. D., Ortega, F., Weishampel, D. B., & Jianu, C. M. (2001). A revision of the crocodyliform *Allodaposuchus precedens* from the Upper Cretaceous of the Hateg Basin, Romania. Its relevance in the phylogeny of Eusuchia. *Journal of Vertebrate Paleontology*, *21*(1), 74-86.

Carpenter, K., & Lindsey, D. (1980). The dentary of *Brachychampsa montana* Gilmore (Alligatorinae; Crocodylidae), a Late Cretaceous turtle-eating alligator. *Journal of Paleontology*, 1213-1217.

Carvalho, I. S., Gasparini, Z. B., Salgado, L., Vasconcellos, F. M., & da Silva Marinho, T. (2010). Climate's role in the distribution of the Cretaceous terrestrial Crocodyliformes throughout Gondwana. *Palaeogeography, Palaeoclimatology, Palaeoecology*, *297*(2), 252-262.

Chiappe, L. M. (1988). Un nuevo *Caiman* (Crocodylia, Alligatoridae) de la Formación Tremembé (Oligoceno), Estado de São Paulo, Brasil, y su significado paleoclimático. *Paula-Coutiana*, *3*, 49-66.

Clark, J. M., (1986). Phylogenetic relationships of the crocodylomorph Archosaurs. PhD thesis, University of Chicago.

Clark, J. M. (1994). Patterns of evolution in Mesozoic Crocodyliformes. In *In the shadow of the dinosaurs: early Mesozoic tetrapods* (N. C. Fraser, H.-D. Sues eds.), New York: Cambridge Univ. Press, 84-97.

Claude, J. (2008). *Morphometrics with R*. Springer Science & Business Media.

Colbert, E. H. (1946). *Sebecus*, representative of a peculiar suborder of fossil Crocodilia from Patagonia. *Bulletin of the American Museum of Natural History*, *87*(4), 217-270.

Cozzuol, M. A. (2006). The Acre vertebrate fauna: age, diversity, and geography. *Journal of South American Earth Sciences*, *21*(3), 185-203.

Croft, D. A. (2007). The middle Miocene (Laventan) Quebrada Honda fauna, southern Bolivia and a description of its notoungulates. *Palaeontology*, *50*(1), 277-303.

Dalrymple, G. H. (1979). On the jaw mechanism of the snail-crushing lizards, *Dracaena* Daudin 1802 (Reptilia, Lacertilia, Teiidae). *Journal of Herpetology*, *13*, 303-311.

Delfino, M., & De Vos, J. (2010). A revision of the Dubois crocodylians, *Gavialis bengawanicus* and *Crocodylus ossifragus*, from the Pleistocene *Homo erectus* beds of Java. *Journal of Vertebrate Paleontology*, *30*(2), 427-441.

Delfino, M., Piras, P., & Smith, T. (2005). Anatomy and phylogeny of the gavialoid crocodylian *Eosuchus lerichei* from the Paleocene of Europe. *Acta Palaeontologica Polonica*, *50*(3), 565-580.

Densmore, L. D. (1983). Biochemical and immunological systematics of the order Crocodilia. In *Evolutionary Biology*, *Volume 16* (M. K. Hecht, B. Wallace, G. H. Prance eds.), New York: Plenum, 397- 465.

Densmore, L. D., & Dessauer, H. C. (1984). Low levels of protein divergence detected between *Gavialis* and *Tomistoma*: Evidence for crocodilian monophyly? *Comparative Biochemistry and Physiology Part B: Comparative Biochemistry*, *77*(4), 715-720.

Densmore, L. D., & Owen, R. D. (1989). Molecular systematics of the order Crocodilia. *American Zoologist*, *29*(3), 831-841.

Densmore III, L. D., & White, P. S. (1991). The systematics and evolution of the Crocodilia as suggested by restriction endonuclease analysis of mitochondrial and nuclear ribosomal DNA. *Copeia*, *1991*, 602-615.

Dessauer, H. C., Glenn, T. C., & Densmore, L. D. (2002). Studies on the molecular evolution of the Crocodylia: footprints in the sands of time. *Journal of Experimental Zoology*, *294*(4), 302-311.

Eaton, M. J., Martin, A., Thorbjarnarson, J., & Amato, G. (2009). Species-level diversification of African dwarf crocodiles (Genus *Osteolaemus*): a geographic and phylogenetic perspective. *Molecular phylogenetics and evolution*, *50*(3), 496-506.

Espurt, N., Baby, P., Brusset, S., Hermoza, W., Antoine, P. O., Salas-Gismondi, R., Pujos, F., Roddaz, M., Regard, V., Tejada, E. R., & Bolaños, R. (2006). Geomorphic and sedimentologic analyses on the Fitzcarrald Arch: evidence of a recent tectonic uplift. *XIII Congreso Peruano de Geología, Lima, Perú*, 273-276.

Espurt, N., Baby, P., Brusset, S., Roddaz, M., Hermoza, W., Regard, V., Antoine, P.-O., Salas-Gismondi, R. & Bolaños, R. (2007). How does the Nazca Ridge subduction influence the modern Amazonian foreland basin? *Geology*, *35*(6), 515-518.

Espurt, N., Baby, P., Brusset, S., Roddaz, M., Hermoza, W., & Barbarand, J. (2010). The Nazca Ridge and uplift of the Fitzcarrald Arch: implications for regional geology in northern South America. *Amazonia, Landscape and Species Evolution: A Look into the Past*, (C. Hoorn, F. P. Wesselingh eds.), Hoboken: Blackwell-Wiley, 89-100.

Figueiredo, J., Hoorn, C., Van der Ven, P., & Soares, E. (2010). Late Miocene onset of the Amazon River and the Amazon deep-sea fan: Evidence from the Foz do Amazonas Basin: Reply. *Geology*, *38*(7), e213-e213.

Fittkau EJ. 1981 Armut in der Vielfalt – Amazonien als Lebensraum fur Weichtiere. *Mitteilungen Zool. Ges. Braunau, 3*, 197-200.

Fortier, D. C., De Souza-Filho, J. P., Guilherme, E., Maciente, A. A., & Schultz, C. L. (2014). A new specimen of *Caiman brevirostris* (Crocodylia, Alligatoridae) from the Late Miocene of Brazil. *Journal of Vertebrate Paleontology*, *34*(4), 820-834.

Fortier, D. C., & Rincón, A. D. (2013). Pleistocene crocodylians from Venezuela, and the description of a new species of *Caiman*. *Quaternary International*, *305*, 141-148.

Friedman, M. (2011). Parallel evolutionary trajectories underlie the origin of giant suspension-feeding whales and bony fishes. *Proceedings of the Royal Society of London B: Biological Sciences*, rspb20111381.

Gasparini, Z. B. (1968). Nuevos restos de *Rhamphostomopsis neogaeus* (Burm.) Rusconi 1933 (Reptilia, Crocodilia) del «Mesopotaminense (Plioceno medio-superior) de Argentina. *Ameghiniana, Buenos Aires*, *5*(8), 299-311.

Gasparini, Z. (1984). New Tertiary Sebecosuchia (Crocodylia: Mesosuchia) from Argentina. *Journal of Vertebrate Paleontology*, *4*(1), 85-95.

Gasparini, Z., Fernandez, M., & Powell, J. (1993). New tertiary sebecosuchians (Crocodylomorpha) from South America: phylogenetic implications. *Historical Biology*, *7*(1), 1-19.

Gatesy, J., & Amato, G. D. (1992). Sequence similarity of 12S ribosomal segment of mitochondrial DNAs of gharial and false gharial. *Copeia*, *1992*: 241-243.

Gatesy, J., & Amato, G. (2008). The rapid accumulation of consistent molecular support for intergeneric crocodylian relationships. *Molecular phylogenetics and evolution*, *48*(3), 1232-1237.

Gatesy, J., Amato, G., Norell, M., DeSalle, R., & Hayashi, C. (2003). Combined support for wholesale taxic atavism in gavialine crocodylians. *Systematic Biology*, *52*(3), 403-422.

Gatesy, J., Baker, R. H., & Hayashi, C. (2004). Inconsistencies in arguments for the supertree approach: supermatrices versus supertrees of Crocodylia. *Systematic Biology*, *53*(2), 342-355.

Gervais, P. (1876) Crocodile gigantesque fossile du Brésil. *Jour. Zool., 5*, 232-236.

Gingras, M. K., Räsänen, M., & Ranzi, A. (2002). The significance of bioturbated inclined heterolithic stratification in the southern part of the Miocene Solimoes Formation, Rio Acre, Amazonia Brazil. *Palaios*, *17*(6), 591-601.

Goillot, C., Antoine, P.-O., Tejada, J., Pujos, F., & Salas-Gismondi, R. (2011). Middle Miocene Uruguaytheriinae (Mammalia, Astrapotheria) from Peruvian Amazonia and a review of the astrapotheriid fossil record in northern South America. *Geodiversitas*, *33*(2), 331-345.

Goloboff, P. A., Farris, J. S., & Nixon, K. C. (2008). TNT, a free program for phylogenetic analysis. *Cladistics*, *24*(5), 774-786.

Guerrero, J. (1997). Stratigraphy, sedimentary environments, and the Miocene uplift of the Colombian Andes. In *Vertebrate Paleontology in the Neotropics: The Miocene Fauna of La Venta, Colombia.* (R. F. Kay, R. H. Madden, R. L. Cifelli, J.J. Flynn), Washington DC, DC: Smithsonian Institution, 5-43.

Gürich, G. (1912). *Gryposuchus Jessei*, ein neues schmalschnauziges Krokodil aus den jüngeren Ablagerungen des oberen Amazonas-Gabietes. *Mitteilungen Mineral.-Geol. Instit. Hamburg*. 4 Beiheft z. Jahrb. Hamburg. Wiss Anat. 29, 59-71.

Harshman, J., Huddleston, C. J., Bollback, J. P., Parsons, T. J., & Braun, M. J. (2003). True and false gharials: a nuclear gene phylogeny of Crocodylia. *Systematic Biology*, *52*(3), 386-402.

Hass, C. A., Hoffman, M. A., Densmore, L. D., & Maxson, L. R. (1992). Crocodilian evolution: insights from immunological data. *Molecular Phylogenetics and Evolution*, *1*(3), 193-201.

Hastings, A. K., Bloch, J. I., Cadena, E. A., & Jaramillo, C. A. (2010). A new small short-snouted dyrosaurid (Crocodylomorpha, Mesoeucrocodylia) from the Paleocene of Northeastern Colombia. *Journal of Vertebrate Paleontology*, *30*(1), 139-162.

Hastings, A. K., Bloch, J. I., & Jaramillo, C. A. (2011). A new longirostrine dyrosaurid (Crocodylomorpha, Mesoeucrocodylia) from the Paleocene of north- eastern Colombia:

biogeographic and behavioural implications for New- World Dyrosauridae. *Palaeontology*, *54*(5), 1095-1116.

Hastings, A. K., Bloch, J. I., Jaramillo, C. A., Rincon, A. F., & MacFadden, B. J. (2013). Systematics and biogeography of crocodylians from the Miocene of Panama. *Journal of Vertebrate Paleontology*, *33*(2), 239-263.

Hastings, A. K., Bloch, J. I., & Jaramillo, C. A. (2014). A new blunt-snouted dyrosaurid, *Anthracosuchus balrogus* gen. et sp. nov. (Crocodylomorpha, Mesoeucrocodylia), from the Palaeocene of Colombia. *Historical Biology*, 1-23.

Hillenius, W. J., & Ruben, J. A. (2004). The evolution of endothermy in terrestrial vertebrates: Who? When? Why? *Physiological and Biochemical Zoology*, *77*(6), 1019-1042.

Hoorn, C. (1993). Marine incursions and the influence of Andean tectonics on the Miocene depositional history of northwestern Amazonia: results of a palynostratigraphic study. *Palaeogeography, Palaeoclimatology, Palaeoecology*, *105*(3), 267-309.

Hoorn, C. (1994). An environmental reconstruction of the palaeo-Amazon River system (Middle–Late Miocene, NW Amazonia). *Palaeogeography, Palaeoclimatology, Palaeoecology*, *112*(3), 187-238.

Hoorn, C., Guerrero, J., Sarmiento, G. A., & Lorente, M. A. (1995). Andean tectonics as a cause for changing drainage patterns in Miocene northern South America. *Geology*, *23*(3), 237-240.

Hoorn, C., Wesselingh, F. P., Hovikoski, J., & Guerrero, J. (2010a). The development of the amazonian mega-wetland (Miocene; Brazil, Colombia, Peru, Bolivia). In *Amazonia, Landscape and Species Evolution: A Look into the Past* (C. Hoorn, F. P. Wesselingh eds.), Hoboken: Blackwell-Wiley, 123-142.

Hoorn, C., Wesselingh, F. P., Ter Steege, H., Bermudez, M. A., Mora, A., Sevink, J., Sanmartín, I., Sánchez-Meseguer, A., Anderson, C. L., Figueiredo, J. P. Jaramillo, C., Riff, D., Negri, F. R., Hooghiemstra, H., Lundberg, J., Stadler, T., Särkinen, T. & Antonelli, A. (2010b). Amazonia through time: Andean uplift, climate change, landscape evolution, and biodiversity. *Science*, *330*(6006), 927-931.

Hovikoski, J. (2001). Sedimentology, ichnology, and sequence stratigraphy of four outcrops from the Early—Late Miocene Pebas Formation, Western Amazonian foreland basin, Peru. PhD thesis, MSc thesis, University of Turku, Finland.

Hovikoski, J., Räsänen, M., Gingras, M., Roddaz, M., Brusset, S., Hermoza, W., & Lertola, K. (2005). Miocene semidiurnal tidal rhythmites in Madre de Dios, Peru. *Geology*, *33*(3), 177-180.

Hovikoski, J., Gingras, M., Räsänen, M., Rebata, L. A., Guerrero, J., Ranzi, A., Melo, J., Romero, L., Nuñez del Prado, H., Jaimes, F. & Lopez, S. (2007). The nature of Miocene Amazonian epicontinental embayment: High-frequency shifts of the low-gradient coastline. *Geological Society of America Bulletin*, *119*(11-12), 1506-1520.

Hovikoski, J., Wesselingh, F. P., Räsänen, M., Gingras, M., & Vonhof, H. B. (2010). Marine influence in Amazonia: evidence from the geological record. In *Amazonia, landscape and species evolution: a look into the past* (C. Hoorn & F. P. Wesselingh eds.), Hoboken: Blackwell-Wiley, 143-160.

Hua, S., & Jouve, S. (2004). A primitive marine gavialoid from the Paleocene of Morocco. *Journal of Vertebrate Paleontology*, *24*(2), 341-350.

Hurlburt, G. R., Heckert, A. B., & Farlow, J. O. (2003). Body mass estimates of phytosaurs (Archosauria: Parasuchidae) from the Petrified Forest Formation (Chinle Group: Revueltian) based on skull and limb bone measurements. *New Mexico Museum of Natural History Science Bulletin*, *24*, 105-113.

Iordansky, N. N. (1964). The jaw muscles of the crocodiles and some relating structures of the crocodilian skull. *Anatomischer Anzeiger, 115*(3), 256-280.

Iordansky, N. N. (1976). The skull of the Crocodilia. In *Biology of the Reptilia 4* (C. Gans, T. Parsons eds.) London: Academic Press, 201-260.

Iturralde-Vinent, M., & MacPhee, R. D. (1999). Paleogeography of the Caribbean region: implications for Cenozoic biogeography. *Bulletin of the American Museum of Natural History, 238*, 1-95.

Jaramillo, C., Rueda, M. J., & Mora, G. (2006). Cenozoic plant diversity in the Neotropics. *Science*, *311*(5769), 1893-1896.

Jouve S. (2004). Etude des Crocodyliformes fini Crétacé-Paléogène du Bassin des Oulad Abdoun (Maroc) et comparaison avec les faunes africaines contemporaines: systématique, phylogénie et paléo-biogéographie. PhD thesis, Museum national d'Histoire naturelle, Paris.

Jouve, S. (2009). The skull of *Teleosaurus cadomensis* (Crocodylomorpha; Thalattosuchia), and phylogenetic analysis of Thalattosuchia. *Journal of Vertebrate Paleontology*, *29*(1), 88-102.

Jouve, S., Iarochene, M., Bouya, B., & Amaghzaz, M. (2006). New material of *Argochampsa krebsi* (Crocodylia: Gavialoidea) from the Lower Paleocene of the Oulad Abdoun Basin (Morocco): phylogenetic implications. *Geobios*, *39*(6), 817-832.

Jouve, S., Bardet, N., Jalil, N. E., Suberbiola, X. P., Bouya, B., & Amaghzaz, M. (2008). The oldest African crocodylian: phylogeny, paleobiogeography, and differential survivorship of marine reptiles through the Cretaceous-Tertiary boundary. *Journal of Vertebrate Paleontology*, *28*(2), 409-421.

Kälin, J. A. 1931. Ueber die Stellung der Gavialiden im System der Crocodilia. *Rev. Suisse Zool. 38*: 379–388.

Kälin, J. A. (1933) Beiträge zur vergleichenden Osteologie des Crocodilidenschädels. *Zoologische Jahrbucher Abteilung Anat., 57*(4), 535-714.

Kälin, J. A. 1955. Zur Stammesgeschichte der Crocodilia. *Rev. Suisse Zool. 62*:347–356

Kay, R. F., & Madden, R. H. (1997). Mammals and rainfall: paleoecology of the middle Miocene at La Venta (Colombia, South America). *Journal of Human Evolution*, *32*(2), 161-199.

Kellner, A. W., Pinheiro, A. E., & Campos, D. A. (2014). A new sebecid from the Paleogene of Brazil and the crocodyliform radiation after the K–Pg boundary. *PLoS ONE*, 9(1): e81386.

Klingenberg, C. P. (2011). MorphoJ: an integrated software package for geometric morphometrics. *Molecular ecology resources*, *11*(2), 353-357.

Kraus, R. (1998). The cranium of *Piscogavialis jugaliperforatus* n. gen., n. sp. (Gavialidae, Crocodylia) from the Miocene of Peru. *Paläontologische Zeitschrift*, *72*(3-4), 389-405.

Langston Jr, W. (1965). Fossil crocodilians from Colombia and the Cenozoic History of the Crocodylia in South America. *University of California Publications of Geological Sciences, 52*: 1-127.

Langston Jr, W. (1976). The Crocodilian skull in historical perspective. In *Biology of the Reptilia 4* (C. Gans, T. Parsons eds.), London: Academic Press, 263-284.

Langston Jr, W. (2008). Notes on a partial skeleton of Mourasuchus (Crocodylia: Nettosuchidae) from the Upper Miocene of Venezuela. *Arquivos do Museu Nacional*, *66*(1), 125-143.

Langston, W., & Gasparini, Z. (1997). Crocodilians, *Gryposuchus*, and the South American gavials. In *Vertebrate Paleontology in the Neotropics: the Miocene Fauna of La Venta, Colombia*, (R. F. Kay, R. H. Madden, R. L. Cifelli, J.J. Flynn eds.), Washington DC, DC: Smithsonian Institution, 113-154.

Larson, A., & Losos, J. B. (1996). Phylogenetic systematics of adaptation. *Adaptation.* San Diego, CA: Academic Press, 187-220.

Leclercq, F., Schnek, A. G., Braunitzer, G., Stangl, A., & Schrank, B. (1981). Direct reciprocal allosteric interaction of oxygen and hydrogen carbonate sequence of the haemoglobins of the Caiman (*Caiman crocodylus*), the Nile crocodile (*Crocodylus niloticus*) and the Mississippi crocodile (*Alligator mississippiensis*). *Hoppe-Seyler's Zeitschrift fãr physiologische Chemie*, *362*(8), 1151-1158.

Losos, J. B., & Miles, D. B. (1994). Adaptation, constraint, and the comparative method: phylogenetic issues and methods. *Ecological morphology: Integrative organismal biology*, 60-98.

Lovejoy, N. R., Bermingham, E., & Martin, A. P. (1998). Marine incursion into South America. *Nature*, *396*(6710), 421-422.

Lundberg, J. G., Marshall, L. G., Guerrero, J., Malabarba, M. C. & Wesselingh, F. (1998). The stage for Neotropical fish diversification: a history of tropical South American rivers. *Phylogeny and classification of Neotropical fishes.* (L. R. Malabarba, R. E. Reis, R. P. Vari, Z. M. Lucena, C. A. S. Lucena eds.), Porto Alegre, Edipucrs, 13-48.

McAliley, L. R., Willis, R. E., Ray, D. A., White, P. S., Brochu, C. A., & Densmore, L. D. (2006). Are crocodiles really monophyletic?—evidence for subdivisions from sequence and morphological data. *Molecular phylogenetics and evolution*, *39*(1), 16-32.

Madden, R. 1997. A new toxodontid notoungulate. In *Vertebrate Paleontology in the Neotropics: the Miocene fauna of La Venta, Colombia* (Kay, R., Madden, R., Cifelli, R., Flynn, J. J. eds.), Washington, DC: Smithsonian Institution Press, 335–354.

Magnusson, W. E., & Campos, Z. (2010). Cuvier's smooth-fronted caiman *Paleosuchus palpebrosus*. *Crocodiles Status Survey and Conservation Action Plan*, 40-42.

Marivaux, L., Salas-Gismondi, R., Tejada, J., Billet, G., Louterbach, M., Vink, J., Bailleul, J., Roddaz, M. & Antoine, P. O. (2012). A platyrrhine talus from the early Miocene of Peru (Amazonian Madre de Dios sub-andean zone). *Journal of Human Evolution*, 63: 696-703.

Martin, J. E. (2007). New material of the Late Cretaceous globidontan *Acynodon iberoccitanus* (Crocodylia) from southern France. *Journal of Vertebrate Paleontology*, *27*(2), 362-372.

Martin, J. E., Buffetaut, E., Naksri, W., Lauprasert, K., & Claude, J. (2012). *Gavialis* from the Pleistocene of Thailand and its relevance for drainage connections from India to Java. *PloS ONE*, *7*(9), e44541.

Martin, J. E., Amiot, R., Lécuyer, C., & Benton, M. J. (2014). Sea surface temperature contributes to marine crocodylomorph evolution. *Nature communications*, *5*:4658.

Matthiessen, P. (1961). The Cloud Forest: A Chronicle of the South American Wilderness. New York, Viking.

Meredith, R. W., Hekkala, E. R., Amato, G., & Gatesy, J. (2011). A phylogenetic hypothesis for *Crocodylus* (Crocodylia) based on mitochondrial DNA: evidence for a trans-Atlantic voyage from Africa to the New World. *Molecular Phylogenetics and Evolution*, *60*(1), 183-191.

Molnar, R. E. (2012). Jaw musculature and jaw mechanics of *Sebecus icaeorhinus* Simpson, 1937 (Mesoeucrocodylia, Sebecosuchia). *Earth and Environmental Science Transactions of the Royal Society of Edinburgh*, *103*(3-4), 501-519.

Monsch, K. A. (1998). Miocene fish faunas from the northwestern Amazonia basin (Colombia, Peru, Brazil) with evidence of marine incursions. *Palaeogeography, Palaeoclimatology, Palaeoecology*, *143*(1), 31-50.

Mook, C. C., (1921a). *Brachygnathosuchus braziliensis, a new fossil crocodilian from Brazil*. *Bulletin of the American Museum of Natural History, 44*: 43-49.

Mook, C. C. (1921b). Skull characters of Recent Crocodilia: with notes on the affinities of the recent genera. *Bulletin of the American Museum of Natural History, 44*: 123-268.

Mook, C. C. (1921c). Individual and age variations in the skulls of recent Crocodilia. *Bulletin of the American Museum of Natural History, 44*: 51-66.

Mook, C. C. (1941). *A new fossil Crocodilian from Colombia*. *Proceedings of the United States National Museum, 91*(3122): 55-58.

Mora, A., Baby, P., Roddaz, M., Parra, M., Brusset, S., Hermoza, W. & Espurt, N. (2010). Tectonic history of the Andes and sub-Andean zones: implications for the development of the Amazon drainage basin. *Amazonia: Landscape and species evolution*, (C. Hoorn, F. P. Wesselingh eds.), Hoboken: Blackwell-Wiley, 38-60.

Moraes- Santos, H., Villanueva, J. B. & Toledo, P. (2011). New remains of a gavialoid crocodilian from the late Oligocene-early Miocene of the Pirabas Formation, Brazil. *Zoological Journal of the Linnean Society*, *163*(s1), S132-S139.

Moreno, F., Hendy, A. J. W., Quiroz, L., Hoyos, N., Jones, D. S., Zapata, V., Zapata, S., Ballen, G. A., Cadena, E., Cárdenas, A. L., Carrillo-Briceño, J. D., Carrillo, J., Delgado-Sierra, D., Escobar, J., Martínez, J. I., Martínez, C., Montes, C., Moreno, J., Perz, N., Sánchez, R., Suárez, C., Vallejo-Pareja, M. C. & Jaramillo, C. (2015). Revised

stratigraphy of Neogene strata in the Cocinetas basin, La Guajira, Colombia. *Swiss Journal of Palaeontology*, 1-39.

Muñoz-Torres, F. A., Whatley, R. C., & Van Harten, D. (2006). Miocene ostracod (Crustacea) biostratigraphy of the upper Amazon Basin and evolution of the genus *Cyprideis*. *Journal of South American Earth Sciences*, *21*(1), 75-86.

Nakaya, H., & Tsujikawa, H. (2006). Late Cenozoic mammalian biostratigraphy and faunal change. In *Human Origins and Environmental Backgrounds* Springer US, 59-70.

Negri, F. R., Bocquentin- Villanueva, J., Ferigolo, J., & Antoine, P. O. (2010). A review of Tertiary mammal faunas and birds from western Amazonia. *Amazonia: Landscape and Species Evolution: A look into the past* (C. Hoorn, F. P. Wesselingh eds.), Hoboken: Blackwell-Wiley, 243-258.

Norell, M. A. (1988). Cladistic approaches to evolution and paleobiology as applied to the phylogeny of the alligatorids. PhD thesis, Yale University.

Norell, M. A. (1989). The higher level relationships of the extant Crocodylia. *Journal of Herpetology*, 325-335.

Norell, M. A., Clark, J.M. (1990) A reanalysis of *Bernissartia fagesii*, with comments on its phylogenetic position and its bearing on the origin and diagnosis of the Eusuchia. *Bull. Inst. R. Sci. Nat. Belg*., *60*: 115-128.

Nuttall C.P. (1990) A review of the Tertiary non-marine molluscan faunas of the Pebasian and other inland basins of north-western South America. *Bull. British Museuem of natural History Geol*. **45**, 165-371.

Oaks, J. R. (2011). A time- calibrated species tree of Crocodylia reveals a recent radiation of the true crocodiles. *Evolution*, *65*(11), 3285-3297.

Ősi, A., & Weishampel, D. B. (2009). Jaw mechanism and dental function in the late Cretaceous basal eusuchian *Iharkutosuchus*. *Journal of Morphology*, *270*(8), 903-920.

Ősi, A., Clark, J. M., & Weishampel, D. B. (2007). First report on a new basal eusuchian crocodyliform with multicusped teeth from the Upper Cretaceous (Santonian) of Hungary. *Neues Jahrbuch für Geologie und Paläontologie-Abhandlungen*, *243*(2), 169-177.

Paolillo, A., & Linares, O. J. (2007). Nuevos cocodrilos sebecosuchia del cenozoico suramericano (Mesosuchia: Crocodylia). *Paleobiologia Neotropical*, *3*, 1-25.

Pearcy, A., & Wijtten, Z. (2011). A morphometric analysis of crocodilian skull shapes. *The Herpetological Journal*, *21*(4), 213-218.

Perutz, M. F., Bauer, C., Gros, G., Leclercq, F., Vandecasserie, C., Schnek, A. G., Braunitzer, G., Friday, A. E. & Joysey, K. A. (1981). Allosteric regulation of crocodilian haemoglobin. *Nature* 291: 682–684.

Petrulevičius, J. F., Nel, A., De Franceschi, D., Goillot, C., Antoine, P. O., Salas-Gismondi, R., & Flynn, J. J. (2011). First fossil blood sucking Psychodidae in South America: a sycoracine moth fly (Insecta: Diptera) in the middle Miocene Amazonian amber. *Insect Systematics & Evolution*, *42*(1), 87-96.

Pierce, S. E., Angielczyk, K. D., & Rayfield, E. J. (2008). Patterns of morphospace occupation and mechanical performance in extant crocodilian skulls: a combined geometric morphometric and finite element modeling approach. *Journal of Morphology*, *269*(7), 840-864.

Pierce, S. E., Angielczyk, K. D., & Rayfield, E. J. (2009). Morphospace occupation in thalattosuchian crocodylomorphs: skull shape variation, species delineation and temporal patterns. *Palaeontology*, *52*(5), 1057-1097.

Pinheiro, A. E., Fortier, D. C., Pol, D., Campos, D. A., & Bergqvist, L. P. (2013). A new *Eocaiman* (Alligatoridae, Crocodylia) from the Itaboraí Basin, Paleogene of Rio de Janeiro, Brazil. *Historical Biology*, *25*(3), 327-337.

Poe, S. (1996). Data set incongruence and the phylogeny of crocodilians. *Systematic Biology*, *45*(4), 393-414.

Pol, D., & Gasparini, Z. (2009). Skull anatomy of *Dakosaurus andiniensis* (Thalattosuchia: Crocodylomorpha) and the phylogenetic position of Thalattosuchia. *Journal of Systematic Palaeontology*, *7*(2), 163-197.

Pol, D., & Powell, J. E. (2011). A new sebecid mesoeucrocodylian from the Rio Loro Formation (Palaeocene) of north- western Argentina. *Zoological Journal of the Linnean Society*, *163*(s1), S7-S36.

Pol, D., Leardi, J. M., Lecuona, A., & Krause, M. (2012). Postcranial anatomy of *Sebecus icaeorhinus* (Crocodyliformes, Sebecidae) from the Eocene of Patagonia. *Journal of Vertebrate Paleontology*, *32*(2), 328-354.

Pol, D., Nascimento, P. M., Carvalho, A. B., Riccomini, C., Pires-Domingues, R. A., & Zaher, H. (2014). A new notosuchian from the Late Cretaceous of Brazil and the phylogeny of advanced notosuchians. *PloS ONE*, *9*(4), e93105.

Polly, P. D., Lawing, A. M., Fabre, A. C., & Goswami, A. (2013). Phylogenetic principal components analysis and geometric morphometrics. *Hystrix, the Italian Journal of Mammalogy*, *24*(1), 33-41.

Pons, D., & De Franceschi, D. (2007). Neogene woods from western Peruvian Amazon and palaeoenvironmental interpretation. *Bulletin of Geosciences*, *82*(4), 343-354.

Price, L. I. (1964). Sobre o cranio de um grande crocodilideo extinto do Alto Rio Jurua, Estado do Acre. *Anais da Academia Brasileira de Ciência, 36*, 59–66.

Price, L. I. (1967). Sobre a mandibula de um gigantesco crocodilideo extinto do alto rio Jurua, Estado do Acre. *Atas do Simposio sobre a Biota Amazonica, Geociências 1,* 359–371.

Pujos, F., Albino, A. M., Baby, P., & Guyot, J. L. (2009). Presence of the extinct Lizard *Paradracaena* (Teiidae) in the middle Miocene of the Peruvian Amazon. *Journal of Vertebrate Paleontology*, *29*(2), 594-598.

Pujos, F., Salas-Gismondi, R., Baby, G., Baby, P., Goillot, C., Tejada, J., & Antoine, P.-O. (2013). Implication of the presence of *Megathericulus* (Xenarthra: Tardigrada: Megatheriidae) in the Laventan of Peruvian Amazonia. *Journal of Systematic Palaeontology*, *11*(8), 973-991.

Quiroz, L. I., & Jaramillo, C. A. (2010). Stratigraphy and sedimentary environments of Miocene shallow to marginal marine deposits in the Urumaco Trough, Falcon Basin, western Venezuela. *Urumaco and Venezuelan Paleontology* (M. Sánchez-Villagra, O. Aguilera, A. Carlini), Bloomington: Indiana University Press, 153-172.

Räsänen M, Linna A, Irion G, Rebata Hernani L, Vargas Huaman R, Wesselingh F. (1998) Geología y geoformas de la zona de Iquitos. In *Geoecología y desarollo Amazónico: estudio integrado en la zona de Iquitos, Peru*, Annales universitatis Turkuensis, Ser A II, 114 (R. Kalliola, S. Flores Paitán eds.), Turku: University of Turku, 59-137.

Rebata LA, Räsänen ME, Gingras MK, Vieira Jr V, Berberi M, Irion G. (2006) Sedimentology and ichnology of tide-influenced Late Miocene successions in western Amazonia: the gradational transition between the Pebas and Nauta formations. *Journal of South American Earth Sciences, 21*: 116-129.

Regard, V., Lagnous, R., Espurt, N., Darrozes, J., Baby, P., Roddaz, M., Calderón, I. & Hermoza, W. (2009). Geomorphic evidence for recent uplift of the Fitzcarrald Arch (Peru): A response to the Nazca Ridge subduction. *Geomorphology*, *107*(3), 107-117.

Riff, D. & Aguilera, C. (2008). The world's largest gharials *Gryposuchus*: description of *G. croizati* n. sp. (Crocodylia, Gavialidae) from the Upper Miocene. *Paläontologische Zitschrift, 82*(2), 178-195.

Riff, D., Romano, R., Seyferth, P., Oliveira, G. R., & Aguilera, O. A. (2010). Neogene crocodile and turtle fauna in northern South America. *Amazonia: Landscape and Species*

Evolution: A look into the past (C. Hoorn, F. P. Wesselingh eds.), Hoboken: Blackwell-Wiley, 259-280.

Roddaz, M., Baby, P., Brusset, S., Hermoza, W., & Darrozes, J. M. (2005). Forebulge dynamics and environmental control in Western Amazonia: the case study of the Arch of Iquitos (Peru). *Tectonophysics*, *399*(1), 87-108.

Roddaz, M., Hermoza, W., Mora, A., Baby, P., Parra, M., Christophoul, F., Brusset, S. & Espurt, N. (2010). Cenozoic sedimentary evolution of the Amazonian foreland basin system. *Amazonia, landscape and species evolution: a look into the past.* (C. Hoorn, F. P. Wesselingh eds.), Hoboken: Blackwell-Wiley, 61-88.

Rohlf, F. J. (1999). Shape statistics: Procrustes superimpositions and tangent spaces. *Journal of Classification*, *16*(2), 197-223.

Roncal, J., Couderc, M., Baby, P., Kahn, F., Millán, B., Meerow, A. W., & Pintaud, J. C. (2015). Palm diversification in two geologically contrasting regions of western Amazonia. *Journal of Biogeography* (first on line).

Roos, J., Aggarwal, R. K., & Janke, A. (2007). Extended mitogenomic phylogenetic analyses yield new insight into crocodylian evolution and their survival of the Cretaceous–Tertiary boundary. *Molecular phylogenetics and evolution*, *45*(2), 663-673.

Rovereto, C. (1912). Los cocodrilos fósiles de las capas del Paraná. *Anales del Museo Nacional de Historia Natural de Buenos Aires*, Serie 3 *22*: 339–368.

Rusconi, C. (1933). Observaciones críticas sobre reptiles Terciarios de Paraná (Fam. Alligatoridae). *Revista de la Universidad Nacional de Córdova*, *20*(6-7), 57-106.

Rusconi C. 1937. Nuevo aligatorino del Paleoceno Argentino. *Boletín Paleontol. Buenos Aires 8*:1–5.

Rylands, A. B., Mittermeier, R. A., Pilgrim, J., Gascon, C., Fonseca, G., Silva, J. M. C., Mittermeier, C. G., et al. (2002). *Amazonia*. (R. A. Mittermeier, C. G. Mittermeier, P. P. Gil, J. F. Pilgrim, J. eds.), Wilderness: Earth's last wild places. CEMEX, Agrupación Sierra Madre, S. C. Mexico, 56-107.

Salas, R. & Urbina, M. (2003). El espécimen de *Purussaurus* (Eusuchia: Alligatoridae) del Mioceno superior del Río Mapuya, Ucayali-Perú. *VI Congreso Latinoamericano de Herpetología*, Lima-Perú: 95R.

Salas-Gismondi, R., Baby, P., Antoine, P.-O., Pujos, F., Benammi, M., Espurt, N., Brusset, S., Urbina, M., and De Franceschi, D. (2006). Late middle Miocene vertebrates from the Peruvian Amazonian Basin (Inuya and Mapuya Rivers, Ucayali): Fitzcarrald Expedition. (2005). *XIII Congreso Peruano de Geología*, Lima, Perú, 643-646.

Salas-Gismondi, R., Antoine, P. O., Baby, P., Brusset, S., Benammi, M., Espurt, N., De Franceschi, D., Pujos, F., Tejada, J. & Urbina, M. (2007). Middle Miocene crocodiles from the Fitzcarrald Arch, Amazonian Peru. *Cuadernos del Museo Geominero*, *8*, 355-360.

Salas-Gismondi, R., Tejada, J. & Antoine, P.-O. (2011). Evidence on the tropical history of Paleogene Cingulata. *IV Congreso Latinoamericano de Paleontología de Vertebrados*, September 21-24, San Juan, Argentina.

Salas-Gismondi, R., Antoine, P. O., Clarke, J. Baby, P. & Urbina, M. (2013). Croc's two realms: New Cenozoic discoveries from the Amazonian basin and the Pacific coast of Peru. *73rd Meeting of the Society of Vertebrate Paleontology*, October 30- November 2, Los Angeles, 203A.

Salas-Gismondi, R., Flynn, J. Baby, P., Tejada-Lara J. & Antoine, P.-O., (2014a). Sobre el origen de la biodiversidad amazónica. In *Iquitos* (Varón Consultores Asociados eds.), Lima: Telefónica del Perú, 84-91.

Salas-Gismondi, R., Antoine, P.-O., Baby, P. Tejada-Lara, J., Urbina, M., (2014b) Evidence from the cloud forest: Matthiessen specimen of *Purussaurus* from the late Middle Miocene of Peruvian Amazonia, *74rd Meeting of the Society of Vertebrate Paleontology*, November 5-8, 2014, Berlin, 219A.

Salas-Gismondi, R., Flynn, J. J., Baby, P., Tejada-Lara, J. V., Wesselingh, F. P., & Antoine, P. O. (2015a). A Miocene hyperdiverse crocodylian community reveals peculiar trophic dynamics in proto-Amazonian mega-wetlands. *Proceedings of the Royal Society of London B: Biological Sciences*, *282*(1804), 20142490.

Salas-Gismondi, R., Tejada-Lara, J.V., & Antoine P.-O. (2015b) Potential role of the northern proto-Amazonian drainage for biotic dispersals from South America to the Caribbean. *4th Meeting of the Network for Neotropical Biogeography*, Smithsonian Tropical Research Institute Ciudad de Panamá, Panamá. January15-16, 2015.

Salisbury, S. W., Molnar, R. E., Frey, E., & Willis, P. M. (2006). The origin of modern crocodyliforms: new evidence from the Cretaceous of Australia. *Proceedings of the Royal Society of London B: Biological Sciences*, *273*(1600), 2439-2448.

Sánchez-Villagra, M. R., & Aguilera, O. A. (2006). Neogene vertebrates from Urumaco, Falcón State, Venezuela: diversity and significance. *Journal of Systematic Palaeontology*, *4*(03), 213-220.

Scalabrini, P. (1887). Cartas Científicas. *Mus. Prov. Entre Ríos*, Paraná.

Shephard, G. E., Müller, R. D., Liu, L., & Gurnis, M. (2010). Miocene drainage reversal of the Amazon River driven by plate-mantle interaction. *Nature Geoscience*, *3*(12), 870-875.

Scheyer, T. M., & Moreno-Bernal, J. W. (2010). Fossil crocodylians from Venezuela in the context of South American faunas. In *Urumaco and Venezuelan Paleontology: The Fossil Record of the Northern Neotropics* (M. Sánchez-Villagra, O. Aguilera, F. Carlini eds.) Bloomington: Indiana University Press, 192-213.

Scheyer, T. M., Aguilera, O. A., Delfino, M., Fortier, D. C., Carlini, A. A., Sánchez, R., Carrillo-Briceño, J. C., Quiroz, L. & Sánchez-Villagra, M. R. (2013). Crocodylian diversity peak and extinction in the late Cenozoic of the northern Neotropics. *Nature communications*, *4*, 1907.

Schumacher, G. H., (1976). The head and hyolaryngeal skeleton of turtles and crocodylians. In *Biology of the Reptilia 4* (C. Gans, T. Parsons eds.), London: Academic Press, 101-199.

Sereno, P. C., Larsson, H. C., Sidor, C. A., & Gado, B. (2001). The giant crocodyliform *Sarcosuchus* from the Cretaceous of Africa. *Science*, *294*(5546), 1516-1519.

Sill, W. D. (1970) Nota preliminary sobre un nuevo gavial del Plioceno de Venezuela y una discusión de los gaviales sudamericanos. *Ameghiniana, 7*: 151-159.

Simpson, G. G. (1933). A new crocodilian from the *Notostylops* beds of Patagonia. *American Museum Novitates, 623*: 1-9.

Simpson, G. G. 1960. Notes on the measurement of faunal resemblance. *American Journal of Science*, *258a*, 300–311.

Souza Filho, J.P. (1993) Ocorrência de *Charactosuchus fieldsi* e *Charactosuchus* n. sp. (Crocodilia, crocodilidae) no Neógeno da Amazônia Brasiliera. *Ameghinana, 30*: 113R.

Souza Filho, J.P., Bocquentin-Villanueva, J. (1989) *Brasilosuchus mendesi*, n. g., n. sp., um novo representante da Família Gavialidae do Neógeno do Acre, Brasil. *Anais XI Congresso Brasileiro de Paleontologia*, Curitiba 1, 457–463.

Spillmann, F. (1949). Contribución a la Paleontología del Perú. Una mamifauna fósil de la región del río Ucayali. Publicaciones del Museo de Historia Natural ‘‘Javier Prado’’, *1*, 1–39.

Stone, J. R. (2003). Mapping cladograms into morphospaces. *Acta Zoologica*, *84*(1), 63-68.

Tarsitano, S. F., Frey, E., & Riess, J. (1989). The evolution of the Crocodilia: a conflict between morphological and biochemical data. *American Zoologist*, *29*(3), 843-856.

Tejada, J., Antoine, P.-O., Baby, P., Pujos, F. & Salas-Gismondi, R. (2011). Basal or not so basal cingulates in the middle Miocene of Peruvian Amazonia. *IV Congreso Latinoamericano de Paleontología de Vertebrados*, San Juan, Argentina.

Tejada- Lara, J. V., Salas- Gismondi, R., Pujos, F., Baby, P., Benammi, M., Brusset, S., De Franceschi, D., Espurt, N., Urbina, M. & Antoine, P.-O. (2015a). Life in proto- Amazonia: Middle Miocene mammals from the Fitzcarrald Arch (Peruvian Amazonia). *Palaeontology*, *58*(2), 341-378.

Tejada-Lara, J., Salas-Gismondi, R. & Antoine, P.-O. (2015b). Pebas, Acre, and Parana systems: connecting the dots to elucidate mammalian biogeographic patterns in the Middle Miocene of South America. *IV Meeting of the Network for Neotropical Biogeography*, Panama City, Panama.

Thorbjarnarson, J. B. (1990). Notes on the feeding behavior of the gharial (*Gavialis gangeticus*) under semi-natural conditions. *Journal of Herpetology*, *24*(1), 99-100.

Tineo, D. E., Bona, P., Pérez, L. M., Vergani, G. D., González, G., Poiré, D. G., Gasparini, Z. & Legarreta, P. (2015). Palaeoenvironmental implications of the giant crocodylian Mourasuchus (Alligatoridae, Caimaninae) in the Yecua Formation (late Miocene) of Bolivia. *Alcheringa: An Australasian Journal of Palaeontology*, *39*(2), 224-235.

Vélez-Juarbe, J., Brochu, C. A., & Santos, H. (2007). A gharial from the Oligocene of Puerto Rico: transoceanic dispersal in the history of a non-marine reptile. *Proceedings of the Royal Society of London B: Biological Sciences*, *274*(1615), 1245-1254.

Vonhof, H. B., Wesselingh, F. P., & Ganssen, G. M. (1998). Reconstruction of the Miocene western Amazonian aquatic system using molluscan isotopic signatures. *Palaeogeography, Palaeoclimatology, Palaeoecology*, *141*(1), 85-93.

Walsh, S. A. & Suárez, M. (2005). First post-Mesozoic record of Crocodyliformes from Chile. *Acta Palaeontologica Polonica*, *50*(3), 595.

Watanabe, A. (2014). R2D3 and C3PO: A companion tool for testing the fidelity of twodimensional geometric morphometric data in a three-dimensional world of vertebrate crania. *74th Annual Meeting of the Society of Vertebrate Paleontology*, Berlin, 253A.

Watanabe, A., & Slice, D. E. (2014). The utility of cranial ontogeny for phylogenetic inference: a case study in crocodylians using geometric morphometrics. *Journal of Evolutionary Biology*, *27*(6), 1078-1092.

Weaver, J. P. (2012). *Geometric morphometrics of Antillean Crocodiles*. PhD thesis, Texas Tech University.

Webster, M. & Sheets, H. D. (2010). A practical introduction to landmark-based geometric morphometrics. *Quantitative Methods in Paleobiology*, *16*, 168-188.

Wesselingh, F. P. (2006). Miocene long-lived lake Pebas as a stage of mollusc radiations, with implications for landscape evolution in western Amazonia. *Scripta Geologica*, *133*, 1-17.

Wesselingh, F. P., & Macsotay, O. (2006). *Pachydon hettneri* (Anderson, 1928) as indicator for Caribbean–Amazonian lowland connections during the Early–Middle Miocene. *Journal of South American Earth Sciences*, *21*(1), 49-53.

Wesselingh, F. P., Räsänen, M. E., Irion, G., Vonhof, H. B., Kaandorp, R., Renema, W., Romero Pittman, L. & Gingras, M. (2002). Lake Pebas: a palaeoecological reconstruction of a Miocene, long-lived lake complex in western Amazonia. *Cainozoic Research*, *1*(1-2), 35-81.

Wesselingh, F. P., & Salo, J. A. (2006). A Miocene perspective on the evolution of the Amazonian biota. *Scripta Geologica*, *133*, 439-458.

Wesselingh, F. P., Hoorn, M. C., Guerrero, J., Räsänen, M. E., Pittmann, L. R., & Salo, J. A. (2006). The stratigraphy and regional structure of Miocene deposits in western Amazonia (Peru, Colombia and Brazil), with implications for late Neogene landscape evolution. *Scripta Geologica*, *133*, 291-322.

Wesselingh, F. P., Ranzi, A., & Räsänen, M. E. (2006). Miocene freshwater Mollusca from western Brazilian Amazonia. *Scripta Geologica*, *133*, 419-437.

Wesselingh, F. P., Guerrero, J., Räsänen, M. E., Pittmann, L. R., & Vonhof, H. B. (2006). Landscape evolution and depositional processes in the Miocene Amazonian Pebas lake/wetland system: evidence from exploratory boreholes in northeastern Peru. *Scripta Geologica*, *133*, 323-363.

Westgate, J. W. 1989. Lower vertebrates from an estuarine facies of the Middle Eocene Laredo Formation (Claiborne Group), Webb County, Texas. *Journal of Vertebrate Paleontology*, 9:282–294.

Whitaker, R. & Basu, D., 1983. The gharial (*Gavialis gangcticus*) a review. I. *Bombay Nat. Hist. Soc*, *79*(3), 19.

Wilberg, E. W. (2012). Phylogenetic and morphometric assessment of the evolution of the longirostrine crocodylomorphs. Ph.D. Thesis.

Wilberg, E. W. (2015). What's in an Outgroup? The Impact of Outgroup Choice on the Phylogenetic Position of Thalattosuchia (Crocodylomorpha) and the Origin of Crocodyliformes. *Systematic Biology*, *64*(4): 621-637.

Willard, B. (1966). *The Harvey Bassler Collection of Peruvian Fossils*. Lehigh University.

Willis, P. M. (1993). *Trilophosuchus rackhami* gen. et sp. nov., a new crocodilian from the early Miocene limestones of Riversleigh, northwestern Queensland. *Journal of Vertebrate Paleontology*, *13*(1), 90-98.

Willis, R. E., McAliley, L. R., Neeley, E. D., & Densmore, L. D. (2007). Evidence for placing the false gharial (*Tomistoma schlegelii*) into the family Gavialidae: inferences from nuclear gene sequences. *Molecular phylogenetics and evolution*, *43*(3), 787-794.

Wing, S. L., Herrera, F., Jaramillo, C. A., Gómez-Navarro, C., Wilf, P., & Labandeira, C. C. (2009). Late Paleocene fossils from the Cerrejón Formation, Colombia, are the earliest record of Neotropical rainforest. *Proceedings of the National Academy of Sciences*, *106*(44), 18627-18632.

Wu, X. C., Russell, A. P., & Brinkman, D. B. (2001). A review of *Leidyosuchus canadensis* Lambe, 1907 (Archosauria: Crocodylia) and an assessment of cranial variation based upon new material. *Canadian Journal of Earth Sciences*, *38*(12), 1665-1687.

Young, M. T., Brusatte, S. L., Ruta, M., & de Andrade, M. B. (2010). The evolution of Metriorhynchoidea (Mesoeucrocodylia, Thalattosuchia): an integrated approach using geometric morphometrics, analysis of disparity, and biomechanics. *Zoological Journal of the Linnean Society*, *158*(4), 801-859.

APPENDICES

APPENDICES

Anatomical abbreviations for figures

an	angular
anp	angular process
ar	articular
bo	basioccipital
bs	basisphenoid
CH	choana
cq	cranio-quadrate canal
cqg	cranio-quadrate groove
d	dentary
dc	dentary crest
d1-d22	dentary tooth positions
DI	diastema
d.s	splenial surface for dentary
ec	ectopterygoid
ec.j	jugal surface for ectopterygoid
ec.mx	maxilla surface for the ectopterygoid
emf	external mandibular fenestra
eo	exoccipital
f	frontal
FAD	mandibular adductor fossa
fae	quadrate foramen aerum
fic	foramen intermandibularis caudalis
fio	foramen intermandibularis oralis
fo	foramina
f.p	parietal surface for frontal
gf	glenoid fossa
j	jugal
if	incisive foramen
ma	maxillary alveolus
mlm	lateral margin of the maxilla
j.mx	maxilla surface for jugal
l	lacrimal
LC	laterosphenoid crest
lsp	laterosphenoid
lcf	lateral carotid foramen
m1-m22	maxillary tooth positions
mcq	medial hemicondyle of quadrate
mg	Meckelian groove
mx	maxilla
mx.ec	ectopterygoid surface for maxilla
mx.j	jugal surface for maxilla
mx.pm	premaxilla surface for maxilla
mxpp	posterior process of the maxilla
n	nasal
n.mx	maxilla surface for nasal
na	narial opening
nac	narial crest
naf	narial fossa

op	occlusal pits
or	orbit
p	parietal;
p1-p5	premaxillary tooth positions
pa	palatine
pa.mx	maxilla surface for palatine
pd1-4	pit for dentary tooth positions
pf	prefrontal
pf.f	frontal surface for prefrontal
pm	premaxilla
pmc	inter-premaxillary contact
pm.mx	maxilla surface for premaxilla
po	postorbital
pob	postorbital bar
pom	orbital margin of the postorbital
pop	postorbital process
ppo	paraoccipital process
pt	pterygoid
ptb	pterygoid bullae
ptf	post-temporal fenestra
q	quadrate
qj	quadratojugal
qj.j	jugal surface for quadratojugal
qj.q	quadrate surface for quadratojugal
QK	knob of quadrate crest A
rar	retroarticular process of the mandible
rac	retroarticular crest
rc	rostral canthi
s	splenial
sa	surangular
sab	surangular bridge
s.d	dentary surface for the splenial
so	supraoccipital
so.sq	squamosal surface for the supraoccipital
sof	suborbital fenestra
sp.d	dentary surface for splenial
sq	squamosal
sqe	squamosal eminences
sqg	squamosal groove
sqp	squamosal prong
sq.po	postorbital surface for the squamosal
stf	supratemporal fenestra
sy	symphysis
V	foramen for cranial nerve V
vo	vomer
vf	vagus foramen;
XII	foramen for cranial nerve XII

Institutional abbreviations and comparative material

AMNH: American Museum of Natural History, New York, USA.

ANSP: Academy of Natural Sciences, Philadelphia, USA.

DMR-KS: Khok Sung Collection, Department of Mineral Resources, Bangkok, Thailand.

IGM: INGEOMINAS, Bogotá, Colombia.

IRSNB: Institut Royal des Sciences Naturelles de Belgique, Brussels, Belgique.

MCNC: Museo de Ciencias Naturales de Caracas, Caracas, Venezuela.

MHN: Museo de Historia Natural, Universidad Nacional de La Plata, La Plata, Argentina.

MNHN: Muséum national d'Histoire naturelle, Paris, France.

MUSM, Vertebrate Paleontology Collection of the Natural History Museum of San Marcos University, Lima, Perú.

MRU: Museo Regional de Ucayali, Pucallpa, Perú.

NHM: Natural History Museum, London, England.

NMC: Canadian Museum of Nature, Ottawa, Canada.

OCP: Office Chérifien des Phosphates, Khouribga, Morocco.

SMNK: Staatliches Museum für Naturkunde Karlsruhe, Karlsrhue, Germany.

SMNS: Staatliches Museum für Naturkunde Stuttgart, Stuttgart, Germany

UCMP: University of California Museum of Paleontology, Berkeley, California, USA.

UF: Florida Museum of Natural History - University of Florida, Gainesville, USA.

UFAC Universidade Federale du Acre, Rio Branco, Brazil

USNM: United States National Museum, Smithsonian Institution, Washington, USA.

Brachychampsa montana: UCMP 128400

Arambourgia gaudryi: MNHN QU 17155 (holotype)

Orthogenysuchus olseni: AMNH 5178 (holotype)

Diplocynodon ratelii: MNHN SG 539, MNHN SG 557

Eocaiman cavernensis: AMNH 3158

Allognathosuchus polyodon: AMHN 2275, AMNH 6049.

Allognathosuchus cf. *polyodon*. AMNH 19080; AMNH 19083, AMNH 19084

Listrognathosuchus multidentatus: AMNH 5179

Navajosuchus mooki: AMNH 6780 (holotype)

Gryposuchus jessei: UFAC 1272

Eogavialis africanus: AMNH 5067, AMNH 5069, AMNH 5071, AMNH 5073, AMNH 5074, AMNH 5075, SMNS 11785, SMNS 50.734.

Piscogavialis jugaliperforatus: SMNK 1282 PAL (holotype); MUSM 439, partial skeleton; MUSM 2528, partial jaw.

cf. *Piscogavialis* sp.: MUSM 1997, complete skull, partial mandibles, osteoderms, scapula.

Pisco gavialoid: MUSM 1513, partial skull and jaws, osteoderms, postcranial elements.

cf. *Barinasuchus*: IGM 85-181, MNHN n/n

Necrosuchus ionensis: AMNH 3219 (holotype)

Eocaiman sp.: UCMP 38878

Purussaurus neivensis: IGM 88-184, IGM LR-320a, UCMP 39704, UCMP 38827, MUSM 927

Purussaurus brasilensis: UFAC 1403, UFAC 1421, UFAC 1488, UFAC 1773, UFAC 2508, UFAC 2509, UFAC 2655, UFAC 4732, UFAC 4770, UFAC 5174, UFAC 5300, AMNH 3855 (*Brachygnathosuchus braziliensis*).

Charactosuchus sp. UFAC 1664 (holotype of *Charactosuchus mendezi*), UFAC 1693, UFAC 1834, UFAC 2122, UFAC 2717, UFAC 3370, UFAC 3531

Leidyosuchus canadensis: NMC 8942

Alligator mississippiensis: UF 10941, UF 84197;

La Venta *Caiman*: UCMP 39978.

Caiman latirostris: MNHN DB 587, UF 62649

Caiman yacare: UF 121263, UF121249

Caiman brevirostris: UFAC 196,

Caiman crocodilus: UF 80913, UF 80914, MUSM

Melanosuchus niger: UF 53600, UF 62641

Paleosuchus trigonatus: MUSM DPV CR1,

Paleosuchus palpebrosus: UF 75023, UF 87980

Mourasuchus nativus: UFAC 1736; UFAC 1799, UFAC 2515

Mourasuchus atopus: UCMP 38012, MNHN n/n,

Caiman niteroiensis: UFAC 3142, UFAC 4678

Alligator mcgrewi: AMNH 7905, AMNH 8700,

Alligator mefferdi: AMNH 7016 (holotype)

Alligator mississippiensis: AMNH 7907 (galushai), UF 10941, UF84197

Alligator sinensis: UF 67829, UF 105540

Alligator olseni: UF 3537, UF205700

Gryposuchus sp.: UFAC 1796.

Eosuchus cf. *minor*: ANSP 10079.

Eosuchus lerichei: IRSNB 1740.

Thoracosaurus macrorhynchus: MNHN 1902-22.

Culebrasuchus mesoamericanus: UF 244434 (holotype)

Centenariosuchus gilmorei: UF 205708, UF252800

Eogavialis africanus: AMNH 5067, AMNH 5071 AMNH 5073, AMNH 5074, AMNH 5075, IMGP-UT n/n, SMNK 11785,

Argochampsa krebsi: OCP DEK-GE 1201

Gryposuchus neogaeus: MHN LP 26-413

Gryposuchus croizati: MCNC 77-72V (holotype), AMU CURS-58, AMU CURS 133.

Gryposuchus colombianus: IGM 184696

Ikanogavialis gameroi: MCNC 143-72V

Gavialis browni: AMNH 6279

Gavialis gangeticus: MNHN A5321, MNHN 1944-249, MNHN 1885-702, MNHN A-5312, UF 70592

Mecistops cataphractus: UF 166780, UF 166781

Crocodylus moreleti: MNHN A-5261, UF 29160

Crocodylus novoguineae: UF 71780

Gavialis bengawanicus: DMR-KS-201202-1

Borealosuchus sternbergii: USNM 6533

Crocodilus niloticus: MNHN n/n, UF 54812, UF 55787

Crocodilus acutus: UF 49953, UF54201, UF 151167

Crocodylus porosus: UF 134586

Osteolaemus tetraspis: UF 33749, UF 166783

Euthecodon arambourgi: MNHN LBE 001 (holotype).

Tomistoma dowsoni: MNHN LBE 311, NHM PV R 4769

Tomistoma cairense: SMNK 50.734, SMNK 50.739 , SMNK 50.741

Tomistoma schlegelii: MNHN A5311, MNHN 1944-233, UF 54210, UF 84888

Thecachampsa americana: AMNH 5663, UF 24127, UF/FGS 564, UF V1201, UF 3000

Relative snout width and length assessment

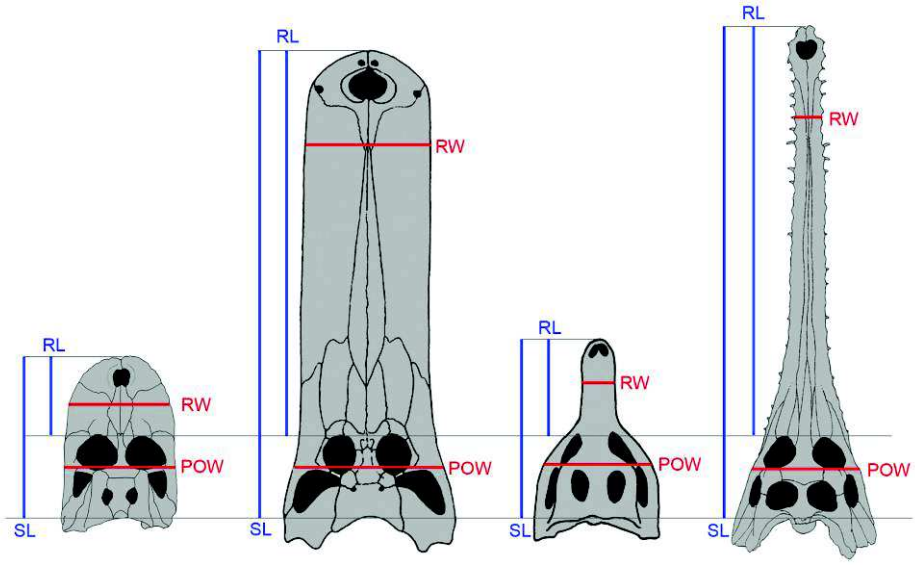

Figure Appendix 1. Cranial measurements within the four idealized snout eusuchian morphotypes. From left to right: short and wide, long and wide, short and narrow, long and narrow. Abbreviations: POW, postorbital width; RL, rostral length; RW, rostral width; SL, skull length.

Table Appendix 1. Cranial indices of Pebas crocodylians (in bold font) and other eusuchians. Potential intraspecific variation is not evaluated. Abbreviations: RL/SL, rostral length-skull length index; RW/POW, rostral width-postorbital width index. For Pebas *Paleosuchus* we used indices of *Paleosuchus trigonatus* as an exemplar.

Taxa	RL/SL	RW/POW
Bernissartia fagesii	0.72	0.58
Acynodon iberoccitanus	0.46	0.69
Iharkutosuchus makadii	0.39	0.51
Allodaposuchus precedens	0.57	0.64
Eothoracosaurus mississippiensis	0.75	0.23
Thoracosaurus neocesariensis	0.78	0.22
Eosuchus lerichei	0.72	0.33
Eogavialis africanus	0.76	0.29
Gryposuchus colombianus	0.74	0.35
Gryposuchus croizati	0.80	0.31
***Gryposuchus* nov. sp.**	**0.75**	**0.27**
Piscogavialis jugaliperforatus	0.83	0.27
Ikanogavialis gameroi	0.84	0.38
Siquisiquesuchus venezuelensis	0.82	0.23
Argochampsa krebsi	0.74	0.31
Gavialis gangeticus	0.76	0.25
Borealosuchus griffithi	0.66	0.56
Borelosuchus acutidentatus	0.67	0.51
Mecistops cataphractus	0.72	0.37
Crocodylus niloticus	0.65	0.76
Crocodylus porosus	0.70	0.67
Crocodylus acutus	0.72	0.67
Osteolaemus tetraspis	0.56	0.60
Australosuchus clarkae	0.65	0.66

Kambara murgoensis	0.59	0.77
Voay robustus	0.61	0.73
Thecachampsa americana	0.76	0.34
Tomistoma schlegelii	0.73	0.33
Crocodylus acer	0.68	0.44
Megadontosuchus arduini	0.73	0.41
Asiatosuchus germanicus	0.64	0.67
Pristichampsus vorax	0.68	0.61
Dollosuchoides desmorei	0.75	0.29
Leidyosuchus canadensis	0.67	0.65
Diplocynodon ratelii	0.63	0.60
Diplocynodon hantoensis	0.67	0.73
Diplocynodon muelleri	0.55	0.80
Diplocynodon darwini	0.57	0.70
Stagerochampsa mccabei	0.51	0.67
Albertochampsa langstoni	0.56	0.77
Brachychampsa montana	0.49	0.69
Alligator sinensis	0.58	0.75
Alligator mississippiensis	0.64	0.79
Alligator mefferdi	0.59	0.79
Alligator thompsoni	0.60	0.76
Alligator olseni	0.55	0.81
Alligator mcgrewi	0.47	0.65
Alligator prenasalis	0.56	0.68
Ceratosuchus burdoshi	0.54	0.62
Navajosuchus mooki	0.47	0.74
Wannaganosuchus brachymanus	0.49	0.65
Procaimanoidea uthaensis	0.49	0.72
Arambourgia gaudryi	0.47	0.59
Tsoabichi greenriverensis	0.59	0.96
Purussaurus brasiliensis	0.70	0.90
Purussaurus neivensis	**0.67**	**0.84**
Orthogenysuchus olseni	0.67	0.61
Mourasuchus amazonensis	0.83	0.70
Mourasuchus atopus	**0.82**	**0.85**
Mourasuchus arendsi	0.82	0.68
Caiman jacare	0.57	0.67
Caiman crocodilus	0.63	0.57
Caiman latirostris	0.58	0.75
Caiman niteroiensis	0.61	0.83
Melanosuchus niger	0.58	0.79
Melanosuchus fisheri	0.48	0.61
Paleosuchus trigonatus	0.59	0.61
Paleosuchus palpebrosus	0.54	0.62
Globidentosuchus brachyrostris	0.49	0.87
Gnatusuchus pebasensis	**0.49**	**0.93**
Pebas *Paleosuchus*	**0.59**	**0.61**
Kuttanacaiman iquitosensis	**0.52**	**0.86**
Caiman wannlangstoni	**0.51**	**0.70**

Character list of the phylogenetic analyses

Skull and mandibles. This character list was basically developed primarily by Brochu (1999, 2011) and Jouve et al. (2008). A small number of characters are derived from previous contributions (Benton & Clark, 1988; Norell, 1988, 1989; Norell & Clark, 1990; Buscalioni et al., 1992, 2001; Willis, 1993; Clark, 1994; Wu et al., 2001; Brochu, 2004b; Hua & Jouve, 2004; Jouve, 2004; Salisbury et al., 2006;; Ösi et al., 2007). Modifications/additions and new characters are indicated in bold font. Three characters are entirely new (i.e., 202-204). This list includes only osteological characters from the skull and jaws. For characters 1-46 see Brochu (2011).

47. Alveoli for dentary teeth 3 and 4 nearly same size and confluent (0), or fourth alveolus larger than third, and alveoli are separated (1).
48. Anterior dentary teeth strongly procumbent (0) or project anterodorsally (1).
49. Dentary symphysis extends to fourth or fifth alveolus (0); or sixth to eighth alveolus (1); **or eighth to twelfth alveolus (2); or beyond twelfth (3). Modified from Brochu (2004b), character 166.**
50. Dentary gently curved (0), or deeply curved (1), or linear (2) between fourth and tenth alveoli.
51. Largest dentary alveolus immediately caudal to fourth is 13 or 14 (0); 11 or 12 (1); no differentiation (2); or behind 14 (3).
52. Splenial with anterior perforation for mandibular ramus of cranial nerve V (0) or lacks anterior perforation for mandibular ramus of cranial nerve V (1).

53. Mandibular ramus of cranial nerve V exits splenial anteriorly only (0) or splenial has singular perforation for mandibular ramus of cranial nerve V posteriorly (1) or splenial has double perforation for mandibular ramus of cranial nerve V posteriorly (2).
54. Splenial participates in mandibular symphysis; splenial symphysis adjacent to no more than five dentary alveoli (0), or splenial excluded from mandibular symphysis; anterior tip of splenial passes ventral to Meckelian groove (1), or splenial excluded from mandibular symphysis; anterior tip of splenial passes dorsal to Meckelian groove (2), or deep splenial symphysis, longer than five dentary alveoli; splenial forms wide V within symphysis (3), or deep splenial symphysis, longer than five dentary alveoli; splenial constricted within symphysis and forms narrow V (4).
55. Coronoid bounds posterior half of foramen intermandibularis medius (0), or completely surrounds foramen intermandibularis medius at maturity (1), or obliterates foramen intermandibularis medius (2) at maturity.
56. Superior edge of coronoid slopes strongly anteriorly (0) or almost horizontal (1).
57. Inferior process of coronoid laps strongly over inner surface of Meckelian fossa (0), or remains largely on medial surface of mandible (1).
58. Coronoid imperforate (0), or with perforation posterior to foramen intermandibularis medius (1).
59. Process of splenial separates angular and coronoid (0) or no splenial process between angular and coronoid (1).
60. Angular–surangular suture contacts external mandibular fenestra at posterior angle at maturity (0) or passes broadly along ventral margin of external mandibular fenestra late in ontogeny (1).

61. Anterior processes of surangular unequal, little or no ventral process (0) or subequal to equal, well development ventral process (1).
62. Surangular with spur bordering the dentary tooth row lingually for at least one alveolus length (0), or lacking such spur (1).
63. External mandibular fenestra absent (0), or present (1), or present and very large; most of foramen intermandibularis caudalis visible in lateral view (2).
64. Surangular–dentary suture intersects external mandibular fenestra anterior to posterodorsal corner (0), or at posterodorsal corner (1).
65. Angular extends dorsally toward or beyond anterior end of foramen intermandibularis caudalis; anterior tip acute (0) or, does not extend dorsally beyond anterior end of foramen intermandibularis caudalis; anterior tip very blunt.
66. Surangular–angular suture lingually meets articular at ventral tip (0), or dorsal to tip.
67. Surangular continues to dorsal tip of lateral wall of glenoid fossa (0), or truncated and not continuing dorsally (1).
68. Articular–surangular suture simple (0), or articular bears anterior lamina dorsal to lingual foramen (1), or articular bears anterior lamina ventral to lingual foramen (2), or bears laminae above and below foramen (3).
69. Lingual foramen for articular artery and alveolar nerve perforates surangular entirely (0), or perforates surangular-articular suture (1).
70. Foramen aerum at extreme lingual margin of retroarticular process (0), or set in from margin of retroarticular process (1).
71. Retroarticular process projects posteriorly (0), projects posterodorsally, not higher than the posterior edge of the articular fossa (1), or projects posterodorsally higher than the posterior edge of the articular fossa (2).

72. Surangular extends to posterior end of retroarticular process (0), or pinched off anterior to tip of retroarticular process (1).
73. Surangular–articular suture orientated anteroposteriorly (0), or bowed strongly laterally within glenoid fossa (1).
74. Sulcus between articular and surangular (0), or articular flush against surangular within the adductor fossa (1).

For characters 75-78 see Brochu (2011).

79. Teeth and alveoli of maxilla and/or dentary circular in cross-section (0), or posterior teeth laterally compressed (1), or all teeth compressed (2).
80. Maxillary and dentary teeth with smooth carinae (0), or serrated (1), or with neither carinae nor serrations (2).
81. Naris projects anterodorsally (0), or dorsally (1).
82. External naris bisected by nasals (0), or nasals contact external naris, but do not bisect it (1), or nasals excluded, at least externally, from naris; nasals and premaxillae still in large contact (2), or nasals excluded from naris and nasals and premaxillae in weak contact (3), or nasals and premaxillae not in contact (4).
83. Naris circular or keyhole-shaped (0), or wider than long (1), or anteroposteriorly long and prominently teardrop-shaped (2).
84. External naris of reproductively mature males remains similar to that of females (0), or develops bony excrescence (ghara) (1).
85. External naris opens flush with dorsal surface of premaxillae (0), or circumscribed by a crest (1).

86. Premaxillary surface lateral to naris smooth (0), or with deep notch lateral to naris (1).

87. Premaxilla has five teeth (0) or four teeth (1) early in posthatching ontogeny.

88. Incisive foramen small, less than half the greatest width of premaxillae (0), or extremely reduced and thin (1), or large, more than half the greatest width of premaxillae (2), or large, and intersects premaxillary–maxillary suture (3).

89. Incisive foramen completely situated far from premaxillary tooth row, at the level of the second or third alveolus (0), or abuts premaxillary tooth row (1), or projects between first premaxillary teeth (2).

90. Dorsal premaxillary processes short, not extending beyond third maxillary alveolus (0), or long, extending beyond third maxillary alveolus (1).

91. Dentary tooth 4 occludes in notch between premaxilla and maxilla early in ontogeny (0), or occludes in a pit between premaxilla and maxilla; no notch early in ontogeny (1).

92. All dentary teeth occlude lingual to maxillary teeth (0), or occlusion pit between seventh and eighth maxillary teeth; all other dentary teeth occlude lingually (1), or dentary teeth occlude in line with maxillary tooth row (2).

93. Largest maxillary alveolus is no. 3 (0), or no. 5 (1), or no. 4 (2), or nos. 4 and 5 are same size (3), or no. 6 (4), or maxillary teeth homodont (5), or maxillary alveoli gradually increase in diameter posteriorly toward penultimate alveolus (6).

94. Maxillary toothrow posterior to first six maxillary alveoli curved medially or linear (0), or curves laterally broadly (1).

95. Dorsal surface of rostrum curves smoothly (0), or bears medial dorsal boss (1).

96. Canthi rostralii absent or very modest (0), or very prominent at maturity (1).

97. Preorbital ridges absent or very modest (0), or very prominent at maturity (1).

98. Antorbital fenestra present (0), or absent (1).

99. Vomer entirely obscured by premaxilla and maxilla (0), or exposed on palate at premaxillary–maxillary suture (1).

100. Vomer entirely obscured by maxillae and palatines (0), or exposed on palate between palatines (1).

101. Surface of maxilla within narial canal imperforate (0), or with a linear array of pits (1).

102. Medial jugal foramen small (0), or very large (1).

103. Maxillary foramen for palatine ramus of cranial nerve V small or not present (0), or very large (1).

104. Ectopterygoid abuts maxillary tooth row (0), or maxilla broadly separates ectopterygoid from maxillary tooth row (1).

105. Maxilla terminates in palatal view anterior to lower temporal bar (0), or comprises part of the lower temporal bar (1).

106. Penultimate maxillary alveolus less than twice the diameter of the last maxillary alveolus (0), or more than twice the diameter of the last maxillary alveolus (1).

107. Prefrontal dorsal surface smooth adjacent to orbital rim (0) or bearing discrete knob-like processes (1).

108. Dorsal half of prefrontal pillar narrow (0) or expanded anteroposteriorly (1).

109. Medial process of prefrontal pillar expanded dorsoventrally (0) or anteroposteriorly (1).

110. Prefrontal pillar solid (0) or with large pneumatic recess (1).

111. Medial process of prefrontal pillar wide (0) or constricted at base (1).

112. Maxilla has linear medial margin adjacent to suborbital fenestra (0) or bears broad shelf extending into fenestra, making lateral margin concave (1).

113. Anterior face of palatine process rounded or pointed anteriorly (0) or notched anteriorly (1).

114. Anterior ectopterygoid process tapers to a point (0) or forked (1).

115. Palatine process extends (0) or does not extend (1) significantly beyond anterior end of suborbital fenestra.

116. Palatine process generally broad anteriorly (0) or in form of thin wedge (1).

117. Lateral edges of palatines smooth anteriorly (0) or with lateral process projecting from palatines into suborbital fenestrae (1).

118. Palatine–pterygoid suture nearly at (0), or far anteriorly from posterior angle (1) of suborbital fenestra.

119. Pterygoid ramus of ectopterygoid straight, posterolateral margin of suborbital fenestra linear (0) or ramus bowed, posterolateral margin of fenestra concave (1).

120. Lateral edges of palatines parallel posteriorly (0) or flare posteriorly, producing shelf (1).

121. Anterior border of the choana is comprised of the palatines (0) or choana entirely surrounded by pterygoids (1).

122. Choana projects posteroventrally (0) or anteroventrally (1) at maturity.

123. Pterygoid surface lateral and anterior to internal choana flush with choanal margin (0) or pushed inward anterolateral to choanal aperture (1).

124. Posterior rim of internal choana not deeply notched (0), or deeply notched (1).

125. Internal choana not septated (0), or with septum that remains recessed within choana (1), or with septum that projects out of choana (2).

126. Ectopterygoid–pterygoid flexure disappears during ontogeny (0), or remains throughout ontogeny (1).

127. Ectopterygoid extends (0), or does not extend (1) to posterior tip of lateral pterygoid flange at maturity.

128. No posterior process of maxilla within lacrimal or within lacrimal and prefrontal (0), or maxilla with posterior process within lacrimal (1), or maxilla with posterior process between lacrimal and prefrontal (2).

129. Prefrontals separated by the frontal and nasals, anterior process of frontal extending far anterior to the anterior margin of the orbit (0), prefrontals separated by the frontal and nasals, anterior process of frontal around the same level or posterior to the anterior margin of the orbit (1), or prefrontals meet medially, anterior process of frontal around the same level or posterior to the anterior margin of the orbit (2).

130. Lacrimal longer than prefrontal (0), or prefrontal longer than lacrimal (1), or lacrimal and prefrontal both elongate and nearly the same length (2).

131. Anterior tip of frontal forms simple acute point (0), or forms broad, complex sutural contact either with the nasals or prefrontals (1).

132. Ectopterygoid extends along medial face of postorbital bar (0), or stops abruptly ventral to postorbital bar (1).

133. Postorbital bar massive and anteroposteriorly oval in cross section (0), or slender and rounded in cross section (1).

134. Postorbital bar bears process that is prominent, dorsoventrally broad, and divisible into two spines (0), or bears process that is short and generally not prominent (1).

135. Ventral margin of postorbital bar flush with lateral jugal surface (0), or inset from lateral jugal surface (1).

136. Postorbital bar continuous with anterolateral edge of skull table (0), or inset (1).

137. Dorsal margin of orbit flush with skull surface (0), or dorsal edges of orbits upturned, or (2) **dorsal and posterior edges upturned**. **Modified from Brochu (1999), character 103.**

138. Ventral margin of the orbit gently circular (0) or with a prominent notch (1) Brochu, 1999, character 139.

139. Palpebral forms from single ossification (0), or from multiple ossifications (1).

140. Quadratojugal spine prominent at maturity (0) or greatly reduced or absent at maturity (1).

141. Quadratojugal spine low, near posterior angle of infratemporal fenestra (0), or high, between posterior and superior angles of infratemporal fenestra (1).

142. Quadratojugal forms posterior angle of infratemporal fenestra (0), jugal forms posterior angle of infratemporal fenestra (1), or quadratojugal–jugal suture lies at posterior angle of infratemporal fenestra (2).

143. Postorbital neither contacts quadrate nor quadratojugal medially (0), or contacts quadratojugal, but not quadrate, medially (1), or contacts quadrate and quadratojugal at dorsal angle of infratemporal fenestra (2), or contacts quadratojugal with significant descending process (3).

144. Quadratojugal bears long anterior process along lower temporal bar (0), or bears modest process, or none at all, along lower temporal bar (1).

145. Quadratojugal extends to superior angle of infratemporal fenestra (0), or does not extend to superior angle of infratemporal fenestra; quadrate participates in fenestra (1).

146. Postorbital–squamosal suture orientated ventrally (0), or passes medially ventral to skull table (1).

147. Dorsal and ventral rims of squamosal groove for external ear valve musculature parallel (0), or squamosal groove flares anteriorly (1).

148. Squamosal–quadrate suture extends dorsally along posterior margin of external auditory meatus (0), or extends only to posteroventral corner of external auditory meatus (1).

149. Posterior margin of otic aperture smooth (0), or bowed (1).

150. Frontoparietal suture deeply within supratemporal fenestra; frontal prevents broad contact between postorbital and parietal (0), or suture makes modest entry into supratemporal fenestra at maturity; postorbital and parietal in broad contact (1), or suture on skull table entirely (2).

151. Frontoparietal suture between supratemporal fenestrae concavoconvex (0), or linear (1).

152. Supratemporal fenestra with fossa; dermal bones of skull roof do not overhang rim at maturity (0), or dermal bones of skull roof overhang rim of supratemporal fenestra near maturity (1), or supratemporal fenestra closes during ontogeny (2).

153. Shallow fossa at anteromedial corner of supratemporal fenestra (0), or no such fossa; anteromedial corner of supratemporal fenestra smooth (1).

154. Medial parietal wall of supratemporal fenestra imperforate (0), or bearing foramina (1).

155. Parietal and squamosal widely separated by quadrate on posterior wall of supratemporal fenestra (0), or parietal and squamosal approach each other on posterior wall of supratemporal fenestra without actually making contact (1), parietal and squamosal meet along posterior wall of supratemporal fenestra (2).

156. Skull table surface slopes ventrally from sagittal axis (0), or planar at maturity (1).

157. Squamosal on skull table is horizontal or nearly so (0), or upturned to form a posterolateral discrete horn (1); or producing a high transversely oriented eminence at the posterior margin (2) late in ontogeny.

158. Mature skull table with broad curvature; short posterolateral squamosal rami along paroccipital process (0), or with nearly straight sides; significant posterolateral squamosal rami along paroccipital process (1), or with nearly straight sides; posterolateral squamosal processes form long “prongs” (2).

159. Squamosal does not extend (0), or extends ventrolaterally to lateral extent of paraoccipital process (1).

160. Supraoccipital exposure on dorsal skull table small (0), or points posteriorly to the caudal margin of the parietal (1), or absent (2), or large (but parietals still in posterior border) (3), or large such that parietal is excluded from posterior edge of table (4).

161. Anterior foramen for palatine ramus of cranial nerve VII ventrolateral (0), or ventral (1) to basisphenoid rostrum.

162. Sulcus on anterior braincase wall lateral to basisphenoid rostrum (0), or braincase wall lateral to basisphenoid rostrum smooth; no sulcus (1).

163. Basisphenoid not exposed extensively (0), or exposed extensively (1), on braincase wall anterior to trigeminal foramen.

164. Extensive exposure of prootic on external braincase wall (0), or prootic largely obscured by quadrate and laterosphenoid externally (1).

165. Laterosphenoid bridge comprised entirely of laterosphenoid (0), or with ascending process of palatine (1).

166. Capitate process of laterosphenoid orientated laterally (0), or anteroposteriorly toward midline (1).

167. Parietal with recess communicating with pneumatic system (0), or solid, without recess (1).

168. Significant ventral quadrate process on lateral braincase wall (0), or quadrate–pterygoid suture linear from basisphenoid exposure to trigeminal foramen (1).

169. Lateral carotid foramen opens lateral (0), or dorsal (1) to basisphenoid at maturity.

170. External surface of basioccipital ventral to occipital condyle orientated posteroventrally (0) or posteriorly (1) at maturity.

171. Posterior pterygoid processes tall and prominent (0), or small and project posteroventrally (1), or small and project posteriorly (2).

172. Basisphenoid thin (0), or anteroposteriorly wide (1) ventral to basioccipital.

173. Basisphenoid not broadly exposed ventral to basioccipital at maturity; pterygoid short ventral to median eustachian opening (0), or basisphenoid exposed as broad sheet ventral to basioccipital at maturity; pterygoid tall ventral to median eustachian opening (1).

174. Exoccipital with very prominent boss on paroccipital process; process lateral to cranioquadrate opening short (0), or exoccipital with small or no boss on paroccipital process; process lateral to cranioquadrate opening long (1).

175. Lateral eustachian canals open dorsal (0) or lateral (1) to medial eustachian canal.

176. Exoccipitals terminate dorsal to basioccipital tubera (0), or send robust process ventrally and participate in basioccipital tubera (1), or send slender process ventrally to basioccipital tubera (2).

177. Quadrate foramen aerum on mediodorsal angle (0), or on dorsal surface of quadrate (1).

178. Quadrate foramen aerum is small (0), or comparatively large (1), or absent (2) at maturity.

179. Quadrate lacks (0), or bears (1) prominent, mediolaterally thin crest on dorsal surface of ramus.

180. Attachment scar for posterior mandibular adductor muscle on ventral surface of quadrate ramus forms modest crests (0), or prominent knob (1).

181. Quadrate with small, ventrally reflected medial hemicondyle (0), or with small medial hemicondyle; dorsal notch for foramen aereum (1), or with prominent dorsal projection between hemicondyles (2), or with expanded medial hemicondyle (3), **or more detached, ventromedially projected medial hemicondyle (4). From Riff & Aguilera (2008), after Brochu (1999), character 112.**

182. Edge of the maxillary tooth alveoli lower or at the same level than the space between toothrow (0) or edge of maxillary tooth alveoli higher than the space between toothrow (toothrow underlined) (1).

183. Ventral border of exoccipital: convex and ventrally projected, hiding the posterior opening of the cranioquadrate passage from the occipital view (0), or straight, sharpen or smoothly convex and does not hide the posterior opening of the cranioquadrate passage from the occipital view (1).

184. Occipital surface sloped, visible in dorsal view (0), or vertical or not visible in dorsal view (1) at maturity.

185. **Ventral premaxillary-maxillary suture mainly transversal to W-shaped (0), or acute, V-shaped suture, exceeds posteriorly the level of the second alveoli (1). Modified from Jouve (2004), character 168.**

186. Less than 18 teeth (0), 18 to 22 teeth (1), or more than 22 teeth (2) on maxilla.

187. Lateral edge of the skull table at the level of the postorbital-squamosal suture situated laterally or at the same level as (0), or medially to (1) the quadrate condyle in dorsal view at maturity.

188. Frontal ends at the same level or posterior (0) or extends well anterior (1) to the anterior extension of the prefrontal.

189. Maxilla posterior process without tooth, short or absent (0), or long, longer to the distance between the three last teeth (1) in ventral view.

190. **Interorbital bridge narrower to equivalent (0), or broader (1) than the width of the orbit. Modified from Jouve (2004), character 181.**

191. **Supratemporal fenestra longer than wide, rounded (0), or quadrangular, wider than long, large (1) at maturity. Jouve et al. (2008), character 199.**

192. Presence (0), or absence (1) of a medial crest on the basioccipital.

193. Absence (0), or presence (1) of a posterior dentary process between splenial and angular on the ventral side.

194 Dorsal margin of the articular on the retroarticular process largely visible in lateral view (0), or slightly or not visible in lateral view (1).

195 Posterior margin of the orbit anterior to the posterior margin of the suborbital fenestra (0), or posterior or at the same level than the posterior margin of the suborbital fenestra (1) measured at the level of the postorbital-frontal suture in the orbital margin.

196 Basioccipìtal-exoccipital process ventral to occipital condyle (basioccipital plate) with parallel or ventrally convergent sides (0) or ventrally divergent sides (1) in posterior view.

197. Absence (0) or presence (1) of a smooth medial depression ventral to the basioccipital and posterior to the medial Eustachian foramen.

198. Dentary teeth series behind to alveoli 12-13 are pointed to slightly blunt (0); **or globular (1);** or molariform multicusped (2). **Modified from Salas-Gismondi et al., 2015a, character 198.**

199. First four alveoli in the dentary are the same size or smaller than other dentary alveoli (0) or are the largest within the dentary (1).

200. Orbits longer than wide (0) or wider than long to rounded (1) late in ontogeny.

201. From the series composed by the three most posterior premaxillary alveoli: (0) the intermediate alveolus is the biggest, or (1) anterior and intermediate alveoli are bigger, similar in size, or (2) the anterior is the biggest. Modified from Salas-Gismondi et al., 2015a, character 201.

202. Frontal plate surface well ornamented with deep pits and furrows (0) or surface only little sculpted to relatively smooth (1). [New]

203. Retroarticular longitudinal crest absent (0) or present (1). [New]

204. Infratemporal fenestra bears an acute to straight dorsal angle, triangular shaped ITF (0); or its dorsal margin forms a gentle curve, not an angle, ovoid-shaped ITF (1). [New]

205. Posterior bar of supratemporal fenestra (i.e., post-temporal bar) thick (0) or thin (1). From Jouve (2004), character 184.

206. Anterolateral margin of the orbit flush with rostral surface (0) or upturned (1). Adapted form Brochu (1999), character 103.

Character matrix

This data matrix is based on Brochu (2011), Jouve et al. (2008), and Salas-Gismondi et al. (2015a). Character score coding has been updated by direct examination of original fossil and recent material (see appendices), as well as by adopting character scores from recent publications. Scores for *Mourasuchus* species are mainly from Bona et al. (2013). *Culebrasuchus mesoamericanus* and *Centenariosuchus gilmorei* were mainly scored after Hastings et al. (2013), complemented by personal observations. *Caiman brevirostris* is scored after Fortier et al. (2014). *Argochampsa krebsi* is scored after Jouve et al. (2008) whereas scores for *Gavialis bengawanicus* are from Delfino & De Vos (2010). *Eosuchus lerichei* is scored after Delfino et al. (2005). Besides *Gryposuchus* nov. sp. from Iquitos bonebeds, South American gharials are represented in this matrix by *Ikanogavialis gameroi* Sill, 1970, *Piscogavialis jugaliperforatus* Kraus, 1998, *Siquisiquesuchus venezuelensis* Brochu & Rincón, 2004, *Gryposuchus colombianus* (Langston 1965), and *Gryposuchus croizati* Riff & Aguilera, 2008. We also include character coding of the Caribbean taxon *Aktiogavialis puertoricensis* based on Velez-Juarbe et al. (2007). *Aktiogavialis* was codable only for 13.1% of the proposed characters (i.e., 27 of 206); and considering that water abrasion affected preservation of the holotype and only specimen (2007), we cautiously scored it as unknown for prootic exposure around the trigeminal foramen (i.e., character 164-?). Although *Gryposuchus neogaeus* (Burmeister, 1885) and *Gryposuchus jessei* Gürich, 1912 were included in anatomical comparisons, these taxa are not included in the current phylogenetic analyses because their tentative scorings are redundant with other *Gryposuchus* species. New material of *Piscogavialis jugaliperforatus*, comprising a well-preserved partial skull and mandibles (MUSM 439; MUSM 2528), was used to complement scores provided by

Delfino et al. (2005) based on the type specimen (SMNK 1282 PAL). Our matrix also includes new scorings for the non-South American taxon *Eogavialis africanus* based on direct examination of original material (AMNH 5067, AMNH 5069, AMNH 5071, AMNH 5073, AMNH 5074, AMNH 5075, SMNS 11785, SMNS 50.734).

Bernissartia fagesii
????? ?0??? 01111 02100 ?00?0 ?000? ??000 0?100 010??
?0010 ?000? ????? ?10?0 ?00?0 01?1? ???00 010?0 000?0
0030? 001?? ???10 00??? ?1?00 00?00 0??01 00?0? ??001
100?0 ?0??0 ?0?00 10?0? ?00?0 0???? ????0 00?00 00?00
0000? 0?000 0??00 0?100 00000 0

Acynodon iberoccitanus
????? ????? ????? ????? ????? ????? ????? ????? ?????
?1010 3101? ????? ??0?? ????? 0?0?? ???00 010?0 00000
10600 00100 ??001 00??? ?0000 00010 1?00? ??200 100?1
100?1 10?00 00??0 10100 000?2 ????? ????1 ???0? ???01
00010 01100 00??1 00100 00000 0

Iharkutosuchus makadii
????? ????? ????? ????? ????? ????? ????? ????? ?????
?1012 3???? ????? 110?? ?00?? 10?1? ???00 01??0 00001
10610 001?0 ???01 10??? ?0000 00100 11000 01201 1001?
100?1 ?0?00 ?0??? 12??? 100?3 ????? 1???1 00000 0??11
00?10 00000 00??1 ?0200 00000 0

Hylaeochampsa vectiana
????? ????? ????? ????? ????? ????? ????? ????? ?????
????? ????? ????? ????? ????? ??0?? ???0? ????? ????0
?0?10 001?0 0??01 10?0? 00000 00100 1000? 0?221 10001
110?? ??1?0 ?0000 10100 00000 0???? 1?001 00100 0?011
0001? ?0000 00??0 00??0 ?0?00 0

Borealosuchus sternbergii
00000 0000? 11001 0?100 10000 00101 00000 1?00? ??0??
?0110 10000 000?0 00100 00000 10000 0??00 020?0 00000
01310 00100 01000 001?0 ?0000 01110 10001 01000 00111
100?0 00100 ?0000 00100 10100 0000? 1?001 00110 00000
00100 11000 00011 00000 00000 0

Eothoracosaurus mississippiensis
????? ?0??? ????? ????0 1??00 0???? ????0 0?00? ??0??
??1?2 ???3? ????? 0???? ?00?0 21?0? ???00 130?0 00??1
02500 0010? ?0000 00??? ?0000 10100 1000? ???00 0?001
100?? ?01?? ?1000 0010? 001?0 0???? ????1 00010 00000
01001 101?1 10?1? 00000 100?0 0

Thoracosaurus neocesariensis
????? ?0??? ???11 1?1?0 10??? ?0011 ??0?? 0?00? ??0??
?1122 ???3? ????? ??10? 000?0 2?0?? ???00 130?0 000?1
02500 00100 ??000 000?0 ?0000 10100 10000 ?0000 00001
110?0 0010? ?1?00 00100 00101 00000 0?001 00?10 00000
0100? ??0?1 10??0 ?00?0 ????0 0

Eosuchus lerichei
????? ????? ?0101 1???0 1???? ???11 ????? ??0?? ?????
?1112 ???3? ????? ????? ????? ????? ???00 120?0 00001
02500 00100 ?0010 000?? ?0000 00100 1000? 01000 10??1
110?0 00?0? 010?2 0010? 00100 ????? ????1 0??10 10100
31010 0?000 00??0 00000 00?10 0

Eosuchus minor
????? ?0??? 0??11 1???0 1?00? 0?01? ??000 0?000 ??0??
?1122 ??030 0?000 0?10? 00000 2100? ???00 120?0 000?1
02500 00100 ?0000 00?00 00000 10100 10000 ?1000 00001
110?? ?0100 ?10?1 00100 001?0 100?? 1???1 01010 10100
31010 0?000 00?10 00000 00010 0

Eogavialis africanus
????? ???1? ????1 1???0 10??? ????? ??0?? ????? ??0??
?11?2 2003? ????0 0?110 000?? 2101? ???00 120?0 00101
02500 00100 ?0000 00000 00000 10100 10000 01000 00001
110?0 00100 ?1001 00100 00101 00?00 0??01 01010 10000
01001 00010 10?00 11001 10010 1

Gryposuchus colombianus
????0 ?0??? 001?? ????0 1??00 0???? ????? ????? ??0??
?1132 2?030 100?0 00110 00000 2100? ???00 13110 011?1
02500 00100 ?0?00 00??0 ?0000 10101 10000 01100 00000
121?0 00100 ?1001 10100 00201 00010 0?001 21010 10000
?100? 10101 21?00 11001 21111 1

Siwalik *Gavialis*
????? ????? ????? ????? ?0??? ????? ????? ?0??? ?????
???32 ???3? ????? 0?100 000?? 2?0?? ???0? ?40?? ??10?
?2??0 ????0 ?0?0? ????0 ?0000 ?0?00 100?0 ?1??? ?0000
?21?0 00100 0100? ?0?00 0?101 ?0??? ??00? 21010 10???
01001 ?0111 21?00 ?1??1 ?0001 1

Gavialis bengawanicus
????? ????? ???11 1???? ????? ????? ????? ??1?? ?????
?1?32 ?003? ????0 00100 00000 2100? ????? ?4??? ????1
02500 00?00 ?000? ??0?? ?01?0 10??? 1??0? ??0?0 ?0000
?21?0 0?100 01001 10100 1?101 ???0? 0?00? ?1010 10???
01?0? 101?1 11??0 11001 ?0001 1

Gavialis gangeticus
02000 0000? 00111 10110 10000 00011 10000 00?00 00000
01132 20030 00000 00100 00000 21000 10000 14010 00101
02500 00100 00000 00000 00000 10100 10000 01100 00000
12100 00100 01001 10100 00101 00000 00001 21010 10000
01001 20111 21100 11001 10001 1

Arktiogavialis puertoricensis
????? ????? ????? ????? ????? ????? ????? ????? ?????
????? ????? ????? ????? ????? ????? ????? ????? ?????
????? ????? ????? ????? ????? ????? ?0?0? ????? ?????
?2??? ????? ??001 10100 0???1 ?00?? 0???? 210?? 1????
???0? ????? 01??? 1???? ?00?0 ?

***Gryposuchus* nov. sp.**
????? ????? ????? ????? ????? ????? ????? ????? ?????
?1132 20?4? ????0 0011? 00?00 211?? ???00 120?0 01101
02500 00100 ?0000 00??? ?0000 10100 1000? 01000 00001
110?0 00000 01?01 0010? 00101 ????? 0???1 ?101? 10000
41001 10111 21000 11001 21111 1

Gryposuchus croizati
????? ????? ????? ????? ????? ????? ????? ????? ?????
?1132 2???? ????? ????? ????? ????? ???00 131?0 01101
02500 00100 ????? ?0??? ?0??0 ??111 1000? ?1?0? ?00?0
121?? ?010? ????1 101?? 0?201 ????? ????? 21010 1????
41?01 10??1 21??? 11?01 211?1 1

Piscogavialis jugaliperforatus
????? ????? ????? ????? ????? ????? ??1?? ????0 ?????
?1132 20030 0?000 001?0 ???10 2?00? ???00 130?0 01101
02500 00100 ?0000 000?0 ?0000 10100 10000 01?00 00001
110?0 00001 01002 00100 00201 ?0?1? 0?0?1 2??1? 10000
41001 20110 2?000 1?000 10111 1

Ikanogavialis gameroi
????? ????? ????? ????? ????? ????? ????? ????? ?????
?1132 ????? ????? 0?10? ??0?0 2?00? ????? ?30?? 0?1?1
02500 0010? ???00 0???? ??0?0 10??0 10??? ??000 ??000
?11?? ?0?0? ????2 10100 00201 ????? ????? 21010 10??0
?1?01 20?10 2???0 11?01 ?01?1 1

Siquisiquesuchus venezuelensis
????? ????? ????? ????? 1???? ????? ????? ????? ?????
?1132 ???3? 0???? ????? ????0 ????? ????? 1?0?? 0???1
02500 001?? ???0? ????? ?0000 10??0 1???? ????? ??000
?20?? ?0??? ?1?0? ?010? 002?1 ????? ???0? 21010 10??0
41?0? 20?10 2??00 ?0?00 ?01?1 1

Argochampsa krebsi
????? 0?00? 0?11? 1???? ????? ?0??? ????? ???0? ?????
?11?2 ????? ????? ????? ????? ????? ????? 130?0 00001
02500 00100 ??0?? 0?1?? ?00?0 10??? 1000? ??000 10111
110?? ?0000 0?001 1010? 00201 ?0??? 0???? ???1? 1?000
01000 200?0 01??0 11?00 10??0 1

Pristichampsus vorax
????0 ?0??? 01001 001?0 1?000 00111 ??010 0?10? ??1??
?1110 ?000? ????0 ??100 0001? ??0?? ???21 010?0 000?0
00300 01100 ?0000 00??0 ?0000 00100 10001 01000 00111
110?? ?0100 00100 00100 10100 0???0 1??11 00110 00000
20110 01000 00??1 000?0 00000 0

Pristichampsus geiseltalensis
????? ????? ???0? 0???0 1?000 ?0??1 ??010 0?1?? ?1???
?1110 1000? ????? 0?1?? ??0?? ??1?? ???21 ?20?0 00000
00300 011?? ?0000 00??? ?0000 00100 1010? ?1000 00111
110?0 ?0?00 ?0?01 0010? 10100 ????? ????1 ???10 00000
2???? ????? ????? ??0?0 0???? ?

Planocrania hengdongensis
????? ????? ????? ????? 1???? ????? ????? ????? ?????
?1110 ???0? ????? ??1?? ??0?0 ??0?? ???20 010?0 ?????
01300 ??1?? ??0?0 00??? ?0??? ?0100 1???? ???0? 0?1?1
100?? ????? ?0?0? 00100 ?0100 ????? 1???1 ???10 ?1000
1???? ????? ????? ??0?0 000?0 0

Leidyosuchus canadensis
????0 ?0??? ????1 ????0 10000 011?1 ??10? 0?11? ?11??
?0110 ?0000 0?0?0 1?110 00001 1101? ???00 010?0 00000
00300 00100 00010 00100 01000 01110 10001 01000 10111
100?0 10100 10010 00100 10100 00000 1?001 00110 01000
10100 11000 00?01 00000 00000 0

Diplocynodon ratelii
????? ?0??? ???00 0???0 10?00 ?1111 00140 0?10? ?21??
?0100 1101? ????0 11100 0001? ?101? ???00 120?0 00010
12300 00100 01010 00??0 ?0000 00111 10001 01000 10111
100?? 10100 10000 00101 10100 00000 1?101 00110 01000
10110 01000 00011 00000 00000 0

Diplocynodon hantoniensis
100?? ?1?1? 01000 01000 10000 11111 ??140 0?101 ?21??
?0110 11010 ????0 11100 00011 2101? ???00 120?0 ?001?
11300 ?0100 ?1010 001?0 ?0000 00101 10001 010?0 10111
100?1 10100 ?0010 10101 10100 0??0? 1??01 0011? 01000
10110 01?00 00011 00?00 ????? 1

Diplocynodon muelleri
????? ????? ????? ????? 1?01? ?1??? ??14? 0?10? ?21??
?0100 1??2? ????0 1110? ?1001 ?100? ???00 120?1 000?0
12300 00100 01010 00??? ?0000 01111 10000 01000 1?1?1
100?1 10??0 ?01?0 10101 10100 ????? ???01 00110 01000
10??? ??0?0 0???1 ??000 0???? ?

Diplocynodon tormis
????? ????? ????? ????? 1???? ?1??? ????? ??10? ?21??
?01?0 11?1? ????0 1?1?0 0???? ?1??? ???0? 120?? 000?0
12300 00100 ?1010 001?? ?0000 00111 100?0 ?1000 10111
100?1 10100 00010 10101 10100 ?0??? 1?001 ?0110 01000
10??? ??0?0 0???? ????0 ?0??? ?

Diplocynodon darwini
10000 1001? 01000 0?000 10000 ?1111 ??140 0?101 121??
?0110 10010 ??0?0 1?100 00011 11010 0??00 020?0 00010
10300 00100 ?0??0 00??0 ?0000 00111 1?001 010?0 1?111
100?1 10100 ?0110 10101 10100 0???? ???01 00110 01000
10110 01?00 0?011 ?0??0 ????? ?

Baryphracta deponiae
100?0 ?0??? ????0 ????0 1?0?? ?1??? ??14? 0?10? ?21??
??1?0 1??0? ????0 1?10? ?0??1 ?10?? ???00 1???0 00??0
10300 001?0 ????0 00??? ??0?0 001?1 1000? 010?0 1?111
100?1 10100 ?0??0 11?0? 101?0 0???? ????1 ???1? ?1000
10??? 0???0 0???? ????? ?0?00 0

Stangerochampsa mccabei
????1 10??? 01001 0?000 10000 01111 00100 0?01? ?11??
?1110 00100 ????0 11111 0000? 110?? ???00 110?0 00311
10200 00100 ?0010 00??? ?0000 00011 11001 01210 11111
100?1 10200 ?0?11 00102 10100 0??1? 1??01 00110 01000
10110 01000 00?11 00?00 00000 0

Albertochampsa langstoni
????? ????? ????? ????? ????? ????? ????? ????? ?????
????? ????? ????? ????? ????? ????? ???00 1?0?0 ?0??1
10200 001?0 ??01? 00??? ?00?? 00011 11001 0?2?0 1?111
100?? ?0?0? ?0?11 00102 10100 ????? ???01 00110 01?00
00??? ????? ????? ????0 00?00 0

Brachychampsa montana
10101 1001? 1100? ??000 1??00 01111 00?00 0?103 111??
?1110 0101? ????0 1110? 00001 11010 0??00 110?0 00311
10100 00100 ?0010 001?0 ?0100 00011 11001 01210 11111
100?1 10200 ?0111 00101 10103 00010 1?001 00110 01000
10110 01000 00011 00100 00000 0

Brachychampsa sealeyi
????? ????? ????? ????? ????? ????? ????? ??10? ??1??
?1110 0??0? ????? ?11?? 00001 ?1?1? ???00 1?0?0 00311
10100 0010? ??010 ????? ????0 0???? ????? 0?210 ?1101
?00?? ????? ????1 00??? ????3 ????? ????? ???1? ?10??
10??? ????? ????? ????? 00?00 0

Alligator sinensis
10101 1101? 11001 01000 10110 11111 00110 00112 11111
01100 00120 ?0010 11200 00011 1101? ?1100 10000 10010
10200 00100 00010 00110 01000 00011 11002 01101 11111
11001 10200 10112 00102 10102 00011 11001 00110 01000
10110 01000 00?11 00000 00000

Alligator mississippiensis
10101 1001? 01001 00000 10110 11111 00110 00112 10110
01100 01120 10010 11200 01011 11010 01100 10000 10010
10200 00100 00010 00111 00000 00011 11002 01101 11111
11001 10200 10112 10102 10102 00011 11001 00110 01000
10110 01000 00011 00000 00000 0

Alligator mefferdi
????? ????? ????? ????? ????? ??1?? ????? ??11? ?????
?1100 00120 10000 11200 01011 11010 0??00 100?0 10010
10200 00100 ?0?10 001?1 ?0000 000?1 11002 01111 11111
110?1 10200 ?0112 10102 10102 0??1? ??001 00110 01000
10110 01?00 00011 00000 00000 0

Alligator thompsoni
????? ????? ????? ????0 1???? ????1 ????? 0?1?? ?????
?1100 00?2? ????0 11200 01001 1101? ???00 100?0 100?0
10200 0010? ?0010 001?1 ?0000 00??? ?1??2 ??1?1 11111
110?1 ?0200 101?2 10102 10102 ?001? 11?01 00110 01000
10??? 01?00 0???? ?0000 00?00 0

Alligator olseni
????? ?0?1? ????1 0???0 1?100 11111 ???10 0?11? ?????
?1101 0010? ????0 11200 00001 1101? ???00 100?0 10010
10200 ??100 ???10 00??0 ?0?00 01011 11102 01111 11111
110?1 10200 ?0112 00102 10102 0???? ??001 00?1? 01000
10?10 01000 00011 ?0000 00?00 0

Alligator mcgrewi
10001 0001? 01001 0?000 10000 111?1 101?? 0?11? ??1??
?1111 0010? 100?0 11100 00011 1101? ???00 000?0 10010
10200 00100 ?0010 001?0 01000 00011 11002 01111 11111
10001 10200 ?0112 00102 10102 0?01? ??001 00110 01000
10110 010?0 00011 00000 00?00 0

Alligator prenasalis
10001 ?0?1? ????1 0?0?0 10000 11111 ??100 0?112 111??
?1111 0010? ????0 11100 00011 11010 0??00 000?0 10010
10200 00100 ?0010 00110 01000 00011 11002 01111 11111
100?1 10200 ?0112 00102 10100 0001? 1?001 00110 01000
10110 01000 0?01? 00000 00000 0

Ceratosuchus burdoshi
????? ????? ????? ????? ????? ????? ????? 0?1?? ?????
?1111 0??0? ????0 1?10? ?00?1 ??01? ???00 010?0 ?0210
10200 00100 ???10 00??0 ????0 0???0 1???? ?1??0 ??111
100?? ????? ?0??? ?010? 111?? ????? ????1 0??10 01000
10??? 010?0 0???? ??100 ?0?00 0

Allognathosuchus polyodon
????? ????? ????? ????? ????? ????? ????? ????? ?????
?1111 0010? ????0 1?11? ?00?1 ?1?1? ???00 010?0 00?10
10200 001?0 ????? 00??0 ?00?0 0?0?1 1100? ?1??1 1?111
100?? ????? ?0??2 0010? 101?? ????? ????1 ???1? ?1???
10??? ??0?0 ????? ??10? 0???? 0

Allognathosuchus wartheni ("Wilwood alligatorid")
????1 ?0??? ????? ????0 ?0000 ?1111 ??100 0?11? ??1??
?1111 0010? 100?0 11110 00001 ?101? ???00 010?0 00010
10200 00100 00010 001?0 ?0000 00?01 11001 ?1111 11111
10??1 10200 ?0112 00102 10100 00?1? 1?001 00110 01?00
10??? ????0 ????? ???0? ????? ?

Navajosuchus mooki
????? ?0?1? ????? 0???0 ?00?? ?1111 ??1?? 0?111 111??
?1111 0010? ????0 1?11? ?00?? 110?? ???00 010?0 00210
10200 001?? ?0?10 00??0 ???00 ?00?1 1100? 01110 11111
100?? ?020? ?0112 ?0102 10100 0???? 1??01 0??10 01000
10110 0?000 000?1 00100 00000 0

Wannaganosuchus brachymanus
????1 ?0??? 1?00? 0???0 10000 ?1111 00100 0?11? ??1??
?1111 00?0? ????0 ??100 ?00?1 ??0?? ???00 110?0 0001?
10200 ??100 ???10 00??0 ?1000 00??? 1??0? ?1111 1?111
100?? ????? ?0?12 001?? 10100 0???? ????1 0011? 01000
10110 01000 00??1 ?0100 00?00 0

Procaimanoidea kayi
????1 10?1? ????? 0???0 10?00 ?1111 ??10? 0?112 121??
???01 0?1?? 100?0 1?110 00001 110?? ???10 ????? 0???0
10?00 001?? ?0?10 00??0 ?0000 00001 11001 011?1 11111
1000? ?0200 ?0112 00102 10102 0???? ???01 00110 01000
10?1? ??00? 00011 ?0?0? 0???? ?

Procaimanoidea utahensis
????? ????? ????? ????? ????? ????? ????? ????? ?????
?1101 00?00 ??010 11110 ??001 1101? ???10 110?0 100?0
1020? 00100 ??010 00??? ?0000 000?1 11001 01111 1?111
100?1 ?0200 ?0112 0010? 10100 0???? ???01 00110 01000
10??? 00000 0??11 ?0000 00000 0

Arambourgia gaudryi
????? ????? ????? ????? ????? ????? ????? ????? ?????
?1111 0??0? ????0 1?100 ?0??1 ?10?? ???00 01??0 00??0
10200 001?0 ?0?10 00100 0?000 0???? 11001 ?1011 1?111
100?1 102?0 10?12 ?0?02 10100 ????? ????0 0011? 01000
1011? ?00?? 00?11 00000 00000 0

Necrosuchus ionensis
????? ?0??? ????? ????0 ???01 ?111? ??130 0?11? ??1??
?1100 0??2? ????? ??1?? ?0??? ??0?? ???00 ????? ?????
????? ????? ????? ????? ????? ????? ????? ????? ?????
????? ????? ????? ????? ????? 0???? ????? ?0??? ?1?0?
1???? ????? ?0??? 00?0? ????? ?

Tsoabichi greenriverensis
????? ????? ????? ????0 1???? ????? ????? ??10? ?20??
?1100 ???2? ????? ??1?? ????1 1???0 1??00 010?1 0????
10??0 001?? ????? ?0??? ????? ????? ????? ??000 1?111
1?0?1 ?0??? ?0??2 11??? 101?3 ????? ????? ????? ?100?
?0??? ?10?0 0???? ???00 00?00 0

Purussaurus mirandai
????? ????? ????? ????? 1?110 01??? ??11? 0?1?? ?????
?1100 ?0?2? ?1?11 ?1201 100?1 1?01? ???0? 112?0 0021?
10000 11100 ???10 00??? ?0000 00011 11?1? 11021 0?111
110?1 10200 10112 000?? 10104 ????? ????? 0011? 2?00?
10??0 01000 00??1 00?10 00000 0
Purussaurus brasiliensis
????? ????? ????? ????? ????? ????? ????? ????? ?????
?1100 1???2? ????1 11??? ????1 10??? ???00 112?0 00211
10000 111?0 ???10 00??? ?0?00 00011 1???? ?1021 0?111
110?1 1???? 101?2 101?? 101?4 ????? ????1 ?0?1? ?1000
10110 010?0 00??1 00010 00000 0

Purussaurus neivensis
101?1 00?1? 00001 0?0?? 1???? 011?? ????? 0?11? ??1??
?1100 ??1?1 010?1 11201 10001 1001? ???00 110?0 00020
10000 01110 ?0010 001?0 ?0000 00011 11011 11021 01111
110?1 10201 ?0112 001?2 10104 00010 1??01 0??10 21000
10?10 01000 00?01 00010 00000 0

Mourasuchus atopus
10??1 00?1? 00?01 0?00? 1?10? 011?? ??130 0?11? ??1??
?1102 ?112? ????0 1110? 10001 1000? ???00 120?1 00001
10500 01100 ?0010 011?? ?0000 00011 11011 ?1021 0?111
111?1 10?00 10??2 111?? 12104 0???? 1???1 00110 ?1000
10110 210?0 00??? ?0?10 00000 1

Mourasuchus amazonensis
????? ????? ????? ????? ????? ????? ????? ????? ?????
????? ????? ????? ????? ????? ????? ????? 120?1 0???1
???0? 01??? 0???? ?1??? ????? ????? ????? ??221 ??111
?12?1 102?0 ?0??2 111?? 1?1?4 ????? ????? ???1? ?????
?0??? 210?0 0???? ????0 00?00 1

Mourasuchus arendsi
????? ????? ????? 1?00? ?1100 11??? ??01? ????? ?????
?11?2 ????? ????? ????? ????? 1?0?? ????? 12??1 ?0?01
??50? 01?00 ????0 ?1??? ??000 0???? ????1 ?1?21 ????1
?12?1 ????1 ????? ????? 1?104 ????? ????? ????0 ?????
?0??? 210?0 0???? ????0 00?00 1

Mourasuchus nativus
????? ????? ????? ????? ????? ????? ????? ????? ?????
?11?2 ?112? ????0 1110? 10?01 1000? ????? ??0?? ????1
??5?? ????? ????? ?0??0 ?1?0? ?0011 1?01? ?1?2? ?????
?1??1 102?0 100?2 11112 12104 ?0010 1000? 00?10 01???
1011? 210?0 0???? ???10 00?00 1

Eocaiman cavernensis
????? ????? ????? ????? ????? ????? ????? ????? ?????
?1110 0??2? ????0 1?1?? ????? ????? ???00 ????0 ?????
?0??? ??1?? ???10 0???0 ?1??0 000?? ????? 0???? ??1?1
1?0?? ???0? ????? ????? ??1?4 ????? ????? 0??1? 2????
?0??? 0?00? ????? ??00? 0???? 0

Caiman yacare
10111 1001? 10001 00000 10101 11111 00110 00111 22111
01100 11121 01011 10101 10201 10010 11100 11000 00020
11200 00100 00010 00110 01000 00011 11011 11120 11111
11001 10201 10112 01112 10104 00010 11001 00110 21000
10110 01000 00011 00000 00000 0

Caiman crocodilus
10111 1001? 10001 00000 10101 11111 00110 00111 22111
01100 11121 01011 10101 10201 10010 11100 11000 00020
11200 00100 00010 00110 01000 00011 11011 11110 11111
11001 10201 10112 01112 10104 00010 11001 00110 21000
10110 01000 00011 00000 00000 0

Caiman latirostris
10111 0001? 10001 00000 1010? 11111 00110 00111 22121
01100 11121 01011 1?101 10201 100?? ?1100 11000 00020
10200 10100 00010 00110 01000 00011 11011 11110 11111
11001 10201 10112 11112 10104 00010 11001 00110 21000
10110 01000 00011 00000 00000 0

La Venta *Caiman* (UCMP. 39978, formerly *Caiman* cf. *lutescens*)
????? ????? ????? ????? ????? ????? ????? ????? ?????
????? ????? ????? ????? ????? ????? ???00 110?0 00010
10200 10100 ?0010 00??? ?1000 00011 11111 111?0 ????1
??0?? ???0? ????? ????? ????? ????? ????? ????? ?1000
10??0 0?00? ????? ????? 0???? 0

Melanosuchus fisheri
????? ?0??? ????? 0???? ????? ????? ????? ????? ?????
????0 1???? ????1 ?1101 1???? 10?1? ???00 1?0?0 0002?
10200 10110 ???10 00??0 ?1?0? ???11 ????1 ?112? ??111
110?? ????? ?0??? ?11?? 1010? ????? ???01 0??1? 2?000
101?0 01??? 0???? ????0 00?00 0

Melanosuchus niger
10111 1001? 1?001 00000 10101 11111 00110 00111 22121
01100 11121 01011 11101 10201 1001? ?1100 11000 00020
10200 10110 00010 00110 01000 00011 11011 11110 11111
11001 10201 10112 11112 10104 00010 11001 00110 21000
10110 01000 00011 00000 00000 0

Paleosuchus trigonatus
10011 1111? 01001 01000 10001 11111 21130 00111 32112
01100 11222 11111 11101 10201 10010 11110 11000 01010
10200 00100 00010 00110 00100 01111 11011 11000 11111
11011 10201 10112 121?2 10103 00010 11001 00110 21000
10110 01000 00011 00000 00000 0

Paleosuchus palpebrosus
10011 1111? 01001 01010 10001 11111 21130 00111 32112
01100 11222 111?1 11101 10201 100?0 11110 11000 01010
10200 00100 00010 00110 00100 01111 11011 11000 11111
11011 10201 10112 121?2 10103 00010 11001 00110 21000
10110 01000 00?11 00000 00000 0

Caiman brevirostris
????? ????? ????? ????? ????? ????? ????? ????? ?????
?1110 ????? ????1 ??1?? ?0201 ????? ???00 110?0 00??1
10200 1010? ????? ????? ????0 000?? ??0?? ??110 ????1
110?? ????? ?01?2 011?? 101?? ????? ???0? ????? 210??
10??? 0?0?0 0???? 00?00 00000 0

Culebrasuchus mesoamericanus
????? ????? ????? ????? ????? ????? ????? ????? ?????
?1100 ???2? ????0 ??20? ????? ????? ???10 ????0 ?????
?000? 0?1?? ????? ????0 ?0??? ????? ????? ????? ??1?1
?00?? ????? ????2 10?0? ??1?4 ????? ????1 ???1? 0????
?0??? ????0 00??? 00000 000?0 0

Centenariosuchus gilmorei
????? ????? ????? ????? ????? ????? ????? ????? ?????
?1100 1??2? ????? ????? ????? ????? ???00 1?0?0 0002?
?020? 1?10? ???1? ????? ?0??0 0???? ????? ????? 1?1??
11??? ????? 10?12 ?1?1? 1?1?4 ????? ????1 ???1? 2????
?0110 01??0 00??? 00?0? 00??0 0

Globidentosuchus brachyrostris
????? ????? ????? ????0 1???? ????? ????? ????? ?????
?1110 0??0? 1???0 ?1101 10311 1001? ???00 1???0 00??0
1?200 00??? ?1?10 ?0??? ?1?0? ??0?1 1???? ?1020 0?1?1
100?? ????0 ?0??2 011?? 101?4 ????? ????1 ???1? ????0
?0?1? 010?0 00??? 00100 00000 0

Gnatusuchus pebasensis
????? ????? ????? ????? ????? ????? ????? ????? ?????
?1020 ?1200 0?011 11101 00001 1001? ???02 110?0 10010
10000 001?? ?0010 ?0??? ?1??? ??11? 10011 01?1? 1???1
100?? ?0?0? 1?012 0111? 10104 ????? 1??01 00110 21001
10110 01000 00011 00101 00000 0

Mecistops cataphractus
10?00 1001? 00001 00000 11100 11111 20120 00111 10110
11110 31010 10001 00100 01110 201?1 00100 12000 00010
02100 00100 01000 00110 10000 10110 10001 01000 00111
11000 01011 00012 00100 10100 01110 10111 10010 00000
30110 01110 00011 00000 00000 0

Crocodylus niloticus
10100 0001? 10101 00010 11100 11111 20120 00111 20110
11100 11010 10001 01100 01110 20111 00100 11000 00010
02100 00100 11000 00110 10010 00110 10010 01000 00111
11000 01011 00012 00100 10100 01110 10111 10011 00000
30110 01000 00011 00000 00000 0

Crocodylus porosus
11100 0001? 00101 01010 11100 01111 20120 00111 20110
11100 11010 10001 01100 01110 20111 00100 11000 00010
02100 01100 11000 00110 10010 00110 10000 01000 00111
11000 01011 00012 00100 10100 01110 10111 10011 00000
30110 01000 00011 00000 00000 0

Crocodylus acutus
00100 0001? 10101 10010 11100 11111 20120 00110 20110
11100 11010 10001 01100 01110 20111 00100 11000 00010
02101 00100 11000 00110 10010 00110 10000 01100 00111
11000 01011 00012 00100 10100 01110 10111 10011 00000
30110 01000 00011 00000 00000 0

Osteolaemus tetraspis
??1?0 0001? 00101 01000 11100 11111 20111 00111 11110
11100 11010 10001 01100 00110 20111 00110 10000 01010
02100 01100 01000 00110 11001 01110 10100 01000 10111
11010 01010 10012 11100 10110 01110 10111 10110 00000
30110 01000 00011 00000 00000 0

Australosuchus clarkae
????? ?0??? ????1 ??0?? 1???? ?11?? ????? 0?10? ??1??
?1110 ?101? ????0 01100 00110 ?011? ???00 110?0 00011
02100 00100 01000 001?0 ?0000 00??? ????0 01000 ?0111
110?0 02011 ?0112 00100 10100 011?? 1??11 ?0010 00?00
10?10 010?0 0?0?1 ????0 0???? ?

Kambara implexidens
????? ?0??? ????? ????0 1???? ?11?? ??110 0?10? ??1??
?1110 1101? ????0 01100 00110 ?011? ???00 110?0 00011
02100 00100 01000 001?0 10000 00100 10000 01000 00111
110?0 02011 ?0012 00100 10100 01110 1?111 10010 00000
10?10 01000 00??1 00??0 ????? ?

Crocodylus acer
????? ????? ????? ????? ????? ????? ????? ????? ?????
????? ????? ????? ????? ????? ????? ???00 110?0 000?1
02100 00100 ??000 001?? ?0001 00?10 10000 01000 10111
100?0 02?01 ?00?2 00100 10100 01??0 ??111 00010 00000
30?10 01000 00?11 00??0 0?000 0

Crocodylus affinis
00100 1001? 10001 00001 11000 01111 00110 0?10? ??1??
?1110 11010 10000 01100 00000 20110 0??00 110?0 00010
01100 00100 ?0100 00??0 ?0001 00110 10000 01000 00111
100?0 ?010? ?0012 00100 10100 01??0 ???11 00010 00000
30?10 01000 000?1 00??0 0??00 0

Tomistoma schlegelii
02100 0001? 00101 00010 11000 11111 10110 00101 30110
11122 ?1040 00001 00100 00000 20100 00100 12000 00011
02100 00101 01000 00110 10001 00000 10000 01100 00111
11000 00110 00012 10100 10100 01100 10111 10010 00000
30110 01000 00011 00000 00000 0

Thecachampsa americana
????? ????? ????1 ????0 1?000 ?1111 ??110 0?00? ??1??
?1122 ???4? ????0 0010? 0031? ?010? ???00 120?0 00011
02100 00100 ?1000 00??? ?0000 10000 10000 ??100 0?111
110?0 00?10 01012 00100 10102 ???0? ???11 10010 0?200
301?0 01000 00??? 00000 00010 0

Kentisuchus spenceri
????? ?0??? ????? ????? 1???? ????? ????? ????? ?????
??1?0 ???4? ????0 ??100 0?110 ??11? ???00 110?0 000?1
02100 00100 ???00 00??0 ?0100 10100 100?0 01100 0?111
110?? ????0 ?0??2 0010? 10100 ????? ??111 ?0?10 0?0?0
30?10 0?0?0 00??1 00??0 000?0 0

Asiatosuchus germanicus
001?0 ?0?1? 00101 0?010 1?000 ?1111 ??1?? 0???? ??1??
?1110 1000? ????0 01100 00??0 101?0 0??00 010?0 000?0
00100 0010? ??100 00??0 ?0001 0???0 10000 01000 0?111
100?? ?0100 ?0011 10100 10100 0???? ???11 00?10 00000
30?10 010?0 0?001 ????0 000?0 0

Kuttanacaiman iquitosensis
????? ????? ????? ????? ????? ????? ????? ????? ?????
?1110 11120 0?010 1110? 10201 1001? ???10 110?0 00010
10200 001?0 ?0010 00??? ?1000 01011 1101? 11020 01??1
100?? ?020? 10?12 11112 10104 ????? 1??01 00?10 21000
10110 01000 00011 00100 00000 0

Caiman wannlangstoni
????? ????? ????? ????? ????? ????? ????? ????? ?????
?1110 1112? ????1 ??10? ????? ????? ???00 010?0 0???0
10200 1010? ?0?10 001?0 ?1?0? ??011 111?? 11120 ??111
110?1 10?01 10112 011?? 10104 ????? 1??01 0??10 21000
10110 01000 00??1 00100 00?00 0

***Paleosuchus* sp. (Pebas *Paleosuchus*)**
????? ????? ????? ????? ????? ????? ????? ????? ?????
?1100 ???2? ????? ????? ????? ????? ???10 1?0?0 01??0
1020? 0?1?? ??010 0???? ?0100 0???? ????? ????? ?????
??0?? ????? ????? ????? ????? ????? ????? ????? ?????
?0??0 0??0? ????? ???0? 0???? ?

Morphometric analysis

(1) Landmark definitions.

1. Anteriormost point of the frontal on the sagittal axis.
2. Fronto-parietal suture on the sagittal axis.
3. Right postorbital-squamosal suture on the lateral margin of skull table.
4. Left postorbital-squamosal suture on the lateral margin of skull table.
5. Right antero-lateral corner of skull table.
6. Left antero-lateral corner of skull table.
7. Right contact of postorbital-frontal suture with the orbital margin.
8. Left contact of postorbital-frontal suture with the orbital margin.
9. Right contact of frontal-prefrontal suture with orbital margin.
10. Left contact of frontal-prefrontal suture with orbital margin.
11. Right contact of prefrontal-lacrimal suture with the orbital margin.
12. Left intersection of prefrontal-lacrimal suture with the orbital margin.
13. Right frontal-prefrontal-nasal junction.
14. Left frontal-prefrontal-nasal junction.
15. Right anteriormost point of prefrontal.
16. Left anteriormost point of prefrontal.
17. Right anteriormost point of jugal.
18. Left anteriormost point of jugal.
19. Right anteriormost point of lacrimal.
20. Left anteriormost point of lacrimal.

(2) Crocodylian skull material studied in the morphometric analysis

1. *Eosuchus* cf. *minor* ANSP 10079
2. *Eosuchus lerichei* IRSNB 1740
3. *Thoracosaurus macrorhynchus*, MNHN 1902-22
4. *Eogavialis africanus*, IMGP-UT
5. *Argochampsa krebsi*, OCP DEK-GE 1201
6. *Gryposuchus* nov. sp., MUSM 1981
7. *Gryposuchus colombianus*, IGM 184696
8. *Ikanogavialis gameroi*, MCNC 143-72V
9. *Piscogavialis jugaliperforatus*, SMNK 1282 PAL
10. cf. *Piscogavialis* sp., MUSM 1997
11. *Gavialis browni*, AMNH 6279
12. *Gavialis gangeticus*, MNHN A5321
13. *Gavialis bengawanicus*, DMR-KS-201202-1
14. *Borealosuchus sternbergii*, USNM 6533
15. *Leidyosuchus canadensis* NMC 8942
16. *Alligator mississippiensis* UF 10941
17. *Caiman crocodilus* UF 80913
18. *Paleosuchus trigonatus*, MUSM DPV CR1
19. *Crocodilus niloticus* MNHN
20. *Crocodilus acutus* UF 49953
21. *Tomistoma schlegelii*, MNHN A5311
22. *Thecachampsa americana* AMNH 5663

(3) Procrustes superimposition analysis [1]. Average shape:

Lmk.	Axis 1 (x)	Axis 2 (y)
1	0.17274774	0.00000000
2	-0.25346838	0.00000000
3	-0.29071048	-0.22922749
4	-0.29071048	0.22922749
5	-0.17876069	-0.20004794
6	-0.17876069	0.20004794
7	-0.15485176	-0.11980901
8	-0.15485176	0.11980901
9	-0.06315062	-0.07431625
10	-0.06315062	0.07431625
11	0.00630870	-0.11563227
12	0.00630870	0.11563227
13	0.06566544	-0.02265320
14	0.06566544	0.02265320
15	0.17356595	-0.04997391
16	0.17356595	0.04997391
17	0.17384811	-0.12972111
18	0.17384811	0.12972111
19	0.30844567	-0.05506090
20	0.30844567	0.05506090

Procrustes sums of squares: 0.7263382866828477
Tangent sums of squares (symmetric component): 0.6888259374667368
Tangent sums of squares (asymmetry component): 0.007601511570988219

(4) Principal Component Analysis (PCA): CovMatrix, newDataset, Symmetric component.

	Eigenvalues	% Variance	Cumulative %
1.	0.01475838	44.993	44.993
2.	0.00831802	25.359	70.352
3.	0.00359941	10.973	81.326
4.	0.00156568	4.773	86.099
5.	0.00125842	3.837	89.935
6.	0.00096193	2.933	92.868
7.	0.00062272	1.898	94.766
8.	0.00043773	1.334	96.101
9.	0.00036539	1.114	97.215
10.	0.00033475	1.021	98.235
11.	0.00020617	0.629	98.864
12.	0.00016015	0.488	99.352
13.	0.00009950	0.303	99.656
14.	0.00005683	0.173	99.829
15.	0.00002574	0.078	99.907
16.	0.00001716	0.052	99.960
17.	0.00000969	0.030	99.989
18.	0.00000355	0.011	100.000

Total variance: 0.03280124

Variance of the eigenvalues: 0.0000136694038
Eigenvalue variance scaled by total variance: 0.01270
Eigenvalue variance scaled by total variance and number of variables: 0.24214

(5) Statistical analysis for fluctuating asymmetry
This analysis takes into account the object symmetry in the data:

Classifiers used for the Procrustes ANOVA:
Individuals: Taxa

Centroid size:

Effect	SS	MS	df	F	P (param.)
Individual	2052.454831	97.735944	21		

Shape, Procrustes ANOVA:

Effect	SS	MS	df	F	P (param.)
Individual	0.68882594	0.0018222908	378	95.93	<.0001
Side	0.00042081	0.0000233781	18	1.23	0.2329
Ind * Side	0.00718071	0.0000189966	378		

Shape, MANOVA tests of effects:

Symmetric component of shape variation:

Effect	Pillai tr.	P (param.)

Note: the test for 'Individual' used the symmetric component of the residual as the 'error' effect.

Asymmetry component of shape variation:

Effect	Pillai tr.	P (param.)
Side	0.78	0.6694

Directional asymmetry vector:

Lmk.	Axis 1 (x)	Axis 2 (y)
1	0.00000000	-0.00067460
2	0.00000000	-0.00200719
3	0.00091023	-0.00064757
4	-0.00091023	-0.00064757
5	0.00035812	0.00091065
6	-0.00035812	0.00091065
7	0.00093445	0.00156955
8	-0.00093445	0.00156955
9	-0.00007215	0.00051097
10	0.00007215	0.00051097
11	0.00019921	0.00019665
12	-0.00019921	0.00019665
13	0.00024572	0.00020511
14	-0.00024572	0.00020511
15	-0.00031841	-0.00043032

16	0.00031841	-0.00043032
17	-0.00028206	-0.00016309
18	0.00028206	-0.00016309
19	0.00053116	-0.00081105
20	-0.00053116	-0.00081105

(6) Phylogenetic mapping

Phylogenetic tree notation (Newick format):
((1,2,(3,(4,(5,(((6,7),(8,(9,10))),(11,12,13))))))),(14,((15,(16,(17,18))),((19,20),(21,22)))))
Dataset: PC scores, CovMatrix, newDataset, Symmetric component [2].
Data type: PC scores.
Method: unweighted squared-change parsimony.
The tree is rooted.
Tree length: 0.23046511

4TH MEETING OF THE NETWORK FOR NEOTROPICAL BIOGEOGRAPHY
Smithsonian Tropical Research Institute
Ciudad de Panamá, Panamá
January 15-16, 2015

Potential role of the northern proto-Amazonian drainage for biotic dispersals from South America to the Caribbean.

Salas-Gismondi, R.[1,2]; Tejada-Lara J.V.[2,3]; Antoine P.-O.[1]

[1]Institut des Sciences de l'Évolution, Université Montpellier 2, CNRS, IRD, 34095 Montpellier, France.
[2]Departamento de Paleontología de Vertebrados, Museo de Historia Natural, Universidad Nacional Mayor de San Marcos; Avenida Arenales 1256, Lima 14, Perú.
[3]Florida Museum of Natural History and Department of Biology – University of Florida, PO BOX 117800, Gainesville, FL 32611, USA.

When and how non-volant vertebrates of South American origin became established in the Caribbean Archipelago is a matter of arduous debate. This phylogenetic disparate assembly includes extinct and/or extant caviomorph rodents, megalonychid sloths, platyrrhine primates, bufonid toads, cichlid fishes, and a gharial crocodylian that might have reached the Caribbean islands sometime during the Cenozoic. Although geological evidence reveals sea barriers isolating this Archipelago from South America since the Paleocene, the occurrence of short-term terrestrial paths has not been fully falsified. Unfortunately, the pre-Quaternary fossil record is scarce and it does not provide significant data about early Cenozoic life within the Caribbean Archipelago. Given the complexity of this scenario, biogeographical hypotheses range from Cretaceous vicariance models to Cenozoic dispersals by land bridges (e.g., GAARlandia) or rafting.

Here, we would like to highlight the overlooked existence of an ancient South American drainage discharging into the Caribbean Sea by the eastern modern coast of Venezuela. This trunk river of northern flow was deeply rooted in western proto-Amazonia, between the growing Andes and the Guyana Craton, from the Paleocene until the Middle-Late Miocene transition. Large rivers in tropical coastal areas have been acknowledged as key elements for the biotic dispersal (i.e., by rafting) through sea barriers, interestingly involving Caribbean clades such as caviomorph rodents and platyrrhine primates as models. In fact, the restricted higher-order taxonomic composition of the Caribbean fauna implies a selective pattern of dispersal within the biotic entities at the source, comprising also secondarily freshwater clades (gharials and cichlid fishes) and taxa with marine relatives (megalonychid sloths). In western Amazonia, most Caribbean groups have been recorded as fossils during the time interval this northern flow drainage might have acted as a dispersal catalyst. Relative to GAARlandia hypothesis, this model fits better with distinct and diachronous events of colonization throughout the Cenozoic, as has been suggested by molecular data analyses. Caribbean Sea currents running northwestward provide further support for the riverine model discussed herein and originally proposed by Hedges in 1996. Although this model is not new, there is now evidence of the South American river that would have promoted dispersals to the Caribbean Archipelago.

Evidence from the cloud forest: Matthiessen specimen of *Purussaurus* from the late Middle Miocene of Peruvian Amazonia

SALAS-GISMONDI, Rodolfo, Université Montpellier 2, CNRS, IRD, Montpellier, France; ANTOINE, Pierre-Olivier, Université Montpellier 2, CNRS, IRD, Montpellier, France; BABY, Patrice, Université de Toulouse, CNRS, IRD, Toulouse, France; TEJADA-LARA, Julia, University of Florida, Gainesville, FL, United States of America; URBINA, Mario, Museo de Historia Natural, UNMSM, Lima, Peru

Peter Matthiessen in his classic of 1961 The Cloud Forest, detailed the discovery of a one-hundredkilogram "giant mandible" in a creek bank of the Mapuya River, Peruvian Amazonia. He canoed with the heavy fossil for around 300 km down the Ucayali River to Pucallpa city where the specimen was retained in the police station and subsequently lost for more than three decades. In 1997, the fossil was recovered by the Ucayali Regional Government and stored at the Museo Regional de Pucallpa (MRP). The fossil specimen (MRP 19), in fact a snout preserved until the level of the suborbital fenestrae, presents a broad, deep, and heavily-sculpted rostrum and large external naris, both diagnostic features of the giant caiman *Purussaurus*. Stratigraphy and paleontology of the *Purussaurus*-bearing outcrops at the Mapuya River and surrounding areas of the Fitzcarrald Arch concur to assign a late Middle Miocene age to this assemblage based on high faunal similarity with La Venta mammals of Colombia. However, MRP 19 resembles more closely to Late Miocene species of *Purussaurus* from Acre (Brazil; P. brasiliensis) and Urumaco (Venezuela; *P. mirandai*) than to the coeval species from La Venta (*P. neivensis*), in having short V-shaped nasals, a postnarial fossa, and huge size. Nonetheless, MRP 19's originality was only unveiled after removing the hard matrix of the rostrum dorsal surface. The narial opening was actually capacious and elongated but it only reached posteriorly the level of the fifth maxillary alveolus, whereas in the Late Miocene species it outreaches the eighth alveolus level. Behind the narial opening and fossa, the dorsal surface between both rostral canthi is not longitudinally depressed. This region is relatively flat in P. neivensis but deeply depressed in the younger species. Ventrally, the vomer is exposed behind the premaxilary-maxillary suture, as we suspect is characteristic for the genus Purussaurus. Within the maxillary dental series, Purussaurus specimens known so far show unambiguously that the third alveolus is slightly bigger than the fourth, a unique feature among caimanines.

During the late Middle Miocene, Fitzcarrald *Purussaurus* and *P. neivensis* inhabited different areas of the vast Pebas System, a complex of mega-wetlands that covered most northwestern South America. By the Late Miocene, strong Andean uplift divided the "pan-Amazonian" region and further favored *Purussaurus* allopatric speciation within the newly born Orinoquia and Amazonia basins.

EVOLUTION OF NEOTROPICAL BIODIVERSITY: PHYLOGENY, ECOLOGY, AND BIOGEOGRAPHY OF THE MESOEUCROCODYLIA (VERTEBRATA: CROCODYLIFORMES) FROM THE MIOCENE OF PERUVIAN AMAZONIA

Abstract: Under the influential role of the Andean mountains, western Amazonia developed distinctive environmental conditions that ultimately led to divergent, higher biodiversity within the Neotropics. Although this intimate geologic-biotic interaction might have produced similar phenomena in the past, our knowledge about the tropical biotic evolution occurring in close proximity to these rapid growing mountains is poorly documented in the deep time. A pivotal time interval for the emergence of the modern Amazonian ecosystems occurred during the Miocene, when major Andean uplift remodeled the landscape of the foreland basin and fostered the onset of the Amazon River System, at about 10.5 million years ago. Proto-Amazonian biotas just prior to this episode are integral to understanding origins of Neotropical biodiversity, yet vertebrate fossil evidence was extraordinarily rare thus far. By studying the evolution, ecology, and biogeography of fossil mesoeucrocodylians (caimans, gharials, and sebecids) documented in new rich paleontological sites of eastern Peru, this research provides a snapshot of the florishing Miocene life of western proto-Amazonia.

The crocodylian assemblage of the Iquitos bonebeds (middle-late Miocene transition) is extraordinary in representing both the highest taxonomic diversity (with up to seven associated species) and the widest range of snout morphotypes ever recorded in any crocodyliform community, recent or extinct. The heterogeneity of snout shapes at the Peruvian Miocene localities covers most of the morphospace range known for the entire crocodyliform clade reflecting the combined influences of long-term evolution, resource abundance and variety, and niche partitioning in a complex ecosystem, with no recent equivalent. Besides the large-bodied *Purussaurus* and *Mourasuchus*, all other crocodylians in Iquitos are new taxa, including a stem caiman—*Gnatusuchus pebasensis*—bearing a massive shovel-shaped mandible, procumbent anterior and globular posterior teeth, and a mammal-like diastema. This unusual species is an extreme exemplar of a radiation of small caimans with crushing dentitions recording peculiar feeding strategies correlated with a peak in proto-Amazonian molluscan diversity and abundance, deep in the so-called Pebas Mega-Wetland System. The sole long-snouted crocodylian in this community is the basalmost gavialoid of the Amazonian basin, a critical taxon that offers evidence for accurately reconstructing the ancestral anatomy and ecology of this clade. Including this new species in phylogenetic-morphometric analyses suggests that the evolution of the similar rostral pattern between South American and Indian gavialoids results from parallel evolution in riverine habitats.

As part of the same prevailing Pebas biome, Fitzcarrald localities correspond to coeval paleoenvironments closer to the Andean influence (late middle Miocene). This fauna includes deep-snouted sebecids (Sebecosuchia) and advanced gavialoids (Gavialoidea) with protruding eyes, associated with a wide array of caimans (*Mourasuchus*, *Purussaurus*, *Paleosuchus* et *Eocaiman*), and further suggesting the presence of terrestrial settings and fluvially-dominated ecosystems. On the other hand, the highly endemic Iquitos faunas evolved within the dysoxic marshes and swamps typical of the long-lived Pebas Mega-Wetland System (early–early late Miocene) and declined with the inception of the transcontinental Amazon drainage, favoring diversification of longirostrine crocodylians and more modern generalist-feeding caimans. Indeed, the end of the Pebas Mega-Wetland System notably resulted in the reduction of the phylogenetic and morphotypical mesoeucrocodylian proto-Amazonian diversity, designating the beginning of the modern Amazonian faunas. The rise and demise of distinctive, highly productive aquatic ecosystems substantially influenced evolution of Amazonian biodiversity hotspots of crocodylians and other organisms throughout the Neogene.

Résumé : L'Amazonie occidentale héberge une biodiversité actuelle foisonnante. Si l'évolution des biomes tropicaux de basse altitude est mal documentée dans le temps profond, il semble que le Miocène ait été une période clé pour l'émergence des écosystèmes amazoniens modernes. Une phase majeure de surrection des Andes a en effet provoqué la mise en place du drainage actuel de l'Amazone au Miocène supérieur (10,5 millions d'années). Pour mieux connaître les modalités de l'émergence de la biodiversité néotropicale actuelle, acquérir une meilleure connaissance des biomes proto-amazoniens – antérieurs au Miocène supérieur – est donc crucial. Malheureusement, le registre fossile correspondant était jusqu'à présent très restreint, en particulier pour les vertébrés. En analysant l'évolution, l'écologie et la biogéographie de mésoeucrocodiliens fossiles (caïmans, gavials et sébécidés) découverts dans de nouvelles localités d'Amazonie péruvienne, le présent mémoire permet de dépeindre un épisode clé de la vie foisonnante de la "proto-Amazonie" occidentale au Miocène.

La faune de crocodiles des gisements de la région d'Iquitos (13-10 Ma), au Nord-est du Pérou, représente à la fois la plus grande diversité taxonomique (sept espèces associées) et la plus grande variété de morphotypes du rostre connues pour une communauté donnée de crocodyliformes (actuels-fossiles). L'hétérogénéité dmorphologique correspondante recouvre la majeure partie du morpho-espace connu pour l'ensemble des crocodyliformes, ce qui reflète les influences conjointes d'une évolution à long terme, d'une grande abondance/variété de ressources alimentaires, et d'une ségrégation de niches dans un écosystème complexe. Outre les caïmans géants *Purussaurus* et *Mourasuchus*, tous les autres crocodiliens sont des taxons nouveaux, parmi lesquels un caïman basal—*Gnatusuchus pebasensis*—présentant une mandibule massive et en forme de pelle, des dents antérieures proclives et postérieures globuleuses, ainsi qu'un diastème de type « mammalien ». Cette espèce très particulière constitue un exemple extrême d'une radiation évolutive de petits caïmans durophages, associée à l'apogée des mollusques proto-amazoniens, au sein du méga-système humide Pebas. Le seul crocodilien longirostre de cette communauté est le gavialoïde le plus basal du bassin amazonien, crucial pour la reconstitution de l'écologie et du morphotype ancestraux des Gavialoidea. Une fois inclus dans des analyses phylogénétiques-morphométriques, ce nouveau taxon permet de démontrer que le patron longirostre des gavialoïdes sud-américains et indiens résulte d'une évolution convergente, dans des habitats fluviatiles.

Situées à la périphérie du biome pébasien et contemporaines des assemblages d'Iquitos, les localités de l'Arche de Fitzcarrald (13-12 Ma) correspondent à une influence plus marquée des Andes, en termes d'environnements. Cette faune de crocodiliens inclut des sébécidés (Sebecosuchia) au crâne comprimé latéralement et des gavials dérivés et aux yeux proéminents (Gavialoidea), associés à divers caïmans (*Mourasuchus*, *Purussaurus*, *Paleosuchus* et *Eocaiman*). La composition de cet assemblage suggère la prédominance de milieux terrestres et fluviatiles dans cette région. Le contraste est fort avec la région d'Iquitos, où les faunes de crocodiles, hautement endémiques, apparaissent plutôt liées à l'existence de marécages dysoxiques typiques du méga-système Pebas.

La mise en place du système de drainage transcontinental amazonien au début du Miocène supérieur a entrainé la disparition du système Pebas et le déclin de ces faunes crocodiliennes proto-amazoniennes, remplacées par des communautés dominées par des caïmans plus généralistes (notamment *Caiman* et *Melanosuchus*) et des gavials très longirostres. Plus généralement, l'essor, la persistance, puis le déclin de ces écosystèmes aquatiques miocènes à forte productivité a laissé une empreinte durable – et encore perceptible – sur la biodiversité amazonienne.